



UNIVERSIDAD DE VALLADOLID
ESCUELA DE INGENIERÍAS INDUSTRIALES

DEPARTAMENTO DE INGENIERÍA QUÍMICA Y
TECNOLOGÍA DEL MEDIO AMBIENTE

*Direct synthesis of H_2O_2 :
study of the influence of N_2 as reaction inert
and optimization of the reactor configuration*

Presentada por Irene Huerta Illera para optar al grado de Doctor por la
Universidad de Valladolid

Dirigida por:

Dr. Juan García Serna

Prof. Dra. M. José Cocero Alonso



UNIVERSIDAD DE VALLADOLID
ESCUELA DE INGENIERÍAS INDUSTRIALES

DEPARTAMENTO DE INGENIERÍA QUÍMICA Y
TECNOLOGÍA DEL MEDIO AMBIENTE

*Síntesis directa de H_2O_2 :
estudio de la influencia de N_2 como inerte de reacción
y selección de la configuración de reactor optima*

Presentada por Irene Huerta Illera para optar al grado de Doctor por la
Universidad de Valladolid

Dirigida por:

Dr. Juan García Serna

Prof. Dra. M. José Cocero Alonso

Memoria para optar al grado de Doctor,
con Mención de Doctorado Internacional
presentada por la Ingeniera Química
Irene Huerta Illera

Siendo los tutores en la Universidad de Valladolid

Dr. D. Juan García Serna

y

Prof. Dra. D^a María José Cocero Alonso

Y en Industrial Chemistry and Reaction Engineering Department of Chemical
Engineering Department, Åbo Akademi University (Finlandia)

Dr. Pierdomenico Biasi

Valladolid, Mayo de 2014

UNIVERSIDAD DE VALLADOLID
ESCUELA DE INGENIERIAS INDUSTRIALES

Secretaría

La presente tesis doctoral queda registrada en el folio número _____ del
correspondiente libro de registro numero _____.

Valladolid, a ____ de _____ de 2014

Fdo. El encargado de registro

Juan García Serna
Profesor Titular de Universidad
Departamento de Ingeniería Química y Tecnología del Medio Ambiente
Universidad de Valladolid

y

María José Cocero Alonso
Catedrática de Universidad
Departamento de Ingeniería Química y Tecnología del Medio Ambiente
Universidad de Valladolid

Certifican:

Que la ingeniera química IRENE HUERTA ILLERA ha realizado en el Departamento de Ingeniería Química y Tecnología del Medio Ambiente de la Universidad de Valladolid, bajo nuestra dirección, el trabajo que, para optar al grado de Doctorado Internacional, presenta con el título "*Direct synthesis of H₂O₂: study of the influence of N₂ as reaction inert and optimization of the reactor configuration*", cuyo título en castellano es "*Síntesis directa de H₂O₂: estudio de la influencia de N₂ como inerte de reacción y selección de la configuración de reactor óptima*", siendo el Dr. Pierdomenico Biasi su tutor durante la estancia realizada en Åbo Akademi University (Finlandia).

Valladolid, a ____ de _____ de 2014

Fdo. Juan García Serna

Fdo. María José Cocero Alonso

Reunido el tribunal que ha de juzgar la tesis doctoral titulada "*Direct synthesis of H₂O₂: study of the influence of N₂ as reaction inert and optimization of the reactor configuration*" presentada por la ingeniera Irene Huerta Illera y en cumplimiento con lo establecido en el Real Decreto 1393/2007 de 29 Octubre ha acordado conceder por _____ la calificación de _____.

Valladolid, a _____ de _____ de 2014

PRESIDENTE

SECRETARIO

1^{er} VOCAL

2^o VOCAL

3^{er} VOCAL

Table of Contents

Resumen.....	1
1. Introducción.....	3
2. Objetivos.....	6
3. Resultados.....	7
4. Conclusiones.....	24
Referencias.....	32
Lista de Figuras.....	34
Summary.....	35
Objectives.....	55
<u>Chapter I: Direct synthesis of H₂O₂: general aspects and influence of reactions conditions</u>	59
1.1. Hydrogen peroxide and general outlook of the methods of production.....	61
1.2. Direct synthesis: operational conditions selection.....	65
1.2.1. <i>Catalyst</i>	66
Active metal.....	66
Oxidation state.....	67
Catalyst's support.....	67
1.2.2. <i>Promoters</i>	68
Halides.....	68
Acids.....	69
1.2.3. <i>Solvent</i>	70
1.2.4. <i>Pressure and temperature</i>	71
1.3. Direct synthesis: reactor configuration.....	71
1.3.1. <i>Slurry bubble column reactor (SBCR)</i>	72
1.3.2. <i>Trickle bed reactor</i>	73
1.4. Industrial production of H ₂ O ₂ by direct synthesis: overview of patents.....	74
1.5. Conclusions.....	78
References.....	79
Table captions.....	83
Figure captions.....	83

Chapter II: Hydrogenation and decomposition kinetic study of H₂O₂ over Pd/C catalyst in an aqueous medium at high CO₂ pressure85

2.1. Introduction	87
2.2. Experimental	89
2.1.1. <i>Material and methods</i>	89
2.1.2. <i>Experimental Set-up and procedure</i>	90
2.3. Mathematical model	91
2.3.1. <i>Mechanism</i>	91
2.3.2. <i>H₂ solubility</i>	92
2.3.3. <i>Mass balance equations</i>	93
2.3.4. <i>Numerical solution strategy</i>	94
2.4. Results and discussion	94
2.4.1. <i>Initial concentration of hydrogen peroxide</i>	97
2.4.2. <i>Halide concentration</i>	98
2.4.3. <i>Acid concentration and pH</i>	100
2.4.4. <i>Reaction temperature</i>	101
2.4.5. <i>Amount of catalyst and Pd loading</i>	102
2.5. Conclusions	104
List of symbols	106
References	107
Table captions	108
Figure captions	108

Chapter III: Direct synthesis of H₂O₂ in water using nitrogen as inert over Pd/C catalysts in semicontinuous mode.....111

3.1. Introduction	113
3.2. Experimental	114
3.2.1. <i>Materials and Methods</i>	114
3.2.2. <i>Experimental Set-up and procedure</i>	114
3.3. Results and discussion	115
3.3.1. <i>Nitrogen vs CO₂</i>	118
3.3.2. <i>Amount of catalyst and Pd loading</i>	120
3.3.3. <i>Pressure and hydrogen partial pressure</i>	123

3.3.4. Reaction temperature.....	127
3.3.5. Gas total flow.....	129
3.3.6. Influence of agitation speed.....	131
3.4. Conclusions.....	133
References	134
Table captions	136
Figure captions	137

Chapter IV: Effect of the low hydrogen to palladium ratio in the direct synthesis of H₂O₂ in water in a trickle bed reactor 139

4.1. Introduction	141
4.2. Materials and methods.....	143
4.2.1. Materials.....	143
4.2.2. Experimental set-up	144
4.2.3. Analytical methods.....	145
4.2.4. Experimental procedure	146
4.3. Results and discussion	146
4.3.1. Overall analysis of maxima and minima	151
4.3.2. Influence of operational pressure.....	153
4.3.3. Influence of liquid flowrate	154
4.3.4. Influence of the ratio between the catalyst, bed volume, catalyst distribution	156
4.4. Conclusions	160
References	161
Table captions	163
Figure captions	164

Chapter V: The development of the H₂O₂ direct synthesis process in water with a commercial catalyst in a continuous reactor. 165

5.1. Introduction.....	167
5.2. Materials and methods.....	170
5.2.1. Materials.....	170
5.2.2. Experimental set-up	170
5.2.3. Methods.....	171
5.2.4. Experimental procedure.....	172

5.3. Results and discussion	172
5.3.1. <i>Hydrogenation experiments</i>	177
5.3.2. <i>Influence of liquid flow rate/gas flow rate and amount of catalyst</i>	179
5.3.3. <i>Influence of total operation pressure</i>	182
5.3.4. <i>Influence of temperature</i>	183
5.3.5. <i>Influence of bromide concentration</i>	185
5.3.6. <i>Influence of palladium concentration in the catalyst</i>	187
5.4. Conclusions	189
References	190
Table captions	193
Figure captions	193

Chapter VI: Determination and model of liquid – gas mass transfer coefficient and interfacial area in a low pressure bubble column

6.1. Introduction	197
6.2. Material and methods	199
6.2.1 <i>Materials</i>	199
6.2.2 <i>Experimental setup</i>	199
6.2.3 <i>Experimental procedure</i>	200
6.3. System modelling and correlations	201
6.3.1. <i>Model as perfect mixed stirred tank (PMST)</i>	201
6.3.2. <i>Empirical correlations from bibliography</i>	202
6.3.3. <i>CFD model of the bubble column</i>	203
6.4. Results and discussion	205
6.4.1. <i>Hold-up</i>	207
6.4.2. <i>Bubble diameter</i>	211
6.4.3. <i>Mass transfer coefficient and interfacial area</i>	214
6.4.4. <i>CFD modelling; results and conclusions</i>	218
6.5. Conclusions	221
Symbols and nomenclature	222
References	223
Table Captions	226
Figure Captions	226

Conclusions	227
Future work.....	239
<u>Appendix I</u> : Supplementary figures for chapter II.....	241
<u>Appendix II</u> : Supplementary data for chapter VI	249
<u>Appendix III</u> : Direct synthesis of H ₂ O ₂ in a slurry bubble column.....	259
A.1. Slurry bubble columns. Applications and design	261
<i>A.1.1. General aspects for the design of slurry bubble column reactors</i>	263
<i>A.1.2. Pre – design of a slurry bubble column reactor</i>	268
A.2. Direct synthesis of H₂O₂ in a low pressure slurry bubble column	271
<i>A.2.1. Materials</i>	271
<i>A.2.2. Experimental setup</i>	271
<i>A.2.3. Results and discussion</i>	272
A.3. Design of a high pressure slurry bubble column reactor	275
A.4. Measuring and analysis of the reaction conditions on the system hydrodynamic	277
List of symbols.....	283
References	283
Table Captions.....	284
Figure Captions.....	285
Mechanical design.....	287
Piping and instrumentation diagrams.....	301
Acknowledgments	311
List of publications.....	313

RESUMEN

Síntesis directa de H_2O_2 .

Estudio de la influencia de N_2 como inerte de reacción
y selección de la configuración de reactor óptima

1. Introducción

El desarrollo de la producción de peróxido de hidrógeno mediante síntesis directa y su aplicación en el entorno de la industria química constituye uno de las principales prioridades en la “Agenda estratégica de Investigación” (SRA) de la Plataforma Tecnológica Europea para la Química Sostenible [1].

El peróxido de hidrógeno, conocido comúnmente como agua oxigenada, es un líquido incoloro con fuertes propiedades oxidantes, y altamente inestable que puede descomponer por acción del calor, la luz o el contacto con metales. Entre sus múltiples aplicaciones, además de medicina y farmacia, están la síntesis química (oxidación de propileno), industria textil y del papel (acción blanqueante), tratamiento de aguas residuales o incluso la industria alimentaria, la aeronáutica o la electrónica. La importancia del peróxido de hidrógeno radica en su carácter “verde” debido a su baja toxicidad, alta degradabilidad y al hecho de que descompone generando agua como único subproducto.

Tradicionalmente la producción industrial de peróxido de hidrógeno ha estado dominada por la ruta de la antraquinona. Mediante un proceso cíclico la 2 – alquil – antraquinona es reducida en presencia de paladio e hidrógeno y oxidada posteriormente con aire para obtener peróxido de hidrógeno. Las condiciones de operación, aunque ventajosas, y la cantidad de subproductos generados que hacen necesaria una posterior purificación y separación limitan la viabilidad de este proceso solo para grandes escalas. Durante las últimas décadas se han desarrollado varios procesos alternativos para la síntesis de peróxido de hidrógeno. La síntesis directa es la más prometedora de todas ellas y la que ha sido más estudiada por varios grupos de investigación. Esta opción no solo reduce notablemente la necesidad de una purificación posterior sino que permite la síntesis *in situ*, eliminando los riesgos asociados al transporte.

Aunque en sí misma la reacción de síntesis es sencilla, el proceso en su totalidad tiene una gran cantidad de limitaciones y complejidades. Además de la reacción principal existen otras tres reacciones secundarias (Esquema 1) que son termodinámicamente favorables y compiten contra la principal, reduciendo la selectividad y eficiencia del proceso. La reacción de síntesis directa necesita la presencia de un catalizador para tener lugar, lo que añade una dificultad extra al proceso puesto que para que se produzca la reacción los reactivos gaseosos tienen que disolverse en el medio de reacción y alcanzar los centros activos de sólido. El carácter inflamable de las mezclas hidrógeno – oxígeno limita la concentración del hidrógeno, que actúa como reactivo limitante, a un valor máximo del 4 % mol [2, 3].

Existen una gran cantidad de trabajos bibliográficos realizados por varios grupos de investigación que estudian la influencia de las condiciones de reacción con el objetivo de minimizar el efecto de las reacciones secundarias, optimizar las condiciones de operación y mejorar la transferencia de materia y la selectividad. La mayoría de referencias bibliográficas disponibles en los principales medios de difusión están enfocadas en tres aspectos del proceso de optimización de la reacción de síntesis:

- El tipo de medio de reacción. Generalmente agua, metanol o etanol (puros o mezclas de ambos) son las opciones más utilizadas como fase líquida; el dióxido de carbono y nitrógeno actúan normalmente como diluyente en la fase gas. La selección de uno u otro dependerá de las condiciones de operación y de la aplicación posterior del peróxido generado [4-6].
- El metal activo y soporte del catalizador. Los metales nobles (oro, paladio, platino) por separado o combinados forman el componente activo en la mayoría de los catalizadores usados en síntesis directa de peróxido de hidrógeno. Los tipos de soporte más estudiados son carbón activo, óxido de titanio, zeolitas y alúmina principalmente [7-9]
- Los promotores o inhibidores, que añadidos en bajas concentraciones al medio de reacción o actuando como modificadores del soporte del catalizador reducen la actividad de las reacciones secundarias [10-12].

Aunque menos numerosos, también es posible encontrar trabajos centrados en el estudio de las reacciones secundarias, la cinética del proceso y el mecanismo de reacción.

El valor e importancia de estos trabajos es innegable y gracias a muchos de ellos se han determinado los mecanismos del proceso y los factores determinantes para la síntesis. Sin embargo, todos estos trabajos están realizados con un enfoque principalmente académico, centrado en los aspectos más formales del proceso y en las condiciones de operación y de control típicas de un proceso a escala laboratorio. Puesto que las principales aplicaciones del peróxido de hidrógeno están relacionadas con procesos industriales a gran escala (la producción anual de H_2O_2 se estima en 3000 kt por año), la única manera de que la síntesis directa pueda ser un proceso equiparable a la ruta de la antraquinona es desarrollando nuevos sistemas de producción que puedan ser extrapolados a escala industrial.

La selección de la configuración del reactor debe estar basada en las condiciones de proceso y las necesidades del sistema de reacción trifásica. Los reactores tipo "slurry bubble column" (reactor de columna de burbujeo) y "trickle bed reactor" (reactor de lecho percolador) son reactores de

tipo continuo ampliamente utilizados en la industria química. Este tipo de reactores favorecen el contacto entre las diferentes fases que toman parte en la reacción de síntesis directa de peróxido reduciéndose así las limitaciones relacionadas con la transferencia de materia y consiguiéndose alcanzar mayores valores de productividad y rendimiento.

2. Objetivos

El objetivo principal de esta tesis es la de encontrar las condiciones óptimas de reacción para diferentes configuraciones de reactores continuas utilizando un catalizador comercial. Aunque la síntesis de peróxido de carbono ya ha sido profundamente estudiada, la mayoría de las patentes e investigaciones tienen un rango de aplicación muy limitado a escala piloto o a escala industrial. Los resultados y conclusiones de este trabajo buscan servir como base para la selección y posible desarrollo de un sistema a escala piloto para la síntesis directa de peróxido de hidrógeno. Para ello se han planteado los siguientes objetivos.

- Estudiar la reacción de hidrogenación – descomposición. Mediante la operación de una planta a escala laboratorio se estudiará la influencia de las principales variables de reacción y se establecerá su influencia sobre las reacciones secundarias (descomposición e hidrogenación). A partir de los resultados experimentales y mediante modelado se obtendrán los valores de los parámetros cinéticos.
- Optimizar el proceso reacción de síntesis directa de peróxido de hidrógeno y estudiar la influencia de las principales variables de reacción. Las condiciones de operación que se estudiarán serán diferentes para cada sistema debido a sus características particulares.
- Analizar la hidrodinámica de las columnas de burbujeo mediante el estudio del “hold – up” y de la transferencia de materia en sistemas a baja y alta presión.
- Optimizar la producción de H_2O_2 en un reactor de lecho percolador (trickle bed reactor), en colaboración con la universidad Abo Akademi (Turku, Finlandia), estudiando las principales variables de operación para un catalizador comercial en base Paladio/Carbón.

3. Resultados y discusión

Capítulo I. *Síntesis directa de peróxido de hidrógeno. Aspectos generales e influencia de las condiciones de reacción.*

El peróxido de hidrógeno se ha convertido gracias a sus excelentes propiedades oxidantes y a su baja toxicidad en uno de los compuestos químicos más utilizados tanto en la industria química de gran escala (textil, papelera, producción de reactivos de alto valor añadido (epoxidación del propileno)) como la producción de artículos de alto valor añadido (electrónica). La demanda global anual de peróxido de hidrógeno es de cercana a 3 millones de toneladas y aumenta aproximadamente un 4% por año.

De todos los procesos existentes la síntesis directa a partir de oxígeno e hidrógeno es la alternativa más prometedora y con más posibilidades de desarrollo para sustituir a los procesos de reacción tradicionales. Mediante síntesis directa puede ser posible la producción de peróxido de hidrógeno *in situ*. La producción a pequeña escala, imposible para los procesos tradicionales que solo son eficientes a gran escala, presenta dos ventajas principalmente:

- Permite el ajuste de las características del peróxido de hidrógeno generado a las necesidades del proceso para el cual se produce.
- Evita la necesidad del transporte desde los centros de producción a los de consumo. El transporte de peróxido de hidrógeno es peligroso debido a que el compuesto se transporta muy concentrado y descompone fácilmente.

Existen una gran cantidad de artículos de investigación y patentes que demuestran el extraordinario esfuerzo necesario para determinar y modelar el mecanismo de reacción y como cada variable del proceso afecta a la productividad y la eficiencia. La mayor parte de todos los trabajos disponibles en las fuentes de referencias habituales están realizados a escala laboratorio y con reactores tipo “*batch*” que aunque proporcionan una información extremadamente valiosa y sientan las bases del proceso no pueden ser aplicadas directamente a gran escala.

El desarrollo de sistemas que permitan la producción de manera continua es clave para la futura implementación de la síntesis directa como un proceso de producción de peróxido de hidrógeno a escala industrial o semi – industrial. De todos los tipos de reactores disponibles los de tipo “*slurry bubble column*” y percolador (*trickle bed reactor*) son los más adecuados en función de las necesidades de la síntesis directa de peróxido de hidrógeno. Permiten la síntesis de peróxido en continuo (clave para el desarrollo de la técnica a escala industrial), la transferencia de materia entre las fases gas – líquida – sólida esta favorecida y son sencillos de operar.

Aunque tanto los reactores de “*slurry bubble column*” y los de tipo percolador (*trickle bed reactor*) tienen numerosas aplicaciones en la industria química, su aplicación para la producción de peróxido de hidrógeno mediante síntesis directa no está completamente desarrollada aún [13-15].

Capítulo II. *Estudio cinético de las reacciones de hidrogenación y descomposición del peróxido de hidrógeno sobre catalizador de Pd/C en medio acuoso de reacción y alta presión de dióxido de carbono.*

La reacción de síntesis directa de peróxido de hidrógeno transcurre acompañada de tres reacciones secundarias y competitivas que reducen la selectividad del proceso global. La reacción de descomposición ($\text{H}_2\text{O}_2 \rightarrow \text{H}_2\text{O} + \frac{1}{2} \text{O}_2$) e hidrogenación ($\text{H}_2\text{O}_2 + \text{H}_2 \rightarrow 2 \text{H}_2\text{O}$) tienen lugar de forma simultánea a la reacción de síntesis y se ven afectadas de la misma manera por las variaciones en las condiciones de operación que la reacción principal [16]. El trabajo desarrollado en este capítulo pretende aportar información sobre el mecanismo de las dos reacciones secundarias y ayudar así determinar las condiciones óptimas de operación en las que dichas reacciones sean minimizadas.

Puesto que la reacción de descomposición tiene lugar incluso en condiciones no agresivas (la luz y el contacto con superficies metálicas puede causar la descomposición del peróxido de hidrógeno) es imposible estudiar el efecto de la hidrogenación individualmente. El dispositivo experimental está formado principalmente por un reactor semicontinuo perfectamente agitado que opera manteniendo la fase líquida en estado estacionario pero permite que la fase gas sea continua y los equipos necesarios para controlar la presión, temperatura y la cantidad de gases alimentados al reactor. Todos los experimentos se realizaron utilizando CO_2 en condiciones cercanas a las críticas ($T_c = 39.98 \text{ }^\circ\text{C}$, $P_c = 73.73 \text{ bar}$) y con un catalizador comercial de tipo Pd soportado sobre carbón activo. Las variables experimentales estudiadas fueron temperatura, concentración de haluro y ácido, cantidad de catalizador, concentración del metal activo y concentración inicial de peróxido de hidrógeno.

Para separar el efecto de cada reacción, cada experimento está formado por dos etapas; la primera, en la que la fase gas del sistema está compuesta únicamente por dióxido de carbono en la que se medirá el efecto de la reacción de descomposición y para la cual se fijó una duración de 45 minutos; y la segunda, en la que se introduce hidrógeno al reactor y la disminución en la

concentración se debe tanto a la descomposición como a la hidrogenación y que dura hasta que el tiempo de reacción alcance las tres horas o se consuma todo el peróxido de hidrógeno.

El desarrollo del modelo de las reacciones de hidrogenación y descomposición se ha basado en los resultados obtenidos en el estudio de cada parámetro de reacción. Las expresiones cinéticas propuestas son las siguientes:

$$r_d = k_d \cdot (C_{H_2O_2})^{\alpha_d} \cdot (n_{Pd})^{\beta_d} \quad (1) \quad r_h = k_h \cdot (C_{H_2O_2})^{\alpha_h} \cdot C_{H_2}^* \cdot (n_{Pd})^{\beta_h} \quad (2)$$

El valor de cada parámetro del modelo (k_{od} , k_{oh} , α_d , α_h , β_d , β_h) se obtendrá en base a la influencia de las variables de reacción.

Respecto a la concentración inicial de peróxido de hidrógeno (1, 3, 5 y 10 % wt/v) se concluyó que la velocidad de descomposición depende de la concentración de peróxido siguiendo una cinética de primer orden ($\alpha_d = 1.031$), mientras que la reacción de hidrogenación depende de la concentración de peróxido con un valor de orden de reacción cercano a orden cero ($\alpha_h = -0.161$) [10]. Una de las principales conclusiones que pueden obtenerse es que la hidrogenación es entre tres y veinte veces mayor que la descomposición, para condiciones de baja concentración de peróxido. Tras treinta minutos de reacción, para el experimento con una concentración inicial de 5 %wt/v la descomposición fue del 2.4% y la hidrogenación del 7.0%. Para el caso de una concentración inicial del 1% wt/v la descomposición fue muy similar, del 2.9% mientras que la hidrogenación alcanzó valores del 63.5 %.

El efecto de los promotores (ácidos y haluros) como limitantes de las reacciones secundarias fue claro y está ampliamente desarrollado en bibliografía. Los resultados mostraron que un ratio Br^-/Pd entre 1.5 y 2.5 mantiene la reacción descomposición en valores bajos y minimiza el efecto de la hidrogenación. También se ha encontrado una relación entre los factores cinéticos y el ratio Br^-/Pd . ($1851.4 < k_{od} < 2555$; $59.90 < k_{oh} < 692.59$). La selección del valor de pH (medida de la cantidad de ácido) debe hacerse en función del punto isoeléctrico del soporte del catalizador. Tal y como se esperaba, debido a resultados obtenidos por otros autores, un valor de pH = 2 demostró ser el más adecuado [17]. La temperatura (de 40 a 60 °C) juega un papel doble en la reacción de síntesis de peróxido puesto que incrementa la velocidad de reacción tanto para la síntesis como para la descomposición y la hidrogenación. La energías de activación calculadas a partir de los resultados experimentales tiene valores relativamente bajos ($E_{ad} = 18803.6 \text{ J}\cdot\text{mol}^{-1}$ (descomposición) y $E_{ah} = 7746.2 \text{ J}\cdot\text{mol}^{-1}$ (hidrogenación)).

El número de centros activos disponibles para reacción depende de la cantidad de catalizador (15 – 100 mg) y del porcentaje de paladio que contenga el catalizador (1, 3 y 5 % wt). Aunque las reacciones tienen lugar principalmente sobre el metal activo, varios autores han observado cierta actividad en el soporte del catalizador. La velocidad de reacción de descomposición aumenta exponencialmente con la cantidad de paladio disponible para los tres catalizadores estudiados, aunque el comportamiento cuando se utiliza el catalizador del 5 %Pd/C es diferente al de los experimentos con 1 % Pd/C y 3 % Pd/C. La velocidad de hidrogenación sigue una dependencia del tipo lineal para los tres catalizadores estudiados. La influencia de la cantidad de catalizador se incluye en el modelo a través de la concentración de centros activos y un coeficiente (β_d y β_h) que cuyo valor depende de tipo de catalizador utilizado y de la etapa de proceso (cinética o transferencia de materia) que sea controlante, (etapa cinética controlante: $0.88 < \beta_d < 1.08$ y $0.88 < \beta_h < 1.08$; etapa de transferencia de materia controlante: $\beta_d = 1.44$ y $\beta_h = 0.71$).

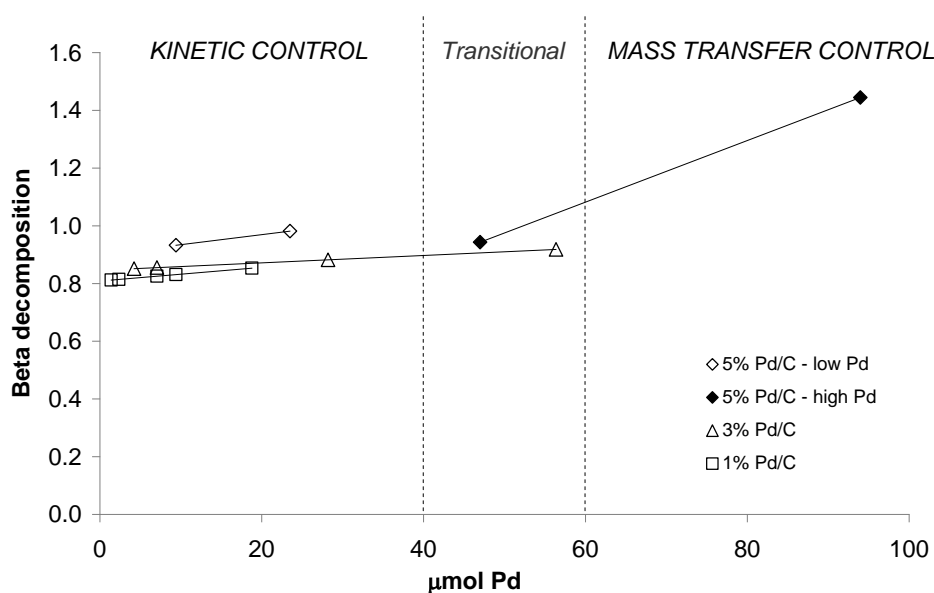


Figura 1. Valores de orden de reacción para la concentración de centros activos en descomposición versus la cantidad de paladio.

Capítulo III. Síntesis directa de peróxido de hidrógeno en agua utilizando nitrógeno como inerte en un reactor semicontinuo.

En la síntesis directa de peróxido de hidrógeno es necesario poner en contacto directo los dos reactivos gaseosos, oxígeno e hidrógeno. Las mezclas de $O_2 - H_2$ son altamente inflamables en un rango de concentración muy amplio (límite inferior de inflamabilidad = 4 % mol H_2 ; límite superior de inflamabilidad = 96 % mol H_2), aunque los límites de dicho intervalo pueden variar según diferentes autores. Usando gases inertes (CO_2 o N_2) se puede reducir la concentración de

hidrógeno hasta niveles seguros. El dióxido de carbono ha demostrado ser una excelente opción como inerte, puesto que no solo mantiene la concentración de H_2 a niveles bajos sino que sus propiedades físicas facilitan la transferencia de materia, reducen el límite de inflamabilidad y ayudan a estabilizar el peróxido de hidrógeno ya formado. El uso de gases puros, oxígeno y dióxido de carbono, puede incrementar enormemente el coste de un proceso.

Por lo tanto, y aunque el dióxido de carbono es mejor inerte y produce mejores resultados, la utilización de nitrógeno debe ser considerada como una alternativa, puesto que reduce el coste de producción del peróxido de hidrógeno y simplifica el proceso; el nitrógeno y el oxígeno pueden suministrarse de forma conjunta utilizando aire en vez de los reactivos puros. En este capítulo se estudia el proceso de síntesis directa usando nitrógeno como inerte en vez de dióxido de carbono, con el objetivo de determinar cuáles son las condiciones óptimas de reacción y cómo las variables de reacción afectan al proceso.

La cantidad de catalizador mostró que el mecanismo de reacción está formado principalmente por dos etapas, transferencia de materia y cinética. El control de una etapa frente a la otra depende de las condiciones de operación y de la cantidad de centros activos disponibles para reacción. Si la cantidad de catalizador es pequeña el sistema estará limitado por la cinética (no hay espacios de reacción suficientes para todos los reactivos que llegan a la superficie del sólido), si la cantidad de catalizador es grande la etapa limitante es la transferencia de materia (los reactivos no se transfieren a los centros activos con la suficiente rapidez). Al utilizar nitrógeno como inerte, se descubre que el intervalo de control de la cinética es mucho más estrecho que cuando se utiliza dióxido de carbono. Debido a esto, el valor óptimo de cantidad de catalizador fue de 30 mg de 5% Pd/C, para el cual se obtuvo una concentración de peróxido de hidrógeno máxima de 0.909 % wt/v, con una selectividad del 70% y una conversión del 17.8%. Los resultados fueron diferentes cuando se utilizaron catalizadores similares (mismo soporte) pero con diferentes concentraciones de paladio (1, 3 y 5 % wt), lo que sugiere que el soporte y la distribución del metal activo son diferentes y actúan de forma diferente.

Respecto a la influencia de la presión total (20 a 90 barg) y la presión parcial de hidrógeno (0.83 barg to 3.23 barg) del sistema, la productividad y la conversión aumentaron con el incremento de ambos parámetros. Sin embargo, para la selectividad, los resultados fueron diferentes. En el caso de la presión parcial, la selectividad permanece constante, con valores comprendidos entre el 30 – 35 %. Por el contrario la selectividad tuvo una fuerte dependencia de la presión total del

sistema, con valores entre 16 % para 20 barg y 48 % para una presión de 90 barg. El diferente comportamiento de la selectividad puede explicarse en función del ratio O_2/H_2 . El valor de O_2/H_2 permanece constante en aquellos experimentos en los que se varía la presión total puesto que la composición de la fase gas no varía, sin embargo cuando la presión parcial de hidrógeno es la variable a estudiar el ratio O_2/H_2 cambia (5.46 – 21.85). Un ratio O_2/H_2 alto implica una gran cantidad de oxígeno disponible en la fase líquida, lo que puede modificar las capacidades del catalizador al ser adsorbido sobre los centros activos o afectando al estado de oxidación del metal activo. La influencia de la temperatura de reacción, el flujo de gas y la velocidad de agitación también fueron analizadas.

Puesto que el objetivo del trabajo recogido en este capítulo es determinar si utilizando nitrógeno como inerte de la fase gas es posible alcanzar valores de productividad y rendimiento tan satisfactorios como los que pueden conseguirse con dióxido de carbono, la comparación de los resultados obtenidos con ambos gases es necesaria. Un primer vistazo a los resultados resumidos en la Figura 2 basta para deducir que los valores obtenidos cuando el dióxido de carbono ($5.77 \text{ mol}\cdot\text{h}^{-1}\cdot\text{gPd}^{-1} < \text{T.O.F} < 96.04 \text{ mol}\cdot\text{h}^{-1}\cdot\text{gPd}^{-1}$; $0.98 \text{ \% wt/v} < \% \text{ H}_2\text{O}_2 < 1.58 \text{ \% wt/v}$; $43 \text{ \%} < \text{Selectividad} < 88 \text{ \%}$) actúa como inerte son mucho mayores que cuando se utiliza nitrógeno ($0.56 \text{ mol}\cdot\text{h}^{-1}\cdot\text{gPd}^{-1} < \text{T.O.F} < 22.20 \text{ mol}\cdot\text{h}^{-1}\cdot\text{gPd}^{-1}$; $0.12 \text{ \% wt/v} < \% \text{ H}_2\text{O}_2 < 1.12 \text{ \% wt/v}$; $10.5 \text{ \%} < \text{Selectividad} < 70 \text{ \%}$). Los valores de T.O.F (“Turnover frequency”) son desde 6 hasta 10 veces mayores.

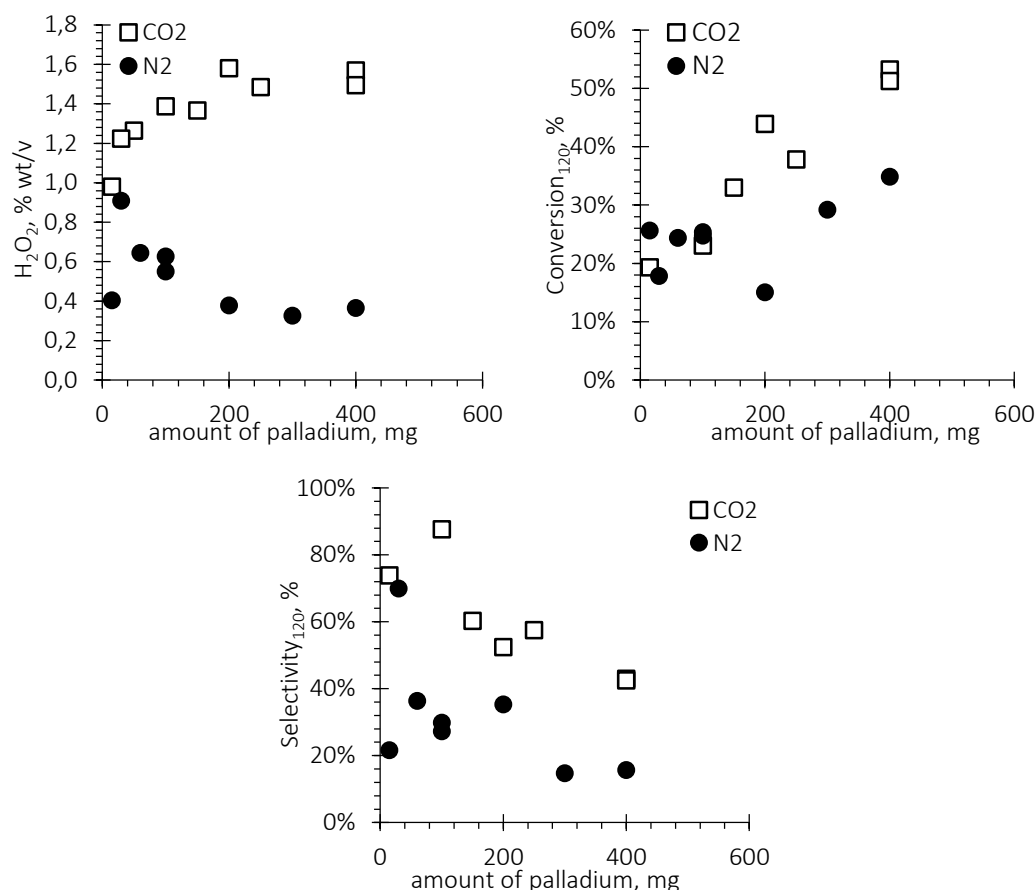


Figura 2. Comparación de los experimentos de síntesis directa realizados utilizando N_2 o CO_2 como inerte.

Capítulo IV. Estudio de la influencia de un bajo valor de ratio hidrógeno – paladio en la reacción en medio acuoso para la síntesis directa de peróxido de hidrógeno en un reactor de lecho percolador (tipo “trickle bed”).

El desarrollo de procesos continuos de síntesis directa de peróxido de hidrógeno es clave para la futura implantación de la síntesis directa a escala industrial. Las limitaciones asociadas a la transferencia de materia y la obligatoriedad de mantener la concentración de hidrógeno en la fase gas por debajo del límite inferior de inflamabilidad (4 % mol), reducen el número de opciones posibles en proceso de selección de un reactor continuo. Los reactores tipo “trickle bed” son reactores de tipo lecho fijo, ampliamente utilizados en procesos industriales a gran escala y que permiten operar en sistemas en los que intervienen las tres fases, sólido – líquido – gas. En la configuración más habitual, la fase sólida esta fija (catalizador, 5% Pd/C, y un soporte inerte, SiO_2), distribuida a lo largo de toda la columna, de forma ordenada o no, mientras que la fase líquida (agua) y la fase gas (2.23 % mol hidrógeno – 11 % mol oxígeno – 86.7 % mol dióxido de carbono) circulan en el sentido de la gravedad a través de los huecos que forma la fase sólida. Varios regímenes de flujo son posibles de acuerdo a la velocidad a la que circulan las fases fluidas

a través del reactor. Para garantizar que el sistema trabaja en régimen de goteo (“trickle”), para el cual el líquido gotea a través de los huecos entre las partículas cubriendo completamente su superficie, es necesario que los valores del Reynolds de la fase líquida y la fase gas tengan valores menores a 10^3 [18]. Las características de los reactores de lecho percolador favorecen enormemente la transferencia de materia entre las fases que intervienen en la reacción de síntesis directa.

Existen gran cantidad de artículos y patentes sobre el uso de reactores de tipo “trickle bed” en la síntesis directa de peróxido de hidrógeno. Sin embargo, debido a la complejidad, tanto de la reacción en si como de los procesos que transcurren en el interior del reactor, es aún necesario seguir estudiando la influencia de las condiciones de reacción para conseguir la optimización del proceso.

Aunque conversión, selectividad y productividad son los objetivos principales a maximizar en la optimización de procesos de reacción, este capítulo está centrado en el estudio de la influencia de la condiciones de operación en la selectividad. Para ello se ha fijado una concentración de hidrógeno en la fase gas del 2.3 %mol, mucho menor que el máximo permitido (4 %mol), de esta manera es posible comprender cuando la selectividad puede ser incrementada debido a la optimización del tiempo de residencia o de las condiciones del catalizador. El objetivo es determinar si un bajo valor de ratio H_2/Pd puede ser beneficioso para el rendimiento del reactor.

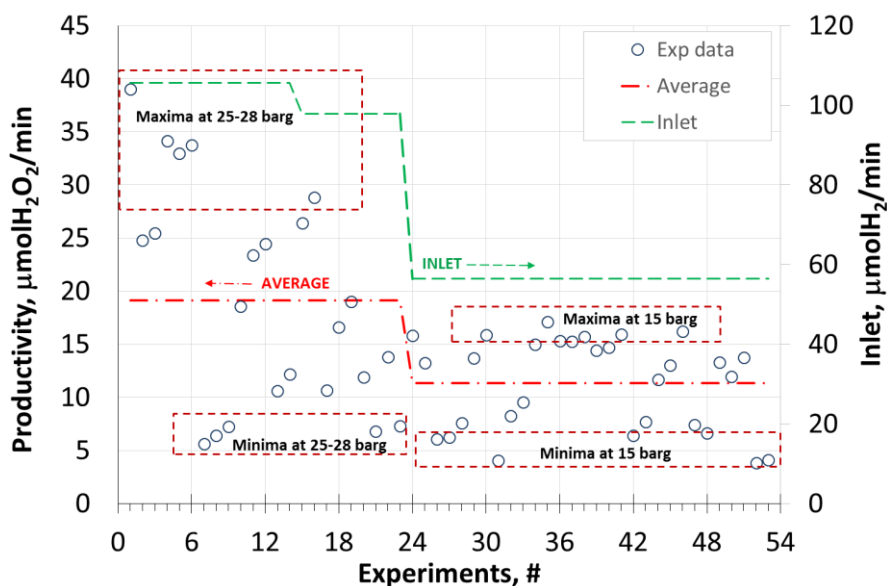


Figura 3. Resumen de los valores de productividad obtenidos durante la optimización de la reacción de síntesis directa de peróxido de hidrógeno en un reactor de tipo “trickle bed”

En la Figura 3 se resumen los valores de productividad de todos los experimentos realizados (0.003 ± 0.001 % wt/v < % H_2O_2 < 0.265 ± 0.019 % wt/v; 5.31 ± 0.29 % < % Yield < 39.97 ± 2.95 %; 3.85 ± 0.02 $\mu\text{mol}\cdot\text{min}^{-1}$ < $F_{H_2O_2}$ < 39.02 ± 0.27 $\mu\text{mol}\cdot\text{min}^{-1}$; 65.05 ± 0.5 $\text{mmol}\cdot\text{h}^{-1}\cdot\text{gPd}^{-1}$ < T.O.F < 782.7 ± 1.6 $\text{mmol}\cdot\text{h}^{-1}\cdot\text{gPd}^{-1}$) en este capítulo. Del estudio de los resultados pueden deducirse las cuatro hipótesis siguientes:

- H-1. Cuanto menor sea la concentración o la presión parcial de hidrógeno en la fase gas, menor será el valor del ratio H_2/Pd .
- H-2. Independientemente del flujo de líquido, la cantidad de hidrógeno disuelto en la fase líquida se mantiene constante, cuando el flujo de líquido es bajo se consigue una concentración local de H_2 mayor y el ratio de H_2/Pd en el centro activo se incrementa.
- H-3. Un aumento de la concentración de catalizador en la zona inicial del reactor es beneficioso para la reacción.
- H-4. Si la cantidad de catalizador permanece constante, un volumen de lecho mayor favorece la disolución del hidrógeno y aumenta el valor del ratio H_2/Pd .

La presión de operación incrementa la productividad del sistema cuando la cantidad de catalizador en el interior del reactor y las condiciones de operación son las adecuadas para que la transferencia de material actúe como etapa limitante. A alta presión (28 – 25) la productividad puede ser entre dos y tres veces mayor que a presión baja (0.265 %wt/v a 0.5 $\text{mL}\cdot\text{min}^{-1}$, 75 mg of cat. y 28 barg; 0.093 %wt/v a 0.5 $\text{mL}\cdot\text{min}^{-1}$, 75 mg of cat. y 15 barg). A baja presión el sistema está limitado por la transferencia de materia, debido a que un aumento en la cantidad de catalizador no incrementa la productividad de la reacción.

Puesto que el catalizador es independiente del soporte inerte, es posible estudiar la influencia de la concentración del catalizador en el interior del reactor y determinar si existe alguna configuración determinada que favorezca la producción de peróxido de hidrógeno. De las cuatro configuraciones analizadas y de acuerdo a los resultados experimentales, una concentración de catalizador mayor (37.5 mg de cat. 5% Pd/C en 13.3 ml de la zona superior del lecho; 25 mg de cat. 5% Pd/C en 13.3 ml de la zona intermedia del lecho y 12.5 mg de cat. 5% Pd/C en 13.3 ml de la zona inferior del lecho) en la zona superior del reactor resulta beneficiosa para la reacción, puesto que se evita que el hidrógeno disuelto en la fase gas y el peróxido de hidrógeno entren en contacto, lo que provocaría la hidrogenación y reduciría el rendimiento y la productividad. Se pueden obtener conclusiones similares cuando en base al valor del ratio Pd/V_b . En cualquier caso para obtener valores altos de T.O.F y de rendimiento es necesario que Pd/V_b sea bajo. Esto

supone que la es necesario un volumen disponible para la transferencia alto, lo que confirmaría la hipótesis H-4.

Capítulo V. *Desarrollo del proceso de síntesis directa de peróxido de hidrógeno en agua un reactor continuo utilizando un catalizador comercial.*

Los reactores de lecho percolador son una de las alternativas más prometedoras para el desarrollo de la síntesis directa de peróxido de hidrógeno a escala industrial. Aunque ya existen varios artículos que analizan el efecto de las principales variables de operación y las características del catalizador es necesario continuar con el estudio para poder determinar de manera más clara la influencia de cada parámetro en la productividad y eficacia del sistema. El desarrollo de una nueva generación de catalizadores más eficientes, sobre los que se haya aplicado todo el conocimiento adquirido hasta ahora es uno de los frentes de investigación claves para conseguir que la síntesis directa de peróxido de hidrógeno sea competitiva frente a los procesos tradicionales. El análisis de los principales parámetros de reacción puede proporcionar información de utilidad para el desarrollo de catalizadores específicos.

Con el objetivo de disponer sin limitaciones de cantidad y garantizar que las propiedades del catalizador son iguales para todos los experimentos, se seleccionó un catalizador comercial. Los parámetros de reacción analizados, flujo de gas y de líquido, flujo molar de hidrógeno, presión, temperatura, cantidad de catalizador y concentración de metal activo en el sólido son considerados como parámetros clave para la eficacia del proceso.

La influencia del flujo de líquido, el flujo de gas y la cantidad de catalizador es analizada simultáneamente puesto que están estrechamente relacionadas. El flujo de líquido debe ser lo suficiente alto para garantizar que todo el lecho en la columna queda completamente y uniformemente humedecido pero no tanto como para el régimen hidrodinámico en el interior del reactor no sea el adecuado. Los resultados muestran que la pérdida de selectividad se debe a la reacción de síntesis de agua al principio del reactor mientras que la hidrogenación y la descomposición únicamente tienen lugar cuando la concentración de peróxido de hidrógeno ha alcanzado un determinado nivel.

Con el flujo de líquido de $4 \text{ ml}\cdot\text{min}^{-1}$ la producción de H_2O_2 aumenta con el flujo molar de hidrógeno, aunque la producción es similar independientemente de la cantidad de catalizador que haya en el lecho (150 – 580 mg). Esto implica que aunque la transferencia de materia es la etapa limitante del proceso (la producción no aumenta al aumentar el número de centros activos), todo el hidrógeno se consume en la zona superior del reactor, antes de que el peróxido

de hidrógeno se haya formado y pueda provocar la hidrogenación. Por el contrario cuando el flujo de líquido es mayor ($6 \text{ ml}\cdot\text{min}^{-1}$), solo cuando la cantidad de catalizador es alta (540 mg) el consumo de hidrógeno es lo suficientemente rápido como para evitar la hidrogenación.

Estos resultados concuerdan con los obtenidos por otros investigadores [13] la eficacia del sistema de reacción depende principalmente del número de centros activos, su distribución a lo largo del reactor y del equilibrio de adsorción entre el H_2 , el O_2 y el peróxido de hidrógeno.

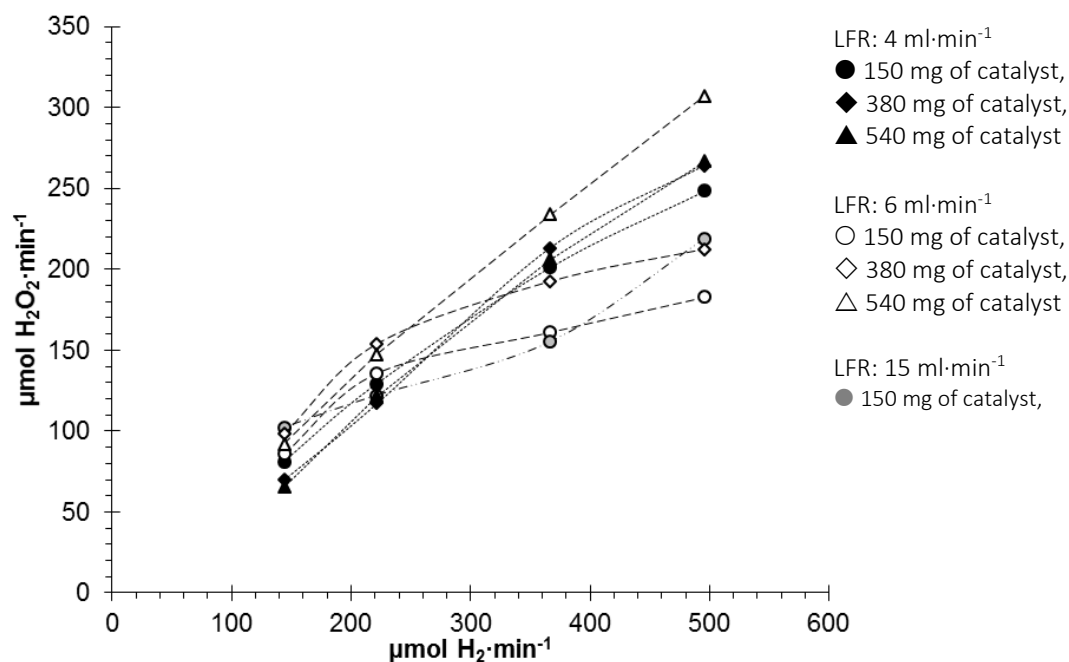


Figura 4. Influencia de flujo de líquido, flujo de gas y cantidad de paladio en la velocidad de producción de peróxido de hidrógeno. 15 barg, 15 °C, 5% Pd/C, $[\text{Br}^-] = 5 \cdot 10^{-4}$.

La presión y temperatura de operación también se incluyeron en el análisis. La influencia de la presión de operación es clara, siempre y cuando el resto de condiciones de reacción sean las correctas un incremento en la presión de operación favorece la solubilidad de los gases en el medio de reacción y reduce las limitaciones por transferencia de materia. Un valor demasiado alto de la presión puede ser perjudicial si la concentración de hidrógeno en la fase líquida es demasiado alta y no se consume con la rapidez necesaria en la zona superior del reactor. El valor mayor de productividad ($307.3 \mu\text{mol H}_2\text{O}_2\cdot\text{min}^{-1}$) del estudio fue obtenido para la mayor presión (26 barg) y de forma equivalente el valor de menor productividad ($93.93 \mu\text{mol H}_2\text{O}_2\cdot\text{min}^{-1}$) se obtuvo para la menor presión (2.8 barg).

La temperatura influye no solo en la cinética de la reacción sino que también en los procesos de adsorción en el catalizador y la solubilidad de los gases en la fase líquida. Debido a esto no es fácil determinar claramente el efecto de la temperatura aunque si es posible dividir el rango

estudiado (5 – 60 °C) en tres zonas diferentes. Para valores de temperatura intermedios (entre 25 y 40 °C) la productividad fue mayor mientras que cuando la temperatura tiene valores bajos (5 y 15 °C) o altos (60 °C) la productividad disminuye debido a que la cinética de reacción es lenta o que hidrogenación y la descomposición se ven favorecidas por temperaturas altas.

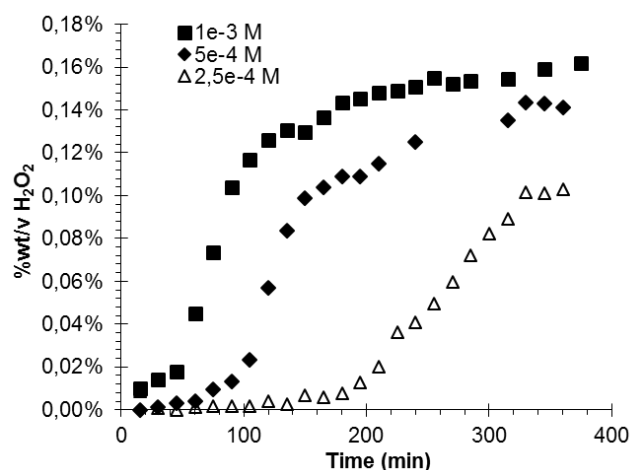


Figura 5. Evolución de la concentración de peróxido de hidrógeno durante la reacción e influencia de la concentración de NaBr

La concentración de promotores en la fase líquida es clave; si la concentración es demasiado alta puede envenenar los centros activos del catalizador. Tres concentraciones diferentes de NaBr han sido estudiadas ($1 \cdot 10^{-3}$ M; $5 \cdot 10^{-4}$ M; $2.5 \cdot 10^{-4}$ M).

La curva de producción de peróxido de hidrógeno frente a tiempo tiene una forma sigmoide con tres zonas diferentes. Cuanto mayor sea la concentración de NaBr mayor será la concentración máxima alcanzada y menor el tiempo de reacción necesario. En análisis de los datos nos permite concluir lo siguiente:

- La cantidad de ion bromuro disponible no afecta tanto a la cantidad de centros activos bloqueados como a la calidad de los mismos. Debido a esto aunque se doble la cantidad de promotor no se puede garantizar que la concentración de peróxido también será la doble.
- El tiempo necesario para que el sistema alcance las condiciones adecuadas para que la producción de peróxido pueda iniciarse depende de la concentración de NaBr de la fase líquida. La concentración de Br⁻ afecta al mecanismo del equilibrio de adsorción – desorción de los reactivos sobre los centros activos y la reconstrucción de los nanoclusters del metal activo.

La distribución del catalizador a lo largo del reactor es determinante en la reacción. Si la concentración de catalizador es demasiado alta en la parte final del reactor puede causar la descomposición del peróxido de hidrógeno generado anteriormente y reducir la selectividad y la productividad del proceso. Manteniendo constante la cantidad total de metal activo se ha estudiado el efecto de la concentración de paladio (5, 10 y 30 % wt/v) en la productividad y el rendimiento del proceso.

Los mejores resultados de productividad ($288.6 \mu\text{molH}_2\text{O}_2 \cdot \text{min}^{-1}$ para $496.0 \mu\text{molH}_2 \cdot \text{min}^{-1}$) y de rendimiento se obtuvieron cuando se utilizó el catalizador más rico en metal activo. Al concentrar el metal activo se consigue un doble efecto; se favorece la aparición de nanoclusters de mayor tamaño y se reduce el porcentaje de hidrogenación del peróxido ya formado puesto que el contacto entre el peróxido de hidrógeno y los centros activos es menos probable.

Por último y puesto que la hidrogenación es la causa de la mayor pérdida del rendimiento de la reacción, se estudió la influencia del flujo molar de hidrógeno y el del tiempo de residencia de la fase líquida en el reactor. La cantidad de H_2O_2 hidrogenado depende directamente del flujo molar de hidrógeno, e inversamente del tiempo de residencia del líquido en el reactor. La tasa de consumo de hidrógeno (directamente relacionado con el porcentaje de hidrogenación) aumenta exponencialmente con el flujo molar de hidrógeno pero linealmente con el tiempo de residencia.

Capítulo VI. *Medida y modelado del coeficiente de transferencia de material líquido – gas y del área interfacial en una columna de burbujeo a baja presión.*

Los reactores de burbujeo numerosas ventajas en comparación con otros reactores multifase (alta transferencia de materia y de calor, ausencia de partes móviles, sencilla operación y bajo coste). Las aplicaciones industriales de los reactores de burbujeo son numerosas y comprenden desde la industria química y petroquímica hasta los procesos biológicos. La importancia de los reactores de burbujeo se ve reflejada en la gran cantidad de estudios publicados relacionados con los procesos de escalado y la investigación de la hidrodinámica del sistema. La influencia de las condiciones de operación (presión, temperatura, densidad de las fases fluidas, velocidad superficial del líquido y el gas), la dimensión de la columna (diámetro, longitud, distribuidor de la fase gas) son las variables típicamente incluidas en los estudios. Sin embargo, la enorme complejidad del proceso y la cantidad de variables que interviene y la dificultad de estudiar todas las fases implicadas de forma simultánea complica la predicción del comportamiento de los reactores de burbujeo.

En este capítulo, se han comparado valores de *hold – up*, diámetro de burbuja y coeficientes de transferencia de materia obtenidos de forma experimental con los obtenidos a partir de correlaciones disponibles en bibliografía. Con el objetivo de utilizar los datos obtenidos en este capítulo para el diseño de un reactor de *slurry bubble column* a alta presión para la síntesis de peróxido de hidrógeno se han propuesto nuevas expresiones para el cálculo del *hold – up* y el diámetro de burbuja. Los valores del coeficiente volumétrico de transferencia de materia se calcularon a partir de la concentración de oxígeno en la fase líquida suponiendo que el sistema se comporta como un tanque perfectamente agitado (PMST). Las correlaciones y modelos [19, 20] con los que se han comparado los valores experimentales han sido seleccionadas de las fuentes bibliográficas habituales teniendo en cuenta que las condiciones para las que fueron obtenidas sean similares a las fijadas en este capítulo.

$$\frac{dC_{O_2}}{dt} = k_L \cdot a \cdot (C^* - C) \quad \text{Ecuación 1. Balance de materia para PMST}$$

La influencia de la altura inicial de líquido ($40 \text{ cm} < h_o < 75 \text{ cm}$), el flujo volumétrico de la fase gas ($200 \text{ mLN} \cdot \text{min}^{-1} < F_{O_2} < 1500 \text{ mLN} \cdot \text{min}^{-1}$ aprox.) y la geometría del difusor (tubo de 1/8" de diámetro externo o difusor poroso) han sido analizadas. Para ninguno de los parámetros estudiados (*hold – up*, diámetro de burbuja, área interfacial y coeficiente de transferencia de materia), la altura inicial de la columna de líquido ha demostrado tener influencia.

La influencia de la velocidad superficial de gas en el valor del *hold – up*, (fracción de volumen de la columna ocupada por la fase gas) depende de tipo de régimen en el que se encuentre la columna y del tamaño de las burbujas [21, 22]. Tal y como era de esperar, la fracción de volumen de la columna ocupada por el gas se incrementó con el flujo de gas, puesto que la cantidad de gas que atraviesa la columna por unidad de tiempo es mayor (de 0.94 % a 1.82 % con un tubo de 1/8" D.E. y de 0.80 % a 1.81 % con el difusor poroso a $200 \text{ mLN} \cdot \text{min}^{-1}$, de 5.20 % a 7.78 % con un tubo de 1/8" D.E. y de 11.83 % a 13.14 % con un difusor poroso a $1500 \text{ mLN} \cdot \text{min}^{-1}$). Las burbujas más pequeñas (obtenidas cuando se utilizó un difusor poroso) también proporcionaron valores de *hold – up* mayores, debido a que el tiempo de residencia de las burbujas pequeñas era mayor, Figura 6.

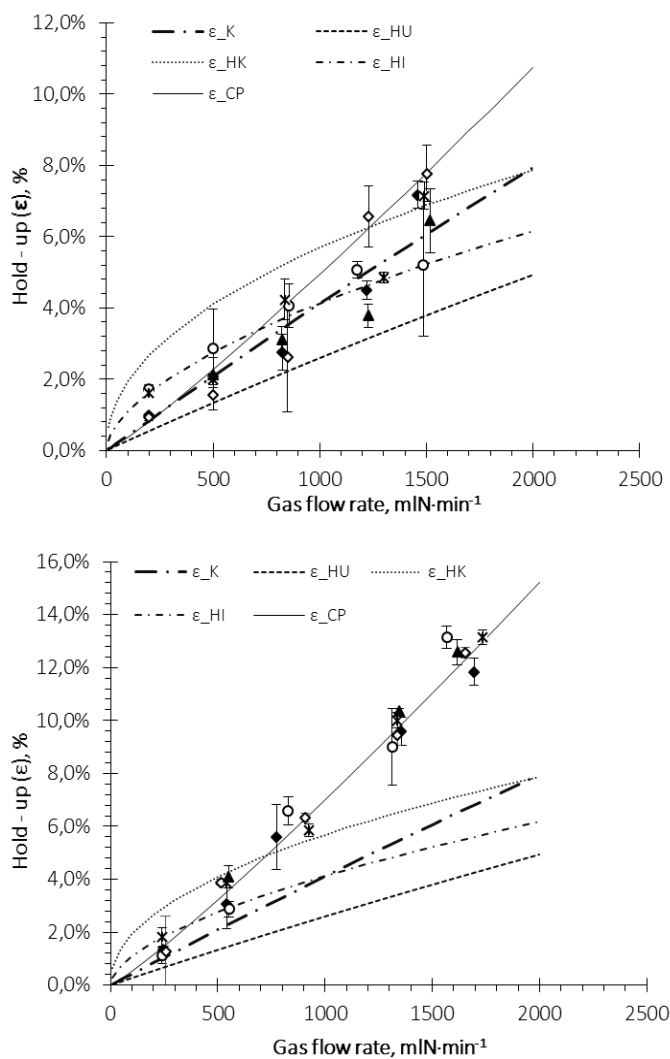


Figura 6. Influencia del flujo de gas y de la altura inicial de líquido en los valores de *hold – up*. Tubo 1/8" D.I. (superior), Difusor poroso (inferior). ◆ $h_0 = 40$ cm; ○ $h_0 = 50$ cm; ◇ $h_0 = 60$ cm; * $h_0 = 70$ cm; ▲ $h_0 = 75$ cm.

Ninguna de las correlaciones seleccionadas de la bibliografía fue capaz de ajustarse a los valores experimentales y por lo tanto una nueva expresión (CP) para el cálculo del *hold – up*, en las condiciones específicas de este capítulo, fue propuesta (Ecuación 2). Con el objetivo de que el cálculo sea lo más sencillo y directo posible, esta nueva expresión se basó en el número de Reynolds, en las propiedades de las fases fluidas y la geometría de la columna. El valor de los factores independientes se obtuvo mediante el ajuste de los valores experimentales (1/8" D.I. tubo: $f_c = 4.03 \cdot 10^{-2}$; difusor poroso: $f_c = 3.41 \cdot 10^{-2}$; todos los exp.: $f_c = 4.82 \cdot 10^{-2}$).

$$\varepsilon = f_{\varepsilon} \cdot d_0 \cdot \text{Re}^{0.7} \left(\frac{u_g}{d_0^5 \cdot g} \right)^{0.21} \quad \text{Ecuación 2. Correlación propuesta para el cálculo de } \textit{hold - up}$$

Respecto a la influencia del flujo de gas en el diámetro de las burbujas, pese a que diferentes autores han obtenido diferentes resultados, en líneas generales, puede concluirse que el diámetro de las burbujas tiende a aumentar con el flujo de gas hasta alcanzar un valor máximo constante [23, 24]. Como ocurre con el *hold-up*, ninguna de las correlaciones seleccionadas de la bibliografía fue capaz de predecir con suficiente precisión el valor del diámetro de burbuja, especialmente cuando el flujo de gas era alto (tubo 1/8" D.E.: 0.71 cm a 1.23 cm; difusor poroso: 0.27 cm a 0.46 cm). Del mismo modo una nueva correlación fue propuesta Ecuación 3, y los valores de los coeficientes individuales fueron calculados a partir de los valores de diámetro de burbuja experimentales (tubo 1/8" D.E.: $f_{db1} = 0,482$ y $f_{db2} = 0,0704$; difusor poroso: $f_{db1} = 0,076$ y $f_{db2} = 0,1683$).

$$d_b = f_{db_1} \cdot \text{Re}_0^{f_{db_2}} \quad \text{Ecuación 3. Correlación propuesta para el cálculo del diámetro de burbuja}$$

El cálculo individual del coeficiente de transferencia de materia (k_L) y del área interfacial (a) puede proporcionar información extra que ayude a determinar el mecanismo del proceso y que parámetro actúa como limitante. El valor del coeficiente volumétrico de transferencia de materia ($k_L \cdot a$) se obtuvo a partir de los valores de concentración de oxígeno en la fase líquida y el modelado del sistema asumiendo que se comporta como un reactor de tanque perfectamente agitado. El valor del área interfacial se calculó a partir de la fracción de volumen de columna ocupado por el gas y el diámetro de las burbujas. En los resultados obtenidos se puede observar que el coeficiente volumétrico de transferencia de materia ($k_L \cdot a$) aumenta con el flujo de gas debido principalmente a que el área interfacial aumenta con el flujo de oxígeno, mientras que el coeficiente de transferencia de manera individual no mostró ninguna dependencia clara (Figura 7).

En análisis y modelado mediante la dinámica computacional de fluidos (CFD) es una alternativa valiosa para la predicción del comportamiento de sistemas como las columnas de burbujeo, en las que intervienen un gran número de variables y parámetros. El modelado con CFD generó valores del diámetro de burbuja mucho menores que los obtenidos experimentalmente y en consecuencia un valor del área interfacial ligeramente mayor. El modelo generado con la ecuación de Lamont y Scott [25], también, proporcionó valores del coeficiente de transferencia de materia mucho menores que los experimentales. Lamont y Scott no limitan el valor del parámetro independiente de la ecuación, sino que proponen un valor en función de la turbulencia del sistema. Con un valor del coeficiente independiente alto (2.5 frente al 1.13

propuesto inicialmente) es posible conseguir valores del coeficiente de transferencia de materia similares a o los obtenidos experimentalmente.

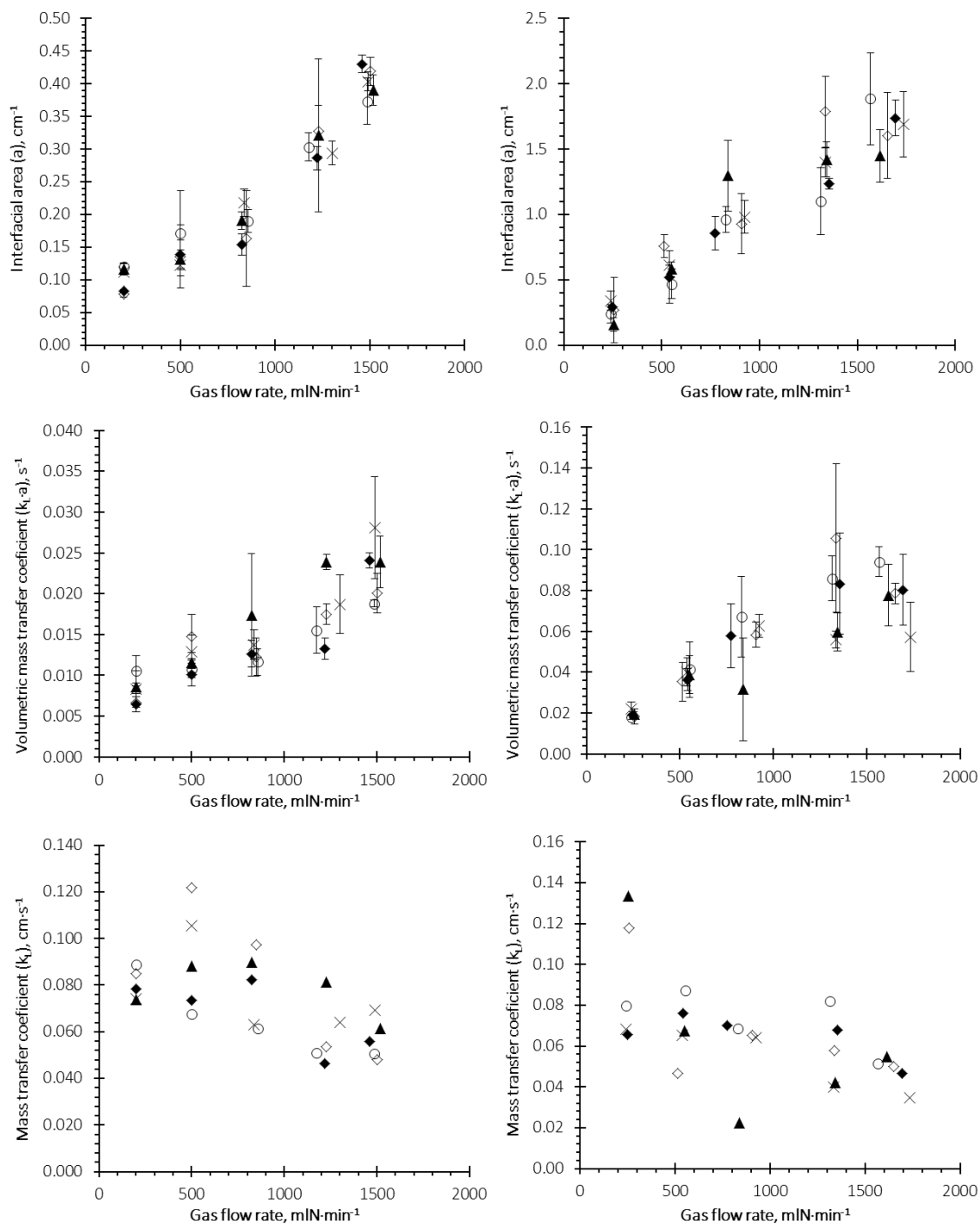


Figura 7. Influencia del flujo de gas y el nivel inicial de líquido en el área interfacial, coeficiente volumétrico de transferencia de material ($k_L \cdot a$) y el coeficiente de transferencia de material (k_L). 1/8" D.E. tubo (izquierda), difusor poroso (derecha). \blacklozenge $h_0 = 40$ cm; \circ $h_0 = 50$ cm; \diamond $h_0 = 60$ cm; $*$ $h_0 = 70$ cm; \blacktriangle $h_0 = 75$ cm.

4. Conclusiones

En este trabajo se ha estudiado la influencia de las principales condiciones de operación en la síntesis de peróxido de hidrógeno en un reactor continuo de tipo percolador. Además se ha realizado una primera aproximación para la sustitución del dióxido de carbono por nitrógeno como compuesto inerte en la fase gas. El análisis de las reacciones de hidrogenación y descomposición ha sido también objeto de estudio en este trabajo.

A continuación se resumen los experimentos con mejores resultados obtenidos en los capítulos III, IV y V. A todas luces las condiciones de operación del capítulo IV son las menos favorables para la producción de peróxido de hidrógeno puesto que tanto la productividad como el rendimiento y el T.O.F obtenidos son los más bajos. Esto se debe a la combinación de bajas presiones de operación, bajos flujos molares de H_2 ($97.8 - 105.6 \mu\text{mol } H_2 \cdot \text{min}^{-1}$) y pequeñas cantidades de catalizador. Estos resultados no son inesperados puesto que en el diseño de los experimentos se decidió sacrificar la productividad en beneficio de un análisis del rendimiento más sencillo.

A pesar de utilizar nitrógeno como inerte, los valores de T.O.F y productividad obtenidos en el capítulo III son los más altos debido a la presión de operación (80 bar) y el alto flujo molar de hidrógeno ($3750 \mu\text{mol } H_2 \cdot \text{min}^{-1}$). Los valores de productividad del capítulo V son similares a los obtenidos en capítulo III, aunque ligeramente menores, lo que indica que con una correcta selección de las variables de operación los reactores continuos de tipo percolador pueden ser tan eficientes como los reactores semicontinuos, incluso trabajando en condiciones mucho menos favorables.

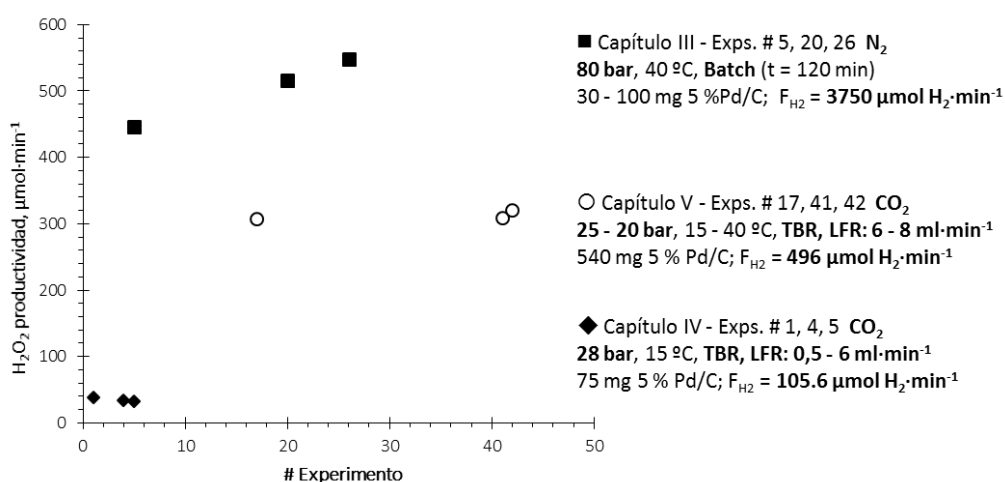


Figura 8. Valores máximos de productividad obtenidos para los capítulos III, IV y V

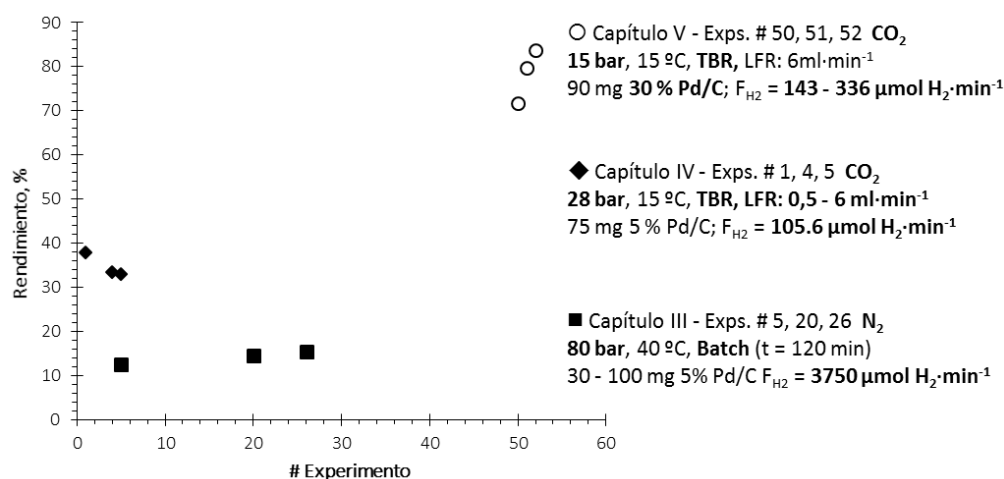


Figura 9. Valores máximos de rendimiento obtenidos para los capítulos III, IV y V

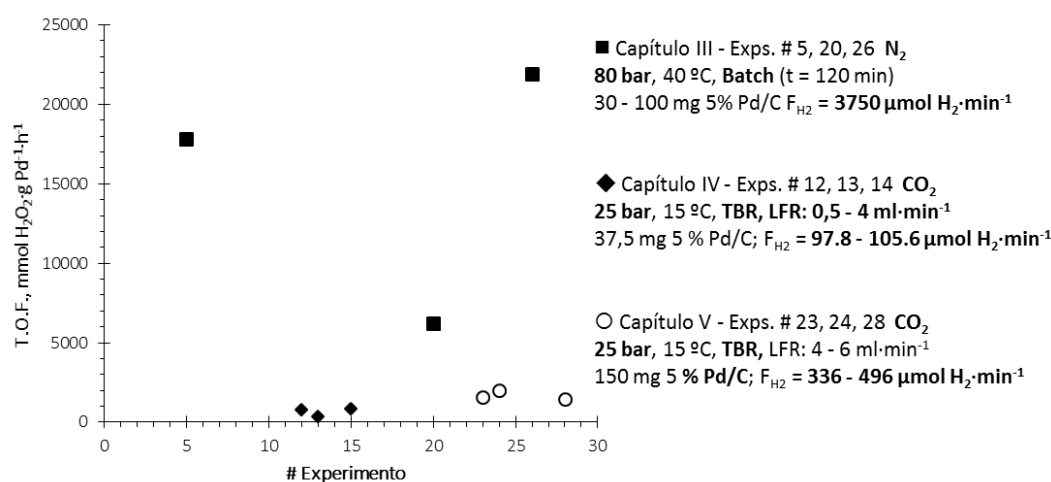


Figura 10. Valores máximos de T.O.F. obtenidos para los capítulos III, IV y V

En función de los resultados obtenidos en los capítulos de esta tesis las conclusiones más relevantes son las siguientes:

Capítulo II. *Estudio cinético de las reacciones de hidrogenación y descomposición del peróxido de hidrógeno sobre catalizador de Pd/C en medio acuoso de reacción y alta presión de dióxido de carbono.*

- El estudio de las reacciones de descomposición e hidrogenación es clave puesto que puede revelar importante información para la optimización de las variables de reacción.

- La hidrogenación es mayor a bajas concentraciones de peróxido de hidrógeno mientras que la descomposición aumentó con la concentración. El orden de reacción, calculado a partir de los datos experimentales, fue $-0,16$ y $1,03$ para la reacción de hidrogenación y descomposición respectivamente.
- La selección del valor óptimo de la concentración de ácido y del ratio Br/Pd puede reducir el efecto de las reacciones secundarias. Un valor de pH cercano a 2 fue suficiente para proteger el peróxido de hidrógeno generado. Respecto al ratio Br/Pd, el efecto de la hidrogenación fue minimizado para un valor comprendido entre 3 y 5 y la descomposición para un valor de 8.
- Se observó una influencia de la cantidad de catalizador en el valor de orden de reacción para el número de centros activos. En el caso de la descomposición, el orden de reacción depende de la cantidad de sólido y de la etapa de proceso que actúe como controlante; $0,812 - 0,981$ para cantidades bajas (control por la cinética) y $1,44$ para cantidades mayores (control debido a la transferencia de materia). Por el contrario para la reacción de hidrogenación el orden de reacción para el número de centros activos aumenta con la cantidad de catalizador ($0,710 - 1,078$) presente en el sistema independientemente de cual sea la etapa controlante del proceso.
- Los valores de energía de activación han sido calculados para ambas reacciones ($E_{a_d} = 18803,6 \text{ J}\cdot\text{mol}^{-1}$ (descomposición) y $E_{a_h} = 7746,2 \text{ J}\cdot\text{mol}^{-1}$ (hidrogenación)).

Capítulo III. *Síntesis directa de peróxido de hidrógeno en agua utilizando nitrógeno como inerte en un reactor semicontinuo.*

- El uso de nitrógeno como inerte es una alternativa válida y viable para la síntesis directa de peróxido de hidrógeno. Los valores máximo de concentración, selectividad y conversión obtenidos en este capítulo fueron respectivamente: $1,13 \text{ \% wt/v}$, 35 \% y 70 \% .
- La productividad ($1,58 \text{ \% wt/v}$ vs. $0,647 \text{ \% wt/v}$) y selectividad (88 \% vs. 48 \%) utilizando nitrógeno son menores que las conseguidas en condiciones similares utilizando dióxido de carbono como inerte, puesto que el nitrógeno no posee las propiedades co-solventes y acidificantes del CO_2 .

- El proceso de transferencia de materia actúa como etapa limitante del proceso para cantidades muy bajas de catalizador (menores de 30 mg 5 % Pd/C) si se compara con un sistema similar utilizando dióxido de carbono. Cantidades de catalizador mayores a 30 mg – 5 %Pd/C redujeron la productividad puesto que incrementan la descomposición. Del mismo modo, con cantidades menores no se pudo garantizar el consumo de hidrógeno con la rapidez suficiente como para evitar la hidrogenación del peróxido ya formado.
- Tanto la conversión (13,2 – 30,2 %), la selectividad (15,8 – 47,8 %) y el T.O.F. (0,897 – 6,193 mol H₂O₂·g Pd⁻¹·h⁻¹) aumentaron al incrementarse la presión del sistema (20 – 90 barg). La influencia de la presión parcial de hidrógeno también ha sido incluida en este capítulo. La conversión y la productividad aumentan con la presión parcial del hidrógeno independientemente de que el incremento se deba a un aumento de la presión total o de la fracción molar de hidrógeno. La selectividad permanece constante (30 – 35 %) siempre y cuando la presión global no varíe, independientemente de valor de la fracción molar de hidrógeno (1 – 4 %). La razón parece estar relacionada con el ratio O₂/H₂ y como la presencia en mayor o menor medida del oxígeno puede alterar los mecanismos de adsorción – desorción y modificar el estado de oxidación del metal activo del catalizador.
- Se calculó el valor del factor pre – exponencial (272,15 mmol·min⁻¹, 520,54 mmol·min⁻¹ y 766,51 mmol·min⁻¹ para los catalizadores con composición 1 % Pd/C, 3 % Pd/C y 5 % respectivamente) y de la energía de activación (2306,7 K, 2348,4 K y 2588,2 K para los catalizadores con composición 1 % Pd/C, 3 % Pd/C y 5 % respectivamente) a partir de la velocidad de reacción observada. De los datos experimentales se pudo apreciar que existe una dependencia lineal entre el factor pre – exponencial y el porcentaje de paladio presente en el sólido. No existe relación entre el factor pre – exponencial y el número de centros activos, lo que implica que el método de preparación o la agregación de las partículas debe ser la razón de este comportamiento.

Capítulo IV. *Estudio de la influencia de un bajo valor de ratio hidrógeno – paladio en la reacción en medio acuoso para la síntesis directa de peróxido de hidrógeno en un reactor de lecho percolador (tipo “trickle bed”).*

- La producción de peróxido de hidrógeno por síntesis directa en un reactor continuo de tipo percolador es posible. Sin embargo, la optimización y análisis de la influencia de las condiciones de operación es clave para asegurar la viabilidad del proceso.
- Bajas concentraciones de hidrógeno (2,23 % mol) en la fase gas permiten obtener valores de productividad y rendimiento muy bajos (valores máximos: $39,02 \mu\text{mol H}_2\text{O}_2 \cdot \text{min}^{-1}$; 37,9 % rendimiento). La relación entre los moles de hidrógeno y la cantidad de paladio en el lecho (H_2/Pd) es un parámetro clave para la optimización de la productividad y el rendimiento.
- La concentración de peróxido de hidrógeno aumentó con la presión del sistema debido a que a altas presiones (28 – 25 barg) la cantidad de hidrógeno disuelto en la fase líquida es mayor. A baja presión (15 barg) el sistema está limitado por la transferencia de materia, ya que la productividad no aumenta al incrementar la cantidad de catalizador ($15,86 \mu\text{mol H}_2\text{O}_2 \cdot \text{min}^{-1}$ con $1 \text{ ml} \cdot \text{min}^{-1}$ y 75 mg of 5 % Pd/C en un lecho de reacción de 40 ml vs. $14,71 \mu\text{mol H}_2\text{O}_2 \cdot \text{min}^{-1}$ con $1 \text{ ml} \cdot \text{min}^{-1}$ y 37,5 mg of 5 % Pd/C en un lecho de reacción de 40 ml).
- La productividad también se vio aumentada al trabajar con bajos niveles de flujo de líquido, debido a que la concentración de hidrógeno disuelto en la fase líquida es mayor. Sin embargo, flujos de líquido extremadamente bajos pueden causar que el goteo de la fase líquida a través del reactor no sea homogéneo lo que reduciría la eficiencia del proceso.
- La distribución del catalizador dentro del lecho de reacción influyó también en la eficiencia del proceso. Mediante una distribución no – homogénea del catalizador (mayor concentración en la parte superior del reactor) fue posible aumentar la productividad y el rendimiento puesto que se reduce el contacto entre el peróxido de hidrógeno, los centros activos del sólido y el hidrógeno.
- Para un valor constante de la cantidad de catalizador, un volumen de lecho de reacción mayor ayudó a la disolución del hidrógeno y en consecuencia la productividad del proceso aumentó notablemente. En términos generales un valor del ratio Pd/V_b menor que $0,094 \text{ mg} \cdot \text{cm}^{-3}$ es el valor recomendado.

Capítulo V. *Desarrollo del proceso de síntesis directa de peróxido de hidrógeno en agua un reactor continuo utilizando un catalizador comercial.*

- La síntesis directa de peróxido de hidrógeno en sistemas continuos es un proceso complejo. A pesar de la gran cantidad de esfuerzos que se han realizado aún se desconocen los detalles del proceso de reacción y como afectan las variables de reacción a la actividad del catalizador.
- La reacción de hidrogenación es la responsable de los bajos valores de productividad y rendimiento obtenidos. La tasa hidrogenación aumentó rápidamente con el flujo molar de hidrógeno alimentado en el reactor (9,2 % de hidrogenación con $74,2 \mu\text{mol H}_2 \cdot \text{min}^{-1}$ and 56,3% of hidrogenación con $219,03 \mu\text{mol H}_2 \cdot \text{min}^{-1}$ para un flujo de líquida de $6 \text{ ml} \cdot \text{min}^{-1}$) y, en menor medida, con el flujo de líquido. Para mayores tiempos de residencia (HRT) la tasa se hidrogenación fue mayor, debido al incremento en el tiempo de contacto entre el peróxido de hidrógeno, el catalizador y el hidrógeno (de 12,4 % hidrogenación para HRT = 5,5 min a 28,6% de hidrogenación para HRT = 44 min y $74,2 \mu\text{mol} \cdot \text{min}^{-1}$).
- El efecto de las reacciones secundarias puede reducirse mediante una adecuada selección de las condiciones de operación y más concretamente de la relación entre el flujo de líquido, el flujo de gas y la cantidad de catalizador. La selección de estas tres variables de reacción debe realizarse de manera que se asegure que el hidrógeno se disuelve en la fase líquida y se consume rápidamente para evitar el contacto entre el gas y el peróxido de hidrógeno formado previamente.
- Valores altos de presión no garantizan altas productividades y rendimientos. No se ha podido determinar con precisión el efecto de la temperatura; valores altos ($60 \text{ }^\circ\text{C}$) favorecen a las reacciones secundarias, del mismo modo que valores demasiado bajos ($15 - 20 \text{ }^\circ\text{C}$) reducen las velocidades de reacción y limitan el proceso.
- La concentración de bromuro en la fase líquida influye en la concentración de peróxido de hidrogeno que el sistema es capaz de alcanzar y el tiempo necesario para su estabilización. Los resultados sugieren que el ion bromuro actúa sobre los centros activos de catalizador bloqueando aquellos que toman parte en la síntesis tanto del peróxido de hidrogeno como del agua, pero que también afectan a la cantidad y la calidad de los sitios que permanecen libres. La reconstrucción de los centros activos y los fenómenos

de adsorción y desorción están influenciados por la concentración de ion bromuro en la fase líquida.

- La concentración y distribución de los centros activos a lo largo del volumen de reacción es clave en la síntesis de peróxido de hidrógeno en un reactor de tipo percolador. Los resultados muestran que un catalizador rico en metal activo (30 % Pd/C) aumenta la productividad y el rendimiento puesto que reduce la probabilidad de hidrogenar el H_2O_2 ya formado. Además, los altos porcentajes de paladio permiten la formación de nanopartículas más grandes que favorecen la reacción de síntesis de H_2O_2 .

Capítulo VI. *Medida y modelado del coeficiente de transferencia de material líquido – gas y del área interfacial en una columna de burbujeo a baja presión.*

- Ninguna de las correlaciones seleccionadas para este capítulo fue capaz de predecir los resultados experimentales, a pesar de que se seleccionaron procurando que las condiciones a las que habían sido obtenidas y las condiciones experimentales fueran similares. Debido a esto, se ha propuesto nuevas expresiones para el cálculo del *hold – up* y el diámetro de burbuja.
- La altura inicial de la columna de líquido no tiene influencia sobre ninguna de las variables analizadas (*hold – up*, diámetro de burbuja o coeficiente de transferencia de materia).
- La fracción de la columna ocupada por la fase gas (*hold – up*) aumenta linealmente con el flujo de gas. El incremento es especialmente pronunciado cuando se utiliza un difusor poroso puesto que el diámetro de las burbujas y su velocidad de ascenso es menor (de 0,94 % a 7,78 % con un difusor formado por un tubo con 1/8" de diámetro externo y de 1,13 % a 13,14 % con un difusor poroso).
- El diámetro de las burbujas depende de la geometría del difusor utilizado y se obtienen valores menores cuando se utiliza un difusor poroso puesto que el diámetro del orificio es menor. El diámetro de la burbuja aumenta inicialmente con el flujo de gas hasta alcanzar un valor máximo constante (tubo 1/8" D.E.: 0,71 – 1,23 cm; difusor poroso: 0,27 – 0,46 cm).

- No se ha apreciado una relación clara entre el flujo de gas y el coeficiente de transferencia de materia (k_L : de $4,63 \cdot 10^{-2}$ a $1,22 \cdot 10^{-1} \text{ cm} \cdot \text{s}^{-1}$ para el tubo de 1/8" D.E. y de $2,52 \cdot 10^{-2}$ a $1,34 \cdot 10^{-1} \text{ cm} \cdot \text{s}^{-1}$ para el difusor poroso) aunque sí que existe entre el flujo de gas y el coeficiente volumétrico de transferencia de materia ($k_L \cdot a$: de $6,48 \cdot 10^{-3}$ a $2,81 \cdot 10^{-2} \text{ s}^{-1}$ para el tubo de 1/8" D.E. y de $1,81 \cdot 10^{-2}$ a $1,06 \cdot 10^{-1} \text{ s}^{-1}$ para el difusor poroso) y el área interfacial (a : de 0,08 a 0,43 cm^{-1} para el tubo de 1/8" D.E. y de 0,16 a 1,89 cm^{-1} para el difusor poroso).
- El modelado mediante dinámica computacional de fluidos puede resultar una alternativa válida para la predicción de la hidrodinámica en columnas de burbujeo.

Referencias

1. Centi, G. and S. Perathoner, *One-step H₂O₂ and phenol syntheses: Examples of challenges for new sustainable selective oxidation processes*. *Catalysis Today*, 2009. **143**(1-2): p. 145-150.
2. Zabetakis, M.G., *Flammability Characteristics of Gases and Vapors*. Bureau of Mines, 1965. **627**.
3. Sierra-Pallares, J., et al. *Flammability limits estimation in high pressure systems. application to supercritical reactors*. in *GPE-EPIC, 2nd International Congress on Green Process Engineering and 2nd European Process Intensification Conference*. 2009. Venice (Italy).
4. Han, Y.F. and J.H. Lunsford, *Direct formation of H₂O₂ from H₂ and O₂ over a Pd/SiO₂ catalyst: The roles of the acid and the liquid phase*. *Journal of Catalysis*, 2005. **230**(2): p. 313-316.
5. Liu, Q., et al., *Direct synthesis of H₂O₂ from H₂ and O₂ over Pd–Pt/SiO₂ bimetallic catalysts in a H₂SO₄/ethanol system*. *Applied Catalysis A: General*, 2008. **339**(2): p. 130-136.
6. Abate, S., et al., *SBA-15 as a support for palladium in the direct synthesis of H₂O₂ from H₂ and O₂*. *Catalysis Today*, 2011. **169**(1): p. 167-174.
7. Dissanayake, D.P. and J.H. Lunsford, *Evidence for the Role of Colloidal Palladium in the Catalytic Formation of H₂O₂ from H₂ and O₂*. *Journal of Catalysis*, 2002. **206**(2): p. 173-176.
8. Olivera, P.P., E.M. Patrito, and H. Sellers, *Hydrogen peroxide synthesis over metallic catalysts*. *Surface Science*, 1994. **313**(1-2): p. 25-40.
9. Edwards, J.K., et al., *Comparison of supports for the direct synthesis of hydrogen peroxide from H₂ and O₂ using Au–Pd catalysts*. *Catalysis Today*, 2007. **122**(3-4): p. 397-402.
10. Choudhary, V.R., C. Samanta, and P. Jana, *Hydrogenation of hydrogen peroxide over palladium/carbon in aqueous acidic medium containing different halide anions under static/flowing hydrogen*. *Industrial and Engineering Chemistry Research*, 2007. **46**(10): p. 3237-3242.
11. Blanco-Brieva, G., et al., *Direct synthesis of hydrogen peroxide on palladium catalyst supported on sulfonic acid-functionalized silica*. *Green Chemistry*, 2010. **12**(7): p. 1163-1166.

12. Choudhary, V.R., C. Samanta, and T.V. Choudhary, *Influence of nature/concentration of halide promoters and oxidation state on the direct oxidation of H₂ to H₂O₂ over Pd/ZrO₂ catalysts in aqueous acidic medium*. Catalysis Communications, 2007. **8**(9): p. 1310-1316.
13. Biasi, P., et al., *Direct synthesis of hydrogen peroxide in water in a continuous trickle bed reactor optimized to maximize productivity*. Green Chemistry, 2013. **15**(9): p. 2502-2513.
14. Biasi, P., et al., *Hydrogen Peroxide Direct Synthesis: Selectivity Enhancement in a Trickle Bed Reactor*. Industrial & Engineering Chemistry Research, 2010. **49**(21): p. 10627-10632.
15. Biasi, P., et al., *Continuous H₂O₂ direct synthesis over PdAu catalysts*. Chemical Engineering Journal, 2011. **176–177**(0): p. 172-177.
16. Campos-Martin, J.M., G. Blanco-Brieva, and J.L. Fierro, *Hydrogen peroxide synthesis: an outlook beyond the anthraquinone process*. Angew Chem Int Ed Engl, 2006. **45**(42): p. 6962-84.
17. Moreno Rueda, T., J. García Serna, and M.J. Cocero Alonso, *Direct production of H₂O₂ from H₂ and O₂ in a biphasic H₂O/scCO₂ system over a Pd/C catalyst: Optimization of reaction conditions*. The Journal of Supercritical Fluids, 2012. **61**(0): p. 119-125.
18. Ranade, V.V., R. Chaudhar, and P.R. Gunjal, *Trickle Bed Reactors: Reactor Engineering & Applications*. 2011, Oxford: Elsevier.
19. Kantarci, N., F. Borak, and K.O. Ulgen, *Bubble column reactors*. Process Biochemistry, 2005. **40**(7): p. 2263-2283.
20. Behkish, A., et al., *Gas holdup and bubble size behavior in a large-scale slurry bubble column reactor operating with an organic liquid under elevated pressures and temperatures*. Chemical Engineering Journal, 2007. **128**(2-3): p. 69-84.
21. Shah, Y.T., et al., *Design parameters estimations for bubble column reactors*. AIChE Journal, 1982. **28**(3): p. 353-379.
22. Kara, S., et al., *Hydrodynamics and axial mixing in a three-phase bubble column*. Industrial & Engineering Chemistry Process Design and Development, 1982. **21**(4): p. 584-594.
23. Akita, K. and F. Yoshida, *Gas Holdup and Volumetric Mass Transfer Coefficient in Bubble Columns*. Effect of Liquid Properties, Ind. Eng. Chem. Process. Des. Dev., 1974. **12**: p. 76.
24. Fukuma, M., K. Muroyama, and A. Yasunishi, *Properties of bubble swarm in a slurry bubble column*. Journal of Chemical Engineering of Japan, 1987. **20**(1): p. 28-33.
25. Lamont, J.C. and D.S. Scott, *An eddy cell model of mass transfer into the surface of a turbulent liquid*. AIChE Journal, 1970. **16**(4): p. 513-519.

Lista de Figuras

Figura 1. Valores de orden de reacción para la concentración de centros activos en descomposición versus la cantidad de paladio.....	10
Figura 2. Comparación de los experimentos de síntesis directa realizados utilizando N ₂ o CO ₂ como inerte.	13
Figura 3. Resumen de los valores de productividad obtenidos durante la optimización de la reacción de síntesis directa de peróxido de hidrógeno en un reactor de tipo “trickle bed”	14
Figura 4. Influencia de flujo de líquido, flujo de gas y cantidad de paladio en la velocidad de producción de peróxido de hidrógeno. 15 barg, 15 °C, 5% Pd/C, [Br ⁻] = 5·10 ⁻⁴	17
Figura 5. Evolución de la concentración de peróxido de hidrógeno durante la reacción e influencia de la concentración de NaBr	18
Figura 6. Influencia del flujo de gas y de la altura inicial de líquido en los valores de <i>hold-up</i> . Tubo 1/8” D.I. (superior), Difusor poroso (inferior). ◆ h ₀ = 40 cm; ○ h ₀ = 50 cm; ◇ h ₀ = 60 cm; ✱ h ₀ = 70 cm; ▲ h ₀ = 75 cm.	21
Figura 7. Influencia del flujo de gas y el nivel inicial de líquido en el área interfacial, coeficiente volumétrico de transferencia de material (k _L ·a) y el coeficiente de transferencia de material (k _L). 1/8” D.E. tubo (izquierda), difusor poroso (derecha). ◆ h ₀ = 40 cm; ○ h ₀ = 50 cm; ◇ h ₀ = 60 cm; ✱ h ₀ = 70 cm; ▲ h ₀ = 75 cm.	23
Figura 8. Valores máximos de productividad obtenidos para los capítulos III, IV y V	24
Figura 9. Valores máximos de rendimiento obtenidos para los capítulos III, IV y V	25
Figura 10. Valores máximos de T.O.F. obtenidos para los capítulos III, IV y V	25

SUMMARY

Direct synthesis of H₂O₂.

Study of the influence of N₂ as reaction inert
and optimization of the reactor configuration

Since the development of the green chemistry the need of a substitute for the traditional organic and chloride oxidants and leaching reagents have increased. One of the most promising alternatives it is the hydrogen peroxide, because its high oxidation potential and its low toxicity and high degradability. Although the traditional routes for H₂O₂ synthesis are the widely used in bulk chemical industry, some alternative routes have been investigated. For all the alternatives, the direct synthesis of hydrogen peroxide from O₂ and H₂ it is the most promising one.

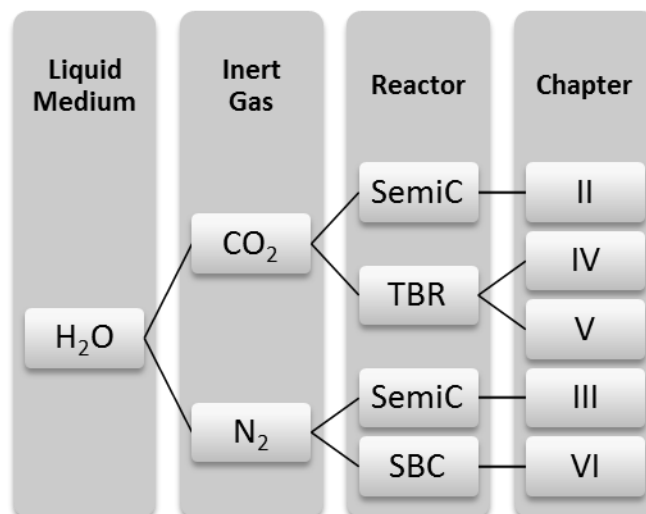


Figure 1. Summarized structure of the chapters that composed this research

Chapter I. The direct synthesis of hydrogen peroxide is a catalytic three phases reaction, what usually supposed that the system is limited by the mass transfer process between the gas, liquid and solid phases. Hydrogen peroxide synthesis is not the only reaction that takes place; there undesired reactions (water synthesis, hydrogen peroxide decomposition and hydrogenation) are also catalyzed by the solid. Most of the investigations paper and patents available in the open literature sources are related with determination of the influence of the catalyst support and the active metal. The adequate selection of the catalyst characteristics could reduce secondary reactions rate and consequently increase the process selectivity. Also the addition of promoters, acids and halides typically, has been studied as a key parameter. Halides and acids are adsorbed over the high activity sites of the catalyst and reduce the hydrogenation reaction rate. In a lower proportion effect of main reaction parameters (temperature and pressure) have been analyzed.

In despite of the great advantages that direct synthesis has in comparison with the traditional production routes, direct synthesis is not yet an available alternative to industrial production because the process is still need for a further investigation in order to achieve higher productions

rates. Slurry bubble column and trickle bed reactors are, because its characteristics, the most optima alternative for the production of hydrogen peroxide at industrial scale. Only a few of papers about continuous direct synthesis of hydrogen peroxide have been published but the results are promising and inspiring.

Chapter II. The main limitations of the direct synthesis reaction are the undesired reactions. Synthesis of water ($\text{H}_2 + \frac{1}{2} \text{O}_2 \rightarrow \text{H}_2\text{O}$), the decomposition ($\text{H}_2\text{O}_2 \rightarrow \text{H}_2\text{O} + \frac{1}{2} \text{O}_2$) and hydrogenation ($\text{H}_2\text{O}_2 + \text{H}_2 \rightarrow 2 \text{H}_2\text{O}$) of the hydrogen peroxide already formed occur simultaneously to the main reaction. The four reactions are catalyzed and influenced by the reaction conditions in the same way since it is almost impossible to minimize the rate of undesired reaction without harm the reaction of synthesis of hydrogen peroxide. Optimization of direct synthesis should not be only focus on the selection of the reaction conditions but also in the study in secondary reactions. A deep knowledge of secondary reactions and its dependence with the system parameter is need.

Influences of the conditions of operation, the concentration of the promoters, the amount of catalyst and the active metal concentration have been analyzed. A kinetic model has been proposed on base on the experimental results. All the experiments have been a carried out at 80 bar in a 0.350 L AISI 316 SS semi – continuous stirred reactor. A commercial Pd catalyst supported over active carbon (1, 3 and 5 %Pd/C) has been used. To separate the effect of the decomposition and hydrogenation, hydrogen was feed only in the second part of the experiment. The specific rate of reaction for both decomposition and hydrogenation were defined as follow, the values of each parameter were obtained by fitting and analysis of the experimental results.

$$r_d = k_d \cdot (C_{\text{H}_2\text{O}_2})^{\alpha_d} \cdot (n_{\text{Pd}})^{\beta_d} \qquad r_h = k_h \cdot (C_{\text{H}_2\text{O}_2})^{\alpha_h} \cdot C_{\text{H}_2}^* \cdot (n_{\text{Pd}})^{\beta_h}$$
$$k_d = k_{0d} \cdot \exp\left(\frac{-E_{a_d}}{R \cdot T}\right) \qquad k_h = k_{0h} \cdot \exp\left(\frac{-E_{a_h}}{R \cdot T}\right)$$

The values of reaction order for decomposition and hydrogenation were obtained by the fitting of the experiments for what the initial hydrogen concentration was studied (1, 3, 5 and 10 % wt/v). The results, $\alpha_d = 1.031$ (%SE_d = 3.56%, %ADD_d = 1.17%) and $\alpha_h = -0.161$ (%SE_h = 33.5%, %ADD_h = 9.78%), are similar to the values proposed in the bibliography looked up ($\alpha_d = 1$ and $\alpha_h = 0$). From the experimental results it was also concluded that hydrogenation is nearly 3 to 20 fold times higher than decomposition. This effect is greater a low hydrogen peroxide

concentration (after 30 min at 5 % wt/v of H_2O_2 decomposition is 2.4% while hydrogenation was 6.97%, for the case of 1% wt/v H_2O_2 decomposition is 2.9% while hydrogenation was 63.5%).

Halides have an inhibitor effect of secondary reactions; however its concentration must be carefully optimized to get the desired effect. Values of Br/Pd between 1.5 and 2.5 are optima due to these values minimize hydrogenation and kept decomposition rate at acceptable values. A non – lineal relation between halide concentration and the pre – exponential factor of the Arrhenius equation have been found ($1859.4 < k_{0d} < 2392.9$; $102.17 < k_{0h} < 623.47$). Not only the halide is need for hydrogen peroxide synthesis but also the concentration (pH) of the acid is a key parameter. As a general rule the pH of the reaction medium must be lower than the isoelectric point of the support. The effect of pH is clear by comparing the values of rate of reaction of the two experiments. In the case of the decomposition reaction rate increases 2.67 times if working in a less acidic medium, pH = 3.8. For hydrogenation the effect is much greater, since the reaction rate increases up to 5.02 times.

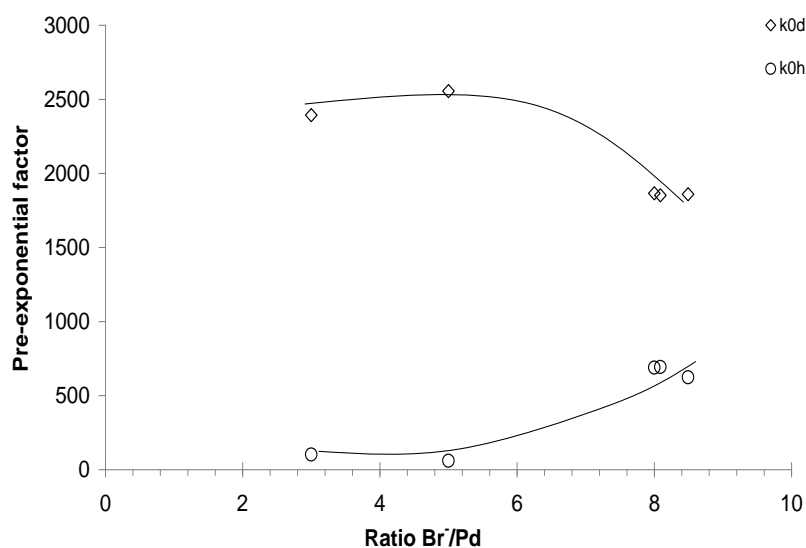


Figure 2. Effect of halide in pre – exponential factor for decomposition and hydrogenation

By the analysis of the influence of the temperature, the values of the energy of activation were obtained ($E_{ad} = 18803.6 \text{ J}\cdot\text{mol}^{-1}$ and $E_{ah} = 7746.2 \text{ J}\cdot\text{mol}^{-1}$). Increasing the temperature the reaction conversion can be increased, however hydrogenation and decomposition reaction rate will be increased too. Only way to overcome hydrogenation and decomposition reaction but have also a high production rate is by made the H_2O_2 already formed inaccessible to the hydrogen.

Decomposition and hydrogenation take place mainly over the active sites of the catalyst but it could be produced over the support. Decomposition rate increased for all the percentage of catalyst tested; although the trend for 5 % Pd/C it is different from the experiments with 1 % and 3 % Pd/C. Differences could be related with the support properties and the adsorption mechanisms. The hydrogenation rate followed a linear tendency for all the catalyst percentages tested. Values of the reactor order over the amount of Pd in the reaction depended on the percentage of palladium in the catalyst but also on the controller step, mass transfer or kinetic.

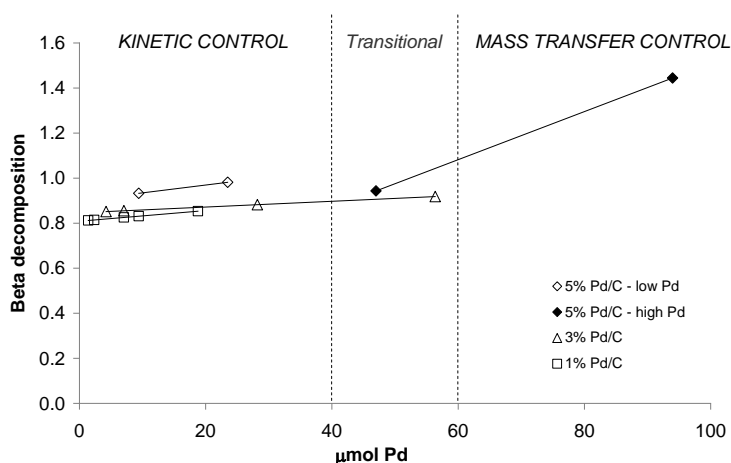


Figure 3. Reaction order for palladium sites in decomposition (β_d) versus amount of Pd.

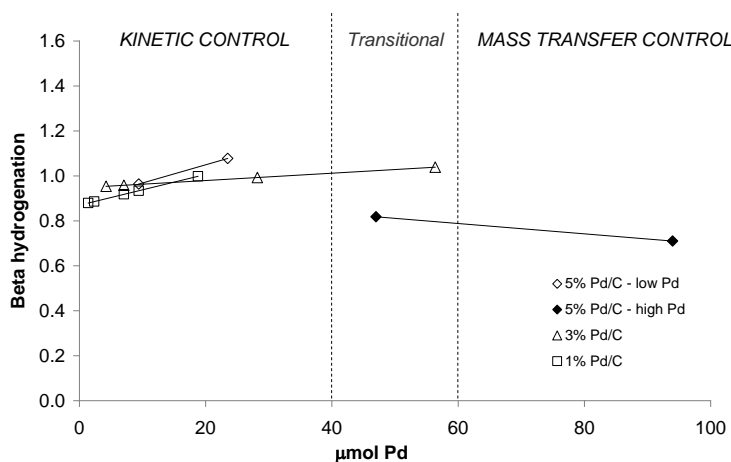


Figure 4. Reaction order for palladium sites in hydrogenation (β_h) versus amount of Pd.

Chapter III. The carbon dioxide has proved to be a great choice as gas phase inert. Because its properties carbon dioxide stabilizes the hydrogen peroxide already formed, increases the flammability limit for $O_2 - H_2$ mixtures and it acts as co - solvent enhancing the mass transfer between gas and liquid. However carbon dioxide is a high value reagent, and its use in hydrogen peroxide direct synthesis could increase the total production. Nitrogen is an alternative to the utilization of carbon dioxide as diluent of the gas phase, nitrogen it is completely inert with all the reagents and material involved in the reaction and it is cheaper in comparison.

Productivity and T.O.F (turn over frequency) obtained by using CO₂ is usually higher. The aim of this chapter it is to optimize the reaction conditions with N₂ in order to obtain values of the productivity similar to the values of the CO₂ experiments. A semi – continuous stirred reactor and a commercial Pd/C (1, 3 and 5 % Pd) catalyst were used. Pressure, temperature and gas flow rate were controlled and H₂O₂ concentration and gas composition outside the reactor were measured continuously. At the same reaction conditions, selectivity, T.O.F and productivity were higher when CO₂ was used as inert, as it was expected (Figure 5).

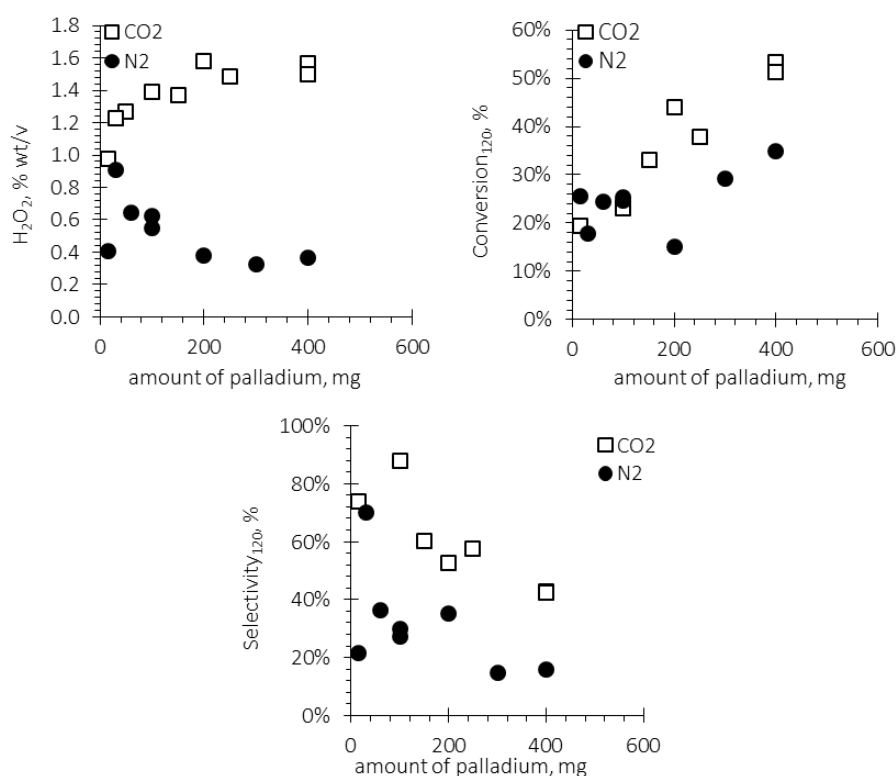


Figure 5. Comparison of direct synthesis experiments using N₂ or CO₂ as gas inert. 80 bar_g, 313.15 K, pH = 2, CO₂: Br⁻/Pd = 8, N₂: Br⁻/Pd = 2, O₂/H₂ = 5.46, 1080 rpm.

The process of direct synthesis of hydrogen peroxide is composed by the mass transfer and the reaction step. The limiting stage depends on the amount of active sites available in the reaction medium. Maximum H₂O₂ concentration obtained was 0.909 % wt/v, with a selectivity of 70% and 17.8% of conversion with only 30 mg of catalyst of 5% Pd/C. When a lower amount of active metal was used the number of active sites was not enough to consume all the hydrogen quickly enough to avoid the hydrogen peroxide hydrogenation. When the amount of catalyst was increased productivity was kept almost constant and even a low decrease was observed, however hydrogen consumption increased. That meant that a higher amount of active metal enhances the decomposition and hydrogenation of the hydrogen peroxide.

Influence of reaction pressure was analyzed in relation with the total reaction pressure but also with the hydrogen partial pressure. Increasing of global pressure had a beneficial effect in the four control parameters (conversion, selectivity, productivity and T.O.F.), because high pressure increased the gas solubility on the liquid phase and reduced the decomposition and the hydrogenation rate. Variation of the hydrogen partial pressure can be due to variations on the total pressure or on the hydrogen molar fraction. Conversion, productivity and T.O.F increased with partial hydrogen pressure in both cases. Selectivity, in the opposite way, was kept constant (30 % – 35 %) when the variation of the hydrogen partial pressure was due to a variation on the hydrogen molar fraction but increased with the hydrogen partial pressure if it changed because the total pressure (16% at 20 barg – 48 % at 90 bar). Influence of the ratio O_2/H_2 can explain these differences. If the ratio O_2/H_2 is kept constant (when total pressure varied the gas composition did not change), the selectivity, conversion and T.O.F increased with pressure. However, at high O_2/H_2 (low hydrogen partial pressure and low hydrogen molar fraction) the amount of oxygen available for reaction is higher, what could affect the adsorption mechanism and modified the metal oxidation state.

For all the series, using different Pd load (1%, 3% and 5% Pd/C) observed reaction rate rose with temperature, as it was expected as four reactions are exothermic. Value of pre – exponential factor ($272.15 \text{ mmol}\cdot\text{min}^{-1}$, $520.54 \text{ mmol}\cdot\text{min}^{-1}$ and $766.51 \text{ mmol}\cdot\text{min}^{-1}$ for 1 % Pd/C, 3 % Pd/C and 5 % Pd/C catalyst respectively) and E_a/R (2306.7 K, 2348.4 K and 2588.2 K for 1 % Pd/C, 3 % Pd/C and 5 % Pd/C catalyst respectively) were obtained using the Arrhenius equation. Pre – exponential factor increased with the percentage of palladium; but not an influence of the palladium percentage over the E_a/R has been found.

Chapter IV: mass transfer limitation between the gas reagents and the liquid phase is one of the main limitations of the process. Trickle bed reactors are widely used in chemistry and petrochemical industry and are one of the most promising alternatives for the continuous production of hydrogen peroxide. Patents and papers about the direct synthesis of hydrogen peroxide have been published yet but the process still needs a further investigation. Influences of the catalyst composition, solvent, pressure and temperature have been studied.

In this case, the hydrogen concentration of the gas phase was set to 2.23 mol % (lower than the low flammability limit). Although because the low hydrogen concentration the productivity was

reduced, this allowed us to understand how the selectivity could be increased by the residence time or the catalyst conditions. Flow regimen must be controlled carefully to ensure that the reactor operated inside the trickle region and that the contact between the solid and the fluids phases is correct. The experimental apparatus is composed by an AISI 316 stainless steel reactor, 30 cm long and 1.15 cm I.D and internally lined with PTFE to avoid hydrogen peroxide decomposition. Pressure, temperature and volumetric gas flow rate was controlled along the reaction progress. A commercial catalyst of palladium (5 % Pd) over active carbon was used as catalyst for all the experiments. Reaction bed is composed by a mixture of the catalyst and SiO₂, that as inert and a support. The volumetric total flow rates corresponded to the specific mass flow rates ranging from 0.017 to 0.032 kg·m⁻²·s⁻¹ for the gas and from 0.047 to 0.566 kg·m⁻²·s⁻¹ for the liquid, respectively.

Maximum productivity was obtained at high pressure (28 – 25 bar) when the lowest liquid flow rate was set (Figure 6). In the opposite the productivity is lower if higher flowrates and shorter silica bed were used. At low – intermediate pressure (15 bar) the productivity was low, in general terms. For the analysis of the overall results four hypotheses have been deducted:

- H-1. The H₂/Pd depends directly on the H₂ concentration or partial pressure.
- H-2. The concentration of hydrogen solved in the liquid phase is higher if the liquid flow decreased, and the ratio H₂/Pd in the active site is higher.
- H-3. Increased catalyst concentration in the catalyst bed at initial reaction stages is beneficial for the reaction.
- H-4. At the same amount of catalyst a longer bed (more SiO₂) helps in a higher H₂ dissolution and H₂/Pd is higher.

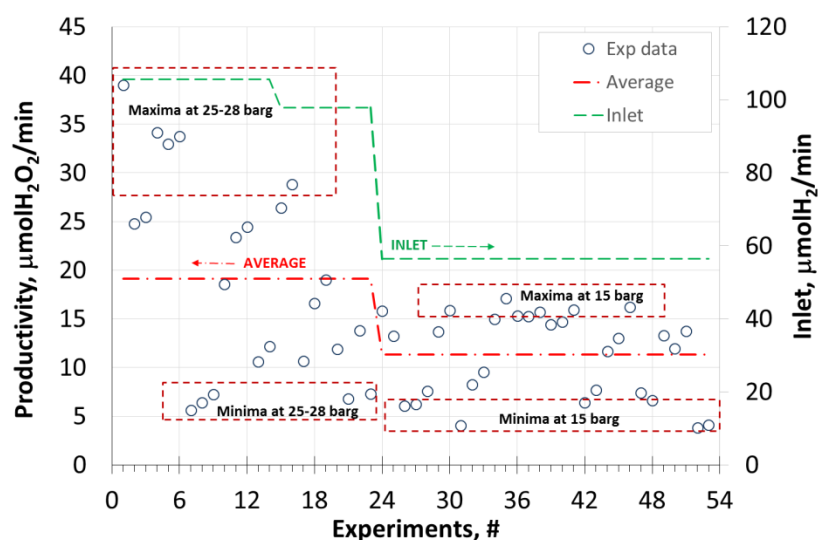


Figure 6. Overview of the experiments

Increasing of pressure could be a simple way to increase the system productivity as high pressure could boost gas solubility in the liquid phase and reduce the mass transfer limitation. Concentration of hydrogen peroxide was 2 – 3 fold times higher when 28 - 25 barg was set in comparison with the values obtained at 15 barg. Analysis of the yield values allows us to conclude that a 15 barg the system was limiting by the mass transfer phenomena (not influence of the catalyst amount was observed). Low flowrate produced always maximum yield, since higher residence time supposed a higher residence time, higher H_2 concentration a low dissolution of the H_2O_2 . However a low liquid flowrate could produce problems in the wetting of the bed on the reactor and reduced the efficiency of the reaction.

The distribution of the catalyst inside the reactor could be modified in order to obtain the maximum productivity or selectivity. At low pressure the same productivity values were obtained independently of the catalyst distribution, because the system was limited by mass transfer and the low H_2 inflow. At high pressure experiments (28 – 25 bar) the effect of the catalyst distribution was clearer, 75 and 37.5 mg of 5 % Pd/C catalysts in 40 and 20 ml of SiO_2 were studied. Hydrogen peroxide concentration was higher when 75 mg of catalyst instead of 37.5 mg was used, with no influence of the volume of the inert, indicating that hydrogen conversion increased with the amount of catalyst.

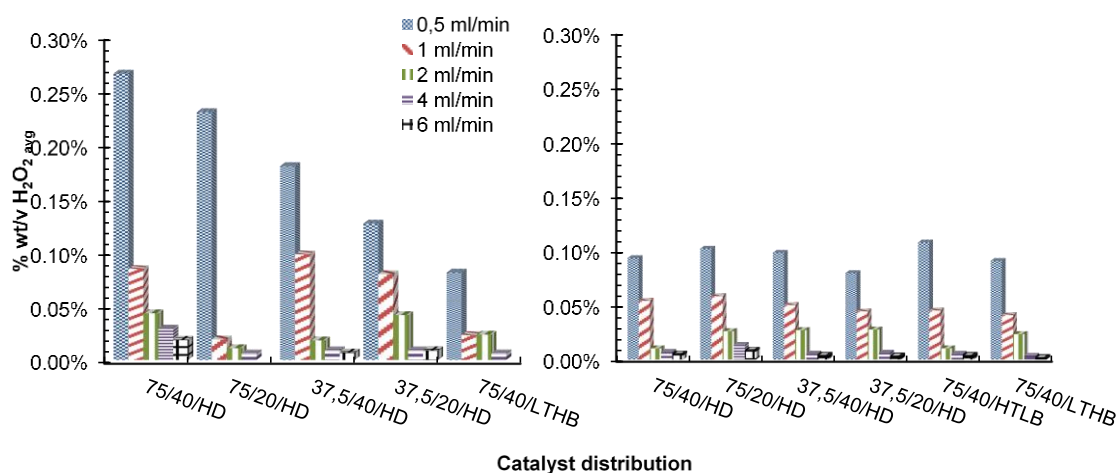


Figure 7. Influence of catalyst distribution and liquid flow rate on final average hydrogen peroxide concentration (Amount of catalyst (mg)/ bed volume (cm³)/distribution). 28 – 25 barg left figure, 15 barg right figure.

For both pressure values the uniform distribution of the catalysts has proved to be the optimum one, since a more distributed catalyst supposed a higher area for mass transfer. Worst results have been obtained when an irregular catalyst distribution (the catalyst concentration in the bottom of the reactor was higher than the concentration of the top), because the contact between the catalyst, the hydrogen and the hydrogen peroxide already formed could cause the decomposition or hydrogenation and reduce the selectivity and productivity of the process (H–3). Hydrogen – palladium ratio (H₂/Pd) must be kept high not only to reduce the effect of secondary reactions but also because the H₂/Pd ratio affects the adsorption/desorption rates. Best yields and T.O.F were obtained at a low Pd/Vb ratio, confirming that way that a long transfer area is needed (H–4).

Chapter V: catalyst design and the determination of its behavior at different reaction conditions is a key step to the development of multiphase reactions as the direct synthesis of hydrogen peroxide. Influence of the main reaction parameters have been studied in this chapter in order to obtain value information that could be used in a more efficient catalyst design. Trickle bed reactor is a flexible solution to support hydrogen peroxide direct synthesis because it guarantees a high mass transfer coefficient between gas, liquid and solid phase. Searching of the most appropriated reaction conditions (liquid flow rate, gas flow rate and amount of catalyst) and minimization of the secondary reactions are necessary.

Liquid flow rate, gas flow rate and the amount of catalyst were closely related in the trickle bed reactors. LFR must be selected carefully to ensure that the flow regime is inside the trickle flow zone but also to ensure the LFR is enough to ensure that the bed is complete and uniformly wetted. For the lower liquid flow rate ($4 \text{ ml}\cdot\text{min}^{-1}$), hydrogen peroxide production increased linearly with the molar flow rate of hydrogen for every amount of catalyst tested (150, 380 and 540 mg). No enhancement of the productivity was found when the amount of the catalyst was increased what implied that the mass transfer was controlling the process. Analysis of the results allowed us to conclude that while the concentration of H_2O_2 is lower, direct synthesis of H_2O_2 and formation of water are the main reactions and that hydrogenation and decomposition only took place when H_2O_2 concentration reached a significant level. At the reaction conditions of these experiments, we could assume that due to the low liquid flow rate the catalyst could consume all the hydrogen at the first part of the reactor, reducing the H_2O_2 hydrogenation.

When a higher liquid flow rate was used ($6 \text{ ml}\cdot\text{min}^{-1}$) only for the experiment with the higher amount of catalyst (540 mg) a linear increasing of the H_2O_2 productivity with the hydrogen molar flow rate was obtained. If a lower amount of catalyst was used (150 mg or 380 mg) for hydrogen molar flow rates higher than $220 \mu\text{mol}\cdot\text{min}^{-1}$ a non – linear tendency or a flattening of the H_2O_2 production was observed; in that case the amount of active sites available to the consumption of the H_2O_2 were not enough and some of hydrogen reacted with the hydrogen peroxide already formed. The adsorption phenomenon that takes place over the active sites of the catalyst is considered as one of the key points of the optimization of the direct synthesis of hydrogen peroxide. The adsorption depends on the catalyst amount, the concentration of the reagents and the liquid and gas flow rates. As the experimental results proved a correct selection of the experimental conditions can shifted the adsorption equilibrium to minimize the hydrogenation reaction.

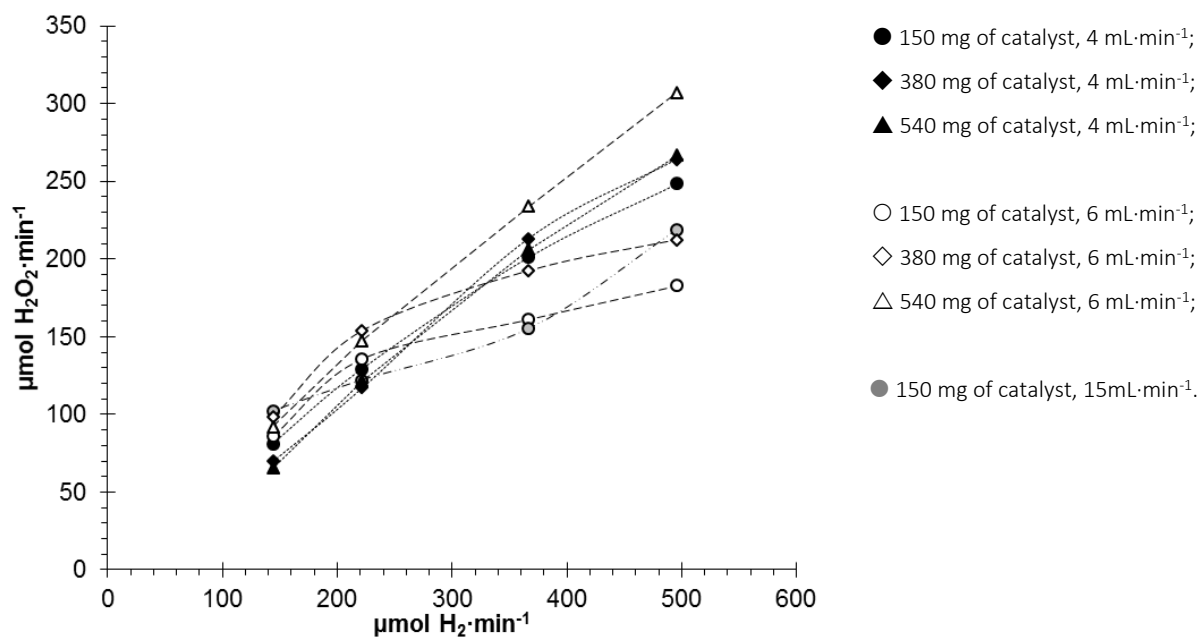


Figure 8. Influence of liquid flow rate, gas flow rate and amount of palladium on hydrogen peroxide production rate. 15 barg, 15 °C, 5% Pd/C, $[\text{Br}^-] = 5 \cdot 10^{-4}$.

Direct relation of the reaction pressure and the H_2O_2 productivity have been found. As it could be expected higher pressures increased productivity since the gas solubility increased also. Maximum hydrogen peroxide productivity was $307.34 \mu\text{mol H}_2\text{O}_2 \cdot \text{min}^{-1}$ obtained for 26 barg. As expected, the lowest productivity rate ($93.93 \mu\text{mol H}_2\text{O}_2 \cdot \text{min}^{-1}$) was obtained at the lowest pressure (2.75 barg). A higher pressure did not guarantee a high productivity, but also the other reaction parameters must be fine-tuned to ensure the reaction was successful (gas and liquid flow rate).

Not a clear relation between the experimental results and the temperature have been found. Temperature affects so many phenomena that take place during the direct synthesis of hydrogen peroxide, as it could be the kinetic of the reactions, the solubility equilibrium and the adsorption – desorption processes. It was possible to divide the temperature interval analyzed in three different sections according to the hydrogen peroxide productivity. Low temperatures (15 °C) retarded the hydrogen consumption, since the kinetics becomes lower, in the opposite way high temperatures (60 °C) increased the reaction rate of decomposition and hydrogenation reducing the productivity and selectivity of the process. Optima values were obtained at intermediate temperatures ($310 \mu\text{mol H}_2\text{O}_2 \cdot \text{min}^{-1}$ and 62.3 % yield at 25 °C; $320 \mu\text{mol H}_2\text{O}_2 \cdot \text{min}^{-1}$ and 64.6 % yield at 40 °C).

Influence of the concentration of the promoters and mechanism of the inhibition of the secondary reactions have been analyzed for three bromide concentration in the liquid flow rate (acid concentration was kept constant, pH = 2). At the first part of the experimentation the hydrogen peroxide concentration increased slowly until that for a specific value of reaction time (it depends on the bromide concentration) the H₂O₂ concentration started to increase sharply to reach a steady – state. Duration of each stage, the increasing velocity and the final H₂O₂ concentration reached depends on the concentration of NaBr in the liquid phase, as the rest of experimental conditions were the same.

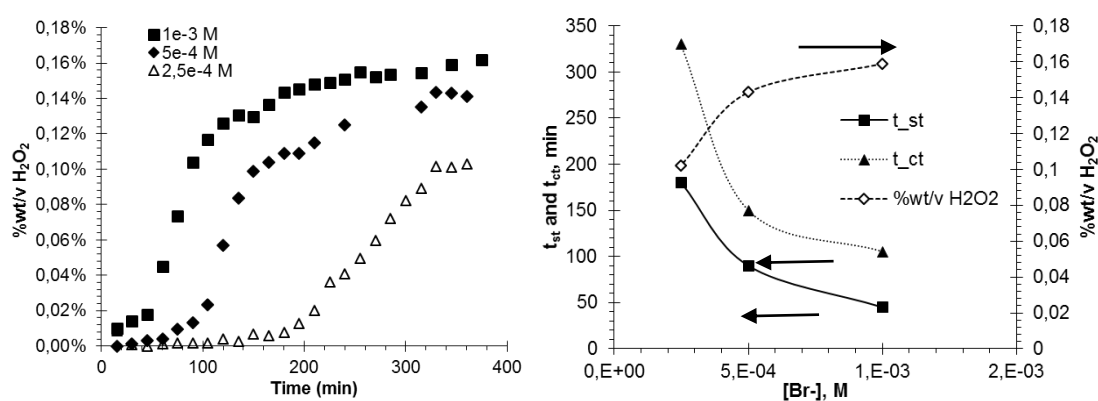


Figure 9. Evolution of hydrogen peroxide during the course of reaction and the influence of bromide concentration (left) and effect of the bromide concentration on the H₂O₂ concentration evolution (right).

Addition of NaBr modifies the shape and the dispersion of the nanoparticles of the catalysts, and acts over the adsorption and desorption phenomena. The more NaBr there is in the solution, the faster is the activation step of the catalyst to reach steady-state conditions and higher the concentration of hydrogen peroxide achieved. Two conclusions could be deduced from the experimental data:

- The concentration of Br⁻ affects only to the quality of the sites that are blocked, not to the quantity, since a double Br⁻ concentration did not imply a double H₂O₂ production.
- Reconstruction of the metal nanoclusters and fitting of the equilibrium phenomena of the Br⁻ on the Pd surface are affected by the Br⁻ concentration.

Distribution of the catalyst along the reaction volume has proved to be decisive (chapter IV). The reaction bed is composed by an inert support and a catalyst that in a similar way it is formed by a support and the active metal. This fact allow us to vary the distribution and the concentration of the active metal inside the reaction bed in order to analyzed how it could influence over the

reaction productivity and efficiency. Influence of the palladium percentage on the catalyst have been studied (5, 10 and 30 % wt.).

In general terms, the catalyst with 30 % wt of palladium gave the best results. As it have been explained before a rapid consumption of the hydrogen at the beginning of the reactor might be the reason. The maximum productivity of $250.5 \mu\text{molH}_2\text{O}_2\cdot\text{min}^{-1}$ (for $496.0 \mu\text{molH}_2\cdot\text{min}^{-1}$) and $288.56 \mu\text{molH}_2\text{O}_2\cdot\text{min}^{-1}$ (for $496.0 \mu\text{molH}_2\cdot\text{min}^{-1}$) were obtained for 10 % Pd/C and 30 % Pd/C, respectively. Yields between 84 % and 60 % for 30 % Pd/C and between 60 % and 50 % for 10 % Pd/C were measured. In general, experiments over 30%Pd/C gave the best values in terms of yield and productivity. Also metal sintering in the catalyst could have a favorable effect over the H_2O_2 direct synthesis, at high concentration of the active nanoparticles they can aggregated more easily favoring the H_2O_2 synthesis.

Hydrogenation is the main cause of the losses of selectivity and productivity during the direct synthesis of hydrogen peroxide. Measuring and study of the hydrogenation rate and how the main reaction parameters influence it have been also done in this chapter. A linear relation between the residence time of the liquid and the hydrogenation rate (represented by the mmol of hydrogen reacted) have been found (16 to $4 \mu\text{mol H}_2\cdot\text{min}^{-1}$ for 3.7 to 44min^{-1} (HRT)). Influence of the hydrogen molar flow rate is greater since the hydrogen consumption rate increased exponentially with the hydrogen molar flow rate feed into the reactor (16 to $99 \mu\text{mol H}_2\cdot\text{min}^{-1}$ for 74.2 to $219.03 \mu\text{mol H}_2\cdot\text{min}^{-1}$).

Chapter VI: Slurry bubble columns are one the main kinds of multiphase reactor and they are used in chemical and petrochemical process since few decades ago. However there is not an easy way to predict the values of the hydrodynamic parameters that define the processes that take place inside a bubble column reactor as the system behavior depends greatly on the experimental conditions and the geometry of the system.

The design of a bubble column is simple but a successful design depends on the prediction of three aspects: mass and heat transfer, mixing characteristics and kinetic of the reaction. There is huge amount of references and equations available of the open literature that allows the calculation of the area for mass transfer, the diameter of the bubbles and the fraction of the column filled by the gas. Prediction of theses parameters using a correlation development for a

different system must be done carefully, ensuring that the correlation and the predictions were obtained at similar conditions.

On this chapter, the influence of the initial liquid level in the column, the gas flow rate and the geometry of the diffuser on the bubble diameter, gas hold – up and mass transfer coefficient have been analyzed. Also new correlations for the prediction of those parameters have been proposed with the objective they could be used for the design of a high pressure slurry bubble column reactor. No influence of the initial liquid level on any parameter have been found.

Hold – up was higher when porous diffuser was used since the small bubbles produced by this diffuser had a higher residence time inside the reactor and on consequence the volume of gas inside the column per unit of time is higher (maximum $\epsilon = 13.14\%$ for diffuser experiments, maximum $\epsilon = 7.17\%$ for 1/8" O.D. tube experiments). As it could be expected, the hold – up value increased also with the gas flow rate (from 0.94 % to 1.82 % for 1/8" O.D. tube and from 0.80 % to 1.81 % for porous diffuser at 200 mLN·min⁻¹ and from 5.20 % to 7.78 % for 1/8" O.D. tube and from 11.83 % to 13.14 % for porous diffuser at 1500 mLN·min⁻¹). None of the proposed correlations from the bibliography was capable to predict the experimental values with a small enough average standard deviation (Figure 10). So, a new expression (Equation 1) was proposed based on the Reynolds number and the physical properties of the gas and the liquid phases. The independent factor of the equation proposed was obtained by the adjustment of the experimental values (tube 1/8" O.D.: $f_c = 4.03 \cdot 10^{-2}$; porous diffuser: $f_c = 3.41 \cdot 10^{-2}$; all the exp.: $f_c = 4.82 \cdot 10^{-2}$).

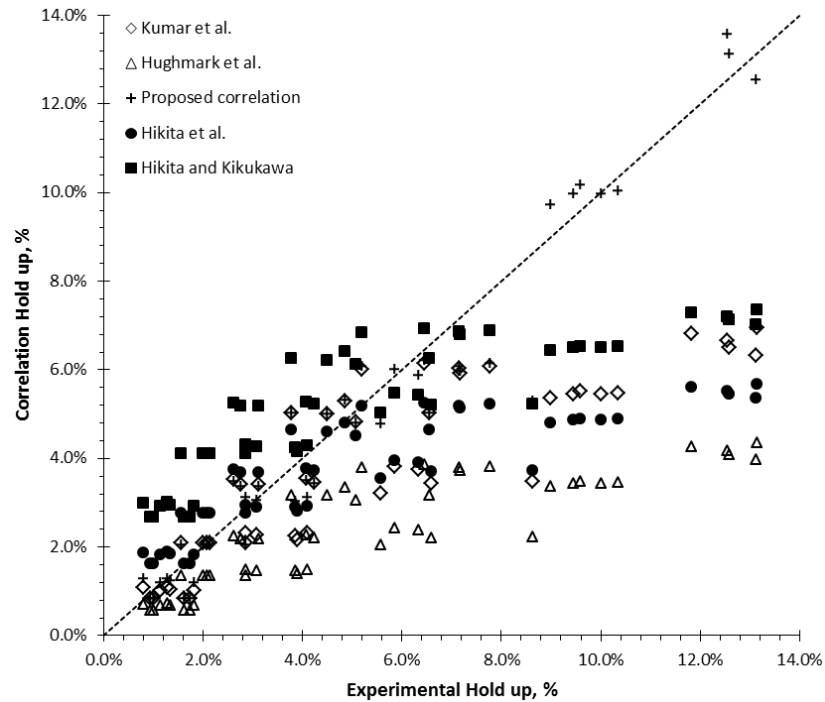


Figure 10. Comparison of the accuracy of the correlations used to the prediction of the hold – up values

$$\varepsilon = f_{\varepsilon} \cdot d_0 \cdot \text{Re}^{0.7} \left(\frac{u_g}{d_0^5 \cdot g} \right)^{0.21} \quad \text{Equation 1. Proposed correlation for hold – up calculation } (\varepsilon_{\text{PC}})$$

The bubble diameter depended on the geometry of the diffuser since the diameter of the orifice determinate the initial shape and size of the bubble. The average diameter of the bubbles obtained when the porous diffuser (0.27 cm – 0.46 cm) was used were smaller than the values used for the experiments with the 1/8" O.D. tube (0.71 cm – 1.23 cm). In relation with the gas flow rate influence, the bubble diameter increased at low gas flow rate until it reached a maximum stable value. As happened with the hold – up values, the correlations selected on the bibliography review could not predict the experimental values (Figure 11) and a new specific correlation have been proposed.

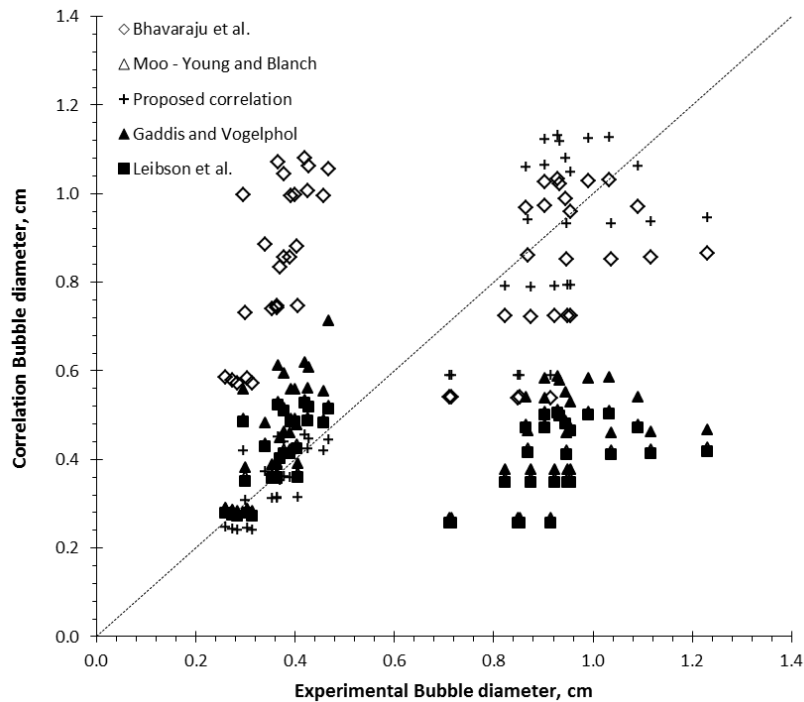


Figure 11. Comparison of the accuracy of the correlations used to the prediction of the bubble's diameter values

Volumetric mass transfer coefficient ($k_L \cdot a$) have been calculated from the experimental values of the oxygen concentration on the liquid phase, assuming that the system behaved as a perfectly stirred batch reactor. The mass transfer volumetric coefficient is a global parameter that combine the mass transfer coefficient (k_L) and the interfacial area (a). The calculation of each parameter individually could give as extra information that allow us to identify which parameter is controlling the mass transfer.

A strong dependence of the interfacial area, and also of the volumetric mass transfer coefficient, on the gas flow rate have been found, as higher the gas flow rate higher the gas inside the column and higher the area between the gas and the liquid phase. On the opposite, the experimental results did not show up a clear relation between the mass transfer and the liquid flow rate.

A preliminary CFD model have been carried out with the objective of predict the bubble diameter, the hold – up and the volumetric mass transfer coefficient of the system. Even the results obtained were similar to experimental ones a further development of the model is still need.

Figure Captions

Figure 1. Summarized structure of the chapters that composed this research	37
Figure 2. Effect of halide in pre – exponential factor for decomposition and hydrogenation	39
Figure 3. Reaction order for palladium sites in decomposition (β_d) versus amount of Pd.	40
Figure 4. Reaction order for palladium sites in hydrogenation (β_h) versus amount of Pd.....	40
Figure 5. Comparison of direct synthesis experiments using N ₂ or CO ₂ as gas inert. 80 barg, 313.15 K, pH = 2, CO ₂ : Br ⁻ /Pd = 8, N ₂ : Br ⁻ /Pd = 2, O ₂ /H ₂ = 5.46, 1080 rpm.	41
Figure 6. Overview of the experiments	44
Figure 7. Influence of catalyst distribution and liquid flow rate on final average hydrogen peroxide concentration (Amount of catalyst (mg)/ bed volume (cm ³)/distribution). 28 – 25 barg left figure, 15 barg right figure.	45
Figure 8. Influence of liquid flow rate, gas flow rate and amount of palladium on hydrogen peroxide production rate. 15 barg, 15 °C, 5% Pd/C, [Br ⁻] = 5·10 ⁻⁴	47
Figure 9. Evolution of hydrogen peroxide during the course of reaction and the influence of bromide concentration (left) and effect of the bromide concentration on the H ₂ O ₂ concentration evolution (right).	48
Figure 10. Comparison of the accuracy of the correlations used to the prediction of the hold – up values	51
Figure 11. Comparison of the accuracy of the correlations used to the prediction of the bubble’s diameter values.....	52

OBJECTIVES

Influence of the reaction conditions, catalyst properties and the concentration of the promoters on the production of hydrogen peroxide by direct synthesis have been widely studied. In despite of the huge amount of papers and patents, the industrial implementation of the direct synthesis as an alternative to the traditional routes for hydrogen peroxide synthesis is still need of investigation. The study of a continuous reaction system (design and optimization of the reaction conditions) is mandatory to achieve the total development of the process.

The global aim of this thesis is the study of viability of different continuous reactor configurations for the direct synthesis of hydrogen peroxide and the determination of the influence of the conditions of reaction and operation, with a special emphasize for the parameters related with the scale up and the design.

For achieve this general purposed the following objectives will addresses

- Studying and modelling of the undesired reactions (decomposition and hydrogenation). A deep knowledge of all the reactions involved in the process is need in order of to select the optima reaction conditions. Undesired reactions cause the decreasing of the selectivity of the process and reduce its competitiveness in comparison with the traditional methods.
- Determination of the influence of the nature of the inert gas selected for the gas phase. Comparison of the productivity and efficiency of the system when nitrogen and carbon dioxide are used. Optimization of the reaction conditions for a semi continuous stirred reactor using N₂ as inert.
- Studying and optimization of hydrogen peroxide production by direct synthesis in a trickle bed reactor. The reaction parameters related with the hydrodynamic of the process and the system scale up, such us gas and liquid flow rate and hydrogen – palladium ratio, are deeply studied. Also catalyst distribution and actives sites concentrations are included in the analysis.
- Analysis of low pressure hydrodynamic regimen in a bubble column reactor. Study of the influence of gas flow rate on hold – up, bubble diameter and mass transfer coefficient values. Development of specific correlations for adjustment and prediction.

- Design, building and setting up of a high pressure slurry bubble column for the direct synthesis of hydrogen peroxide. Slurry bubble columns are a three phases reactors that have widely prove that their properties are adequate to their application into heterogeneous reactions. Even if the running of these kind of reactor is easy in comparison with other typical reactor configuration, the design is an extremely complicated process in which a huge amount of parameters and process should be predicted and considerate.

CHAPTER I

Direct synthesis of H₂O₂.

General aspects and influence of the reactions conditions

1.1. Hydrogen peroxide and general outlook of the methods of production

Known since 1818, when it was discovered by the chemist Louis – Jacques Thénard, the hydrogen peroxide has become, nowadays, in one of the most useful chemical compounds in the bulk chemistry industry. Hydrogen peroxide it is one of the cleanest and most versatile oxidants available due to its high active oxygen content (47 %), and it can be considered as a green oxidant because: 1) its decomposition produced water as the only product and 2) its high degradability and low toxicity index.

Total annual hydrogen peroxide production is estimated around three millions of tons per annum (according from data of 2010), and the production grows at about a 4% rate per year [1]. Industrial applications of hydrogen peroxide are varied: paper industry (bleaching, chloride free chemical), textile industry (bleaching agent replacing sodium chlorite, as a component in detergents), chemical industry (as initiator of polymerization, oxidation, epoxydation and hydroxylation), electronic industry (semiconductor cleaning), wastewater treatment (disinfectant), inorganic synthesis (sodium percarbonate, sodium perborate) and domestic uses (disinfectant, cosmetic and detergents).

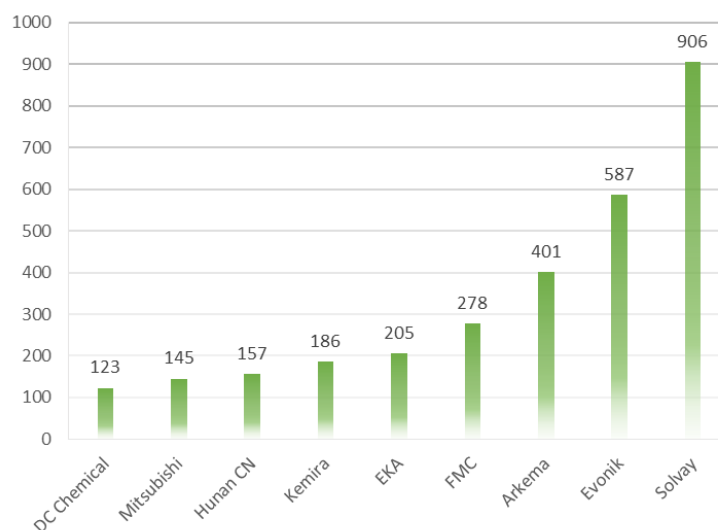


Figure 1. Distribution of the world market of hydrogen peroxide production (kt/year)

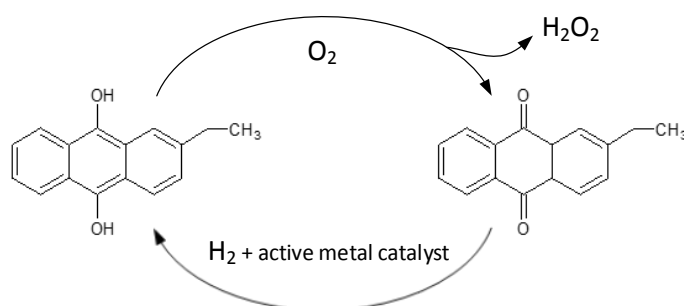


Figure 2. Anthraquinone reaction route for hydrogen peroxide synthesis

Main highlights of the AOP are the fact that it avoids the direct contact of the hydrogen and oxygen and allows a continuous production at mild reaction conditions (40 – 60 °C). However a large amount of by – products are produced and separation, purification and concentration steps are needed to obtain an hydrogen peroxide solution with the suitable characteristics needed for its use in chemical processes. Because of the needed of the purification and concentration steps, AOP route for hydrogen peroxide’s synthesis is only economically viable in large scale plants, what supposed that H₂O₂ must be transported from the production plants to the consumption place. Hydrogen peroxide can decomposed easily (heat, light or metal surfaces could act as activation agents of decomposition) which implies some risk on transportation processes. This fact joined to the wide range of applications of hydrogen peroxide (each application need for a different hydrogen peroxide supply, with different concentrations and purity) suggest the need to developed a reaction process sustainable and optimized for a small scale production rate.

The “Strategic Research Agenda” (SRA) of the European Technology Platform of Sustainable Chemistry supports the production of hydrogen peroxide by direct synthesis and its use in chemical processes in the context of the development of sustainable chemistry industry. Direct synthesis technology would benefit chemical industries by lowering of the hydrogen peroxide price and the reduction of the amount the sub products and waste generated by the auto – oxidation process [2] . Although direct synthesis is not enough developed to be considered an actual alternative to the auto – oxidation process, the research efforts are trying to solve all the issues related to selectivity, mass transfer and safety.

Table 1. Auto – oxidation and direct synthesis comparison

Process	Auto – oxidation	Direct synthesis
Principle	Cyclic oxidation and hydrogenation of organic molecules.	$H_2 + O_2 \rightarrow H_2O_2$
General feature	Well known but complex, developed	Simple process but still need

	during a long time	further development
Catalyst	Pd just in hydrogenation step	Pd and Au based catalyst
Reaction medium	Solution with the mixture of the organic compounds	Water, methanol or ethanol, CO ₂ as co – solvent
Reaction system	Complex system, compound by various reactors	Just one reactor is needed
Selectivity	High	More research is needed
Safety	Safe	Possible
On site production	Impossible	Possible

The direct synthesis (DS) of H₂O₂ from H₂ and O₂ in presence of an active metal catalyst has become a truly alternative to the traditional synthesis processes since it was patented by Henke and Weber in 1914. Direct synthesis not only half the cost of hydrogen peroxide more than half, it could be considered a green process since water is the only by product, that will reduce the global environmental impact of hydrogen peroxide. Although direct synthesis of hydrogen peroxide could seem to be an easy reaction (one mol of oxygen reacts with one mol of hydrogen to produce one mol of hydrogen peroxide) there are some many limitations and difficulties of development that made that the direct synthesis of hydrogen peroxide is not yet a complete optimized process.

The first difficulty of hydrogen peroxide direct synthesis is related with the reactions involved in the global process. Thus, not only the main reaction (H₂O₂ formation) takes place, but also exist three secondary reactions which compete with H₂O₂ synthesis, *i.e.* water formation, decomposition of hydrogen peroxide and hydrogenation of hydrogen peroxide.

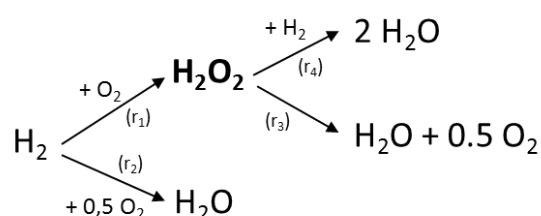


Figure 3. Scheme of reaction of hydrogen peroxide's direct synthesis

Four reactions are thermodynamically favored, highly exothermic and catalyzed by the same catalyst. Secondary reactions do not produce toxic products (only oxygen and water) but cause a decrease in selectivity of the reaction limiting the concentration of the final product.

Table 2. Reactions of direct synthesis of hydrogen peroxide

			ΔH^0 , kJ·mol ⁻¹	ΔH^0 , kJ·mol ⁻¹
r ₁	H ₂ O ₂ formation	$\text{H}_2(\text{g}) + \text{O}_2(\text{g}) \rightarrow \text{H}_2\text{O}_2(\text{l})$	-187.8	-120.9
r ₂	Water formation (highly undesired)	$\text{H}_2(\text{g}) + 0.5 \text{O}_2(\text{g}) \rightarrow \text{H}_2\text{O}(\text{l})$	-285.8	-273.7
r ₃	Decomposition (undesired)	$\text{H}_2\text{O}_2(\text{l}) \rightarrow \text{H}_2\text{O}(\text{l}) + 0.5 \text{O}_2(\text{g})$	-98.2	-116.8
r ₄	Hydrogenation (undesired)	$\text{H}_2\text{O}_2(\text{l}) + \text{H}_2(\text{g}) \rightarrow 2 \text{H}_2\text{O}(\text{l})$	-379.4	-354.4

Safety issues are a drawback for the development of direct synthesis. Mixtures of O₂ and H₂ are explosive in a wide concentration range. The lower flammability limit (LFL) has been measured by some different research groups, and its value varies between 4 % – 4.5 %mol depending on the source and the experimental conditions. For instance, increasing the operational pressure increases the LFL [3]. Although the operation inside the flammability limits used to be common few decades ago, actually almost all the research groups operate inside the safety region. In this sense, to keep the hydrogen concentration below the 4 %mol an inert gas (carbon dioxide or nitrogen mainly) is added to the gas phase. The addition of the inert gas reduces the efficiency of the system, by reducing concentration of one of the reagents, but it is mandatory due to the high flammability of the O₂ – H₂ mixtures.

Direct synthesis is a heterogeneous reaction, in which three phases are involved, the catalyst is a solid, the medium of reaction (water, methanol or ethanol) are liquids and the reagents (O₂, H₂) and the diluents (CO₂, N₂, He, Ar) are gases. Because of system heterogeneity the reaction process is composed by a group of stages in series:

- Convection in the gas phase (m_{t1})
- Gas liquid equilibrium at the interphase (m_{t2})
- Convection in the liquid phase (m_{t3})
- Adsorption of the H₂ and O₂ to the catalyst sites (m_{t4})
- Surface reaction between adsorbed H₂ and O₂ (m_{t5})
- Desorption of the H₂O₂ to the bulk liquid phase (m_{t6})

- Convection in the bulk liquid phase (m_{t7})

Not all the stages have the same weight in the global rate of the process. A correct selection of the experimental device and the operation conditions could reduce the influence of the controlling steps and allow increasing the efficacy of the reaction.

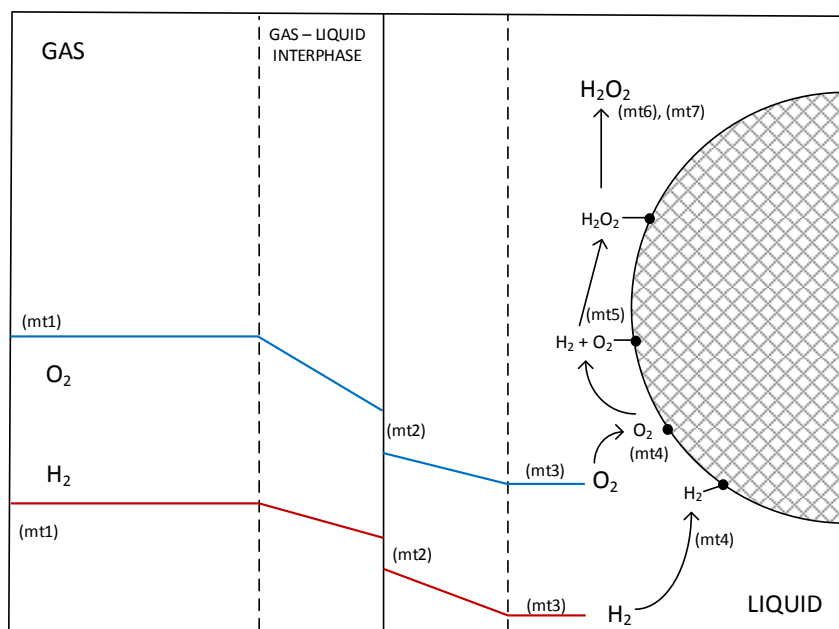


Figure 4. Mass transfer phenomena in direct synthesis reaction process

Other alternative methods to the production of hydrogen peroxide are possible, such as photocatalytic reactions over semiconductor, from the hydrolysis of peroxomono- and peroxodisulfuric acid oxides obtained by the electrolysis of the sulfuric acid, direct synthesis for $CO/O_2/H_2O$ mixtures, enzymatic synthesis, oxygen hydrogenation or from H_2/O_2 mixtures using plasma as reactor initiator. In despite of the limitations of the direct synthesis it has proved to be the most promising of all of them.

1.2. Direct synthesis: operational conditions selection

A large number of studies about direct synthesis are available in the literature, and new publications appear continuously, not only on academic sources but also on the industrial sources. The efforts of the process's optimization are typically focused on the development of the catalyst (support and active metal) and reduction of secondary reactions by the adding of promoters that inhibited those reactions. In a lower proportion, the influence of the solvent has been analyzed too.

1.2.1. Catalyst

Active metal

Only noble metal catalysts have been probed active for direct synthesis of hydrogen peroxide. Palladium, gold, platinum and silver are the most commonly used, especially Pd and Au. Although Dissanayake *et al.* [4, 5] showed that colloidal palladium was very active to reaction, the catalyst are usually composed by an active metal and inert solid that acts as support. The performance of some different active metals have been tested on zeolite – Y support at low temperature [6]. It had been proved that Pd have the best productivity (8 mol H₂O₂· kg cat⁻¹· h⁻¹) followed by Pt (4 mol H₂O₂· kg cat⁻¹· h⁻¹) and Au (3 mol H₂O₂· kg cat⁻¹· h⁻¹). Also Ag, Cu, Rh and Ru were tested but a low productivity was obtained. Based on a theoretical study of the energetics of the reactions involved, Olivera *et al.* [7] predicted that gold based catalyst would be more active than Pd or Pt ones. Influence of the process of manufacturing of the catalyst was analyzed by Li *et al.* [8] (20 °C and 3. MPa) that concluded that only calcined Au catalyst are stable enough to be reused.

Also active metal combinations catalysts have been studied. A significant higher production rate of H₂O₂ was obtained by Landon *et al.* when a 5 wt% Pd – Au over alumina catalyst was used (4.46 mol H₂O₂· kg cat⁻¹· h⁻¹ vs. 1.53 mol H₂O₂· kg cat⁻¹· h⁻¹ only Au catalyst or 0.37 mol H₂O₂· kg cat⁻¹· h⁻¹ Pd catalyst). Palladium acts as promoter for the Au, as this was proved due to the fact that Au – Pd alloy catalyst have a greater productivity than the both metals by separately. Same effect was reported by Edwards *et al.*[9] and Li *et al.* [10] (best catalyst compositions suggested is 2.5 wt% Au / 1.8 wt% Pd over zeolite; 101.6 mol H₂O₂· kg cat⁻¹· h⁻¹). Effect of the addition of different metals, such Re or Co, was studied by Ishihara *et al.* [11], hydrogen peroxide productivity was impaired but the addition of these metals because an increasing in the activity of decomposition and hydrogenation reactions. Other bimetallic catalyst have been studied, Abate *et al.* [12] investigated the efficiency of alumina catalyst with Pd – Ag and Pd –Pt mixtures as active metal. On alumina ceramic membranes, the Pd – Ag catalyst showed higher selectivity values (12 % selectivity) than when the membrane surface is cover with a thin carbon layer before the addition of the metal. Even better results were obtained when Pd – Pt bimetallic catalyst were used (0.5 mol H₂O₂· kg cat⁻¹· h⁻¹, 29 % of selectivity).

Type and concentration of the active metal in the catalyst must be chosen carefully, not only due the influence of the metal characteristics over the reaction but also because the availability and the prize of the metal (palladium prize has been increased form 2100 \$ per kg in 1990 to 26000 \$ per kg in 2000).

Oxidation state

Active metal on catalyst could have different productivity rates as a function of its oxidation state. Results of the study of the influence of the oxidation state are contradictory. Hâncu *et al.* [13], Burch *et al.* [14] and Liu *et al.* [15] explored the use of Pd⁰, and reported that Pd⁰ catalyst had a significant superior activity in the generation of H₂O₂. Liu *et al.* concluded that when a fully reduced was used the rate of H₂O₂ production was close to three times higher (4.1 vs. 10.9 mol H₂O₂ · g Pd⁻¹·min⁻¹).

Melada *et al.* [16] reached a contradictory conclusion. The Pd catalyst supported on zirconia was reduced in the reaction medium by the flowing of a pure hydrogen flow and after that pure oxygen was fed to ensure the complete oxidation of the metal. During the reaction, it was observed that the surface oxidation induced very high catalyst activity (maximum productivity: 800 mol H₂O₂ · g Pd⁻¹·min⁻¹ at 20 °C and atmospheric pressure). Also undiluted H₂/O₂ mixtures (4 % H₂) was used, although the productivity was lower at the beginning of the reaction it increased after a long reaction time (550 mol H₂O₂ · g Pd⁻¹·min⁻¹ after 5 h). The water production rate was 50 times lower than in air, which implies a higher selectivity that it could be kept constant for few hours.

Catalytic support

Carbon, silica, zirconia and zeolite are generally the most used supports on the direct synthesis of hydrogen peroxide because its acidity characteristics help to stabilize the hydrogen peroxide. Edwards *et al.* [17] confirmed the great influence of the support over the productivity and the selectivity of the reaction. Some catalyst based on Au – Pd with different supports were compared and the order of reactivity was set: C > TiO₂ > SiO₂ > Al₂O₃ > Fe₂O₃. Ntainjua *et al.* [18] resolved that support's isoelectric point is the major parameter affecting the hydrogen peroxide selectivity. Degussa – Huls AG showed up that oxidic and silicate supports are the most desirable, carbon active supports were not include because it could be burnt under oxidizing conditions. Independently of the support, a general conclusion was obtained by all the authors, catalyst must be calcinated in order to increase its stability and avoid that the composition of the catalyst changes because the reuse. Functional resins have been reported as suitable supports for H₂O₂ direct synthesis. Sulphonic groups have proved to be capable to interact and stabilize the Pd^{II} ions and avoid its reduction to Pd⁰, which supposed an increasing in the H₂O₂ production rate to values closed to 1100 mol H₂O₂ · g Pd⁻¹·min⁻¹ when methanol was used as solvent at 40 °C and 10. MPa [19].

Also the additions of different dopants could modified the properties and effects of the catalyst support. Melada *et al.* [16] successfully tested the effect of the addition of SO₄²⁻, Cl⁻, F⁻ and Br⁻ on a Pd over zirconia catalyst under mild conditions (20 °C and 1 bar). Dopants usually improved the production rate and the selectivity towards H₂O₂, but a correct selection of the pair support – dopants and the solvent is need. It has been found that silica funcionalized with sulfonic acid could be used in hydrogen peroxide direct synthesis showing a higher selectivity, yield and final hydrogen peroxide concentration higher than the non – funcionalized one. Functionalization did not affect to hydrogenation reaction rate but greatly inhibit the decomposition reaction.

1.2.2. Promoters

As it has been discussed in previous sections, hydrogen peroxide synthesis is not the only reaction that takes place during direct synthesis reaction process. Noble metals used as actives centers act as catalyst also for water synthesis, hydrogen peroxide decomposition and hydrogen peroxide hydrogenation. The competition between four reactions reduced process' selectivity and supposes one of the main drawbacks for the industrial scale implantation of the direct synthesis for H₂O₂ production.

Reaction rate of secondary reactions could be reduced or controlled by the addition to the reaction medium of small amounts of promoters. Although for some catalyst (Au – Pd) the use of promoters could results into a decrease of the activity [9], the use of promoters is general crucial when Pd based catalysts are used. Promoters most used are typically of two categories: halides and acids.

Halides

The beneficial effect of adding a mineral acid, as HCl, to the reaction medium was early reported by Pospelova *et al.* [20]. According to the most of the articles, the halides acts over the catalyst by poisoning the high energy active sites responsible for the dissociative chemisorption of the O₂ and re – adsorption of H₂O₂, and retarding the water production. This statement is consistent with Dissanayake and Lundsford [5] observations that suggested that only diatomic oxygen acts during the formation of the hydrogen peroxide over the palladium. Electronegativity of the anion have proved to be directly related with the capability of the halide to reduce secondary reactions influence. Choudhary *et al.* [21] studied the hydrogenation of H₂O₂ in aqueous acidic medium employing Pd/C catalyst. I⁻ caused complete deactivation of the catalyst because of poisoning, in presence of Cl⁻ and Br⁻ especially hydrogenation is appreciably inhibited, while the effect of F⁻ is

almost negligible. Determination of the optimum amount of halide is usually based on the concentration of the promoter in the reaction medium although some authors suggested that the ratio between halide and the amount of active metal in the catalyst could be the key parameter [22]. Maximum H_2O_2 yield was obtained by Choudhary *et al.* [23] when reaction medium concentration values of $0.9 \text{ mmol}\cdot\text{dm}^{-3}$ for Br^- and $1.5 \text{ mmol}\cdot\text{dm}^{-3}$ for Cl^- solutions were used. Those results suggested that halides concentration must be chosen carefully in order to avoid the catalyst poisoning.

Acids

The stabilizing effect of the presence of acid or protons on the reaction medium have been clearly statement by some authors [24, 25].

The protons prevent hydrogenation and enhancement the adsorption of the halides over the catalyst surface [26]. Effect of the acid is related to the catalyst support structure and its (IEP) isoelectric point (measure of the surface charge). Ntainjua *et al.* [18] determined that hydrogen peroxide productivity was higher when catalyst' supports with a low isoelectric points were used, for Pd and Pd – Au catalyst maximum activity was observed a $\text{pH} = 2$. As general rule, it could be set that for obtained the maximum activity the pH of the reaction medium must be equal or lower than the isoelectric point of the support of the catalyst.

Most of the common solids used as support for the catalyst have values of isoelectric point that are contain in a small interval (*e.g.* $1.0 < \text{IEP: SiO}_2 < 2.0$; $7.0 < \text{IEP: } \alpha, \gamma - \text{Al}_2\text{O}_3 < 8.0$) [27], the isoelectric point of the active carbon could be greatly modified by the pretreatment with acid or base compounds (1.3 – 3.0 and 7.5 – 8.8) [28]. Acidic treatment of active carbon reduces the hydrogenation reaction and cause an increasing in hydrogen peroxide selectivity when an Au – Pd catalyst is used. The reason of this beneficial effect is attributed to modifications on the dispersion of the gold particles along the support [29].

Hydrogen halides are a popular choice for promoters, due to the benefit of the acid and the halide are combine in just one reagent. Phosphoric acid has also proved to be a good option to be used as acidic promoter in the direct synthesis reaction. Choudhary *et al.* [21] tested it and compared it with other mineral acids obtaining very good results, phosphoric acid also proved to be the less corrosive acid in comparison with the rest of the compounds studied. Phosphate anions could act as stabilizers for hydrogen peroxide molecules, so it can be a very desirable option.

Metal leaching and the loses of active metal due to the presence of acid in the reaction medium must be take into account if the reuse of the catalyst is need. When phosphoric acid is used,

metal leaching was only observed at high acid concentrations (higher than 0.3 M). Metal leaching was observed and measured for some authors; lower than 5% when 0.019 M solutions of H₂SO₄, 0.6 % – 4.0% of leaching with a 0.03 M solution of H₃PO₄, 2.5% of leaching with a solution of 0.003 – 0.005 M of H₃PO₄ [30], and even with reaction medium with low concentration of HCl, HBr and HNO₃ an appreciable metal leaching could be observed [21].

A correct and well based selection of the catalyst active metal and support and the nature and concentration of promoters could be the key for the success of direct synthesis of hydrogen peroxide. For all the different options studied and summarized in the bibliography references the most promising results have been obtained Edwards *et al.* [31] who claimed hydrogen peroxide selectivity closed to 98% using a Au – Pd catalyst supported by active carbon pretreated with HNO₃. The understanding about how the promoters increased the selectivity and acts over the reaction mechanism and how the support pretreatment modified the catalyst structure have been the aim of so many investigations but a further researching is still need [1].

1.2.3. Solvent

Water is always the first selection as reaction solvent because of it is non-toxic, non-flammable and its highly miscible with the hydrogen peroxide, however gas solubility on water is really low which limits the production of hydrogen peroxide. By the adding of the additives (organic solvents) it is possible to increase the solubility of the H₂ and O₂ in the water [11, 14, 32]. Although it was found that conversion increased the selectivity was keep low, because the additives were immiscible in water and the contact between them and the catalyst was deficient. Alcohols in general were found as the best option as additives because they are miscible in water (75/25 ethanol – water mixture gave a 34% of selectivity). Pure methanol and ethanol have been successful used as solvent for hydrogen peroxide direct synthesis [24, 33-35].

Carbon dioxide could be used also as co – solvent to enhance system productivity, carbon dioxide increases the lower flammability limit and its acidic character helps to stabilize the hydrogen peroxide. Used of carbon dioxide as co – solvent almost double the hydrogen peroxide selectivity under mild pressure in comparison with similar experiments took out with nitrogen [36]. However some authors have reported that carbon dioxide may cause the deactivation of the palladium of the catalyst [37]. Also supercritical carbon dioxide could be used as solvent (hydrogen and oxygen are completely miscible in scCO₂ what reduce mass transfer limitations) and although CO₂ reach supercritical conditions for not relatively high temperature and pressure

the decompression stage need after reaction could supposed safety a technical problems that would limit the industrial implementation of the process.

1.2.4. *Pressure and temperature*

The influence of pressure is directly related with the mass transfer of the gas phase. The higher the pressure the higher the concentration of gas dissolved in the liquid phase. High pressure also decreases bubble diameter increasing the area for mass transfer. Enhancements of productivity and yield have been reported by so many authors [38], but not an enhancement in selectivity was found [39]. Operation pressure in most of the patents screened was in the range of 20.0 MPa.

Temperature influence is difficult to measure because it interferes with some many stages in the reaction (desired and undesired reactions, adsorption and desorption mechanism, gas solubility). Reaction temperature for direct synthesis has been studied in the range from $-10\text{ }^{\circ}\text{C}$ to $60\text{ }^{\circ}\text{C}$, and in function of the reaction conditions and system specifications a different optimum value was obtained [21, 40, 41].

1.3. **Direct synthesis: reactor configuration**

As it has been discussed in the previous sections, the production of hydrogen peroxide by direct synthesis is a complex process that needs a careful selection of the operational conditions in order to obtain successful results. Selection of the most appropriate reactor configuration (phase distributions) could help to reduce the mass transfer limitations, to increase the productivity and encourage the industrial implementation of the direct synthesis as a method for hydrogen peroxide production.

Most of the investigations at laboratory scale have been carried out using a stirred batch reactors since with this reactors is easy to obtain a huge amount of very precise experimental data, although the concentration of the liquid and gas phases change over the time, which could be measured carefully to ensure the kinetic analysis is correct. In general terms and in the context of an industrial production of hydrogen peroxide, the operation with continuous reactors is wished due to stable operations conditions are kept easily one the stationary state is reached. As the reaction for H_2O_2 production by direct synthesis is a three phase reaction, the selection of the reactor configuration is limited; slurry bubble column, trickle bed reactor and structured reactor are the main options and the most used reactor configurations.

1.3.1. *Slurry bubble column reactor (SBCR)*

Slurry bubble columns are reactors for what the solid is homogeneously dispersed in the liquid phase along the volume of the reactor. The gas phase is bubbled by a gas distributor situated in the bottom of the column what improve the bubble generation; the liquid phase could flow downwards or upwards as the reactor configurations was determinate. Industrial applications of slurry bubble columns are numerous and include applications related to oxidation, hydrogenations, chlorination, alkylation and polymerization reactions and biological processes as fermentations and wastewater treatment.

Slurry bubble columns reactors present some characteristics that could be beneficial for the development of the direct synthesis of hydrogen peroxide at industrial scale. The residence time of the gas phase is higher in comparison with semi – continuous stirred reactor, what ensure the total consumption of the reagents. Liquid phase can be considered perfectly mixed due to the turbulence caused by the gas bubbling, while the gas phase operates in plug flow model without back mixing effects. The combine effect of the turbulence and the big interphase area between the bubbles and the liquid phase improve the mass transfer process and consequently the reaction productivity. Turbulence and mixing have also a beneficial effect over the heat transfer and the control of the temperature of the reactions what have a special importance when, as happen in direct synthesis, the reactions involve in the process are highly exothermic. Main disadvantage of slurry bubble column is related with the catalyst. As the contact between the catalyst and the hydrogen peroxide causes its decomposition the solid must be recovered quickly at the liquid outlet. In the opposite of the trickle bed reactors or the batch stirred reactors, the volume of the reactor is mostly occupied by the liquid phase. So, the concentration of hydrogen peroxide that can be generated is low, unless the liquid residence time or the amount of hydrogen feed into the reactor will be increased.

None paper have been found in the open literature about the use of a slurry bubble column reactor to produce hydrogen peroxide direct synthesis, although Degussa AG has published a patent in what a slurry bubble columns reactor is proposed as a viable alternative to continuously production of H₂O₂ by direct synthesis [42].

1.3.2. Trickle bed reactor

Trickle bed reactors received that name because the liquid phase flows down intermittently, as drops or rivulets, wetting the solid particles. The solid phase fills the most of the reactor volume and its distribution could follow an organized model or not according to the system design (heterogeneous distribution of the active metal is possible). The reaction bed it is composed by the catalyst or by a mixture of the catalyst and an inert support. For the specific case of the direct synthesis of hydrogen peroxide the most advisable flow configuration is the co – current one because that way it is avoid the hydrogenation of the H_2O_2 just produced by the contact with a gas phase rich in hydrogen.

System hydrodynamics and flows have proved to be the key parameter to enhancement of the hydrogen peroxide productivity due to that the high contact area created by the dropping of the liquid over the solid particles improves the gas mass transference to the liquid phase. Because of that, in order to ensure that the hydrodynamic of the reactor is the adequate, the operation parameters must kept carefully inside the limits that guarantee that the system is operating on the selected flow regimen (according to Ranade *et al.* trickle flow regime is possible when gas and liquid phases Reynolds' number is kept lower than 10^3 [43]).

Trickle bed reactors are an excellent choice if a high concentration of hydrogen peroxide is required, because the liquid phase occupies a small portion of the total reactor volume. Two main drawbacks must be taken into account before the selection of reactor type trickle bed for H_2O_2 direct synthesis:

TBR are not the best alternative if an unstable catalyst is used or due to process conditions the reaction bed must be replace frequently because that would imply the reaction should stop.

Heat release and temperature control could be difficult if the reactor diameter is high. Hotspot could appear easily and lead a temperature runaway.

The capability of trickle bed reactors to support production of hydrogen peroxide by direct synthesis has been deeply studied by a researching group at Åbo Akademi University of Turku (Finland). The influence of the liquid and gas flow rate and different types of palladium catalysts were studied and values of hydrogen peroxide concentration up to 1.2 % wt were reported [40, 44, 45]. Also several patents about the industrial application of TBR's for hydrogen peroxide direct synthesis have been published [46].

1.4. Industrial production of H₂O₂ by direct synthesis: overview of patents

Since the direct synthesis of hydrogen peroxide was discovered and its statements were fixed, some many efforts to develop an industrial scale production have been done in many companies. In general terms about a 120 US patents and 40 international patents about the direct synthesis of hydrogen peroxide have been published from 1987 to 2004. Conditions and characteristics of patents have been modified along the time according to the new discoveries and limitations [47].

Almost about one hundred of patents were published form 1980s to 1990s. Hydrogen concentration of the gas phase was not always limited to the flammability region. DuPont [48] and others patents published during the 1980s – 1990s were operated within the explosive region. Explosion of the pilot scale plant at DuPont, the investigation of the direct synthesis as a viable alternative to hydrogen peroxide production was suspended since new catalysts and reactors configurations were carried out and the industrial interest of the direct synthesis of hydrogen peroxide rose again.

Table 3. Selected patents of H₂O₂ production by direct synthesis (1980 – 1990)

Company	Catalyst	H ₂ O ₂ , % wt.	Selectivity, %	Reaction Conditions
DuPont [48]	Pd – Pt (8 % Pt) Colloidal on alumina	19.6	69	136 bar, 5 – 8 °C, 18 % H ₂ in O ₂ , aqueous acid solution (0.1 N HCl)
ENI [49]	1 % Pd – 0.1 % Pt on carbon	7.3	74	100 bar, 8 °C, (autoclave, after 600 h), 3.6% H ₂ , 11% O ₂ and inert, 95:5 methanol:H ₂ O solution (+ additives)
BASF [50]	Pd on monolith	7.0	84	144 bar, 10 % H ₂ in O ₂ , methanol (+ additives)
HTI [51]	Pd(-Pt) on carbon black (140 m ² ·g ⁻¹)	9.1 (276 g·g Pd ⁻¹ ·h ⁻¹)	99	120 bar, 35°C, (autoclave after 600 h), 3 % H ₂ in air, solvent with additives not indicated
Degusa [52]	2.5 % Pd – Au (95:5) on α – Al ₂ O ₃	5.1 (13.8 g·g Pd ⁻¹ ·h ⁻¹)	72	50 bar, 25 °C (tricked bed), 3 % H ₂ , 20 % O ₂ , methanol (+ additives)

Low hydrogen concentration on the gas phase avoids the explosion risk but also reduced the maximum productivity that could be reached. Because of that, some patents proposed new reactor models that allow working with high global hydrogen concentration without the explosion risk. Advanced Peroxide Technology and Princeton Advanced Technology [53, 54] patented a novel reaction configuration center on the dispersion of tiny bubbles of oxygen and hydrogen in enough liquid phase to eliminate any runaway reaction. BASF [50] also patented a

method to produce hydrogen peroxide using a hydrogen concentration within the flammability limits. In that case the reactor was formed by a layer of a woven catalyst monolith and between them the hydrogen was fed, oxygen was fed from the bottom of the reactor, where a gas diffuser is used to generate fine bubbles and the need for mixing turbulence.

Independently of the reaction configuration the operation inside the flammability limits is dangerous especially for large scale reactors. Microreactors are a good alternative since the high surface to volume ratio allows the quenching of the radical reactions. Cost of production at high scale is too high and some problems related to plugging of the microchannels reduce the chances of a high scale implementation. FMC has developed a microreactor able to produce more than 2 % wt. of H_2O_2 in a single channel reaction and it is still working on the process optimization to obtain a pilot plant to achieve a 5 % wt. H_2O_2 concentration stream [55]. Microreactors have also been shown as an alternative for the gas phase epoxidation of propene using in situ produced hydrogen peroxide [56, 57].

Degussa Headwaters, completed in 2007 the first experimentation phase of the demonstration plant for direct synthesis of H_2O_2 and announced the start of the design/construction of a 200,000 tons per year plant in 2008.

Last decade patents are focused on catalyst preparation and improvement of the reaction conditions with especially attention to the safety considerations.

- Palladium is the typically most used metal on catalyst for hydrogen peroxide direct synthesis. Palladium doped with other noble metal (Pt or Au) improved the selectivity. Brill [58] patented the method for production of H_2O_2 at high pressure (40 – 150 bar) in an acidic aqueous solution using a noble metal supported catalyst. Gosser *et al.* [48] stated that doping the catalyst with Pt the activity of the catalyst was increased and consequently the amount of H_2O_2 was maximized.
- Even if the maximum hydrogen concentration was limited by the flammability limits the composition of the gas phase has proved to be determinant for the success of the process. Izumi *et al.* [59] showed up that the optimal ratio of O_2 to H_2 must be compressed between 5 to 20. Huckins [60] patented a continuous process to operate within the explosive region but with a special inner design to avoid explosion conditions. Also it has been reported trickle bed reactor system in which it is possible to use 5 % H_2 and 60 % O_2 [61], although this is only possible when aqueous solutions are

used since the explosions risks of the methanol – H₂ – O₂ mixtures is too high to operated inside the flammability limits.

- The use of organic solvents, or mixtures of water and organic solvent, could increase the productivity and the catalyst life time. Dalton and Skinner [62] concluded that the use of methanol, acetone or acetonitrile could improve the hydrogen peroxide production. Use of methanol as solvent increased one order of magnitude the productivity. Zhou *et al.* [63] obtained a productivity of 900 g H₂O₂·g Pd⁻¹·h⁻¹ when methanol and NaBr, as promoter, were used. Only 400 g H₂O₂·g Pd⁻¹·h⁻¹ was obtained when no NaBr was added to the liquid phase.

Some of the patents published are summarized on Table 4 [47]. As it can be seen the catalyst productivity is not reported frequently and the comparison of the results obtained by the different researching is complicated. In general terms it could be statement that H₂ conversion was typically low, between 30 % to 70 %, and on consequence the recycling of the H₂ would be necessary. The sequential addition of hydrogen to keep uniform the ratio O₂:H₂ has proved to be beneficial to the productivity. Operation pressure varied from 50 – 100 bar, and temperature fixed on the patents analyzed was comprise between 4 °C to 605 °C.

The use of non – corrosive solutions has been also one of the main interest points on the patents. Relative high acid concentration could have a promoting effect for hydrogen peroxide production but also it could create corrosion problems.

Reference	CSIR	Degussa	Repsol	ENI	Headwaters	Headwaters	ENI	BASF	Arkema	Degussa	Headwater	Polymeri Eur.
Main feature	Halogen as promoter in the catalyst	Contact time limited to avoid corrosion	Non corrosive sol., use metal supported on an acid halogen free resin	Sequence of deposition Pd and Pt on sulfonated carbon	Controlled surface coordination catal., water soluble organic additives	Staged or sequential feed of H ₂	Use of polyolefin additives to improve performance	Electroless deposition of Pd and Pt on steatite	Aq. Solution + surfactants	Non-explosive mixture, trickle bed reactor, Pd – Au catal.	Controlled coordination of catal. Solvent selection of parameters	Prod. concn. H ₂ O ₂ with stage evap./distill
Catalyst	Pd (5%) on alumina	0.25% wt Pd – Au (95:5) on α – alumina	1.5 % Pd on Lewatit KZ641	Pd (1%) + Pt (0.1%) on carbon	Pd – Pt/C (from resin)	0.75 % Pd on carbon	Pd (1%) – Pt(0.33%)/carbon funct. with SO ₃ H and polyST	Pd – Pt on steatite	0.7 Pd% - 0.03% Pt on silica	Pd – Au (95:5) on α – alumina.	1 % Pd + 0.02 % Pt on carbon black	Pd – Pt/ carbon
H₂O₂ % wt.	0.72	5.2	5.8	6.6	1.25	10	5.9	10.2	10.7	5.1	2.5	6.8 – 7.2
Select, %	41	74	77	76	56	90	80	72	92	72	91	72 – 75
Gas phase composition (H₂ – O₂ %)	50 – 50	3 – 20	2 – 48	3.6 – 10	3.3 – 20	Note	3.6 – 11	3 – 97	4 – 96	3 – 20	3 – 97	3.6 – 13
P (bar); T (°C)	1; 30	50; 25	100; 40	100; 6	51; 35	28; 45	60; 25	50; 40	63; 60	50; 25	97; 35	130; 4
Solvent	Aq. (+ Br ⁻ , H ₃ PO ₄)	Methanol (+ Br ⁻ , H ₃ PO ₄)	Methanol – water (95:5) + 12 ppm HBr	Methanol – water (95:5) + 9 ppm HBr + 300 ppm H ₂ SO ₄	Aq. + 1% H ₂ SO ₄ + 5 ppm NaBr + 2% methanol	Methanol, 1 % H ₂ SO ₄ + 5 ppm NaBr	Methanol – water (95:5) + 6 ppm HBr + 200 ppm H ₂ SO ₄	Aq. Sol. + H ₃ PO ₄ + HBr	Aq. Sol. + 3.4 % H ₃ PO ₄ + 90 ppm NaBr, 5 ppm Br ₂ + 5 mg surfactant	Methanol + 2 ppm NaBr + 100 ppm H ₂ SO ₄	Methanol, 1 % H ₂ SO ₄ + 5 ppm NaBr	Methanol – water (95:5) + 4 ppm HBr + 200 ppm H ₂ SO ₄
Notes	2h, 14.1 g H ₂ O ₂ ·gPd ⁻¹ ·h ⁻¹	2 h	50h, deposition first Pd then Pt,	50% H ₂ – 50 O ₂ , 2.3% H ₂ O ₂ and 60 % select.	O ₂ :H ₂ ratio about 2 per stage, 17 % O ₂ excess on overall basis	50 h	C ₆ F ₁₃ C ₂ H ₅ SO ₃ H as surfactant	10 h, 67% H ₂ conv.	150 h, 40 % H ₂ conv.	110 h, conc. H ₂ O ₂ 60 % after 2h distillation		

Table 4. Summarized recent H₂O₂ direct synthesis patents

1.5. Conclusions

Hydrogen peroxide direct synthesis seems to be an attractive alternative to high scale traditional production process. Direct synthesis from H₂/O₂ has some characteristics that made it a good alternative to hydrogen peroxide production. No by – products are generated during the reaction, so purification or separations steps are not needed. As direct synthesis process could be feasible a low production scale the transportation of the H₂O₂ from the production plants to the consumption point is not necessary and the transportation risks are eliminated.

As the huge amount of published papers and patents demonstrate, great efforts has been made in order to determinate and understand the mechanism of the reaction and the processes that controls the hydrogen peroxide production. Combination of the active metal and the support that constitute the catalyst and the specific characteristics of the solid (size of the particle, oxidation state of the active metal) have been statement as the key parameter for a successful production of hydrogen peroxide. Also the influence of the reaction conditions, liquid and gas phase solvent, kind and concentration of the promoters were studied. To determine the optimum operation range for each kind of catalyst available for DS is essential to de development of the bases of the process. In the chapters that form this thesis, the investigation have been focus on the observation of the global reaction process and its rules of behavior, and because of this only one catalyst have been studied.

Although the research at laboratory scale has established the base of the hydrogen peroxide by direct synthesis, the development of the direct synthesis as an alternative to the auto – oxidation process and its implementation at industrial scale is still needed of a further investigation. Selection of the optima conditions for reaction at industrial scale and the development of the process in a continuous reactor are the main targets of the current lines of investigation. Because of its characteristics (hydrodynamic regime, distribution of the phases, *etc.*) the slurry bubble column and the trickle bed reactors have been selected as feasible alternatives for continuous hydrogen peroxide production.

References

1. Garcia-Serna, J., et al., *Engineering in direct synthesis of hydrogen peroxide: targets, reactors and guidelines for operational conditions*. Green Chemistry, 2014.
2. Biasi, P., Garcia Serna J., Salmi T., Mikkola J.P., *Hydrogen peroxide direct synthesis: enhancement of selectivity and production with non - conventional methods*. Chemical Engineer Transactions, 2013. **32**: p. 673 - 678.
3. Sierra-Pallares, J., et al. *Flammability limits estimation in high pressure systems. application to supercritical reactors*. in *GPE-EPIC, 2nd International Congress on Green Process Engineering and 2nd European Process Intensification Conference*. 2009. Venice (Italy).
4. Dissanayake, D.P. and J.H. Lunsford, *Evidence for the Role of Colloidal Palladium in the Catalytic Formation of H₂O₂ from H₂ and O₂*. Journal of Catalysis, 2002. **206**(2): p. 173-176.
5. Dissanayake, D.P. and J.H. Lunsford, *The direct formation of H₂O₂ from H₂ and O₂ over colloidal palladium*. Journal of Catalysis, 2003. **214**(1): p. 113-120.
6. Li, G., et al., *Direct synthesis of hydrogen peroxide from H₂ and O₂ and in situ oxidation using zeolite-supported catalysts*. Catalysis Communications, 2007. **8**(3): p. 247-250.
7. Olivera, P.P., E.M. Patrito, and H. Sellers, *Hydrogen peroxide synthesis over metallic catalysts*. Surface Science, 1994. **313**(1-2): p. 25-40.
8. Li, G., et al., *Direct synthesis of hydrogen peroxide from H₂ and O₂ using zeolite-supported Au catalysts*. Catalysis Today, 2006. **114**(4): p. 369-371.
9. Edwards, J.K., et al., *Au-Pd supported nanocrystals as catalysts for the direct synthesis of hydrogen peroxide from H₂ and O₂*. Green Chemistry, 2008. **10**: p. 388-394.
10. Li, G., et al., *Direct synthesis of hydrogen peroxide from H₂ and O₂ using zeolite-supported Au-Pd catalysts*. Catalysis Today, 2007. **122**(3-4): p. 361-364.
11. Ishihara, T., et al., *Synthesis of hydrogen peroxide by direct oxidation of H₂ with O₂ on Au/SiO₂ catalyst*. Applied Catalysis A, 2005. **291**(1-2): p. 215-221.
12. Abate, S., et al., *Performances of Pd-Me (Me = Ag, Pt) catalysts in the direct synthesis of H₂O₂ on catalytic membranes*. Catalysis Today, 2006. **117**(1-3): p. 193-198.
13. Hâncu, D. and E.J. Beckman, *Generation of hydrogen peroxide directly from H₂ and O₂ using CO₂ as the solvent*. Green Chemistry, 2001. **3**: p. 80-86.
14. Burch, R. and P.R. Ellis, *An investigation of alternative catalytic approaches for the direct synthesis of hydrogen peroxide from hydrogen and oxygen*. Applied Catalysis B, 2003. **42**(2): p. 203-211.

15. Liu, Q., et al., *The Active Phase in the Direct Synthesis of H₂O₂ from H₂ and O₂ over Pd/SiO₂ Catalyst in a H₂SO₄/Ethanol System*. Catalysis Letters, 2009. **132**(3): p. 342-348.
16. Melada, S., et al., *Direct synthesis of H₂O₂ on monometallic and bimetallic catalytic membranes using methanol as reaction medium*. Journal of Catalysis, 2006. **237**(2): p. 213-219.
17. Edwards, J.K., et al., *Comparison of supports for the direct synthesis of hydrogen peroxide from H₂ and O₂ using Au–Pd catalysts*. Catalysis Today, 2007. **122**(3-4): p. 397-402.
18. Ntainjua, E., et al., *The role of the support in achieving high selectivity in the direct formation of hydrogen peroxide*. Green Chemistry, 2008. **10**: p. 1162-1169.
19. Blanco-Brieva, G., E. Cano-Serrano, and J.M. Campos-Martin, *Direct synthesis of hydrogen peroxide solution with palladium-loaded sulfonic acid polystyrene resins*. Chemical Communications, 2004: p. 1184-1185.
20. Pospelova, T.A., N.I. Kobozev, and E.N. Eremin, *Palladium catalyzed synthesis of hydrogen peroxide from its elements. I. Conditions for the formation of hydrogen peroxide*. Russian Journal of Physical Chemistry, 1961. **35**(2): p. 143-147.
21. Choudhary, V.R., C. Samanta, and P. Jana, *Hydrogenation of hydrogen peroxide over palladium/carbon in aqueous acidic medium containing different halide anions under static/flowing hydrogen*. Industrial and Engineering Chemistry Research, 2007. **46**(10): p. 3237-3242.
22. Blanco-Brieva, G., et al., *Direct synthesis of hydrogen peroxide on palladium catalyst supported on sulfonic acid-functionalized silica*. Green Chemistry, 2010. **12**(7): p. 1163-1166.
23. Choudhary, V.R., C. Samanta, and T.V. Choudhary, *Influence of nature/concentration of halide promoters and oxidation state on the direct oxidation of H₂ to H₂O₂ over Pd/ZrO₂ catalysts in aqueous acidic medium*. Catalysis Communications, 2007. **8**(9): p. 1310-1316.
24. Menegazzo, F., et al., *Effect of the addition of Au in zirconia and ceria supported Pd catalysts for the direct synthesis of hydrogen peroxide*. Journal of Catalysis, 2008. **257**(2): p. 369-381.
25. Menegazzo, F., et al., *Influence of the preparation method on the morphological and composition properties of Pd-Au/ZrO₂ catalysts and their effect on the direct synthesis of hydrogen peroxide from hydrogen and oxygen*. Journal of Catalysis, 2009. **268**(1): p. 122-130.
26. Landon, P., et al., *Direct synthesis of hydrogen peroxide from H₂ and O₂ using Pd and Au catalysts*. Physical Chemistry Chemical Physics, 2003. **5**: p. 1917 - 1923.

27. Toebes, M.L., J.A. van Dillen, and K.P. de Jong, *Synthesis of supported palladium catalysts*. Journal of Molecular Catalysis A: Chemical, 2001. **173**(1–2): p. 75-98.
28. Solar, J.M., et al., *On the importance of the electrokinetic properties of carbons for their use as catalyst supports*. Carbon, 1990. **28**(2-3): p. 369-375.
29. Edwards, J.K., et al., *Switching Off Hydrogen Peroxide Hydrogenation in the Direct Synthesis Process*. Science, 2009. **323**(5917): p. 1037-1041.
30. Moreno Rueda, T., J. García Serna, and M.J. Cocero Alonso, *Direct production of H₂O₂ from H₂ and O₂ in a biphasic H₂O/scCO₂ system over a Pd/C catalyst: Optimization of reaction conditions*. The Journal of Supercritical Fluids, 2012. **61**(0): p. 119-125.
31. Edwards, J.K., et al., *Switching Off Hydrogen Peroxide Hydrogenation in the Direct Synthesis Process*. Science, 2009. **323**(5917): p. 1037-1041.
32. Krishnan, V.V., A.G. Dokoutchaev, and M.E. Thompson, *Direct production of hydrogen peroxide with palladium supported on phosphate viologen phosphonate catalysts*. Journal of Catalysis, 2000. **196**(2): p. 366-374.
33. Han, Y. and J. Lunsford, *Direct formation of HO from H and O over a Pd/SiO catalyst: the roles of the acid and the liquid phase*. Journal of Catalysis, 2005. **230**(2): p. 313-316.
34. Liu, Q., et al., *Direct synthesis of H₂O₂ from H₂ and O₂ over Pd–Pt/SiO₂ bimetallic catalysts in a H₂SO₄/ethanol system*. Applied Catalysis A: General, 2008. **339**(2): p. 130-136.
35. Liu, Q. and J. Lunsford, *The roles of chloride ions in the direct formation of H₂O₂ from H₂ and O₂ over a Pd/SiO₂ catalyst in a H₂SO₄/ethanol system*. Journal of Catalysis, 2006. **239**(1): p. 237-243.
36. Abate, S., et al., *SBA-15 as a support for palladium in the direct synthesis of H₂O₂ from H₂ and O₂*. Catalysis Today, 2011. **169**(1): p. 167-174.
37. Abate, S., S. Perathoner, and G. Centi, *Deactivation mechanism of Pd supported on ordered and non-ordered mesoporous silica in the direct H₂O₂ synthesis using CO₂-expanded methanol*. Catalysis Today, 2012. **179**(1): p. 170-177.
38. Moreno, T., et al., *Direct synthesis of H₂O₂ in methanol at low pressures over Pd/C catalyst: Semi-continuous process*. Applied Catalysis A: General, 2010. **386**(1-2): p. 28-33.
39. Freakley, S.J., et al., *Effect of Reaction Conditions on the Direct Synthesis of Hydrogen Peroxide with a AuPd/TiO₂ Catalyst in a Flow Reactor*. ACS Catalysis, 2013. **3**(4): p. 487-501.
40. Biasi, P., et al., *Kinetics and Mechanism of H₂O₂ Direct Synthesis over a Pd/C Catalyst in a Batch Reactor*. Industrial & Engineering Chemistry Research, 2012. **51**(26): p. 8903-8912.

41. Gemo, N., et al., *Mass transfer and kinetics of H₂O₂ direct synthesis in a batch slurry reactor*. Chemical Engineering Journal, 2012. **207**: p. 539-551.
42. Haas, T. and R. Jahn, *Process for the production of hydrogen peroxide*. 2008, Degussa AG: United States.
43. Ranade, V.V., R. Chaudhar, and P.R. Gunjal, *Trickle Bed Reactors: Reactor Engineering & Applications*. 2011, Oxford: Elsevier.
44. Biasi, P., et al., *Direct synthesis of hydrogen peroxide in water in a continuous trickle bed reactor optimized to maximize productivity*. Green Chemistry, 2013. **15**(9): p. 2502-2513.
45. Biasi, P., et al., *Hydrogen Peroxide Direct Synthesis: Selectivity Enhancement in a Trickle Bed Reactor*. Industrial & Engineering Chemistry Research, 2010. **49**(21): p. 10627-10632.
46. Gosser, L.W. and J.-A.T. Schwartz, *Catalytic process for making hydrogen peroxide from hydrogen and oxygen employing a bromide promoter* 1988.
47. G. Centi, S. Perathoner, and S. Abate, *Direct Synthesis of Hydrogen Peroxide: Recent Advances.*, in *Modern Heterogeneous Oxidation Catalysis*, W.-. VCH, Editor. 2009.
48. Gosser, L.W. and J.A.T. Schwartz, *Hydrogen peroxide production method using platinum/palladium catalysts*. 1989, Du Pont de Nemour & Co. (S).
49. Papparatto, G., et al., *Process for the continuous production of hydrogen peroxide*. 2003, Eni and Enichem (Italy).
50. Fischer, M., et al., *Process for the manufacture of hydrogen peroxide*. 2002, BASF (Germany).
51. Zhou, B. and L.K. Lee, *Catalyst and process for direct catalytic production of hydrogen peroxide, (H₂O₂)*. 2001, Hydrocarbon Techn. Inc. (US).
52. Haas, T., G. Stochniol, and J. Rollmann, *Direct synthesis of hydrogen peroxide and integration thereof into oxidation processes* 2006, Degussa AG (Germany).
53. Huckins, H., *Method for producing hydrogen peroxide from hydrogen and oxygen*. 1998, Advanced Peroxide Technology (US).
54. Harold, H., *Method for producing hydrogen peroxide from hydrogen and oxygen*. 2003, Princeton Advanced Techn. (US).
55. in *Chem. & Eng. News*. 2004.
56. Brasse, C. and B. Jaeger, *Degussa Science Magazine*, 2006. **17**(4).
57. Zhou, B. in *US EPA Presidential Green Chemistry Award*. 2007.
58. Brill, W.F., *Preparation of hydrogen peroxide*. 1987, Halcon SD Group (US).

59. Izumi, Y., H. Miyazaki, and S. Kawahara, *Process for producing hydrogen peroxide*. 1981, Toyuyama Soda Ka. Ka. (Japan).
60. Huckins, H.A., *Method for producing hydrogen peroxide from hydrogen and oxygen*. 2004, Advanced Peroxide Techn. (US).
61. Delattre, V., et al., *Process for the manufacture of hydrogen peroxide by direct synthesis from hydrogen and oxygen*. 1996, Solvay (Belgium).
62. Dalton, J.A.I., E.J. Greskovich, and R.W. Skinner, *Process for producing hydrogen peroxide* 1982.
63. Zhou, B., M. Rueter, and S. Parasher, *Supported catalysts having a controlled coordination structure and methods for preparing such catalysts*. 2006, Headwaters Nanokinetix Inc. (US).

Table Captions

Table 1. Auto – oxidation and direct synthesis comparison.....	62
Table 2. Reactions of direct synthesis of hydrogen peroxide.....	64
Table 3. Selected patents of H ₂ O ₂ production by direct synthesis (1980 – 1990).....	74
Table 4. Summarized recent H ₂ O ₂ direct synthesis patents.....	75

Figure Captions

Figure 1. Distribution of the world market of hydrogen peroxide production (kt/year).....	61
Figure 2. Anthraquinone reaction route for hydrogen peroxide synthesis.....	62
Figure 3. Scheme of reaction of hydrogen peroxide’s direct synthesis.....	63
Figure 4. Mass transfer phenomena in direct synthesis reaction process.....	65

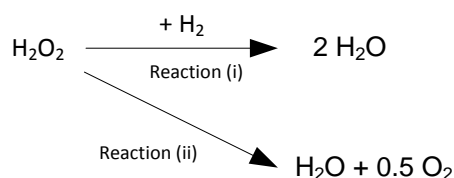
CHAPTER II

Hydrogenation and decomposition kinetic study of H₂O₂ over Pd/C catalyst in an aqueous medium at high CO₂ pressure

Hydrogenation and decomposition of H₂O₂ cause an undesired decrease in selectivity when producing H₂O₂ over Pd/C catalysts via direct synthesis. Hydrogenation accounts for more than 70-85% of the decrease in selectivity itself, which means that the rate of hydrogenations is 3-4-fold the decomposition rate. In this study we have studied the operational interval for H₂O₂ concentration (1 to 10% wt/v) temperature (23 to 50 °C), pH (2 to 3.8), halide to active metal ratio (1.5 to 8.0), catalyst amount and palladium loading (1, 3 and 5%wt Pd/C) at 80 bar using CO₂ as inert gas. A kinetic model coupling both decomposition and hydrogenation was fit to the results of a semicontinuous reactor achieving average deviations lower than 5% in most cases. Using the righty proportion of promoters the activation energies obtained were $E_{ad}=18803.6$ J/mol (decomposition) and $E_{ah}=7746.2$ J/mol. The order of reaction for decomposition respect to H₂O₂ was 1.031 and with hydrogenation -0,161. Turn Over Frequencies of decomposition and hydrogenation rates between 0.31 to 9.62 mol_{H₂O₂}·h⁻¹·molPd⁻¹ and 1.39 to 23.01 mol_{H₂O₂}·h⁻¹·molPd⁻¹ respectively have been observed in this study.

2.1. Introduction

Hydrogen peroxide disappears during direct synthesis following to undesired reactions paths, *i.e.* decomposition and hydrogenation. These reactions decrease H₂ selectivity towards H₂O₂ and causes an increase in the OpEx of the process. The direct coproduction of H₂O also decreases selectivity (see Scheme 1). A number of studies have determined the kinetics of both reactions at low pressures and low H₂O₂ concentrations; however, the direct synthesis at industrial scale will only be feasible at high pressures to overcome mass transfer limitations. Moreover, many authors state that hydrogenation is the principal cause of loss of selectiveness, while this is only true at low H₂O₂ concentrations, as we demonstrate in this work.



Scheme 1. Hydrogenation (i) and decomposition (ii) reactions scheme.

Voloshin and Lawal,[1] studied the kinetics of the global reaction in a microreactor, of 765 μm ID and a length of 4 to 6 cm long, which was packaged with a 2% Pd on PiO_2 catalyst. The model developed to predict the performance of the reactor included the mass transfer, as it required low gas flow rates to achieve a sufficiently high peroxide concentration (ca. 1% w/w). Volsohin's modeling assumed that the phases behave according to a Taylor – type flow model, although the observations of experimental data indicate that Taylor model is only an approximation to the actual flow regime that exists in these reactors. Comparing experimental values (30 to 50 ° C, 7 to 30 mg of catalyst, 3 to 20 bar, 10 ppm NaBr) with the simulated data, it was found that despite the simplifications the fit was good enough, 10% difference between experimental and model data. Despite the low error obtained between the experimental and modeling, the model is limited by the conditions of operation (only valid for gas liquid ratio of 440, measured at standard pressure and temperature).

Deguchi and Iwamoto [2] has developed perhaps one of the most comprehensive kinetic models for low pressures. The reaction was carried out in a 300 mL flask glass perfectly agitated using a magnetic stirred. The catalyst 5% Pd / C has a particle size of about 20 micron. All experiments were performed at atmospheric pressure and temperature of 30 ° C approximately. HBr was

added to the reaction medium, final concentration 0.001 N, as a promoter. The hydrogen partial pressure is between 0.026 – 0.176 bar, oxygen partial pressure between 0.140 and 0.926 bar.

This model includes the mass transfer of hydrogen from the gas phase to the solid surface, the process of adsorption and desorption of products and reactants. The model has been developed for a stirred tank system. The effect of agitation, catalyst pretreatment and partial pressure of oxygen and hydrogen was included. Rate of consumption of hydrogen obtained with this model (18.5 mmol L⁻¹h⁻¹ for hydrogen partial pressure of 0.076 kPa and oxygen partial pressure of 0.156 kPa), remains constant throughout the reaction, which implies that neither catalyst losses effectiveness nor concentration of H₂O₂ affects H₂ consumption.

Most viewed articles in the literature study the direct synthesis reaction using the global observed rate, without differentiating each separate reaction, or in contrast, they do deal only with the decomposition and hydrogenation as single reactions.

Choudhary *et al.* studied intensively, with different catalysts, Pd (5%wt) over carbon [3], decomposition and hydrogenation reactions, focusing on the inhibitory effect of the promoters. The system consisted in a glass reactor of 0.250 L capacity, although the volume of the aqueous phase is 0.150 L, 100 mg of catalyst, different for each study is added to the liquid phase before starting the experiment. The temperature was kept constant using a water bath and all the experiments were performed at atmospheric pressure.

In the absence of proton or presence of F⁻, the hydrogen peroxide concentration decreases very quickly, predominantly the decomposition reaction to hydrogenation (70% of the conversion of peroxide is due to decomposition). Chloride and bromide anions, in acid medium, reduced the effect of decomposition, and the % H₂O₂ decreases slowly due only to the hydrogenation. The rate of hydrogenation decreased with increasing concentration of halide in general.

From the experimental data, under static H₂, Choudhary *et al.* [3] obtained values of reaction order, 1 and 0 respectively for the decomposition and hydrogenation, and values of activation energy (chloride: E_a = 20.61 kJ·mol⁻¹; bromide: E_a = 27.10 kJ·mol⁻¹) and frequency factor (chloride: A = 3.17 x 10⁴ h⁻¹; bromide: A = 3.82 x 10⁵ h⁻¹). Values of activation energy and frequency factor were higher in experiments with Br⁻ than in which Cl⁻ is used.

In experiments in which a steady stream of H₂ was fed to the reactor, the decomposition prevailed over hydrogenation at lower chloride concentrations as 2.7 mmol·L⁻¹. When using bromide as a promoter, even low concentrations from 0.18 to 0.54 mmol·L⁻¹, hydrogenation prevails. In both cases, hydrogenation order reaction was zero to hydrogen peroxide

concentration, and reaction rate is decreased with increasing halide concentration [3]. Cation associated with bromine or chloride anion had a little effect on the H₂O₂ destruction. For the Pd/C the rate of consumption of hydrogen varied between 8.0 %·h⁻¹ (when using HCl) and 8.6%·h⁻¹ (when using NH₄Cl).

Edwards *et al.* [4], studied the role of the catalyst support and stated that the proper selection of it and its treatment can improved the catalytic efficiency towards direct synthesis. For several catalysts, using gold/palladium mixtures as active metals may be reduced activity compared to the hydrogenation using acid pretreatment on the support before impregnating with the metal. Productivity of catalyst was measured examining the stability of higher concentrations of H₂O₂. Solutions of H₂O₂ were stirred at high pressure H₂ (5% H₂/CO₂, 30 bar) in the presence of the support or the catalyst (10 mg) for 30 min at 2 °C. The selectivity to H₂O₂ increased from 80% to 98% for catalyst Au – Pd, after treatment with nitric acid. Productivity rised from 110 mol kg⁻¹ h⁻¹ to 160 mol kg⁻¹ h⁻¹. Thanks to these pretreatment is favoured nucleation of small (2 – 5 nm) particles, Pd – rich alloy, and intermediate (10 to 50 nm) Au – Pd homogeneous alloy particles, compared to other larger composed of gold – rich alloys. The improvement in selectivity was maintained regardless of the time the catalyst was used. But for the catalysts of Pd (productivity increase from 50 to 52 mol kg⁻¹ h⁻¹) or Au monometallic (0.5 mol kg⁻¹ h⁻¹) acid treatment has no appreciable effect.

The aim of this research is to determine the effect of operating conditions, catalyst quantity and concentration of promoters in the hydrogenation and decomposition reactions at high CO₂ pressures, modelling the process to obtain the kinetic parameters.

2.2. Experimental

2.2.1. Materials and Methods

The catalyst used in this study was fine particles with an average of 1, 3 and 5 wt% Pd over carbon support purchased form Aldrich and used fresh for each experiment. It has been selected because it has been used by Moreno *et al.* in previous works [5 – 7] and the activity and stability are acceptable. Bulk and surface properties of fresh 5 wt. % Pd/C catalyst and TEM and SEM analysis can be found in bibliography references [5].

H₂O₂ 33 wt/v%, reagent grade, was purchased from Sigma Aldrich and used to prepare the starting solution. NaBr and H₃PO₄ (PRS – Codex, Panreac Química S.A.U) were used as promoters.

In order to determine the initial concentration of H₂O₂, KI (PRS – Codex, Panreac Química S.A.U), H₂SO₄ (PA – ISO, Panreac Química S.A.U) and Na₂S₂O₃·5H₂O (PA – ACS, Panreac Química S.A.U), were used for conventional iodometric titration [8].

Research grade hydrogen and industrial grade carbon dioxide were purchased from Carburos Metálicos (Spain) and used without further modification.

2.2.2. Experimental Set – up and procedure

All tests were carried out at 80 bar and different temperatures in a 0.350 L AISI 316 SS stirred reactor described elsewhere [6] operating in batch in the liquid phase and continuous in the gas phase (assuring a constant concentration and pressure in gas phase during each experiment). Reaction pressure was controlled by an EL – FLOW Bronkhorst® back pressure regulator. Hydrogen flowrate was controlled by EL – FLOW Bronkhorst® model F – 231M Mass Flow Controller for high pressure applications. Temperature was measured using internal thermocouples and datalogged automatically using PicoTech TC – 08. The initial mixture consisted of 0.1 L aqueous solution aprox. 3.0 wt/v % H₂O₂, with promoters, *i.e.* NaBr and H₃PO₄. Initial concentration of hydrogen peroxide was determined by iodometric titration. Then the catalyst was added and the system (for this study we have used fresh catalyst for each experiment). During the addition of the catalyst O₂ release is clearly visible in the reactor, this is because as the catalyst is fresh it decomposes quite fast several mmol of H₂O₂ and then behaves in a stable way. This is the only pretreatment that we do to the catalyst. We have measured this decomposition in all experiments but we do not include the values in the manuscript because it introduces confusion as the behaviour is unpredictable. It normally causes a sudden decomposition between 5 and 20% of the initial H₂O₂. The experiments started after this conditioning period (*i.e.* 2 to 5 min maximum), in which the system was pressurized with CO₂ until 80 bar, which implies that the “gas phase” is in near – critical conditions.

To separate the effect of decomposition and hydrogenation reactions, each experiment was divided into two distinct steps. In the first part, with a minimum duration of 45 minutes, no hydrogen was fed, so only the decomposition reaction occurred. After the decomposition stage, hydrogen was fed into the reactor at a constant flow rate. In this second stage, in addition to the decomposition reaction, hydrogenation of H₂O₂ takes place. The experiments were stopped either by achieving complete a reaction or 180 minutes. Hydrogen peroxide was quantified by i – Raman spectroscopy [9] and iodometric titration.

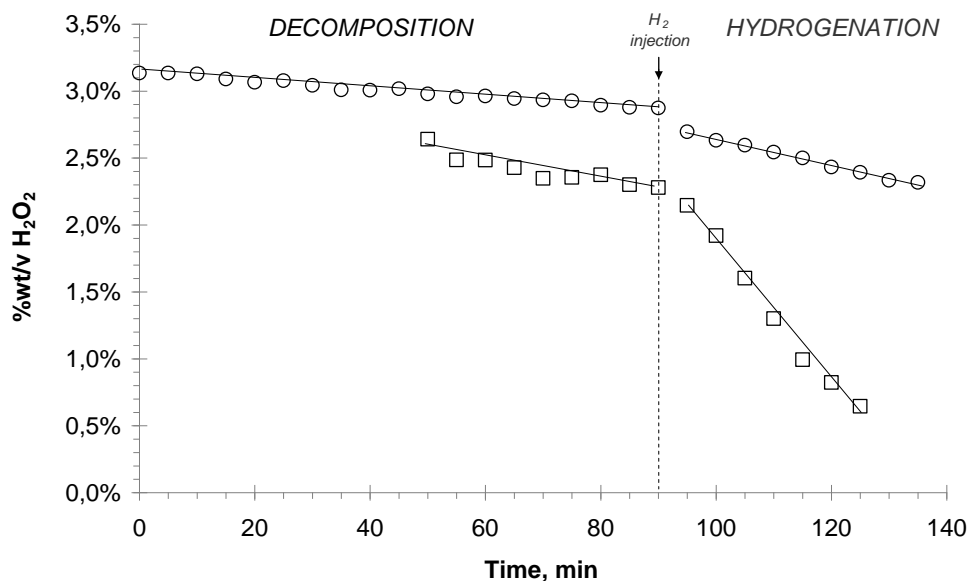


Figure 1. Effect of pH on H₂O₂ decomposition – hydrogenation rate (exp # 1, 22). 40 °C, 100 mg 5% Pd/C, 100 mL, 3 %wt/v H₂O₂ initial, Br⁻/Pd = 8, 80 bar CO₂. ○ pH = 2; □ pH = 3.8.

2.3. Mathematical model

2.3.1. Mechanism

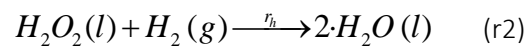
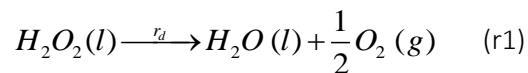
Palladium is an advantageous active metal for H₂O₂ production but, as it has been extensively demonstrated, at the same time the palladium sites produce undesired side reactions; in this case the H₂O₂ decomposition and H₂O₂ hydrogenation. These undesired reactions are one of the decisional drawbacks that keep H₂O₂ direct synthesis technology outside the industrial battle field. A low conversion can be overcome by recycling but low selectivity causes extensive OpEx costs in H₂ side. Understanding these reactions will aid H₂O₂ technology.

It must be considered the difficulty of separating the effects of decomposition and hydrogenation with respect to hydrogen and oxygen, and more important, that the four reactions may affect each other. In this work H₂O₂ is exposed to a gas phase containing only hydrogen and an inert gas (*i.e.* CO₂). The only oxygen present in the system will come from the decomposition reaction, but the quantity will be almost negligible in terms of reaction. It has to be considered that the presence of oxygen in similar quantities than H₂ can modify the decomposition and hydrogenation path inhibiting the reaction somehow, as the O₂ can attach to active sites, thus reducing decomposition and hydrogenation rates. Nevertheless, the study of the four reactions at the same time is difficult as the activation energies create optimization problems. So in this work we have studied the decomposition reaction independently and, afterwards, decomposition

and hydrogenation together to obtain a set of parameters valid for a subsequent H₂O₂ production study.

Based on previous works [5, 7, 10] we have prepared a model to explain the decomposition with subsequent hydrogenation at near – critical conditions. The reactor is considered to be a perfectly mixed reactor in the liquid phase. The quantity of catalyst is negligible (between 0.0075 and 0.2 % wt.), so the system behaves like a pure liquid – gas phase system. The system is modelled simplifying the transport phenomena by assuming two steps mass transfer from bulk gas to catalyst active site and surface catalytic reaction. These two steps are in series, so, in a pseudo – steady state, the rate of each step relies on the other. The limitations to mass transfer between the liquid phase and the catalyst are neglected due to the low diameter of the catalyst particles. Furthermore, the limitations to mass transfer in the gas phase are neglected too provided H₂ is in excess (as the H₂ conversion is lower than 25% in all runs), so, H₂ concentration in the liquid phase was considered similar to the solubility conditions.

Each surface reaction has its own kinetic equation (r1, r2).



2.3.2. H₂ solubility

Hydrogen solubility under reaction conditions has been estimated by thermodynamic equilibrium using Aspen Plus 2006.5 simulation software selecting the Peng – Robinson property package. The Aspen solubility values have been fit using an experimental equation (eq. 1 – 4) for H₂ partial pressures between 0.799 and 3.799 bar and temperatures between 5 and 70 °C. The maximum relative error between Aspen and our simulated liquid molar fraction was lower than 3.5%, with an average relative error of 0.8% (for 124 data points).

$$x_{H_2}^* = A \cdot P_{H_2}^B \quad (1)$$

$$A = -8.25 \cdot 10^{-9} \cdot T^2 + 1.19 \cdot 10^{-6} \cdot T - 3.18 \cdot 10^{-5} \quad (2)$$

$$B = 3.00 \cdot 10^{-3} \cdot T^2 - 0.368 \cdot T - 12.9 \quad (3)$$

$$c_{H_2}^* = \frac{x_{H_2}^* \cdot n_{liq}}{V_{liq}} \quad (4)$$

2.3.3. Mass balance equations

The mass balance for the perfectly mixed batch reactor is then:

Decomposition conditions:

$$\frac{dC_{H_2O_2}}{dt} = -r_d \quad (5)$$

Hydrogenation conditions:

$$\frac{dC_{H_2O_2}}{dt} = -r_d - r_h \quad (6)$$

According to our experimental results (see next section), the velocity reaction, r_d and r_h , is a function of several variables, namely, pH, Br^-/Pd ratio, H_2O_2 initial concentration, number of active sites, %Pd/C (or type of catalyst) and temperature. The large number of variables and how they all relate to each other make it very difficult the resolution of the model and the reaction mechanism. To avoid non – linearity problems that might hinder the adjustment, the experiments should be designed so as to follow the same trend, with no sudden changes in behaviour, but differ enough between them to provide useful information. To determine exactly the effect of each of variables five different sets of experiments were proposed.

The specific rate of reaction for both decomposition and hydrogenation are defined in eqs. 7 – 10.

$$r_d = k_d \cdot (C_{H_2O_2})^{\alpha_d} \cdot (n_{Pd})^{\beta_d} \quad (7)$$

$$r_h = k_h \cdot (C_{H_2O_2})^{\alpha_h} \cdot C_{H_2}^* \cdot (n_{Pd})^{\beta_h} \quad (8)$$

$$k_d = k_{0d} \cdot \exp\left(\frac{-E_{a_d}}{R \cdot T}\right) \quad (9)$$

$$k_h = k_{0h} \cdot \exp\left(\frac{-E_{a_h}}{R \cdot T}\right) \quad (10)$$

2.3.4. Numerical solution strategy

A final set of 2 ODEs (Ordinary Differential Equations) formed by eq. 5 – 6 has been solved using Excel – VBA with a Runge – Kutta algorithm. The model has eight adjustable parameters, k_{d0} , k_{h0} , α_d , α_h , β_d , β_h , E_{ad} and E_{ah} . Objective function (O.F., eq. 11) was minimized using a Excel Solver add – in (Simplex method).

$$O.F = 10^6 \cdot \left(C_{H_2O_2}^{exp} - C_{H_2O_2}^{sim} \right)^2 \quad (11)$$

The goodness of fit has been checked using as reference Deviation Absolute Average (AAD) and Standard Error (SE) values, where n_{data} is the number of data, “exp” stands for the experimental data and “sim” for the data simulated using the model.

$$AAD(\%) = \frac{1}{n_{data}} \cdot \sum_{l=1}^{n=data} \left| \frac{C_{H_2O_2}^{exp} - C_{H_2O_2}^{sim}}{C_{H_2O_2}^{exp}} \right| \cdot 100 \quad (12)$$

$$SE(\%) = \left| \frac{C_{H_2O_2}^{exp} - C_{H_2O_2}^{sim}}{C_{H_2O_2}^{exp}} \right| \cdot 100 \quad (13)$$

2.4. Results and discussion

To demonstrate and understand the behaviour of the system regarding the controllable variables we have carried out a total of 22 experiments. We varied as illustrated in Table 1. Some of the effects cannot be separated easily, such as halide and pH. In this study we have determined the influence of H₂O₂ initial concentration. Then we studied the pH and halide values to reduce hydrogenation and decomposition and we have chosen one condition (related also to a future synthesis step) to continue the study analysing the effect of temperature and amount of catalyst (number of palladium sites more specifically).

All the results from the modelling are presented in Table 2 and Table 3 and analysed thoroughly next. In general the model has an average error lower than ca. %ADD_d = 1% in decomposition (%SE_d max.< 4.0%) and %ADD_h = 1.5% in hydrogenation (%SE_d max.< 5.5 %).

Table 1. Experimental details

Exp.	Pressure bar	Temp . °C	%wt/v H ₂ O ₂	Pd/C wt%	Catalyst mg	Br ⁻ /Pd	pH	H ₂ mmol·min ⁻¹	CO ₂ mmol·min ⁻¹	H ₂ % mol
1	80	40	3.709	5	100	8.5	2.0	3.60	84.2	3.93
2	80	40	3.420	5	200	8.0	2.0	3.20	87.4	3.39
3	80	40	3.320	5	50	8.0	2.0	3.20	91.1	3.25
4	80	40	3.398	5	20	8.0	2.0	2.70	91.1	2.76
5	80	50	3.630	5	100	8.0	2.0	2.70	91.1	2.76
6	80	58	3.426	5	100	8.0	2.0	2.60	102.0	2.38
7	80	60	3.388	5	100	8.0	2.0	2.70	102.0	2.47
8	80	40	3.420	5	100	5.0	2.0	2.60	90.7	2.67
9	80	40	3.329	5	100	3.0	2.0	2.70	102.0	2.47
10	80	40	1.025	5	100	8.0	2.0	2.70	113.0	2.24
11	80	40	5.634	5	100	8.0	2.0	2.70	113.0	2.24
12	80	40	10.962	5	100	8.0	2.0	2.70	113.0	2.24
13	80	40	3.205	1	15	8.0	2.0	2.70	102.0	2.47
14	80	40	3.195	1	25	8.0	2.0	2.70	102.0	2.47
15	80	40	3.082	1	75	8.1	2.0	2.70	102.0	2.47
16	80	40	3.228	1	100	8.0	2.0	2.70	102.0	2.47
17	80	40	3.232	1	200	8.0	2.0	2.70	102.0	2.47
18	80	40	3.193	3	15	8.0	2.0	2.70	102.0	2.47
19	80	40	3.108	3	25	8.0	2.0	2.70	102.0	2.47
20	80	40	3.190	3	100	8.0	2.0	2.70	102.0	2.47
21	80	40	3.233	3	200	8.0	2.0	2.70	102.0	2.47
22	80	40	3.147	5	100	8.0	3.8	2.70	102.0	2.47

Table 2. Results of the fitting to the model (Eq. (5 – 10)). r_d and r_h evaluated for reaction time $t = 30$ min.

Exp.	β_d	β_h	k_d	k_h	mol·min ⁻¹		mol·h ⁻¹ ·mol _{Pd} ⁻¹	
					r_d (10 ⁶)	r_h (10 ⁶)	TOF _d	TOF _h
1	0.94	0.82	1.36	31.82	0.87	2.23	1.09	2.8
2	1.58	0.97	1.49	25.19	1.58	6.77	0.99	4.25
3	0.97	1.06	1.49	25.11	0.35	2.04	0.88	5.12
4	0.93	0.95	1.48	25.35	0.24	1.62	1.51	10.17
5	0.94	0.82	1.86	29.03	1	4.06	1.26	5.1
6	0.94	0.82	2.2	32.32	1.15	3.84	1.44	4.82
7	0.94	0.82	2.29	33.18	1.21	3.75	1.52	4.71
8	0.94	0.82	1.87	3.08	1.15	3.49	1.44	4.38
9	0.94	0.82	1.75	5.21	1.08	4.48	1.36	5.62
10	0.94	0.82	1.49	25.18	0.25	2.26	0.31	2.84

11	0.94	0.82	1.49	25.18	1.28	1.42	1.61	1.78
12	0.94	0.82	1.49	25.18	2.5	1.11	3.14	1.39
13	0.81	0.87	1.49	25.18	0.23	0.55	9.62	23.01
14	0.81	0.87	1.49	25.18	0.32	0.83	8.03	20.84
15	0.82	0.9	1.47	26.29	0.68	1.42	5.69	11.88
16	0.82	0.92	1.49	25.18	0.82	1.87	5.15	11.74
17	0.84	0.98	1.49	25.18	1.13	1.8	3.55	5.65
18	0.84	0.94	1.49	25.18	0.33	0.69	4.6	9.62
19	0.85	0.94	1.49	25.18	0.48	0.86	4.02	7.2
20	0.87	0.98	1.49	25.18	1.18	2.27	2.47	4.75
21	0.91	1.02	1.49	25.18	1.46	3.06	1.53	3.2

Table 3. Errors and deviations of the fitting to the model (Eq. (5 – 10)). Reaction evaluated for t = 30 min

Exp.	max %SE		%AAD		n _{data}	
	Dec.	Hydr.	Dec.	Hydr.	Dec.	Hydr.
1	0.8	0.91	0.31	0.32	19	9
2	2.38	10	0.83	3.8	14	15
3	0.65	0.94	0.25	0.41	23	6
4	1.51	1.58	0.63	0.64	13	17
5	2.93	28.64	1.3	12.66	16	9
6	1.87	2.07	0.63	1.12	17	5
7	0.97	7.35	0.46	3.34	13	7
8	1.79	2.6	0.56	0.73	15	9
9	1.18	1.47	0.5	0.67	13	7
10	3.56	33.49	1.17	9.78	10	8
11	0.41	2.65	0.19	1.12	10	8
12	0.67	0.82	0.34	0.35	13	17
13	1.73	1.6	0.48	0.6	11	20
14	1.46	1.62	0.92	0.88	5	11
15	1.02	1.97	0.44	0.8	11	22
16	1.34	1.62	0.6	0.66	11	6
17	0.93	3.85	0.33	1.97	10	20
18	0.99	1.95	0.38	0.66	11	23
19	1.01	1.46	0.45	0.67	11	23
20	2.56	5.36	0.96	3.32	11	23
21	1.85	5.14	0.84	1.6	11	20

2.4.1. Initial concentration of hydrogen peroxide (exp. # 1, 10 – 12)

According to previous studies [11] the order of the decomposition and hydrogenation reactions with respect to the concentration of hydrogen peroxide was 1 and 0 respectively. We have taken those values as a seed for our fitting, considering a general reaction order, $C_{H_2O_2}^\alpha$ (see eqs. 7 – 8).

The main reason for the decomposition of H_2O_2 remains in the adsorption of the molecule in the active sites that can cleavage the bond O-H and O-O forming H_2O and O_2 . On the other hand, whenever H_2 is adsorbed in a near site the probability of cleavage, by hydrogenation in this case, is higher, as it can be seen in Figure 2 and Figure 3.

In Figure 2 decomposition is analysed for H_2O_2 initial concentrations of 1, 3, 5 and 10 %wt/v. in this case the order of reaction is almost one, according to our modelling results the best fit was obtained at: $\alpha_d = 1.031$ (%SE_d = 3.56%, %ADD_d = 1.17%).

For the case of hydrogenation, the study with similar initial concentrations we have obtained an order or reaction close to zero, in this case: $\alpha_h = -0.161$ (%SE_h = 33.5%, %ADD_d = 9.78%). These experiments exhibited the highest average and maximum errors of this research but the higher error was obtained for 1% wt/v of H_2O_2 initial concentration (exp. #10) (and it has to be considered that errors at lower concentration have higher influence). Following this argument, in Figure 3 is illustrated that low H_2O_2 concentrations exhibit extraordinary high hydrogenation rates. In all cases the concentration of H_2 in the medium was constant (as it operates at the same temperature, pressure and flow conditions), so, this explains the negative exponent for alpha ($\alpha_h = -0.161$) mainly caused by the behaviour at low H_2O_2 concentrations.

One of the main conclusions is that hydrogenation is nearly 3 to 20 fold times higher than decomposition at low H_2O_2 concentrations. For instance, after 30 min at 5 % wt/v of H_2O_2 decomposition is 2.4% while hydrogenation was 6.97%, for the case of 1% wt/v H_2O_2 decomposition is 2.9% while hydrogenation was 63.5%. However we have tested a broader interval and, at high H_2O_2 concentrations (e.g. runs #11 and #12) decomposition can be similar or even higher than hydrogenation. Thus, at 5% wt. H_2O_2 the TOF_d/TOF_h = 0.90 and at 10% wt. H_2O_2 the TOF_d/TOF_h = 2.26, in contrast with the results of other authors [12].

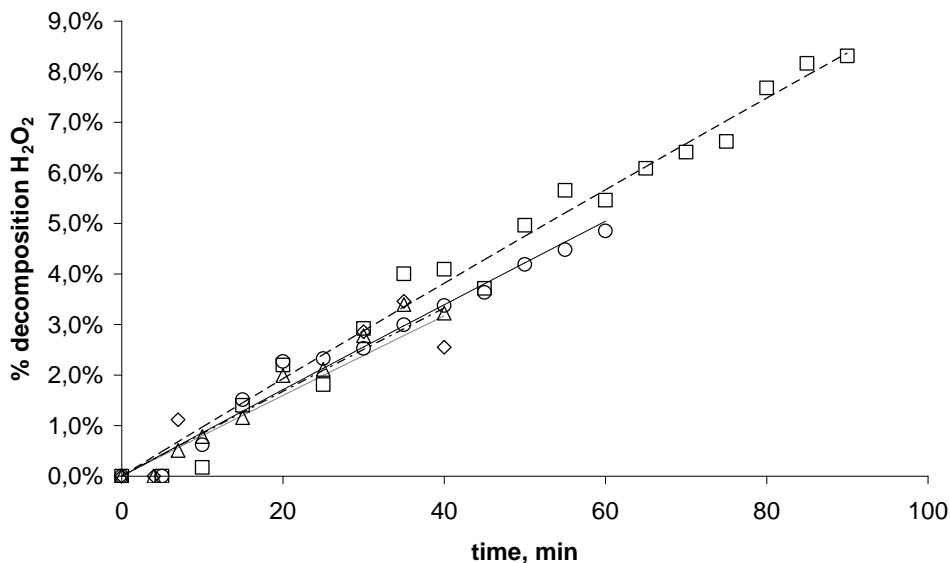


Figure 2. Effect of initial H₂O₂ concentration on decomposition rate (Exp # 1, 10 – 12). 40 °C, 100 mL, 100 mg 5% Pd/C, H₃PO₄=0.03 mol/L, Br⁻/Pd = 8, pH= 2, 80 bar CO₂. ◇ 1% wt/v H₂O₂ initial; □ 3% wt/v H₂O₂ initial; △ 5% wt/v H₂O₂ initial; ○ 10% wt/v H₂O₂ initial. Dashed line represents the values of the simulation.

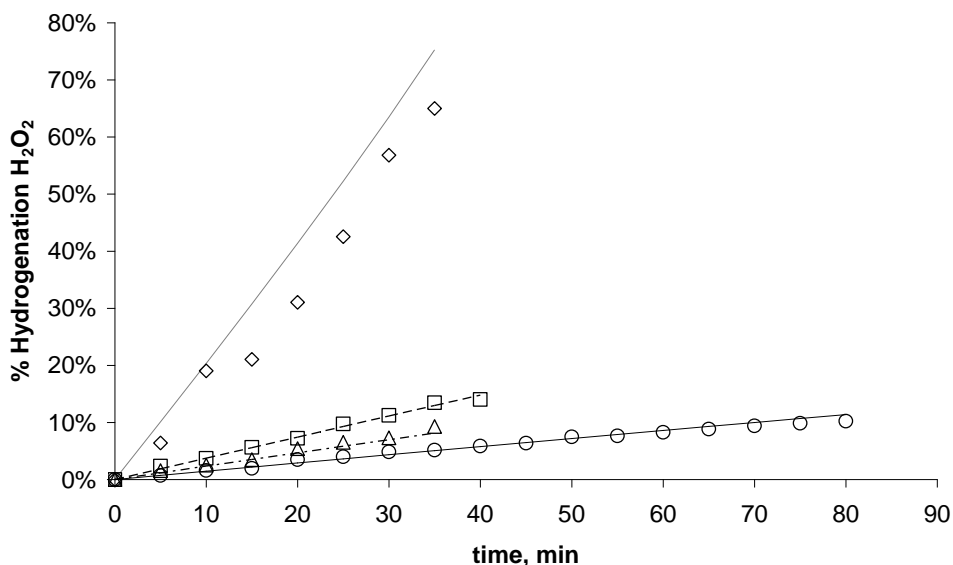


Figure 3. Effect of initial H₂O₂ concentration on hydrogenation rate (Exp # 1, 10 – 12). 40 °C, 100 mL, 100 mg 5% Pd/C, H₃PO₄=0.03 mol/L, Br⁻/Pd = 8, pH= 2, 80 bar CO₂. ◇ 1% wt/v H₂O₂ initial; □ 3% wt/v H₂O₂ initial; △ 5% wt/v H₂O₂ initial; ○ 10% wt/v H₂O₂ initial. Dashed line represents the values of the simulation.

2.4.2. Halide concentration (exp. # 1, 9,10)

Several authors have demonstrated the effectiveness of halides minimizing or preventing the decomposition and hydrogenation. Choudhary and Samanta [13] proposed that the increase in selectivity is due to the effect that the halides are on palladium. These interactions modify the properties of palladium inhibiting the cleavage of the O–O bond present in the molecule of H₂O₂

and O₂. The catalyst performance varies greatly depending on the concentration of halides present in the reaction medium, and, in particular with the molar ratio halide/metal as demonstrated before [7]. This should be taken into account during modelling because it will introduce a high non linearity. In this paper we assume that the protective effect of halides, expressed as a molar ratio between bromine and palladium, is included in the rate constant's pre – exponential factor, k_{od} and k_{oh} . It is difficult to find an appropriate expression for the whole interval due to the high non linearity.

The results obtained (see Figure 4) demonstrate that values of Br⁻/Pd between 1.5 and 2.5 are optima for operation meanwhile minimize the hydrogenation while keep decomposition at acceptable values. At high Br⁻/Pd ratios decomposition decreases while, hydrogenation increases considerably and for this reason are highly non recommended terms of hydrogenation levels, as it would further cause a sharp decrease in the selectivity.

However, as it has been demonstrated in previous studies in terms of synthesis a Br⁻/Pd = 8 is acceptable to reach a stable production, so in this study even when hydrogenation is faster, a ratio Br⁻/Pd = 8 is used.

When analysing the Arrhenius parameters (see also section 1.4.4) the pre – exponential factor is a clear function of the ratio Br⁻/Pd as shown in Figure 5, Table 3 and Supplementary Figures 1 and 2.

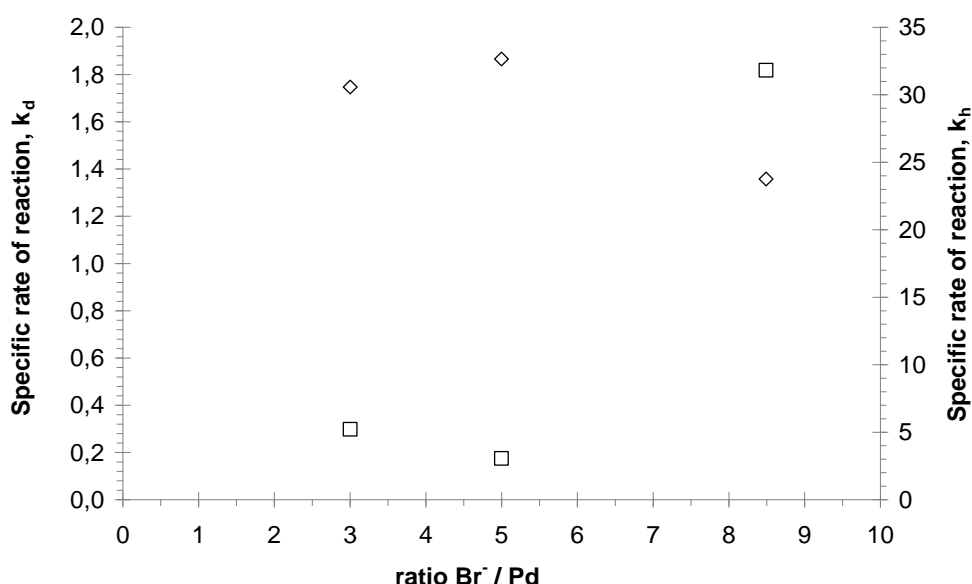


Figure 4. Effect of Br⁻ concentration on H₂O₂ decomposition (◇) and hydrogenation (□) specific rate of reaction (Exp # 1, 8, 9). 40 °C, 100 mg 5% Pd/C, 100 mL, 3 %wt/v H₂O₂ initial, pH= 2, 80 bar CO₂.

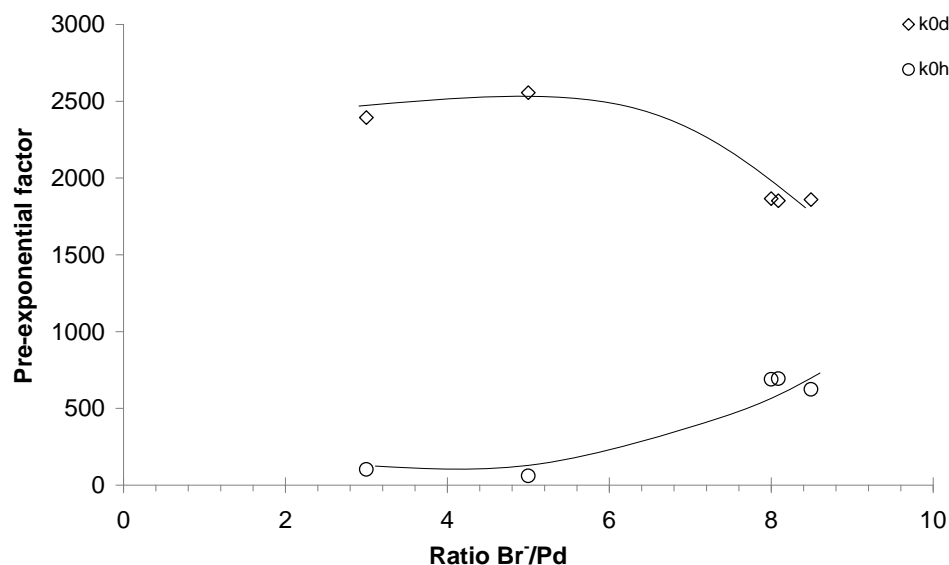


Figure 5. Effect of halide in pre – exponential factor for decomposition and hydrogenation.

Table 4. Arrhenius parameters for decomposition and hydrogenation

Br ⁻ /Pd	k _{0d}	k _{0h}
3.00	2392.9	102.17
5.00	2555.0	59.90
8.00	1865.1	688.42
8.09	1851.4	692.59
8.49	1859.4	623.47

2.4.3. Acid concentration and pH (exp. #1, 22)

The pH coupled with the amount of halide are the two parameters that most affect the reaction process. The selection of an appropriate pH value makes the difference, since catalysts behave differently if the pH value is equal to or lower than the pH of the isoelectric point. We believe that the operation at low pH (lower than the isoelectric point) modifies the charge of the support increasing the desorption rate of H₂O₂ onto the support and active sites. The lower the H₂O₂ available at the active sites the lower the decomposition and hydrogenation reaction rates (*i.e.* selectivity in synthesis is increased). In this work we have chosen phosphoric acid as acid promoter, considering the good results obtained in previous studies [5, 6, 10] and its low corrosion in the system.

In this case two experiments were conducted at different pH values as shown in Figure 1. Experiment #1 at pH = 2.0 ([H₃PO₄] = 0.018 M), very close to that determined as optimal in previous works [7], the decomposition was 2.92% and hydrogenation 7.68% after the first 30

minutes of reaction. In the experiment with pH = 3.8, ($[\text{H}_3\text{PO}_4] = 0$, hydrogen peroxide reduces pH value) both reactions were faster, decomposition was 22.83% and hydrogenation 62.37% after 30 min.

The experiment #22 behaves in a too nonlinear way, so it was not possible to include it in the model. For that reason observed reaction rate values have been used as compiled in Table 5, r_d^{obs} and r_h^{obs} , calculated directly from the data concentration of hydrogen peroxide and its variation in time.

Table 5. Values of the reaction rate observed for experiments # 2 and # 22.

	Run #2, pH = 2.0	Run #22, pH = 3.8
r_d^{obs} , mol $\text{H}_2\text{O}_2 \cdot \text{min}^{-1}$	$8.95 \cdot 10^{-5}$	$2.34 \cdot 10^{-4}$
r_h^{obs} , mol $\text{H}_2\text{O}_2 \cdot \text{min}^{-1}$	$2.80 \cdot 10^{-4}$	$1.41 \cdot 10^{-3}$

The effect of pH is clear by comparing the values of rate of reaction of the two experiments. In the case of the decomposition reaction rate increases 2.67 times if working in a less acidic medium, pH = 3.8. For hydrogenating the effect is much greater, since the reaction rate increases up to 5.02 times.

From these results the rest of the experiments were conducted at $\text{pH} \leq 2.0$ to keep both decomposition and hydrogenation at low levels. It must be considered that working with acid concentrations over 0.03 M may cause severe corrosion in the reactor and undesired leaching active metal in the catalyst [13]. This is the main reason why pH near 2.0 is recommended [5, 7].

2.4.4. Reaction temperature (exp. # 1, 5 – 7)

The effect of temperature on the kinetics, Supplementary Figures 3 and 4, for this reaction will affect in both surface reaction as well as adsorption/desorption rates. In this work, we will consider only the surface reaction step, so the other effects will be included in its constants, determined by an Arrhenius type equation. In this case the activation energies obtained were: $E_{ad} = 18803.6 \text{ J} \cdot \text{mol}^{-1}$ (decomposition) and $E_{ah} = 7746.2 \text{ J} \cdot \text{mol}^{-1}$ (hydrogenation). Such low activation energies explains the main problems that direct synthesis as an industrial process had been facing and will face to be implemented. Hydrogen is expensive as raw material; the recycling from the low concentrated off – gas is expensive so full conversion is required. To

increase the conversion minimizing CapEx costs the increase in temperature is needed, but, increasing temperature increases both hydrogenation and decomposition and this dramatically decreases selectivity. The only way to overcome this problem is to operate in conditions where H₂O₂ is inaccessible to H₂ once it is formed. This is why more specific catalysts and promoters are required. Several authors operate at low temperature (under ambient conditions) but this could not be assumed in terms of OpEx costs for an industrial plant.

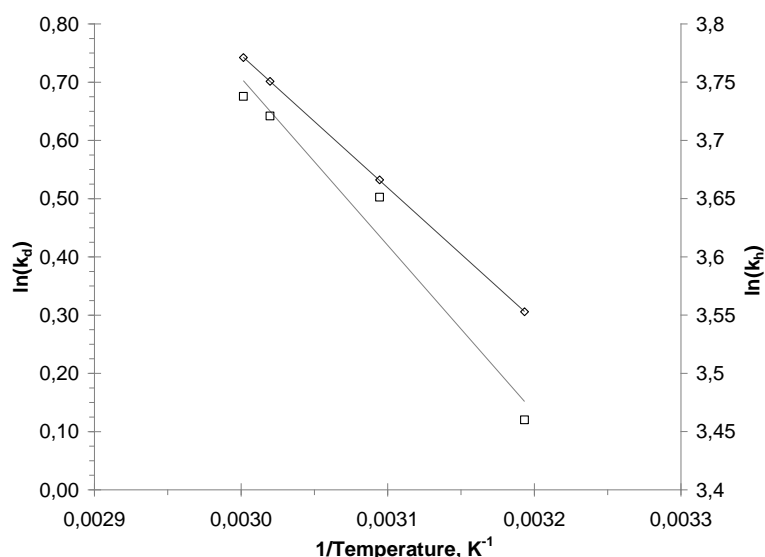


Figure 6. Temperature dependence, Arrhenius plot for decomposition (\diamond) and hydrogenation reactions (\square), (Exp # 1, 5 – 7). 100 mg 5% Pd/C, 100 mL, 3 %wt/v H₂O₂ initial, Br/Pd = 8, pH = 2, 80 bar CO₂.

2.4.5. Amount of catalyst and Pd loading (exp. # 1, 2 – 4, 13–21)

The number of initial active sites is a function of the amount of catalyst, Pd loading and the type of catalyst and catalyst history (*i.e.* activation, preparation, poisoning, leaching in previous uses, etc.).

Decomposition and hydrogenation take place mainly over active metal, but also appears over the support as other authors have pointed out [4]. There is an important effect between the support surface (*i.e.* active carbon) and palladium in this case. At high Pd loadings the system may experience mass transfer limitations so, to determine the kinetics is necessary to work at low Pd amounts. This can be achieved with low catalyst amounts of high Pd% or higher amounts of low Pd%. This effect can be clearly observed in Figure 7 and Figure 8 and Supplementary Figures 5 to 10. Decomposition rate (r_d) increases with Pd for all the catalyst tested. Although it seems that in this case 1%Pd/C and 3%Pd/C had a similar trend, while 5% Pd/C had a different behaviour at low Pd amounts. This can be explained by assuming that the catalyst support behaves differently in

terms of H_2O_2 adsorption. However, for hydrogenation (r_h) has a fairly linear trend in all cases (1%, 3% and 5%Pd/C).

To model these results we have used the order of reaction β_d and β_h over Pd sites (see eqs. 4 – 5). Both β_d and β_h are in the interval 0.88 – 1.08 at low Pd amounts, as expected in the traditional heterogeneous kinetics theory. At high Pd loadings the interactions between the support, the active sites and the H_2O_2 and H_2 coupled to the macroscopic mass transfer of H_2 and this cause a non – linearity requiring $\beta_d = 1.44$ and $\beta_h = 0.71$ (see Figure 9 and Figure 10).

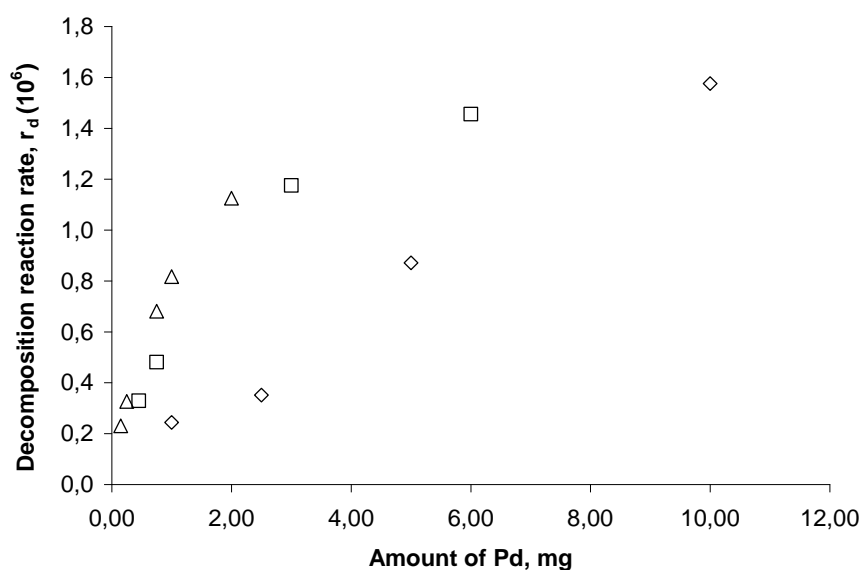


Figure 7. Effect of amount of Pd on decomposition reaction rate, $t = 30$ min (Exp #1, 2 – 4, 13 – 22). 40 °C, 100 mL, 3 %wt/v H_2O_2 initial, $\text{Br}^-/\text{Pd} = 8$, $\text{pH} = 2$, 80 bar CO_2 . \triangle 1 wt %Pd /C, \square 3 wt. Pd/C, \diamond 5 wt. Pd/C.

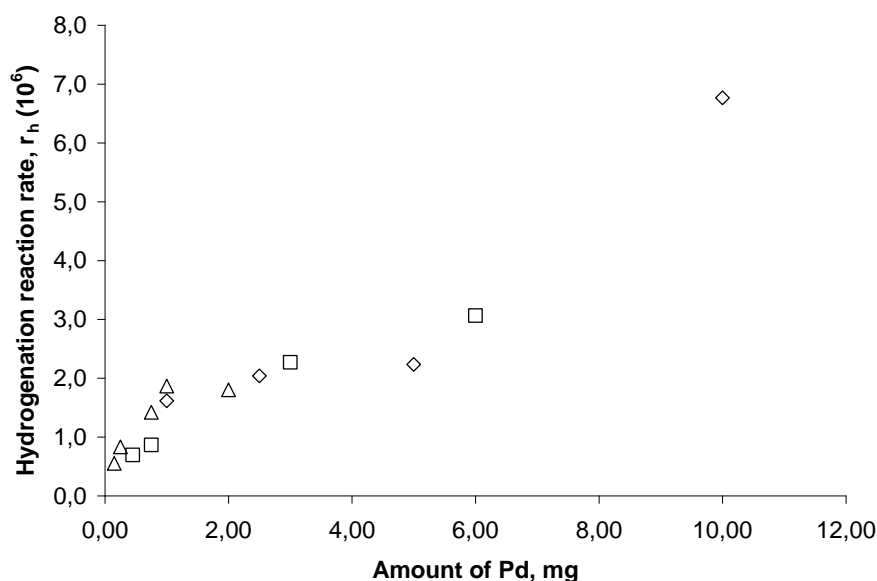


Figure 8. Effect of amount of Pd on hydrogenation reaction rate (Exp #1, 2 – 4, 13 – 22). 40 °C, 100 mL, 3 %wt/v H_2O_2 initial, $\text{Br}^-/\text{Pd} = 8$, $\text{pH} = 2$, 80 bar CO_2 . \triangle 1 wt %Pd /C, \square 3 wt. Pd/C, \diamond 5 wt. Pd/C.

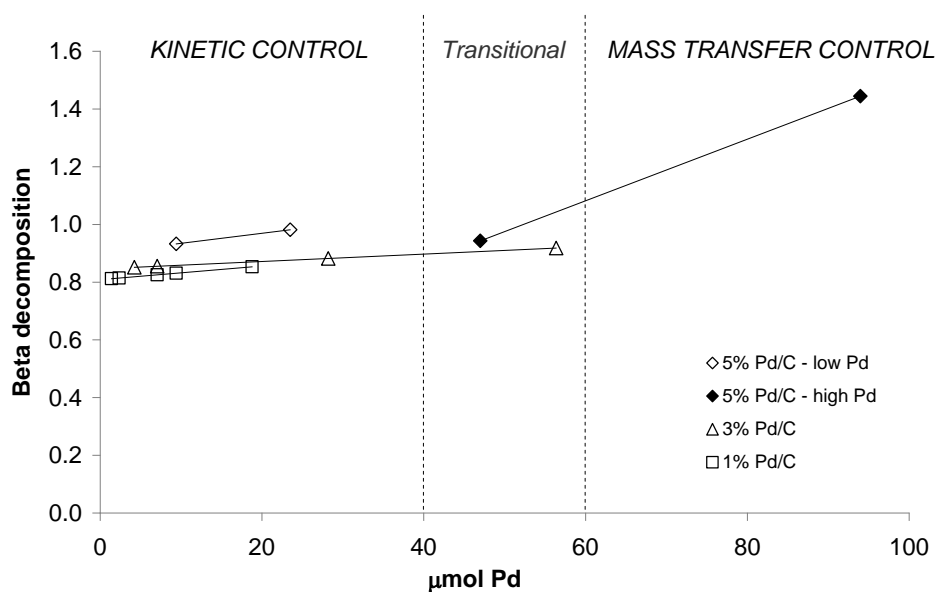


Figure 9. Reaction order for palladium sites in decomposition (β_d) versus amount of Pd.

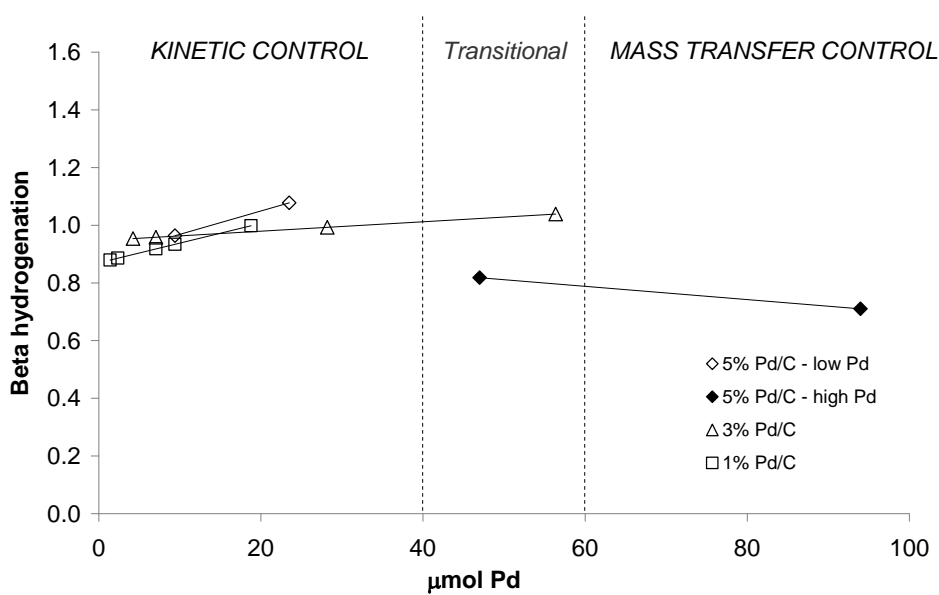


Figure 10. Reaction order for palladium sites in hydrogenation (β_h) versus amount of Pd.

2.5. Conclusions

Although decomposition and hydrogenation reactions are undesired side reactions within direct synthesis of H₂O₂, they can reveal important details for the direct synthesis and reduce experimentation for the optimization of the process variables.

We have proved that hydrogenation is proportionally more severe at low H₂O₂ concentrations, while decomposition increases considerably along with H₂O₂ concentration. This can be observed

from the kinetic results indicating that the order of reaction of hydrogenation is -0.16 and for decomposition is 1.031 (close to zero and linear respectively as other authors have indicated previously). Therefore, during direct synthesis operating at low H_2O_2 concentrations (which are the common option, with H_2O_2 concentrations under 1% wt/v) when the catalyst sites are and hydrogen are available we strongly recommend to optimize the conditions minimizing hydrogenation.

Hydrogenation requires transferring H_2 , so obviously, at high H_2O_2 concentrations the rate of hydrogenation will compete with synthesis (whenever O_2 is present) or be limited by mass transfer. Note that decomposition only relies on H_2O_2 concentration and the active site availability so in several cases this must be the target for minimisation (to increase selectivity).

We have found that the complexity of creating a general kinetic model is driven by the interaction between the catalyst and the environment, *i.e.* protons and halides. For the case of Pd/C pH values round 2.0 are enough to protect from both decomposition and hydrogenation. The halide/Pd ratio between 3.0 and 5.0 are recommended to decrease hydrogenation, and ratios of 8.0 to minimise decomposition. In this work we have studied the catalyst at pH = 2.0 and $\text{Br}^-/\text{Pd} = 8.0$.

The behaviour of the catalyst is function of the number of active sites (%Pd loading) but also of a number of variables, such as support, preparation, history, etc. In this work we have compared the kinetics of 3 commercial catalysts based on activated carbon as support and 1, 3 and 5% wt. Pd loadings. The order of reaction as a function of the number of sites has been 0.812 – 0.981 for decomposition at low Pd amounts and up to 1.444 at high Pd amounts. For hydrogenation the order was 0.710 – 1.078. This indicates that not all of the Pd sites are available or active.

Using the kinetic model we have identified the activation energies of both reactions $E_{a_d} = 18803.6 \text{ J/mol}$ (decomposition) and $E_{a_h} = 7746.2 \text{ J/mol}$ (hydrogenation) as average values for all the catalysts used, obtaining average errors of $\%AAD_d = 0.6\%$ and $\%AAD_h = 2.20\%$ respectively. Such low activation energies explain the small window of operation of the system investigated in the literature, normally between 20 and 40°C and, more uncommon in the interval -10°C and 60 °C.

List of symbols

A = solubility parameter as per eq. (2), bar⁻¹

AAD = absolute average deviation, defined in eq. (12)

B = solubility parameter as per eq. (3)

c_{H₂O₂} = concentration of H₂O₂, mol·L⁻¹

c_{H₂} = concentration of H₂ in the liquid phase, mol·L⁻¹

c_{H₂}^{*} = solubility of H₂ in the liquid phase, mol·L⁻¹

E_a = activation energy, J·mol⁻¹

k_j = specific rate of reaction as per eqs. (9) and (10),

$$k_d [=] \text{molH}_2\text{O}_2^{(1-\alpha_d)} \cdot \text{molPd}^{-\beta_d} \cdot \text{L}^{\alpha_d} \cdot \text{min}^{-1}, \quad k_h [=] \text{molH}_2\text{O}_2^{(1-\alpha_h)} \cdot \text{molPd}^{-\beta_h} \cdot \text{mol H}_2^{-1} \cdot \text{L}^{(1+\alpha_h)} \cdot \text{min}^{-1}$$

k_{j0} = preexponential factor, min⁻¹·mol_{Pd}⁻¹

n_{data} = number of data points in the experimental set

n_{liq} = total number of liquid mol, mol

n_{Pd} = mol of palladium

P_{H₂} = partial pressure of H₂ in the gas phase, bar

P = global reaction pressure, bar

r_j = reaction rate according to eqs. (7) and (8), molH₂O₂·min⁻¹

R = ideal gas constant, 8.314 J·mol⁻¹·K⁻¹

%SE = Percentage of Standard Error as defined in eq. (13)

t = time, min

T = temperature, K

TOF_j = Turn Over Frequency, mol_{H₂O₂}·h⁻¹·mol_{Pd}⁻¹

V_{liq} = volume of the liquid phase, L

x_{H₂} = molar fraction of H₂ in the liquid phase

x_{H₂}^{*} = solubility of H₂ in the liquid phase as per eq. (1)

y_{H₂} = molar fraction of H₂ in the gas phase

Greek letters

α_j = order of reaction of H₂O₂ according to eq. (7) and (8)

β_j = order of reaction of n_{Pd} according to eq. (7) and (8)

Subindex

d = decomposition

h = hydrogenation

Superindex

exp = experimental data point

sim = simulated data point

Acknowledgements

The authors thank the Spanish Economy and Competitiveness Ministry (former Science and Innovation Ministry) Project Reference: CTQ2011-23293 and Junta de Castilla y León Project Reference: VA254B11-2 for funding. The authors also wish to thank Centro de Tecnología de REPSOL (Móstoles, Spain) for scientific advice and project funding.

References

1. Voloshin, Y. and A. Lawal, *Overall kinetics of hydrogen peroxide formation by direct combination of H₂ and O₂ in a microreactor*. Chemical Engineering Science, 2010. **65**(2): p. 1028-1036.
2. Deguchi, T. and M. Iwamoto, *Kinetics and Simulation Including Mass-Transfer Processes of Direct H₂O₂ Synthesis from H₂ and O₂ over Pd/C Catalyst in Water Containing H⁺ and Br⁻ Ions*. Industrial & Engineering Chemistry Research, 2011. **50**(8): p. 4351-4358.
3. Choudhary, V.R., C. Samanta, and P. Jana, *Hydrogenation of hydrogen peroxide over palladium/carbon in aqueous acidic medium containing different halide anions under static/flowing hydrogen*. Industrial and Engineering Chemistry Research, 2007. **46**(10): p. 3237-3242.
4. Edwards, J.K., et al., *Switching Off Hydrogen Peroxide Hydrogenation in the Direct Synthesis Process*. Science, 2009. **323**(5917): p. 1037-1041.
5. Moreno, T., J. García-Serna, and M.J. Cocero, *Decomposition reaction of H₂O₂ over Pd/C catalyst in an aqueous medium at high pressure: Detailed kinetic study and modelling*. The Journal of Supercritical Fluids, 2011. **57**(3): p. 227-235.
6. Moreno, T., J. García-Serna, and M.J. Cocero, *Direct synthesis of hydrogen peroxide in methanol and water using scCO₂ and N₂ as diluents*. Green Chemistry, 2010. **12**: p. 282-289.

7. Moreno, T., J. Garcia-Serna, and M.J. Cocero, *Semi-continuous production of H₂O₂ directly from H₂ and O₂ in a biphasic H₂O/scCO₂ system over a Pd/C catalyst: optimization of reaction conditions*. 2011.
8. Cohen, I.R., T.C. Purcell, and A.P. Altshuller, *Analysis of the oxidant in photooxidation reactions*. Environmental Science and Technology, 1967. **1**(3): p. 247-252.
9. Moreno, T., et al., *Quantitative Raman determination of hydrogen peroxide using the solvent as internal standard: Online application in the direct synthesis of hydrogen peroxide*. Chemical Engineering Journal, 2011. **166**(3): p. 1061-1065.
10. Moreno, T., et al., *Direct synthesis of H₂O₂ in methanol at low pressures over Pd/C catalyst: Semi-continuous process*. Applied Catalysis A: General, 2010. **386**(1-2): p. 28-33.
11. Choudhary, V.R., C. Samanta, and P. Jana, *Formation from direct oxidation of H₂ and destruction by decomposition/hydrogenation of H₂O₂ over Pd/C catalyst in aqueous medium containing different acids and halide anions*. Applied Catalysis A: General, 2007. **317**(2): p. 234-243.
12. Deguchi, T. and M. Iwamoto, *Reaction mechanism of direct H₂O₂ synthesis from H₂ and O₂ over Pd/C catalyst in water with H⁺ and Br⁻ ions*. Journal of Catalysis, 2011. **280**(2): p. 239-246.
13. Choudhary, V.R. and C. Samanta, *Role of chloride or bromide anions and protons for promoting the selective oxidation of H₂ by O₂ to H₂O₂ over supported Pd catalysts in an aqueous medium*. Journal of Catalysis, 2006. **238**(1): p. 28-38.

Table Captions

Table 1. Experimental details	95
Table 2. Results of the fitting to the model (Eq. (5 – 10)). r _d and r _h evaluated for reaction time t = 30 min.	95
Table 3. Errors and deviations of the fitting to the model (Eq. (5 – 10)). Reaction evaluated for t = 30 min	96
Table 4. Arrhenius parameters for decomposition and hydrogenation	100
Table 5. Values of the reaction rate observed for experiments # 2 and # 22.....	101

Figure Captions

- Figure 1. Effect of pH on H₂O₂ decomposition – hydrogenation rate (exp # 1, 22). 40 °C, 100 mg 5% Pd/C, 100 mL, 3 %wt/v H₂O₂ initial, Br⁻/Pd = 8, 80 bar CO₂. ○ pH = 2; □ pH = 3.8.....91
- Figure 2. Effect of initial H₂O₂ concentration on decomposition rate (Exp # 1, 10 – 12). 40 °C, 100 mL, 100 mg 5% Pd/C, H₃PO₄=0.03 mol/L, Br⁻/Pd = 8, pH= 2, 80 bar CO₂. ◇ 1% wt/v H₂O₂ initial; □

3% wt/v H ₂ O ₂ initial; △5% wt/v H ₂ O ₂ initial; ○ 10% wt/v H ₂ O ₂ initial. Dashed line represents the values of the simulation.	98
Figure 3. Effect of initial H ₂ O ₂ concentration on hydrogenation rate (Exp # 1, 10 – 12). 40 °C, 100 mL, 100 mg 5% Pd/C, H ₃ PO ₄ =0.03 mol/L, Br ⁻ /Pd = 8, pH= 2, 80 bar CO ₂ . ◇ 1% wt/v H ₂ O ₂ initial; □ 3% wt/v H ₂ O ₂ initial; △5% wt/v H ₂ O ₂ initial; ○ 10% wt/v H ₂ O ₂ initial. Dashed line represents the values of the simulation.	98
Figure 4. Effect of Br ⁻ concentration on H ₂ O ₂ decomposition (◇) and hydrogenation (□) specific rate of reaction (Exp # 1, 8, 9). 40 °C, 100 mg 5% Pd/C, 100 mL, 3 %wt/v H ₂ O ₂ initial, pH= 2, 80 bar CO ₂	99
Figure 5. Effect of halide in pre – exponential factor for decomposition and hydrogenation.	100
Figure 6. Temperature dependence, Arrhenius plot for decomposition (◇) and hydrogenation reactions (□), (Exp # 1, 5 – 7). 100 mg 5% Pd/C, 100 mL, 3 %wt/v H ₂ O ₂ initial, Br ⁻ /Pd = 8, pH = 2, 80 bar CO ₂	102
Figure 7. Effect of amount of Pd on decomposition reaction rate, t = 30 min (Exp #1, 2 – 4, 13 – 22). 40 °C, 100 mL, 3 %wt/v H ₂ O ₂ initial, Br ⁻ /Pd = 8, pH = 2, 80 bar CO ₂ . △ 1 wt %Pd /C, □ 3% wt. Pd/C, ◇ 5% wt. Pd/C.....	103
Figure 8. Effect of amount of Pd on hydrogenation reaction rate (Exp #1, 2 – 4, 13 – 22). 40 °C, 100 mL, 3 %wt/v H ₂ O ₂ initial, Br ⁻ /Pd = 8, pH = 2, 80 bar CO ₂ . △ 1 wt %Pd /C, □ 3% wt. Pd/C, ◇ 5% wt. Pd/C.....	103
Figure 9. Reaction order for palladium sites in decomposition (β _d) versus amount of Pd.	104
Figure 10. Reaction order for palladium sites in hydrogenation (β _h) versus amount of Pd.....	104

CHAPTER III

Direct synthesis of H₂O₂ in water using nitrogen as inert over Pd/C catalysts in semicontinuous mode

Study of synthesis direct hydrogen peroxide reaction was carried out using air in a semicontinuous stirred bath reactor. Nitrogen acted as inert instead of CO₂ and complexity and cost of process are lower. Some reactions conditions were studied; pressure varied from 20 to 90 bar_g, temperature from 303.15 K to 333.15 K and 495 to 1980 Nml·min⁻¹ gas flow rate with different hydrogen molar fraction from 1.04 % to 4.04 %. Also three different catalysts were used with a palladium percentage equal to 1, 3 or 5 %. Influence of the amount of catalyst in the reaction was also studied. We demonstrated that it is possible to produce hydrogen peroxide using air. A maximum H₂O₂ productivity of 0.516 mmol·min⁻¹ and a maximum selectivity of 70 % were obtained. Experimental results obtained in this paper were compared with CO₂ experiments from a bibliography reference.

3.1. Introduction

Hydrogen peroxide is mainly produced *via* the auto-oxidation route, using 2 – ethyl anthraquinone for the normal plants and the new amyl anthraquinone for the mega plants (200 – 310 kt/y). The direct synthesis route may compete with the current industrial process mostly for small capacities (ca. 10 – 20 kt/y) achieving solutions of at least 15 – 20% wt. H₂O₂. Main drawback in hydrogen peroxide direct synthesis is the need to put in contact hydrogen and oxygen at low H₂ percentage (to avoid explosive range). The need of an inert implies the need for extra compression. In traditional anthraquinone synthesis route hydrogen and oxygen are never in direct contact. This reason made anthraquinone route much safer than direct synthesis process [4].

Hydrogen – oxygen mixtures are explosives in a wide concentrations range. Flammability limits to hydrogen in oxygen or air are (at 25 C and atmospheric pressure) 4 % H₂ (Lower flammability limit, LFL) and 96 % H₂ (upper flammability limit, UFL) [24]. Using inert gases, like N₂ or CO₂, hydrogen gas concentration can be reduced to safety values.

From all the possible gasses can be used as inert carbon dioxide is one of the most used and studied. CO₂ is a green solvent, is completely miscible with reaction gases and has a low solubility with the products which means purification and separation of final product will be easier [2]. Also acidic CO₂ character helps with hydrogen peroxide stabilization in liquid phase and reduce promoters need [1].

CO₂ as inert can modifies flammability limits of H₂/air and H₂/O₂ mixtures. Pande and Tonheim [20] concluded that in presence of CO₂, LFL increases to 9.5% H₂ at atmospheric pressure. However, Piqueras *et al.* [21] estimated that at high pressures safety range for a CO₂/H₂/O₂ mixtures is narrower, and for a H₂ concentration higher than 3.5%mol at 100 bar there is explosion risk. Differences between the safety LFL values gave for every author supposed a difficulty in order to select the conditions of operation that must be safe and secure the maximum system's yield is obtained.

Some other authors have studied N₂ influence as gas phase diluent. The main advantage is the possibility of using air, thus reducing the costs of the oxidant. Moreno et al. [15] checked out, using a batch reactor, the effect of replace CO₂ with N₂ for experiments using water or methanol as liquid phase. In methanol experiments, amount of hydrogen peroxide produced with CO₂ was 135% higher than in N₂ experiments. This is due, mainly, to the high methanol solubility in CO₂ at

reaction condition and CO₂ acidification effect. In water experiments the best result was obtained with N₂, after 165 minutes of reaction a yield of 82.6% and a hydrogen peroxide concentration of 1.38 wt/v were achieved.

Moreno *et al.* [14] revealed, in a following paper, that productivity of a semicontinuous reactor is 4 times lower when N₂ is used as inert instead CO₂. System behavior in face of change in reaction variables is quite similar using CO₂ or N₂ as inert.

Using pure oxygen and pure carbon dioxide can increase the product final cost so it is preferable using air or high oxygen air as reactive and inert. Using N₂ as inert instead of CO₂ is a first approximation to transform a laboratory scale system into an industrial scale system. The main objective in this study is substitute CO₂ by N₂ for hydrogen peroxide direct synthesis without losing selectivity or productivity.

3.2. Experimental

3.2.1. *Materials and Methods*

Catalysts used in this study were microparticles with an average of 1, 3 and 5 wt.% Pd₀ (3 – 5 nm size) over carbon support purchased from Aldrich and used fresh without pretreatment for each experiment [16]. Compressed air and premier grade hydrogen and argon were purchased from Carbueros Metálicos (Spain) and used without further modification. NaBr and H₃PO₄ (PRS – Codex, Panreac Química, Spain) were used as promoters. KI (PRS – Codex, Panreac Química), H₂SO₄ (PA – ISO, Panreac Química) and Na₂S₂O₃·5H₂O (PA – ACS, Panreac Química) were used for conventional iodometric titration [5]. H₂ and O₂ in the gas phase were analyzed every 5 min by Micro Gas Chromatography (Varian CP 4900 with a 5A molecular sieve column operating at 90 °C and equipped with a TCD detector, injector initial temperature was 110 °C and pressure 20 psi).

3.2.2. *Experimental set-up and procedure*

The H₂O₂ synthesis reaction was carried out in a 350 mL AISI 316L agitated reactor described elsewhere [15], for experiments presented in this work the gas mixture is continuously bubbled through the liquid medium (semi – continuous system). All tests were carried out in 200 mL of an aqueous solution with the corresponding amount of promoters (i.e. NaBr and H₃PO₄). The

catalyst was introduced in the reactor together with the solvent before each run. Reaction temperature was measured via an internal thermocouple and datalogged automatically using PicoTech TC. The reactor was first flushed with air, then air was introduced until the reaction pressure was reached. At that point, H₂ was introduced using Bronkhorst EL – FLOW mass flow meter controllers and the reaction time was set to zero.

The reaction pressure was controlled using a Bronkhorst EL – PRESS pressure controller coupled to a Badger's ReCo valve. Reaction time was 2 h unless otherwise stated. To increase mass transfer between the liquid and the catalyst, the system was stirred vigorously with a magnetic stirrer lined with DuPont™ Teflon® and a magnetic stirrer.

Hydrogen peroxide determination during reactor was carried out using a Raman spectrometer BWTEK i – Raman (BWS415) [18]. Samples were taken from the bottom the reactor and pumped through a high pressure cell of 3 ml of volume with a window cap supporting a UV grade quartz window of 20 mm of diameter. Raman equipment was connected to a computer and data were collected every 5 minutes.

In this paper, H₂O₂ selectivity, H₂ conversion and turnover frequency (TOF) are defined as follows:

$$H_2O_2 \text{ Selectivity (\%)} = 100 \cdot \frac{H_2O_2 \text{ generated (mol)}}{H_2 \text{ reacted (mol)}}$$

$$H_2O_2 \text{ Conversion (\%)} = 100 \cdot \frac{H_2 \text{ reacted (mol)}}{H_2 \text{ added to reactor (mol)}}$$

$$T.O.F \left(\frac{\text{mmol } H_2O_2}{\text{h} \cdot \text{g Pd}} \right) = 1000 \cdot \frac{H_2O_2 \text{ generated (mol)}}{\text{amount of Pd (g)} \cdot \text{reaction time (h)}}$$

3.3. Results and discussion

The objective in this paper was to study the influence of the main process variables in hydrogen peroxide direct synthesis using N₂ as inert, demonstrating that productivity and selectivity values cannot be as high as the values obtained using CO₂ as inert but they can get close when the system is optimized.

A total of 39 experiments have been carried out at different operational conditions. The main reaction variables studied were: pressure, temperature, amount of catalyst, supported palladium percentage, gas composition and flow rate and agitation speed.

Table 1. Experimental values of the main operational variables

# Exp	Pressure, barg	Temperature K	Amount of catalyst, mg	nominal Pd % wt.	O ₂ /H ₂	Total gas flow mL·min ⁻¹	Agitation Speed rpm
1	80	313.15	75	1	5.46	1980	1080
2	80	313.15	25	3	5.46	1980	1080
3	80	313.15	15	5	5.46	1980	1080
4	80	313.15	50	3	5.46	1980	1080
5	80	313.15	30	5	5.46	1980	1080
6	80	313.15	150	1	5.46	1980	1080
7	80	313.15	60	5	5.46	1980	1080
8	80	313.15	83	3	5.46	1980	1080
9	80	313.15	125	3	5.46	1980	1080
10	80	313.15	500	1	5.46	1980	1080
11	80	313.15	167	3	5.46	1980	1080
12	80	313.15	100	5	5.46	1980	1080
13	80	313.15	100	5	5.46	1980	1080
14	80	313.15	200	5	5.46	1980	1080
15	80	313.15	300	5	5.46	1980	1080
16	80	313.15	400	5	5.46	1980	1080
17	20	313.15	100	5	5.46	1980	1080
18	40	313.15	100	5	5.46	1980	1080
19	60	313.15	100	5	5.46	1980	1080
20	90	313.15	100	5	5.46	1980	1080
21	80	303.15	75	1	5.46	1980	1080
22	80	323.15	75	1	5.46	1980	1080
23	80	333.15	75	1	5.46	1980	1080
24	80	303.15	50	3	5.46	1980	1080
25	80	323.15	50	3	5.46	1980	1080
26	80	333.15	50	3	5.46	1980	1080
27	80	303.15	15	5	5.46	1980	1080
28	80	323.15	15	5	5.46	1980	1080
29	80	333.15	15	5	5.46	1980	1080
30	80	313.15	100	5	21.85	1920	1080
31	80	313.15	100	5	10.93	1940	1080
32	80	313.15	100	5	7.28	1960	1080
33	80	313.15	100	5	5.46	495	1080
34	80	313.15	100	5	5.46	990	1080
35	80	313.15	100	5	5.46	1485	1080
36	80	313.15	100	5	5.46	1980	0
37	80	313.15	100	5	5.46	1980	600
38	80	313.15	100	5	5.46	1980	840
39	80	313.15	100	5	5.46	1980	1080

A key in hydrogen peroxide synthesis are the promoters. Promoters have a double effect, avoid water formation and protect hydrogen peroxide decomposition and hydrogenation [7, 13, 19, 22]. There are some many bibliographic papers focus on inhibition capacity of promoters both in terms of chemical compound used or promoters concentration [6, 8, 9, 11, 23].

In this paper, H_3PO_4 and NaBr have been used as promoters as their efficiency has been proved in similar systems [14 – 17]. For all the experiments it have been used the amount of phosphoric acid enough to guarantee $\text{pH} = 2.0$ and the amount of sodium bromide necessary to keep a $\text{Br}^-/\text{Pd}=2$. Gas composition was fixed by two limitations, the necessity to keep hydrogen concentration below 4% to avoid explosive mixtures zone and the aim to use air instead of fed oxygen and nitrogen separately.

Table 2. Main results of experimentation

# Exp	TOF ₁₂₀ mol·h ⁻¹ ·gPd ⁻¹	%H ₂ O ₂ t = 120 min	Conversion, % t = 120 min	Selectivity, % t = 120 min	Yield, % t = 120 min	r _{obs} mmoles H ₂ O ₂ ·min ⁻¹
1	11.345	0.335	27.4	16.6	4.5	0.142
2	20.236	0.516	22.7	31.2	7.1	0.253
3	15.831	0.404	25.6	21.6	5.5	0.198
4	10.336	0.527	23.8	30.5	7.2	0.258
5	17.826	0.909	17.8	70.0	12.5	0.446
6	4.113	0.210	27.3	10.5	2.9	0.103
7	6.319	0.645	24.3	36.4	8.9	0.316
8	4.584	0.529	23.6	30.1	7.1	0.190
9	4.319	0.551	28.0	27.0	7.6	0.270
10	1.420	0.241	28.1	11.8	3.3	0.118
11	3.295	0.561	34.7	24.3	8.4	0.275
12	2.899	0.626	24.8	27.3	6.8	0.242
13	3.242	0.551	25.3	29.8	7.6	0.270
14	1.113	0.379	15.0	35.3	5.3	0.186
15	0.564	0.326	29.2	14.7	4.3	0.141
16	0.538	0.366	34.8	15.7	5.5	0.179
17	0.897	0.152	13.2	15.8	2.1	0.075
18	1.764	0.300	20.5	20.1	4.1	0.147
19	1.827	0.311	21.9	19.5	4.3	0.152
20	6.193	1.053	30.2	47.8	14.5	0.516
21	10.366	0.264	21.7	16.7	3.6	0.130
22	13.431	0.342	21.6	21.7	4.7	0.168
23	20.999	0.535	28.6	25.7	7.4	0.262
24	9.663	0.493	24.2	27.9	6.8	0.242
25	10.803	0.551	23.9	31.6	7.6	0.270
26	21.917	1.118	35.4	43.3	15.3	0.548

27	12.152	0.310	21.9	19.4	4.3	0.152
28	19.631	0.501	20.6	33.4	6.9	0.245
29	22.203	0.566	27.0	28.8	7.8	0.278
30	0.681	0.116	19.0	33.4	6.4	0.057
31	1.608	0.250	21.2	35.4	7.5	0.134
32	2.674	0.455	25.6	32.5	8.3	0.223
33	1.063	0.181	44.5	22.3	9.9	0.089
34	2.250	0.383	38.8	27.0	10.5	0.187
35	1.877	0.319	26.1	22.4	5.8	0.156
36	3.537	0.601	27.4	30.1	8.3	0.295
37	2.377	0.404	26.3	21.1	5.5	0.198
38	2.446	0.416	22.1	25.9	5.7	0.204
39	4.010	0.682	28.0	33.5	9.4	0.334

3.3.1. Nitrogen vs CO₂

In order to determine if nitrogen is as good inert as scCO₂ a comparison of experimental results obtained with both gasses is necessary. In this paper we have used N₂ as inert. The values for the synthesis using CO₂ have been extracted from a previous work Moreno *et al.* [14]. That paper was selected because the experimental set – up used in both cases is the same.

Experimental conditions (Exp. # 3, 7, 12, 13, 15, 16) were fixed in order to be similar to Moreno *et al.* experiments and simplify the comparison. However there are some small differences that did not affect to global results. For CO₂ experiments Br⁻/Pd = 8 and H₂/O₂ = 4.00, instead of Br⁻/Pd = 2 and H₂/O₂ = 5.46 of nitrogen experiments. All the CO₂ experiments were carried out at 80 barg, 313.15 K and with 5 %Pd/C catalyst.

Table 3. Results of experiments from Moreno et al. [8]

# Exp	Amount of catalyst, mg	TOF ₁₂₀ mol·h ⁻¹ ·gPd ⁻¹	%H ₂ O ₂ t = 120 min	Conversion, % t = 120 min	Selectivity, % t = 120 min	Yield, % t = 120 min
CO ₂ – 1	400	5.77	1.57	53%	43%	23%
CO ₂ – 2	400	5.50	1.50	51%	43%	22%
CO ₂ – 3	100	20.41	1.39	23%	88%	20%
CO ₂ – 4	250	8.79	1.49	38%	58%	22%
CO ₂ – 5	150	13.39	1.37	33%	60%	20%
CO ₂ – 6	200	11.62	1.58	44%	52%	23%
CO ₂ – 7	50	37.21	1.27	N.A.	N.A.	18%
CO ₂ – 8	30	60.01	1.22	N.A.	N.A.	18%
CO ₂ – 9	15	96.04	0.98	19%	74%	14%

At the first look, it can be observed that the yield with CO₂ was clearly higher than with N₂, under similar conditions. Comparing experiments with same amount of Pd, T.O.F values are between 6 and 10 times higher. Results are consistent with our initial hypotheses, CO₂ acts not only as inert but also increases system acidity (reduce secondary reactions) and improves hydrogen and oxygen transfer from gas to liquid phase.

Hydrogen peroxide final concentration was quite high for experiments with CO₂ as inert (1.58 % wt/v vs. 0.647 % wt/v). Moreno *et al.* concluded that, depending on the amount of catalyst, there are two different steps that limit the process. For experiments with an amount of catalyst lower than 100 mg, kinetics controlled the reaction meanwhile when the amount of catalyst was higher the controlling step was the mass transfer (hydrogen peroxide concentration did not increase with increasing amount of catalyst). Conversion increased linearly with the amount of catalyst, the more catalyst in the reaction the more active sites would be available for hydrogen consumption and conversion would be higher. Selectivity had a maximum value (88%) for 100 mg of catalyst. Decrease of selectivity was due to that decomposition and hydrogenation's rate reaction increase, because there were more active centers and because hydrogen peroxide concentration was higher (hydrogenation rate increases when H₂O₂ concentration is higher [12]).

Experimental results using nitrogen as inert will be discussed deeply in the next section. However, Figure 1 shows that nitrogen has a different influence over reaction process. Concentration is lower, does not keep constant when a high amount of catalyst is used and conversion increases but not linearly. Selectivity keeps the same tendency than for CO₂ experiments but values are lower.

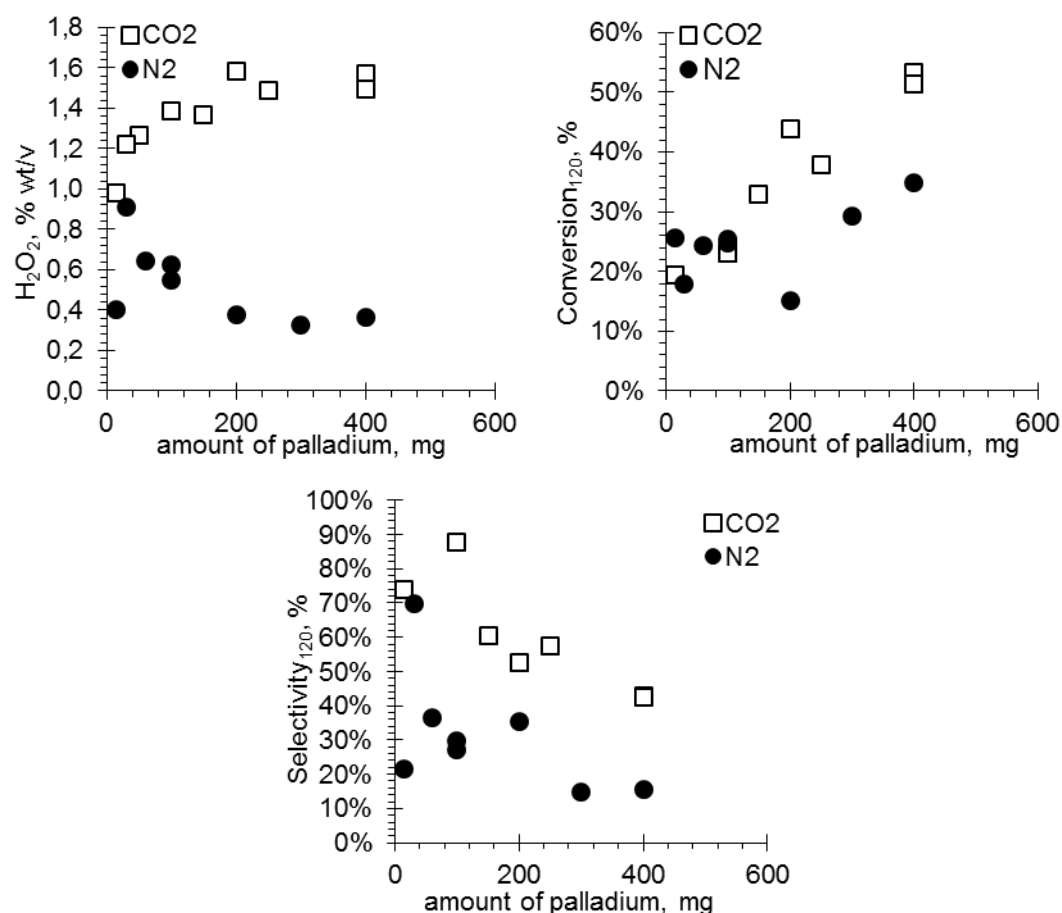


Figure 1. Comparison of direct synthesis experiments using N₂ or CO₂ as gas inert. (N₂ – Exp. # 3, 7, 12, 13, 15, 16; CO₂ – Exp. # 1 – 9) 80 barg, 313.15 K, pH = 2, CO₂: Br⁻/Pd = 8, N₂: Br⁻/Pd = 2, O₂/H₂ = 5.46, 1080 rpm.

3.3.2. Amount of catalyst and Pd loading

The reaction process consists of two steps in series, gas transfer to the liquid phase and chemical reaction on the catalyst active sites. Thus, our reaction system behaves like a slurry bubble column reactor with a short length and intense mixing. Depending on the process conditions, the controlling step will be mass transfer or kinetics. The hydrogen conversion in all the experiments was between 13.2 and 44.5%. Although a higher conversion was desirable, the variables studied were modified to operate either in mass transfer or kinetic regime extracting the maximum information from the system.

The amount of catalyst (15 – 500 mg) and palladium percentage (1, 3, and 5% Pd) were varied finding that the maximum H₂O₂ concentration was 0.909 % wt/v, with a selectivity of 70% and 17.8% of conversion. This value was obtained with only 15 mg of catalyst of 5% Pd/C. It is possible to obtain higher values of H₂ conversion increasing catalyst amount, but that implies a lower

selectivity and lower hydrogen peroxide concentration (figure 1). A similar behavior was obtained for 1% Pd/C and 3% Pd/C.

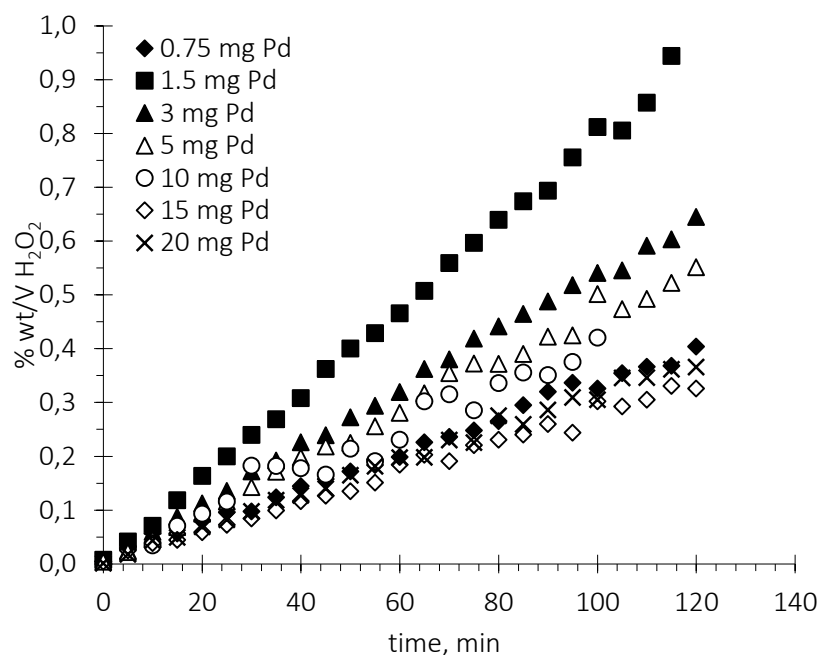


Figure 2. Influence of amount of catalyst (5% Pd/C) in the synthesis of hydrogen peroxide as a function of reaction time. (Exp. # 3, 5, 7, 12 – 16). 80 barg, 313.15 K, pH = 2, Br-/Pd = 2, O₂/H₂ = 5.46, 1080 rpm.

Using small amounts of catalyst, 15 mg of 5% Pd/C (0.75 mg of Pd), the number of active sites were not enough to guarantee that all the H₂ is converted and it was consumed fast enough to avoid hydrogenation of the hydrogen peroxide already produced. That will explain the low final hydrogen peroxide concentration, and the low selectivity and conversion values (figure 1). When the catalyst was increased to 30 mg (1.5 mg of Pd), hydrogen peroxide final concentration rose from 0.404 %wt/v to 0.909 %wt/v.

From our previous study [14] it was known that using CO₂ as inert there is a gap in which kinetics is the controlling step. Operating in those conditions, for amounts of catalyst lower than 100 mg of 5% Pd/C (5 mg of Pd), increasing amount of solid hydrogen peroxide concentration will rise too. However when N₂ is used as inert the gap where kinetic controls the system is narrower than when using CO₂.

That is consistent with the results shown in Figure 2. Using 60 mg of catalyst (3 mg of Pd) or 100 mg of catalyst (5 mg of Pd) values of hydrogen peroxide were quite similar. From 60 mg of

catalyst, increasing catalyst amount there is not a rise in hydrogen peroxide concentration, which means mass transfer stage is the control step.

For higher amounts of catalyst there is not a further improvement in synthesis ability to produce hydrogen peroxide otherwise it gets worse. Figure 3 and 4 are consistent with this statement. Hydrogen consumption increased together with amount of catalyst, although the increased is lower in comparison with the amount of catalyst's increased, for 5 %Pd/C hydrogen consumption increased from 0.914 mmol H₂·min⁻¹ with 0.75 mg of catalyst to 1.244 mmol H₂·min⁻¹ with mg of catalyst. The amount of hydrogen consumed rose but H₂O₂ productivity did not do it, it is because decomposition and hydrogenation reaction's rate were higher, and that will explain that selectivity decreased.

Results are different based on the palladium percentage of the catalyst, even if the total amount of palladium and the operation conditions are the same. The catalyst are different, so the main reason for this behavior can be the differences in structure and characteristics for each catalyst, even when the solid support might be similar.

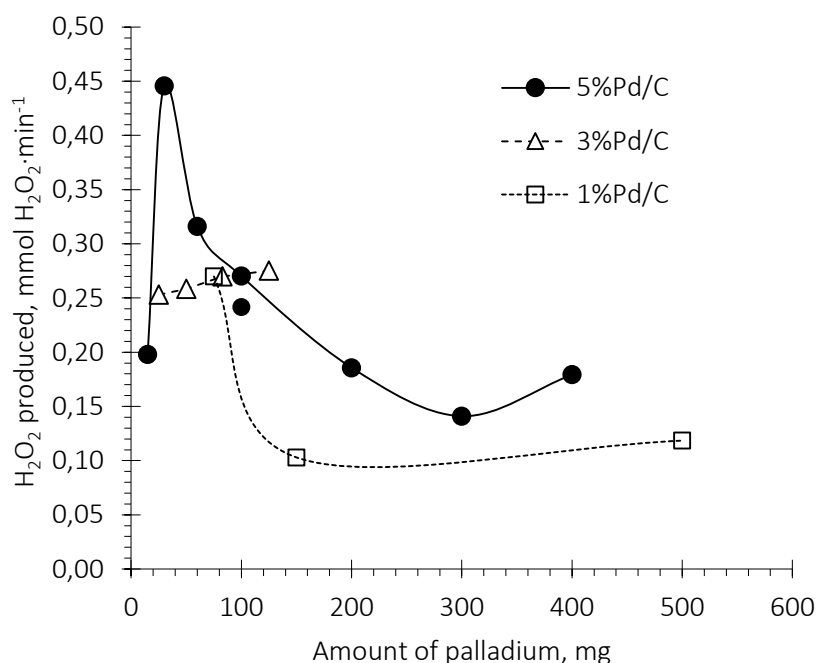


Figure 3. Influence of amount of Pd over H₂O₂ productivity, evaluated at 120 min of reaction time. (Exp. # 3, 5, 7, 12 – 16). 80 barg, 313.15 K, pH = 2, Br⁻/Pd = 2, O₂/H₂ = 5.46, 1080 rpm..

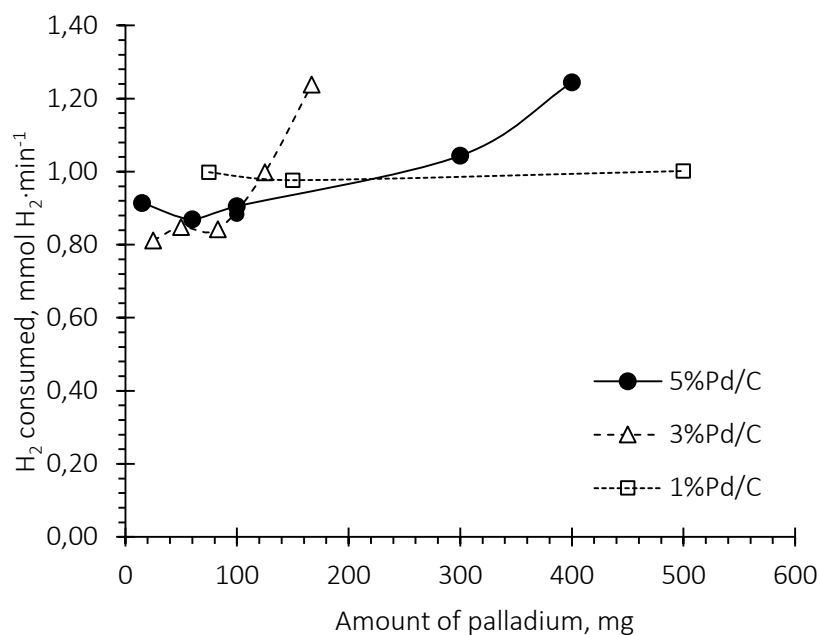


Figure 4. Influence of amount of Pd over H₂ consumed rate, evaluated at 120 min of reaction time. (Exp. # 3, 5, 7, 12 – 16). 80 barg, 313.15 K, pH = 2, Br⁻/Pd = 2, O₂/H₂ = 5.46, 1080 rpm.

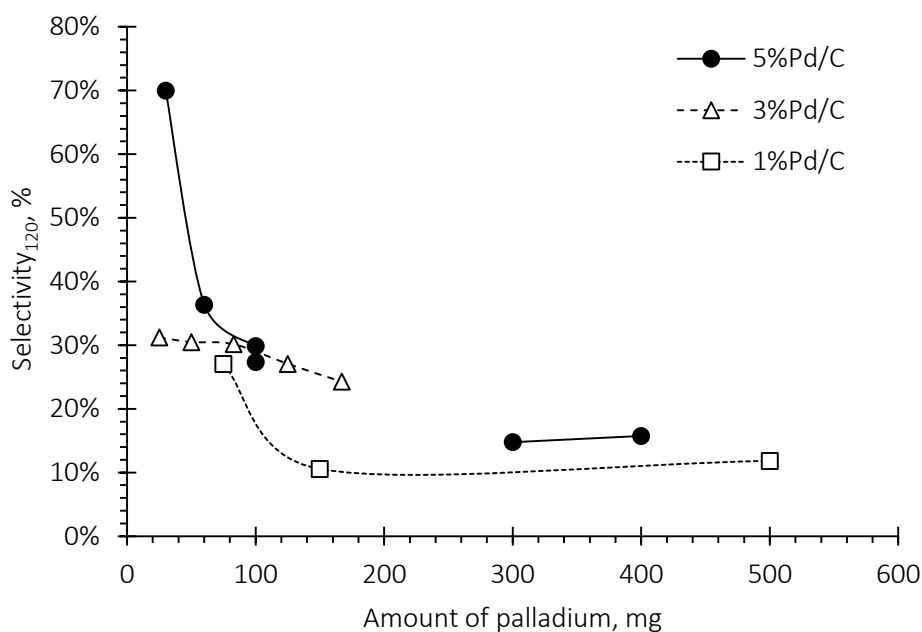


Figure 5. Selectivity towards H₂O₂ versus the amount of Pd, evaluated at 120 min of reaction time. (Exp. # 3, 5, 7, 12 – 16). 80 barg, 313.15 K, pH = 2, Br⁻/Pd = 2, O₂/H₂ = 5.46, 1080 rpm.

3.3.3. Pressure and hydrogen partial pressure

Pressure influence has been studied for pressure values between 20 and 90 barg and for partial hydrogen pressure values form 0.83 barg to 3.23 barg. To guarantee system is operating in mass

transfer control region all the experiments in this series were carried out with 100 mg of 5% Pd/C catalyst. Other reaction conditions were kept equal as experiments in previous section.

Pressure has a positive role in hydrogen peroxide synthesis. The four control parameters of process, productivity, selectivity, conversion and turnover frequency (TOF) rose with total pressure following an exponential curve, as can be seen in figures 6 and 7. Increasing of H₂O₂ productivity is due higher gas solubility in liquid phase. High pressures enhance gas solubility improving mass transfer coefficients, so the observed reaction rate increases also, so hydrogen was consumed faster and secondary reactions effects were reduced.

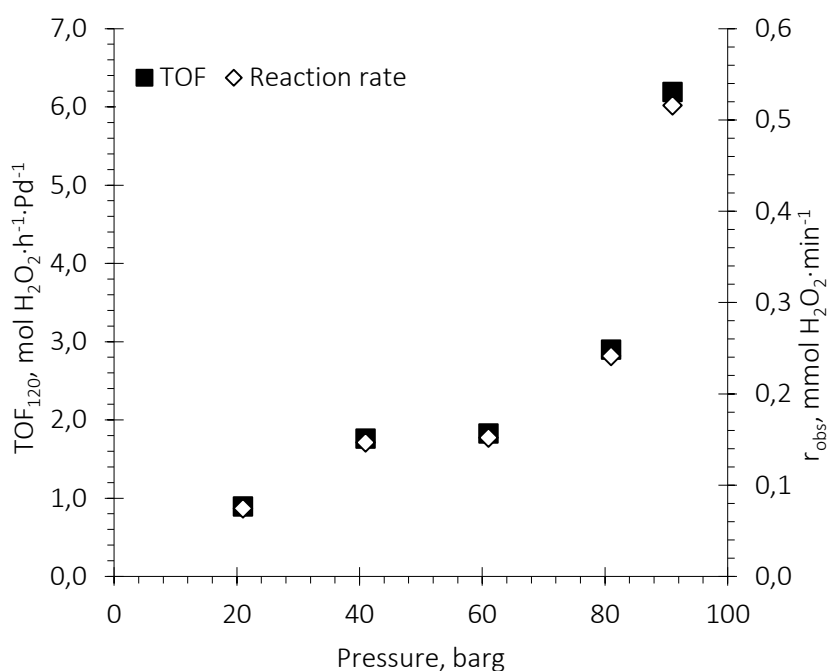


Figure 6. Influence of total pressure on turnover frequency, evaluated at reaction time 120 min, and productivity values (Exp. # 12, 17 – 20) at 313.15 K, 100 mg catalyst, 5 % Pd/C, pH = 2, Br⁻/Pd = 2, O₂/H₂ = 5.46, 1080 rpm.

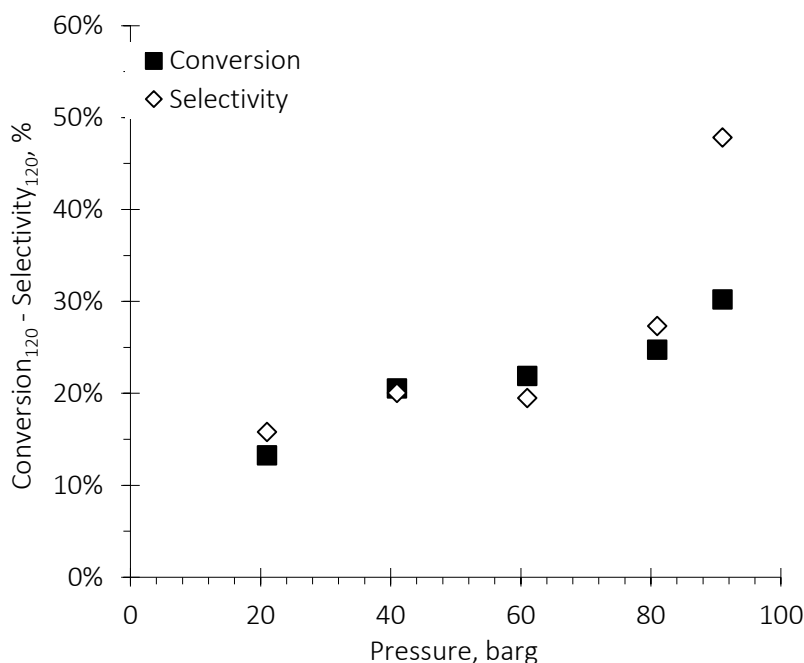


Figure 7. Influence of total pressure on conversion and selectivity, evaluated at reaction time 120 min (Exp. # 12, 17 – 20) at 313.15 K, 100 mg catalyst, 5 % Pd/C, pH = 2, Br⁻/Pd = 2, O₂/H₂ = 5.46, 1080 rpm.

In order to study hydrogen partial pressure two series of experiments were carried out. In the first one, hydrogen molar fraction was kept constant and total system pressure varied between 20 and 90 barg. In the other series total system's pressure was kept constant at 80 barg and hydrogen molar fraction changed between 1% and 4%.

Regardless of variations in hydrogen partial pressure, caused by both variations in total pressure or molar fraction of H₂ in the gas phase, TOF and conversion had the same value and increased linearly at low hydrogen partial pressures. Selectivity was almost constant when hydrogen molar fraction varied, its values oscillated between 30% and 35% but there was a small decrease when molar fraction of 4% was reached. However, selectivity depended strongly of hydrogen partial pressure if it changed due total pressure. At low pressures, 20 barg, selectivity took values around 16% but it can reach 48% when pressure rose until 90 barg.

It can be explained as a function of O₂/H₂ ratio. When hydrogen partial pressure changed due to total pressure the O₂/H₂ ratio was constant because gas composition is the same. In that case, selectivity behaved as conversion and T.O.F. and increased lineally. However if hydrogen partial pressure varied as results of a variation of hydrogen molar fraction the O₂/H₂ ratio varied as well. A high O₂/H₂ ratio or a low hydrogen partial pressure implies a high amount of oxygen available in the liquid phase that can affect catalyst's selectivity by being adsorbed over active centers [3] or modifying active metal oxidation state [10]. Although for low hydrogen partial pressures (0.8

barg) a higher selectivity was obtained when a high value of O₂/H₂ was used (33.4 % at 80 barg and O₂/H₂ = 21.85 vs. 16% at 20 barg and O₂/H₂ = 5.46) the productivity of the system, measured by the T.O.F, was extremely low in comparison with the values obtained at a higher hydrogen partial pressures even if the selectivity decreased (0.681 mol H₂O₂·h⁻¹·g Pd⁻¹ at 80 barg, O₂/H₂ = 21.58, 33.4% selectivity vs. 2.899 mol H₂O₂·h⁻¹·g Pd⁻¹ at 80 barg, O₂/H₂ = 5.46, 27.3 % selectivity).

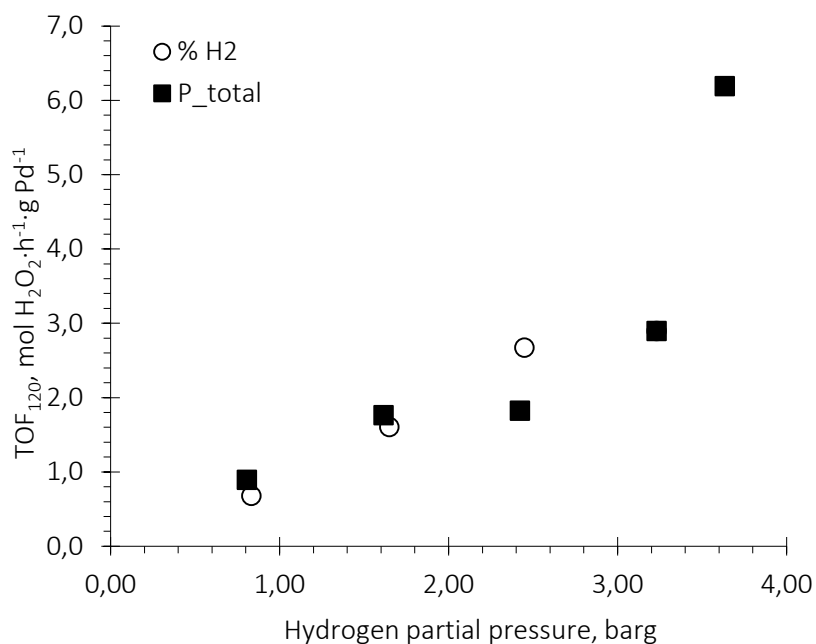


Figure 8. Influence of partial pressure of hydrogen on turnover frequency, evaluated at 120 min. (Exp. # 12, 17 – 20, 30 – 32) at 313.15 K, 100 mg of catalyst, 5 % Pd/C. ■; 20 – 90 barg, 4% H₂, ○; 80 barg, 1% – 4% H₂

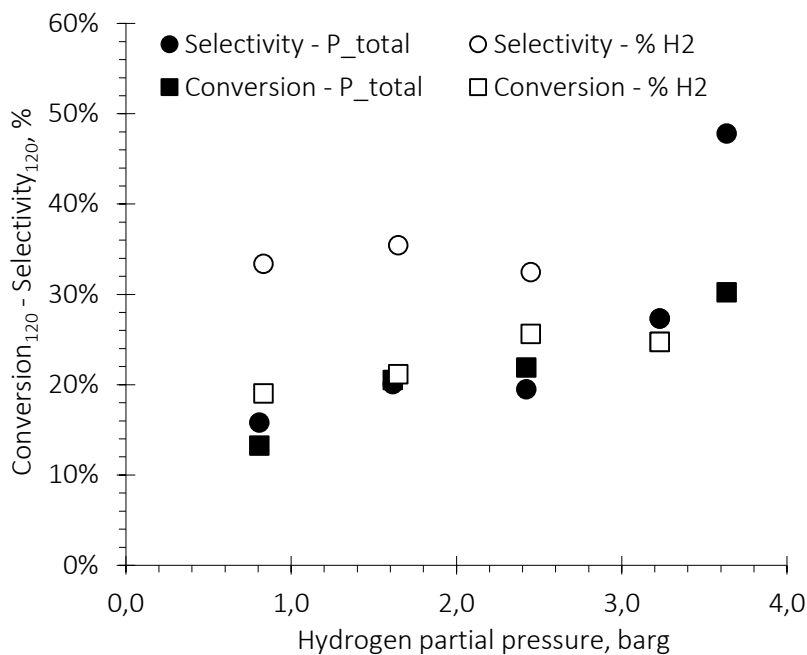


Figure 9. Influence of partial pressure of hydrogen on conversion and selectivity, evaluated at 120 min. (Exp. # 12, 17 – 20, 30 – 32) at 313.15 K, 100 mg of catalyst, 5 % Pd/C. ■; 20 – 90 barg, 4% H₂, ○; 80 barg, 1% – 4% H₂

3.3.4. Reaction temperature

To study influence of temperature all the experiments in this section had been carried out with a low amount of catalyst to sure that kinetic is the controlling step. Observed reaction rate has been calculated from hydrogen peroxide concentration results, assuming that oxygen and hydrogen concentration in liquid phase is constant for each temperature. For all the series, using different Pd load (1%, 3% and 5% Pd/C) observed reaction rate rose with temperature, as it was expected as four reactions are exothermic.

Comparing results of the three series it is perceived that experiments carried out with 1% Pd/C (0.130 – 0.262 mmol H₂O₂/min) and 5% Pd/C (0.152 – 0.278 mmol H₂O₂/min) had similar values of observed reaction rate (r_{obs}). For 3 %Pd/C experiments, reaction rate was greater (0.242 – 0.548 mmol H₂O₂/min). The amount of actives sites is the reason for these differences. The number of actives sites in experiments with 1% Pd/C and 5 % Pd/C was the same, what explains that results are very similar, in experiments with 3% Pd/C the amount of Pd is double and so reaction rate is higher.

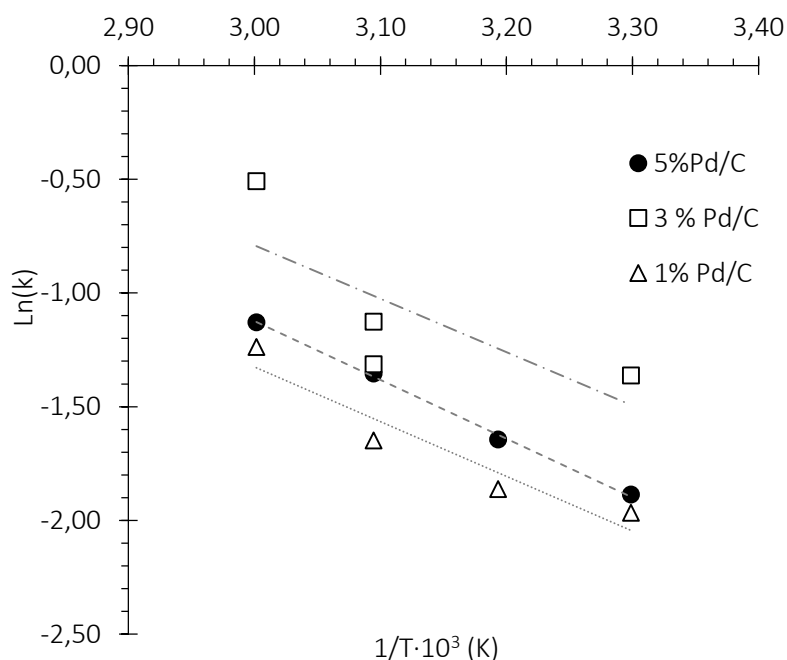


Figure 10. Temperature dependence, Arrhenius plot, (Exp. # 1, 3, 4, 21 – 29) at 80 barg, pH = 2, Br⁻/Pd = 2, O₂/H₂ = 5.46, 1080 rpm.

Hydrogen peroxide productivity increased linearly with the reaction time (Figure 2). That implies that the reaction rate did not depend on the H₂O₂ concentration and in consequence it could be assumed that the reaction constant could be obtained directly by the representation of the productivity of hydrogen peroxide against the reaction time. Pre – exponential factor and activation energy divided by gas constant (E_a/R) can be calculated graphically from figure 10 according to the Equation 2.

$$\frac{d[H_2O_2]}{dt} = r = k; \text{ Equation 1} \quad k = k_0 \cdot e^{\frac{-E_a}{R \cdot T}}; \text{ Equation 2}$$

Pre-exponential factor represents the frequency of collisions between reactant molecules. The values of the pre – exponential factor (272.15 mmol·min⁻¹, 520.54 mmol·min⁻¹ and 766.51 mmol·min⁻¹ for 1 % Pd/C, 3 % Pd/C and 5 % Pd/C catalyst respectively) increased linearly with the palladium percentage on the catalyst which suggest that higher the amount of catalyst faster the reaction (a higher pre – exponential factor implies that molecules collide more frequently). A quick reaction is desired because high consumption of the hydrogen reduce the risk of the hydrogenation of the H₂O₂ already generated. However a high amount of catalyst could be undesired since hydrogen peroxide could be decomposed by the active sites of the solid. No relation between the amount of palladium (0.75 mg for 1 % Pd/C, 1.5 mg for 3 % Pd/C and 0.75 mg for 5 % Pd/C) and the pre – exponential factor or the activation energy have been found, that

suggest that not only the total amount of active metal but also the concentration of the metal on the solid have influence over the system productivity.

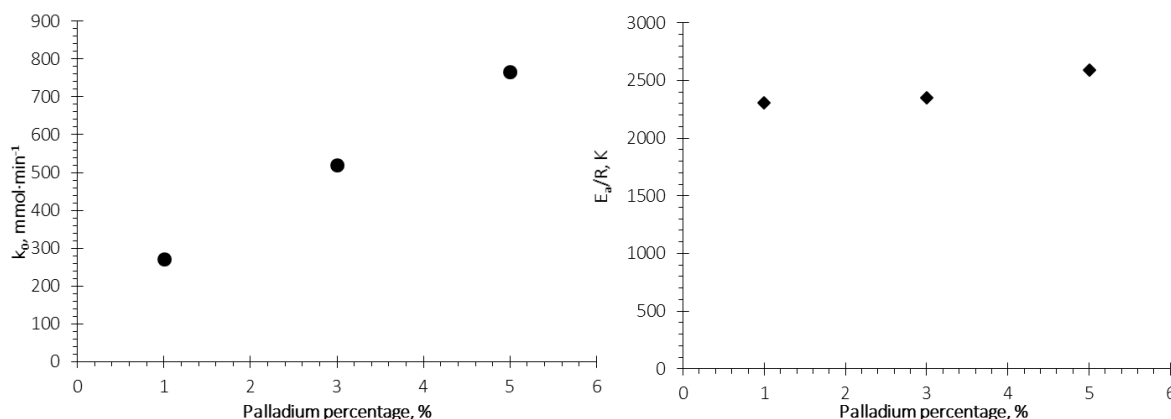


Figure 11. Pre – exponential factor (left) and E_a/R (right) values obtained for the direct synthesis of H_2O_2 using N_2 as inert. (Exp. # 1, 3, 4, 21 – 29) at 80 barg, pH = 2, $Br^-/Pd = 2$, $O_2/H_2 = 5.46$, 1080 rpm.

Also a relation between the percentage of palladium in the catalyst and the E_a/R have been found 2306.7 K, 2348.4 K and 2588.2 K for 1 % Pd/C, 3 % Pd/C and 5 % Pd/C catalyst respectively. Higher the palladium percentage in the catalyst higher the value of the E_a/R and consequently lower the value of the reaction rate constant. However, effect of the palladium rate over the value of k_0 is greater than the effect over the E_a/R and in consequence, according to our experimental results, the reaction rate is higher when rich active metal catalyst is used.

3.3.5. Gas total flow rate

Influence of gas total flow rate has been studied from values between 495 and 1980 $NmL \cdot min^{-1}$. Hydrogen and oxygen inlet gas phase concentration are kept constant at 4.04% and 22.7% respectively. Hydrogen peroxide production rate and TOF increase with gas flow because there is more hydrogen and oxygen available to reaction. As it can be seen in figure 11, hydrogen consumed and hydrogen peroxide productivity increased linearly with gas flow rate. That means that selectivity was constant close to 25 %. Conversion decreased with gas flow rate from 45% to 25% because at high flow rate, gas residence time inside the reactor is lower and reduces the conversion.

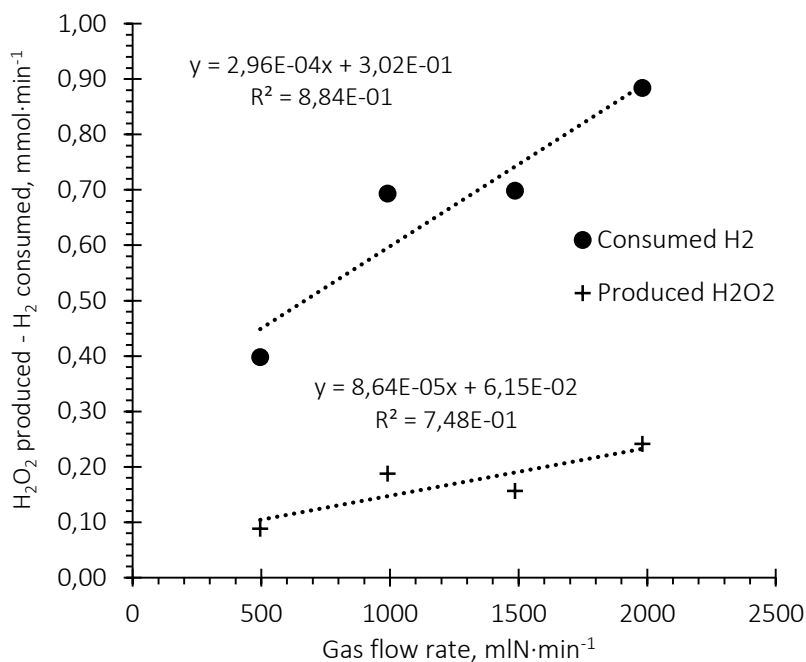


Figure 12. Influence of gas flow rate over H₂O₂ production and H₂ consumption, evaluated at reaction time 120 min. (Exp. # 12, 33 – 35) at 80 barg, 313.15 K, 100 mg catalyst, 5 % Pd/C, pH = 2, Br⁻/Pd = 2, O₂/H₂ = 5.46, 1080 rpm.

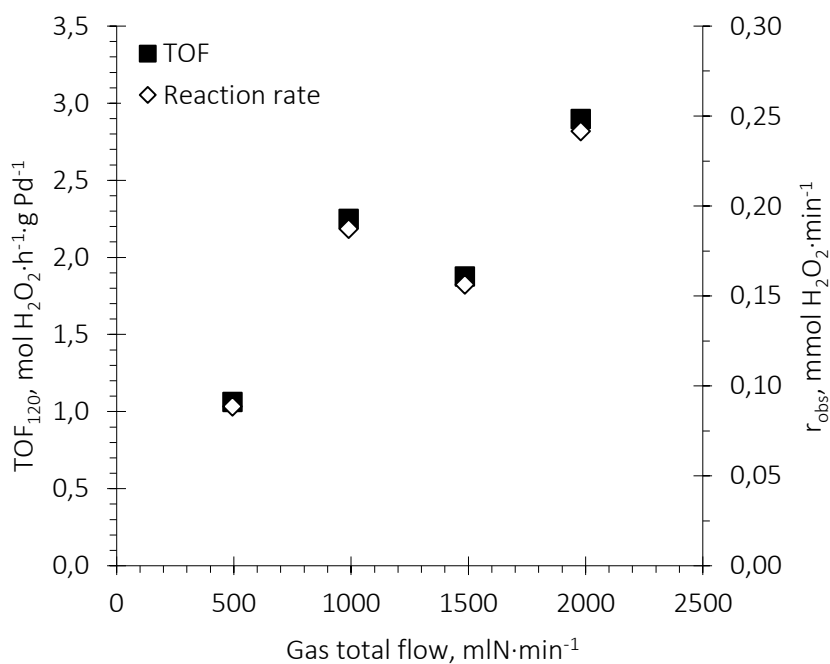


Figure 13. Influence of gas total flow on turnover frequency (TOF), evaluated at reaction time 120 min, and productivity (Exp. # 12, 33 – 35) at 80 barg, 313.15 K, 100 mg catalyst, 5 % Pd/C, pH = 2, Br⁻/Pd = 2, O₂/H₂ = 5.46, 1080 rpm.

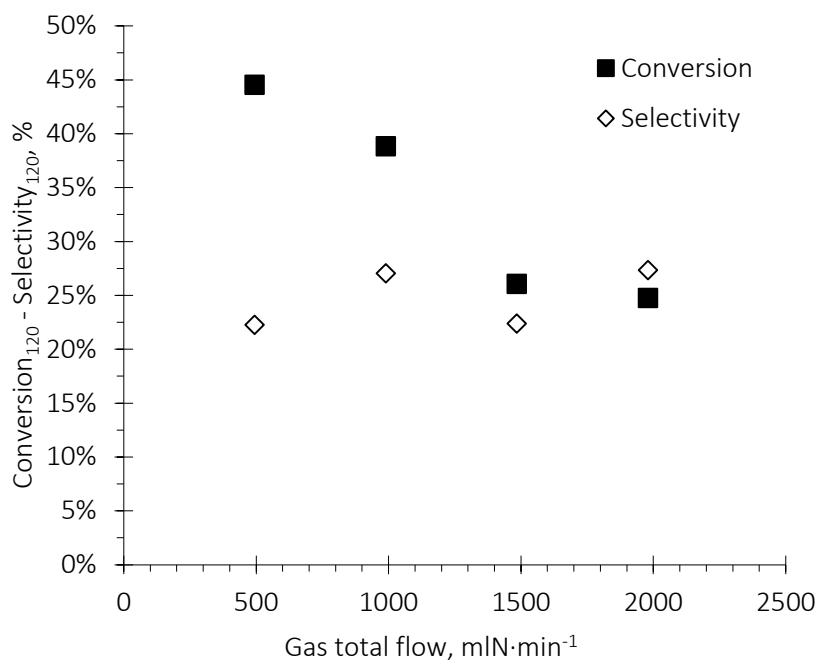


Figure 14. Influence of gas total flow on conversion and selectivity, evaluated at reaction time 120 min, (Exp. # 12, 33 – 35) at 80 barg, 313.15 K, 100 mg catalyst, 5 % Pd/C, pH = 2, Br⁻/Pd = 2, O₂/H₂ = 5.46, 1080 rpm.

3.3.6. Influence of agitation speed

As this is a process that takes places in three different phases it is limited by mass transfer step. It is obvious that agitation speed might be a key parameter in process optimization.

Results from experiments 36 to 39 showed, by contrast, that agitation speed has not a sharp effect. At the studied interval, from 0 to 1080 rpm none of the four parameters, TOF, conversion, selectivity or productivity, changes so much enough as agitation speed can be considered as a decisive parameter. These results can be seen at figures 14 and 15.

These unexpected results might be due to the special design of the gas inlet system. Gases are feeding into the reactor through a micro porous diffuser which transforms the gas stream into micro bubbles. That way it is possible to increase exchange surface and liquid phase turbulence improving mass transfer coefficient. Results, however, showed that agitation system did not work perfectly caused a gas stream bypass that reduced its residence time inside the reactor and also the amount of gas solved into the liquid phase.

Regarding the results, an agitation speed of 1080 rpm was used for all the experiments to ensure at any operation conditions that the system is perfectly mixed.

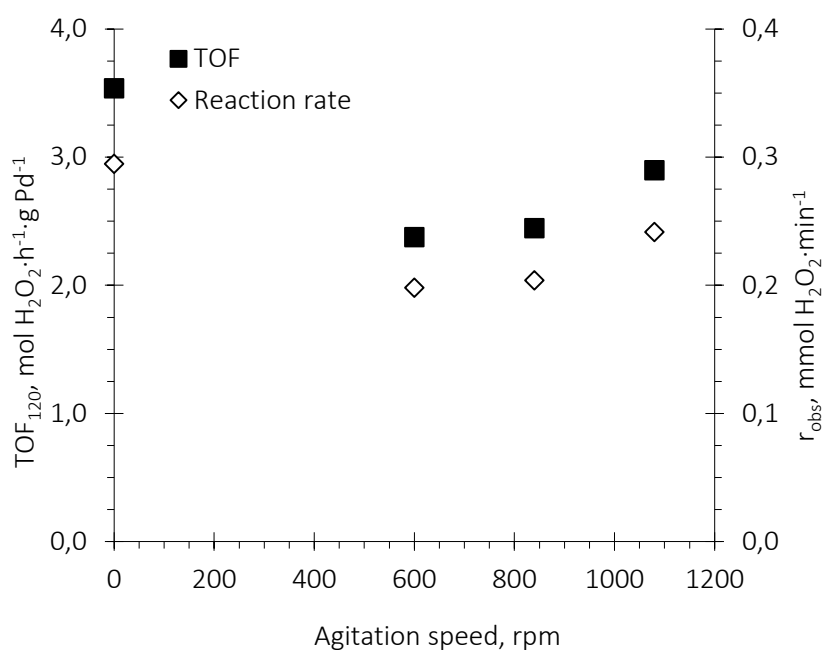


Figure 15. Influence of agitation speed on conversion and selectivity, evaluated at reaction time 120 min, (Exp. # 12, 36 – 39) at 80 barg, 313.15 K, 100 mg catalyst, 5 % Pd/C, pH = 2, Br⁻/Pd = 2, O₂/H₂ = 5.46.

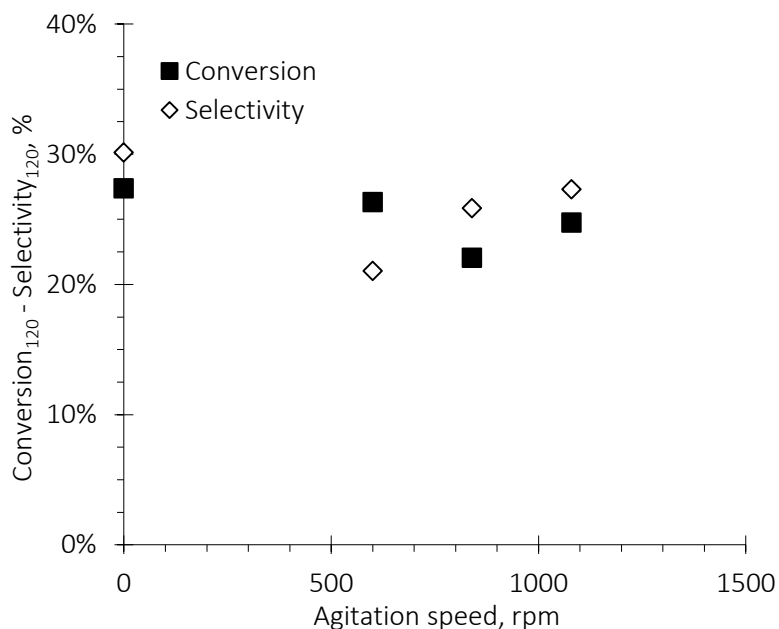


Figure 16. Influence of agitation speed on conversion and selectivity, evaluated at reaction time 120 min, (Exp. # 12, 36 – 39) at 80 barg, 313.15 K, 100 mg catalyst, 5 % Pd/C, pH = 2, Br⁻/Pd = 2, O₂/H₂ = 5.46.

3.4. Conclusions

From experimental results and data analysis it can be concluded that it is possible to produce hydrogen peroxide in a semicontinuous stirring reactor using nitrogen as inert. It has been achieved hydrogen peroxide concentration values of 1.13 %wt/v and values of selectivity and conversion of 70% and 35% respectively. Productivity (measured by the hydrogen peroxide concentration) and selectivity of the reaction were higher when carbon dioxide was used as inert (CO₂: 1.58 % wt/v vs. N₂: 0.647 % wt/v), since the CO₂ properties boosted the mass transfer and stabilized the hydrogen peroxide. Even if nitrogen has not an acidity effect over the system at low pH values (pH = 2) it is possible to avoid decomposition and hydrogenation of hydrogen peroxide.

Mass transfer phenomena act as the controlling step of the reaction even when the amount of catalyst in the reaction is low. Optimum value of the amount of catalyst have been found to be 30 mg (5 % Pd/C); if the concentration of actives sites is lower the hydrogen is not consume quickly enough and the hydrogen peroxide is hydrogenated. Increasing the amount of catalyst it is not possible to enhance the efficiency or productivity of the reaction because the mass transfer is the controlling stage but also because a rising of the decomposition could be expected. This behavior is more pronounced when high percentage catalyst was used. Conversion (13.2 % – 30.2 %), selectivity (15.8 % – 47.8 %) and T.O.F (0.897 mol·h⁻¹·g Pd⁻¹ – 6.193 mol·h⁻¹·g Pd⁻¹) increased with operation total pressure (20 barg to 90 barg), as it was expected. Influence of the O₂/H₂ on the selectivity (measured indirectly throw the variation of the hydrogen partial pressure) have been determinate. At high O₂/H₂, the selectivity decreases due to the high oxygen concentration that could affect the adsorption mechanism or modified the oxidation state of the active metal.

Influence of reaction temperature was also studied and the values of pre – exponential factor (272.15 mmol·min⁻¹, 520.54 mmol·min⁻¹ and 766.51 mmol·min⁻¹ for 1 % Pd/C, 3 % Pd/C and 5 % Pd/C catalyst respectively) and the ratio E_a/R (2306.7 K, 2348.4 K and 2588.2 K for 1 % Pd/C, 3 % Pd/C and 5 % Pd/C catalyst respectively) were calculated from the experimental results using the Arrhenius equation. A strong dependence of the pre – exponential factor with the palladium percentage of the catalyst has been found. Effect of the gas flow rate over the conversion, selectivity and productivity was analyzed. As the selectivity remained constant the productivity increased because the amount of hydrogen and oxygen were higher. However conversion decreased with the gas flow rate due to the residence time of the gas inside the reactor is

shorter. No influence of the agitation speed was found due mainly to experimental errors and the reactor design.

Although results are quite good, it has been impossible to achieve the main objective of this study. Results with N₂ are worse than results obtained with CO₂ due N₂ has not the same chemical and mass transfer properties that CO₂ has and that can increase oxygen and hydrogen ability to dissolve in liquid phase. However using air as reactive and inert allows reducing the operation cost and simplifies the system as oxygen and inert are feeding into the reactor simultaneously and using only one mass flow controller.

Even the results are not as good as it could be expected, future work might be targeted on different reaction systems and reaction with other mass transfer configurations that might increase efficiency and yield.

Acknowledgements

The authors thank the Spanish Economy and Competitiveness Ministry (former Science and Innovation Ministry) Project Reference: CTQ2011-23293, ENE2012-33613 and Junta de Castilla y León Project Reference: VA254B11-2 for funding. Also authors want to thank Teresa Moreno Rueda for CO₂ experiments' dates and results.

References

- [1] E.J. Beckman, Production of H₂O₂ in CO₂ and its use in the direct synthesis of propylene oxide, *Green Chemistry* 5 (2003) 332-336.
- [2] E.J. Beckman, Supercritical and near-critical CO₂ in green chemical synthesis and processing, *Journal of Supercritical Fluids* 28 (2004) 121-191.
- [3] P. Biasi, J. Garcia-Serna, A. Bittante, T. Salmi, Direct synthesis of hydrogen peroxide in water in a continuous trickle bed reactor optimized to maximize productivity, *Green Chemistry* 15 (2013) 2502-2513.
- [4] J.M. Campos-Martin, G. Blanco-Brieva, J.L.G. Fierro, Hydrogen Peroxide Synthesis: An Outlook beyond the Anthraquinone Process, *Angewandte Chemie International Edition* 45 (2006) 6962-6984.
- [5] I.R. Cohen, T.C. Purcell, A.P. Altshuler, Analysis of the oxidant in photooxidation reactions, *Environmental Science and Technology* 1 (1967) 247-252.

- [6] V.R. Choudhary, P. Jana, Direct oxidation of H₂ to H₂O₂ over Br and F-promoted Pd/Al₂O₃ in aqueous acidic medium: Influence of the concentration of Br and F and the method of incorporation of the two halogens in the catalyst on their beneficial synergetic effect on the net H₂O₂ formation, *Applied Catalysis A: General* 329 (2007) 79-85.
- [7] V.R. Choudhary, C. Samanta, Role of chloride or bromide anions and protons for promoting the selective oxidation of H₂ by O₂ to H₂O₂ over supported Pd catalysts in an aqueous medium, *Journal of Catalysis* 238 (2006) 28-38.
- [8] V.R. Choudhary, C. Samanta, P. Jana, Formation from direct oxidation of H₂ and destruction by decomposition/hydrogenation of H₂O₂ over Pd/C catalyst in aqueous medium containing different acids and halide anions, *Applied Catalysis A: General* 317 (2007) 234-243.
- [9] V.R. Choudhary, C. Samanta, P. Jana, Hydrogenation of hydrogen peroxide over palladium/carbon in aqueous acidic medium containing different halide anions under static/flowing hydrogen, *Industrial and Engineering Chemistry Research* 46 (2007) 3237-3242.
- [10] T. Deguchi, M. Iwamoto, Reaction mechanism of direct H₂O₂ synthesis from H₂ and O₂ over Pd/C catalyst in water with H⁺ and Br⁻ ions, *Journal of Catalysis* 280 (2011) 239-246.
- [11] Y.F. Han, J.H. Lunsford, Direct formation of H₂O₂ from H₂ and O₂ over a Pd/SiO₂ catalyst: The roles of the acid and the liquid phase, *Journal of Catalysis* 230 (2005) 313-316.
- [12] I. Huerta, J. García-Serna, M.J. Cocero, Hydrogenation and decomposition kinetic study of H₂O₂ over Pd/C catalyst in an aqueous medium at high CO₂ pressure, *The Journal of Supercritical Fluids* 74 (2013) 80-88.
- [13] P. Landon, P.J. Collier, A.F. Carley, D. Chadwick, A.J. Papworth, A. Burrows, C.J. Kiely, G.J. Hutchings, Direct synthesis of hydrogen peroxide from H₂ and O₂ using Pd and Au catalysts, *Physical Chemistry Chemical Physics* 5 (2003) 1917 - 1923.
- [14] T. Moreno Rueda, J. García Serna, M.J. Cocero Alonso, Direct production of H₂O₂ from H₂ and O₂ in a biphasic H₂O/scCO₂ system over a Pd/C catalyst: Optimization of reaction conditions, *The Journal of Supercritical Fluids* 61 (2012) 119-125.
- [15] T. Moreno, J. García-Serna, M.J. Cocero, Direct synthesis of hydrogen peroxide in methanol and water using scCO₂ and N₂ as diluents, *Green Chemistry* 12 (2010) 282-289.

- [16] T. Moreno, J. García-Serna, M.J. Cocero, Decomposition reaction of H₂O₂ over Pd/C catalyst in an aqueous medium at high pressure: Detailed kinetic study and modelling, *The Journal of Supercritical Fluids* 57 (2011) 227-235.
- [17] T. Moreno, J. García-Serna, P. Plucinski, M.J. Sánchez-Montero, M.J. Cocero, Direct synthesis of H₂O₂ in methanol at low pressures over Pd/C catalyst: Semi-continuous process, *Applied Catalysis A: General* 386 (2010) 28-33.
- [18] T. Moreno, M.A. Morán López, I. Huerta Illera, C.M. Piqueras, A. Sanz Arranz, J. García Serna, M.J. Cocero, Quantitative Raman determination of hydrogen peroxide using the solvent as internal standard: Online application in the direct synthesis of hydrogen peroxide, *Chemical Engineering Journal* 166 (2011) 1061-1065.
- [19] E. Ntainjua, J.K. Edwards, A.F. Carley, J.A. Lopez-Sanchez, J.A. Moulijn, A.A. Herzing, C.J. Kiely, G.J. Hutchings, The role of the support in achieving high selectivity in the direct formation of hydrogen peroxide, *Green Chemistry* 10 (2008) 1162-1169.
- [20] J.O. Pande, J. Tonheim, Ammonia plant NII: Explosion of hydrogen in a pipeline for CO₂, *Process Safety Progress* 20 (2001) 37-39.
- [21] C.M. Piqueras, J. García-Serna, M.J. Cocero, Estimation of lower flammability limits in high-pressure systems. Application to the direct synthesis of hydrogen peroxide using supercritical and near-critical CO₂ and air as diluents, *The Journal of Supercritical Fluids* 56 (2011) 33-40.
- [22] T.A. Pospelova, N.I. Kobozev, E.N. Eremin, Palladium catalyzed synthesis of hydrogen peroxide from its elements. I. Conditions for the formation of hydrogen peroxide, *Russian Journal of Physical Chemistry* 35 (1961) 143-147.
- [23] C. Samanta, Direct synthesis of hydrogen peroxide from hydrogen and oxygen: An overview of recent developments in the process, *Applied Catalysis A: General* 350 (2008) 133-149.
- [24] M.G. Zabetakis, Flammability Characteristics of Gases and Vapors, Bureau of Mines 627 (1965).

Table Captions

Table 1. Experimental values of the main operational variables	116
Table 2. Main results of experimentation	117
Table 3. Results of experiments from Moreno et al. [8].....	118

Figure Captions

- Figure 1. Comparison of direct synthesis experiments using N_2 or CO_2 as gas inert. (N_2 – Exp. # 3, 7, 12, 13, 15, 16; CO_2 – Exp. # 1 – 9) 80 barg, 313.15 K, pH = 2, CO_2 : $Br^-/Pd = 8$, N_2 : $Br^-/Pd = 2$, $O_2/H_2 = 5.46$, 1080 rpm..... 120
- Figure 2. Influence of amount of catalyst (5% Pd/C) in the synthesis of hydrogen peroxide as a function of reaction time. (Exp. # 3, 5, 7, 12 – 16). 80 barg, 313.15 K, pH = 2, $Br^-/Pd = 2$, $O_2/H_2 = 5.46$, 1080 rpm..... 121
- Figure 3. Influence of amount of Pd over H_2O_2 productivity, evaluated at 120 min of reaction time. (Exp. # 3, 5, 7, 12 – 16). 80 barg, 313.15 K, pH = 2, $Br^-/Pd = 2$, $O_2/H_2 = 5.46$, 1080 rpm..... 122
- Figure 4. Influence of amount of Pd over H_2 consumed rate, evaluated at 120 min of reaction time. (Exp. # 3, 5, 7, 12 – 16). 80 barg, 313.15 K, pH = 2, $Br^-/Pd = 2$, $O_2/H_2 = 5.46$, 1080 rpm..... 123
- Figure 5. Selectivity towards H_2O_2 versus the amount of Pd, evaluated at 120 min of reaction time. (Exp. # 3, 5, 7, 12 – 16). 80 barg, 313.15 K, pH = 2, $Br^-/Pd = 2$, $O_2/H_2 = 5.46$, 1080 rpm..... 123
- Figure 6. Influence of total pressure on turnover frequency, evaluated at reaction time 120 min, and productivity values (Exp. # 12, 17 – 20) at 313.15 K, 100 mg catalyst, 5 % Pd/C, pH = 2, $Br^-/Pd = 2$, $O_2/H_2 = 5.46$, 1080 rpm. 124
- Figure 7. Influence of total pressure on conversion and selectivity, evaluated at reaction time 120 min (Exp. # 12, 17 – 20) at 313.15 K, 100 mg catalyst, 5 % Pd/C, pH = 2, $Br^-/Pd = 2$, $O_2/H_2 = 5.46$, 1080 rpm..... 125
- Figure 8. Influence of partial pressure of hydrogen on turnover frequency, evaluated at 120 min. (Exp. # 12, 17 – 20, 30 – 32) at 313.15 K, 100 mg of catalyst, 5 % Pd/C. ■; 20 – 90 barg, 4% H_2 , O; 80 barg, 1% – 4% H_2 126
- Figure 9. Influence of partial pressure of hydrogen on conversion and selectivity, evaluated at 120 min. (Exp. # 12, 17 – 20, 30 – 32) at 313.15 K, 100 mg of catalyst, 5 % Pd/C. ■; 20 – 90 barg, 4% H_2 , O; 80 barg, 1% – 4% H_2 127
- Figure 10. Temperature dependence, Arrhenius plot, (Exp. # 1, 3, 4, 21 – 29) at 80 barg, pH = 2, $Br^-/Pd = 2$, $O_2/H_2 = 5.46$, 1080 rpm. 128
- Figure 11. Pre – exponential factor (left) and E_a/R (right) values obtained for the direct synthesis of H_2O_2 using N_2 as inert. (Exp. # 1, 3, 4, 21 – 29) at 80 barg, pH = 2, $Br^-/Pd = 2$, $O_2/H_2 = 5.46$, 1080 rpm..... 129
- Figure 12. Influence of gas flow rate over H_2O_2 production and H_2 consumption, evaluated at reaction time 120 min. (Exp. # 12, 33 – 35) at 80 barg, 313.15 K, 100 mg catalyst, 5 % Pd/C, pH = 2, $Br^-/Pd = 2$, $O_2/H_2 = 5.46$, 1080 rpm. 130
- Figure 13. Influence of gas total flow on turnover frequency (TOF), evaluated at reaction time 120 min, and productivity (Exp. # 12, 33 – 35) at 80 barg, 313.15 K, 100 mg catalyst, 5 % Pd/C, pH = 2, $Br^-/Pd = 2$, $O_2/H_2 = 5.46$, 1080 rpm. 130
- Figure 14. Influence of gas total flow on conversion and selectivity, evaluated at reaction time 120 min, (Exp. # 12, 33 – 35) at 80 barg, 313.15 K, 100 mg catalyst, 5 % Pd/C, pH = 2, $Br^-/Pd = 2$, $O_2/H_2 = 5.46$, 1080 rpm..... 131
- Figure 15. Influence of agitation speed on conversion and selectivity, evaluated at reaction time 120 min, (Exp. # 12, 36 – 39) at 80 barg, 313.15 K, 100 mg catalyst, 5 % Pd/C, pH = 2, $Br^-/Pd = 2$, $O_2/H_2 = 5.46$ 132

Figure 16. Influence of agitation speed on conversion and selectivity, evaluated at reaction time 120 min, (Exp. # 12, 36 – 39) at 80 barg, 313.15 K, 100 mg catalyst, 5 % Pd/C, pH = 2, Br⁻/Pd = 2, O₂/H₂ = 5.46.....132

CHAPTER IV

Effect of low hydrogen to palladium molar ratios in the direct synthesis of H₂O₂ in water in a trickle bed reactor

Application of a trickle bed reactor (TBR) renders a very compact solution to carry out direct synthesis of hydrogen peroxide in water over a carbon supported palladium. The laboratory scale reactor was filled with silica particles (50-70 mesh) physically mixed with 37.5 to 75 mg of 5%Pd/C particles. The reaction conditions applied were 15°C, 15-28 barg, 0.5 to 6 mL·min⁻¹ of liquid and 4.0-4.5 mL·min⁻¹ of gas flowrate. The system was fed with a 2.23% H₂ concentration inflow (far below the low flammability limit) and the balance was O₂ and CO₂. Thus, we demonstrated that the ratio between H₂ and Pd is one of the key factors to achieve optimized, higher yields of hydrogen peroxide. Consequently, low H₂ concentrations lead to low productivities. One of the less studied parameters addressed here is the ratio between the bed filling (SiO₂) and the catalyst; i.e. the active catalytic species dilution effect. In short, it was found that when the amount of Pd was reduced below 0.094 mgPd·cm⁻³ SiO₂, higher productivity of H₂O₂ could be achieved. The selectivities obtained were between 5.3 and 38.0%, respectively, corresponding to turn-over-frequencies (TOF) ranging from 65 to 921 mmolH₂O₂·gPd⁻¹·h⁻¹.

Huerta, I., *et al.*, *Effect of low hydrogen to palladium molar ratios in the direct synthesis of H₂O₂ in water in a trickle bed reactor* Catalysis Today 2014. **Accepted.**

4.1. Introduction

The need of products and processes that promote development of more sustainable industrial practices over the traditional approaches is today a self – evident goal. Thus, as an example, the hydrogen peroxide demand has recently increased considerably, as it is an excellent chemical oxidant in a wide range of applications, such as pulp and paper bleaching, electronic and textile industries, metallurgy and chemical synthesis [8]. Solvay (30%), followed by Evonik (20%) and Arkema (13%) lead the annual production volumes whereby close to 3000 kt/y is being produced *via* the auto – oxidation process [19].

Direct synthesis process can compete with the auto – oxidation process (traditional process with more than 95% H₂O₂ production quota, nowadays) if H₂O₂ solutions similar to the ones produced with current technology after dilution, i.e. around 15 – 17 %wt, can be made in an economical way [11, 18, 27]. Therefore, direct synthesis is conceived as an on – site process for continuous production of H₂O₂ on – demand.

Direct synthesis of H₂O₂ is a classic example of a three phase process. The gas phase is composed of H₂ and O₂ plus an inert gas in order to maintain the H₂ concentration below the low flammability limit (LFL = 3.6 – 4.0 %mol). The most common inert gases are N₂ (when air is used) or CO₂ when an enhancement in mass transfer is pursued [18, 30]. Typically, the liquid phase is water, methanol, ethanol or a mixture. The solid phase, on the other hand, consist of a mass – transfer enhancing support (e.g. ceramic or metallic rings, etc.) and the active metal supported on it or in another specific support (e.g. zeolites, micro – particulates of activated carbon or zirconia, etc.).

Trickle bed reactors (TBRs) are type of three – phase fixed bed reactors widespread in the operations of petrochemical industry and in the production of bulk chemicals. In a classical setup, the liquid phase flows in downward direction (gravity) and gas is fed either as a down – flow (co – current) or up – flow (counter – current or concurrent) over a bed of solid catalyst particles. The special feature of TBRs is that the liquid flows down intermittently like a chaotic rain wetting the solid particles in the form of droplets, films or rivulets [24]. To assure that, indeed, trickle flow conditions are achieved, the reactor must operate under restricted liquid or gas availability characterized by Reynolds numbers in the order of $Re_G < 10^3$ and $Re_L < 10^3$ [13, 24].

The direct synthesis of H₂O₂ can be schematized by a system of four reactions, appearing as both consecutive and parallel ones. Thus, H₂ and O₂ can directly react to form H₂O₂ (desired) and H₂O (undesired). Further, the H₂O₂ produced can be hydrogenated with H₂ or can decompose thus

producing H₂O (undesired) as a side product, in both cases. Reaction scheme is displayed in Figure 1.

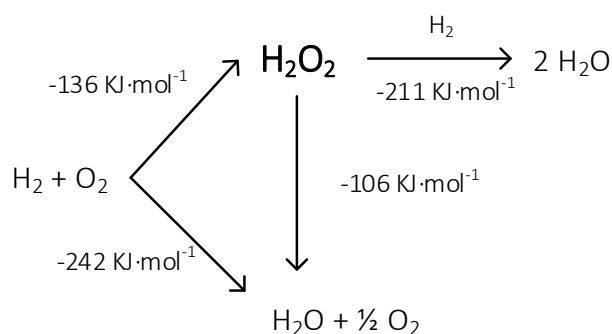


Figure 1. Reactions involved in the direct synthesis of hydrogen peroxide

The minimization of the undesired reactions can be tackled at all levels: the configuration and properties of the catalyst, solvent, transport phenomena and reactor itself are all important. Consequently, a number of research groups have tried to optimize the catalyst composition by combining different active metals [10, 16, 22, 28] or by functionalizing the support [4, 6, 7, 14, 15, 23, 26]. At the reactor level, for instance, the co – current downflow is the best option to minimize the hydrogenation reaction by avoiding the contact between H₂ and H₂O₂ when the highest H₂O₂ concentration appears (at the reactor outlet).

Currently, an increased number of research groups investigates the direct synthesis in continuous setups, mainly in trickle bed reactors [12, 17, 29] and in microreactors [21, 25, 31, 32].

One of the first demonstrations of a TBR for direct synthesis was patented by Haas *et al.* They used a TBR of I.D. = 16 mm, length = 40 cm charged with 148 g of catalyst and with a metal concentration between 0.25 and 2.5 %wt of Pd (95%) and Au (5%). Both water and methanol mixtures were evaluated as the solvent media, at 50 bar and maintaining a ratio of H₂:O₂:N₂ (3:20:77%mol) at 25°C. In addition, bromide (a promoter) concentrations between 0.0002 and 0.001 mol·L⁻¹ and H₂SO₄ concentration in the range of 0.01 mol·L⁻¹ were applied. Consequently, conversions between 47% and 68%, selectivity ranging from 29% to 72%, and palladium productivities (or Turnover frequency, TOF) between 1.6 and 16.5 g H₂O₂·g Pd⁻¹·h⁻¹ were reported.

Biasi *et al.*, on the other hand, have devoted serious efforts in investigations focused on the direct synthesis reaction in a trickle bed reactor using methanol as a solvent and in the absence of any promoters (halides or other). Thus, it was concluded that upon operations at -10°C and 10 – 20 bar, the maximum TOF was 6.1 g H₂O₂·g Pd⁻¹·h⁻¹, corresponding to a productivity of 0.0035 mmol·min⁻¹ [5, 12]. The selectivity achieved was higher when a ratio of 4:22:76 %mol (H₂:O₂:CO₂) in the feed gas was applied at lower flowrates, while the selectivity was increased upon higher

flow rates when a ratio of 2:22:78 %mol ($\text{H}_2:\text{O}_2:\text{CO}_2$) was applied. In this work, this phenomenon was studied in more detail, always operating at low H_2 concentrations in order to unravel the influence of the different parameters. Biasi et al. studied the influence of the support on the selectivity for different palladium catalysts was assessed, demonstrating that the best selectivity was achieved over sulphonated zirconia (ZS), followed by zirconia (Z), sulphonated ceria (CeS) and finally silica (*i.e.* $\text{ZS} > \text{Z} \approx \text{SC} > \text{SiO}_2$) [29]. In addition, the direct synthesis was also tried when water was the liquid medium over a 5%Pd/C catalyst and using NaBr and H_3PO_4 as promoters. In this case, a high productivity of H_2O_2 up to $0.15 \text{ mmol}\cdot\text{min}^{-1}$ of H_2O_2 was achieved with 63% molar yield [3].

In order to optimize a particular heterogeneously catalyzed reaction, a lot of experimental efforts are required but also understanding of the impact of the various operational parameters and other variables that influence the product yield and selectivity. Undoubtedly, the key parameter for this process is the catalytic activity of the metal or combination of metals used – supported on an optimal support. In fact, the selectivity towards H_2O_2 is the main measurable parameter, when complete H_2 conversion is achieved. However, not only the synthesis of the catalyst matters, but also the reaction environment matters, too [3].

Maximum conversion, selectivity or productivity are, typically, the main targets. In this case, we decided to study the reaction at 2.23%mol H_2 inlet concentration, this being considerably lower than the maximum allowed (4.0%mol is the lower flammability limit [20]), thus aiming at understanding whether the selectivity can be increased by optimized residence times or catalyst conditions, although the productivity was sacrificed because of these conditions. Consequently, the amount of catalyst loaded was studied but also the catalyst concentration in the bed. Our aim was to determine whether a low H_2 – to – palladium ratio can be beneficial or not, in terms of the overall catalytic performance.

4.2. Materials and methods

4.2.1. Materials

Fresh 5 %Pd/C (Sigma – Aldrich) was used as catalyst without any modifications. SiO_2 microparticles (200 – 500 μm Sigma – Aldrich) were used as inert diluent in the trickled bed reactor. Glass wool (from Carl Roth) was applied as the support used to immobilize the catalyst bed.

Potassium iodide (99.5 % Sigma – Aldrich), sulphuric acid (98 % J.T. Baker), starch (Merck), sodium thiosulfate pentahydrate (99.5% Sigma – Aldrich) and ammonium molybdate tetra – hydrate (99.0 % Fluka) were used upon hydrogen peroxide titration.

Deionized water was used as the reaction medium. Phosphoric acid (99.0 % Sigma – Aldrich) and sodium bromide (99.5 % Sigma – Aldrich) were used as hydrogen peroxide promoters to prevent decomposition and hydrogenation. Premium grade (99.999%) oxygen, nitrogen and carbon dioxide – hydrogen mixture (2.5 % H₂) were purchased from AGA (Linde Group, Finland) and used as the reactants and inert diluting gases, respectively.

4.2.2. *Experimental set – up*

The scheme of the complete apparatus is shown in Figure 2. The reactor (1) was made of AISI 316 stainless steel, 30 cm long and 1.15 cm I.D., it was internally lined with PTFE to avoid hydrogen peroxide decomposition. An external chiller (9) allowed for operations at low temperatures. Three mass flow controllers (7) (MFC, Brooks 5850 series) were used to control the gas mass flowrate into the reactor. MFCs were calibrated using mass flow rate and the volumetric flow rates were calculated using mixture densities determined with a Redlich – Kwong – Soave equation of state, using Aspen® Properties code [12, 17]. The liquid phase (2) was fed into the reactor by an HPLC pump (6) (Eldex MicroPro up to 20 mL/min), whereas the gas and liquid flows were mixed before the reactor which was fed concurrently downwards.

The total pressure inside the reactor was measured and regulated with a back pressure controller (11) (BPC; Brooks 5866 series). The maximum operational pressure was limited by the maximum pressure in the feed bottles. In fact, the H₂/CO₂ mixture had a maximum pressure of 32 barg. Considering the required minimum pressure drop of 4 bar in the mass flow controller, the maximum reaction pressure attainable was 28 barg. A bypass was used to achieve the desired pressure inside the reactor more rapidly by filling up with N₂ in the start – up. For safety reasons a rupture disk (12) was installed before BPC. Two micrometric valves (13) were used to sample the liquid and gas phases, respectively. A product vessel (10) provided gas – liquid separation and accumulated the liquid phase during the reaction.

The apparatus was located inside a fume hood, equipped with a H₂ sensor that automatically switched off the H₂ flow to the reactor if the H₂ concentration in the ambient air was too high.

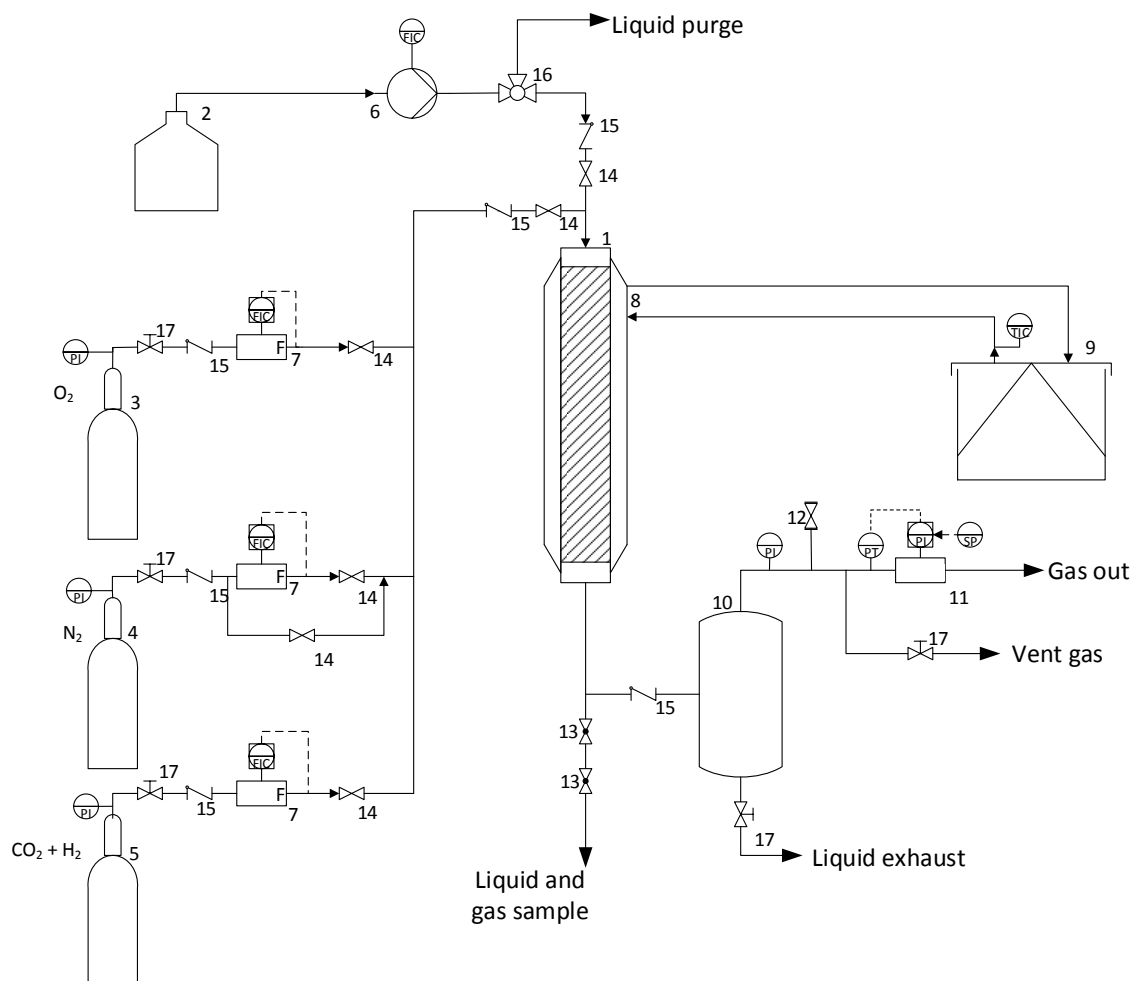


Figure 2. Scheme of the apparatus used in the H_2O_2 experiments. (1) Trickle bed reactor. (2) Liquid solvent supply. (3, 4, 5) Gas bottles, O_2 , N_2 and CO_2/H_2 (97.5/2.5 %). (6) Pump. (7) Mass flow controller. (8, 9) External cooling and chiller with temperature controller. (10) Liquid collection vessel. (11) Pressure controller. (12) Vent valve. (13) Micrometric valve. (14) On/off valve. (15) Check valve. (16) Three – way valve. (17) Ball valve.

4.2.3. Analytical methods

H_2O_2 concentration in water was determined by means of iodometric titration [9]. Gas composition was measured using a Varian 6890 GC Chromatograph equipped with two Agilent capillary columns (Q04 + MS6 HP – PLOT Q and HP – MOLSIV 5A).

4.2.4. Experimental procedure

At first, the reactor was filled with a mixture of catalyst and pure SiO₂, thus ensuring that the solids were perfectly distributed along the bed and to avoid preferential flow paths. After pressurizing, the liquid phase was pumped into the reactor at a high flow rate for the first 30 – 60 min to guarantee that the solids were completely and homogeneously wetted. Once the gases were introduced into the reactor, liquid and gas samples were withdrawn every 15 minutes. The system was considered to be stable and in steady – state when the results of three consecutive samples demonstrated less than 3% deviation. Consequently, the chosen operational conditions were determined and new samples were taken.

4.3. Results and discussion

A set of 53 experiments was designed in order to reveal the influence of pressure, liquid flow rate, amount of catalyst and catalyst distribution inside the reactor. The direct synthesis experiments were carried out at a constant temperature, 15 °C. The gas composition was constant 86.7/11/2.23 %mol (CO₂/O₂/H₂) and volumetric gas flow rate was kept constant at approximately 4.0 – 4.5 mL·min⁻¹, under reaction conditions. The H₂ concentration was 2.23 %mol, i.e. far below the explosive limit (ca. 4.0 %mol [20]).

The volumetric total flow rates corresponded to the specific mass flow rates ranging from 0.017 to 0.032 kg·m⁻²·s⁻¹ for the gas and from 0.047 to 0.566 kg·m⁻²·s⁻¹ for the liquid, respectively. All the experiments were carried out within the trickling regime (Figure 3).

Table 1. Experimental table for H₂O₂ direct synthesis in a trickled bed reactor.

Run #	Pressure barg	Catalyst mg	V _b cm ³	Pd/V _b mg·cm ⁻³	LFR mL·min ⁻¹	GFR ml·min ⁻¹	F _{H₂} μmol·min ⁻¹	Pd/H ₂ mol·mol ⁻¹	Catalyst distribution
1	28	75.0	40	0.094	0.5	4.0	105.61	0.35	HD
2	28	75.0	40	0.094	1	4.0	105.61	0.35	HD
3	28	75.0	40	0.094	2	4.0	105.61	0.35	HD
4	28	75.0	40	0.094	4	4.0	105.61	0.35	HD
5	28	75.0	40	0.094	6	4.0	105.61	0.35	HD
6	28	75.0	20	0.188	0.5	4.0	105.61	0.35	HD
7	28	75.0	20	0.188	1	4.0	105.61	0.35	HD
8	28	75.0	20	0.188	2	4.0	105.61	0.35	HD
9	28	75.0	20	0.188	4	4.0	105.61	0.35	HD
10	25	37.5	20	0.094	0.5	4.5	105.61	0.17	HD
11	25	37.5	20	0.094	1	4.5	105.61	0.17	HD

12	25	37.5	20	0.094	2	4.5	105.61	0.17	HD
13	25	37.5	20	0.094	4	4.5	105.61	0.17	HD
14	25	37.5	20	0.094	6	4.5	105.61	0.17	HD
15	25	37.5	40	0.047	0.5	4.2	97.85	0.19	HD
16	25	37.5	40	0.047	1	4.2	97.85	0.19	HD
17	25	37.5	40	0.047	2	4.2	97.85	0.19	HD
18	25	37.5	40	0.047	4	4.2	97.85	0.19	HD
19	25	37.5	40	0.047	6	4.2	97.85	0.19	HD
20	25	75.0	40	0.094	0.5	4.2	97.85	0.37	HTLB
21	25	75.0	40	0.094	1	4.2	97.85	0.37	HTLB
22	25	75.0	40	0.094	2	4.2	97.85	0.37	HTLB
23	25	75.0	40	0.094	4	4.2	97.85	0.37	HTLB
24	15	75.0	40	0.094	0.5	4.0	56.42	0.65	LTHB
25	15	75.0	40	0.094	1	4.0	56.42	0.65	LTHB
26	15	75.0	40	0.094	2	4.0	56.42	0.65	LTHB
27	15	75.0	40	0.094	4	4.0	56.42	0.65	LTHB
28	15	75.0	40	0.094	6	4.0	56.42	0.65	LTHB
29	15	75.0	40	0.094	0.5	4.0	56.42	0.65	HD
30	15	75.0	40	0.094	1	4.0	56.42	0.65	HD
31	15	75.0	40	0.094	2	4.0	56.42	0.65	HD
32	15	75.0	40	0.094	4	4.0	56.42	0.65	HD
33	15	75.0	40	0.094	6	4.0	56.42	0.65	HD
34	15	75.0	20	0.188	0.5	4.0	56.42	0.65	HD
35	15	75.0	20	0.188	1	4.0	56.42	0.65	HD
36	15	75.0	20	0.188	2	4.0	56.42	0.65	HD
37	15	75.0	20	0.188	4	4.0	56.42	0.65	HD
38	15	75.0	20	0.188	6	4.0	56.42	0.65	HD
39	15	37.5	40	0.047	0.5	4.0	56.42	0.32	HD
40	15	37.5	40	0.047	1	4.0	56.42	0.32	HD
41	15	37.5	40	0.047	2	4.0	56.42	0.32	HD
42	15	37.5	40	0.047	4	4.0	56.42	0.32	HD
43	15	37.5	40	0.047	6	4.0	56.42	0.32	HD
44	15	37.5	20	0.094	0.5	4.0	56.42	0.32	HD
45	15	37.5	20	0.094	1	4.0	56.42	0.32	HD
46	15	37.5	20	0.094	2	4.0	56.42	0.32	HD
47	15	37.5	20	0.094	4	4.0	56.42	0.32	HD
48	15	37.5	20	0.094	6	4.0	56.42	0.32	HD
49	15	75.0	40	0.094	0.5	4.0	56.42	0.65	HTLB
50	15	75.0	40	0.094	1	4.0	56.42	0.65	HTLB
51	15	75.0	40	0.094	2	4.0	56.42	0.65	HTLB
52	15	75.0	40	0.094	4	4.0	56.42	0.65	HTLB
53	15	75.0	40	0.094	6	4.0	56.42	0.65	HTLB

(V_b : volume of the bed of SiO_2 together with the catalyst Pd/C, cm^3 ; LFR: liquid flowrate; GFR: gas flowrate;

F_{H_2} : hydrogen molar inlet flowrate; HD: catalyst uniform distributed (or 37.5 or 75 mg Pd/C in the total),

HTLB: higher catalyst concentration on upper third of reactor and lower catalyst concentration on reactor's

third bottom (37.5/25/13.5 mg Pd/C), LTHB: lower catalyst concentration on upper third of reactor and higher catalyst concentration on reactor's third bottom (13.5/25/37.5 mg Pd/C))

The hydrogen peroxide production rate ($\mu\text{mol H}_2\text{O}_2 \cdot \text{min}^{-1}$) was calculated from H₂O₂ %wt/v values obtained from iodometric titration and liquid flow rate. Hereupon the yield was defined as the moles of hydrogen peroxide produced divided by the moles of H₂ fed into the reactor. H₂ concentration in gas phase at the reactor outlet was close to 0% and, consequently, for calculation purposes, the overall conversion was assumed to reach 100 %.

One should note that maintaining the operational gas flowrate constant at 4.0 – 4.5 mL·min⁻¹ implies that the molar flowrate of the gases actually change during an experimental run, at different pressures. This implies that, at higher pressure, more H₂ was entering the reactor and, consequently, more H₂O₂ left the reaction zone. Therefore, when comparing the results obtained between 25 – 28 barg and 15 barg, it must be kept in mind using not only absolute parameters (such as %H₂O₂ or $\mu\text{mol}/\text{min}$ produced) but also relative parameters (selectivity or yield). To motivate our choice, we decided to use a constant gas flow rate to ensure similar gas hydrodynamics although that, in turn, resulted in variable H₂ molar flowrates when varying the pressure. For this reason, experiments #1 – #23 were performed injecting 97.8 – 105.6 $\mu\text{mol} \cdot \text{min}^{-1}$ of H₂ and experiments #24 – #53 with 56.4 $\mu\text{mol} \cdot \text{min}^{-1}$ of H₂.

Discussion on hydrodynamics

Considering the operation of solid – liquid – gas columns six main flow regimes can be encountered: bubble, trickle, spray, pulse, dispersed and slug flow. In this research, considering the liquid and gas flowrates, the system operated mainly in trickle flow (close to pulse flow in few cases) as depicted in Figure 3. The behavior of a laboratory scale TBRs and an industrial TBRs do not necessary be similar. Thus, considering the main forces governing the hydraulic movement in a TBR, we find inertial (velocity – direction), gravitational (density – direction), viscous (viscosity) and capillary forces (surface tension) [2]. In industrial scale, the gravity forces may control, while in laboratory scale the capillary forces have a strong influence. Alsolami *et al.* stated that the different behaviors at TBRs in industrial and laboratory scales might even result into an absence of the trickle flow in laboratory scale [1]. There are not many references clearly indicating the flow regimes obtained in laboratory scale and, thus we accept that the general flow regime charts for TBR can be applied under certain restrictions [24]. The trickled bed region operating with low gas and liquid flow rates, the gas – liquid interaction is small and liquid flows as films or rivulets over the packed particles. It is recommended to check the flow regime according to the

gas and liquid flow rates for each and every experiment to ensure that the system is, in fact, operating at the trickle flow region. In our experimental system, trickle flow region was assumed, although upon experiments with the highest liquid flowrate the pulsing region was approached, as depicted in Figure 3 (light blue dots). Operating close to the pulsing region is common for industrial reactors whereupon both the liquid phase turbulence and the reactor throughput are increased.

Analyzing the system using the Eötvös number ($E\ddot{o}$ = gravitational force / capillary force) [1], (particle diameters between mesh 70 and 50, i.e. 0.21 and 0.30 mm) we found that $0.006 < E\ddot{o} < 0.012$. This very low values indicates that the capillary forces play an important role over the gravitational forces. However, the length – to – diameter of the reactor ($L/D=26$) reduces the capillary forces, although it is not considered in the $E\ddot{o}$ number. The study of the real behavior of our laboratory scale TBRs in the terms of hold – up will be a matter of a future work.

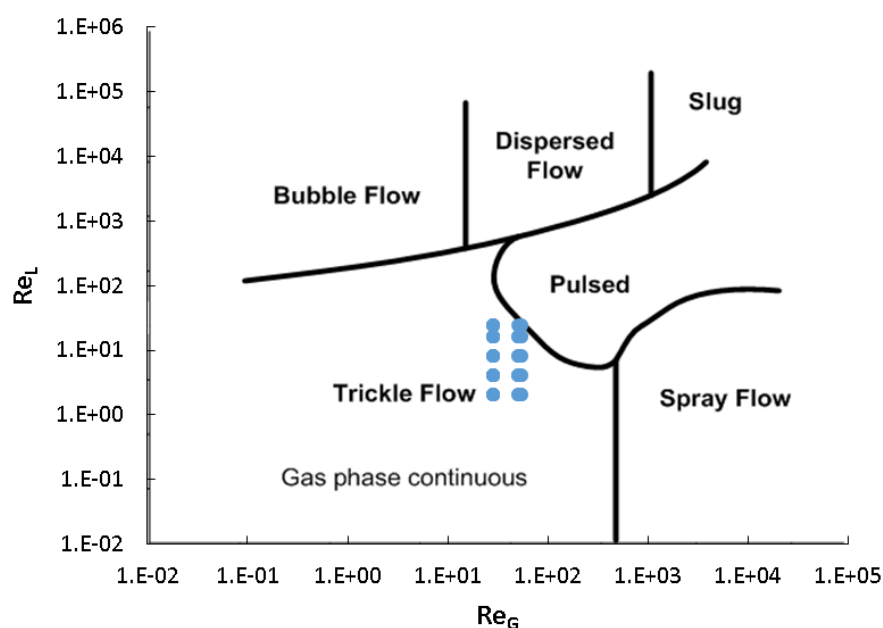


Figure 3. Trickle bed region and operational window (adapted from Ranade *et al.* [24])

As for any heterogeneous system, this reaction system is influenced by two different reaction steps occurring in series: mass transfer followed by kinetic phenomena. Reaction pressure, liquid flow rate, mass of catalyst and catalyst distribution were the parameters studied in this work. A change in each of these variables might influence the apparent kinetics or mass transfer behavior, or both of them at the same time. The complexity of trickled bed reactor hydrodynamics, the numerous chemical and physical stages involved in the process render it extremely complicated to define exactly how each and every reaction variable influences the

system. However, it is possible to understand, in a simplified way, the global behavior analyzing the influence of the reaction variables to the main system parameters: hydrogen peroxide concentration, yield, productivity (measured as $F_{\text{H}_2\text{O}_2} = \mu\text{mol H}_2\text{O}_2 \cdot \text{min}^{-1}$) and turn over frequency (TOF, as $\text{mmol H}_2\text{O}_2 \cdot \text{h}^{-1} \cdot \text{g Pd}^{-1}$). Therefore, as it is defined, the productivity is strongly related with the system reactor – catalyst, while the TOF is more related to the catalyst itself.

Summary of results

The main results obtained are summarized next in Table 2 and discussed thoroughly in the following sections.

Table 2. Summary of main experimental results and standard deviation values

Run #	Average Values			
	[H ₂ O ₂] %wt/v	Yield %	F _{H₂O₂} $\mu\text{mol} \cdot \text{min}^{-1}$	TOF $\text{mmol H}_2\text{O}_2 \cdot \text{h}^{-1} \cdot \text{g Pd}^{-1}$
1	0.265±0.019	37.97±2.95	39.02±0.27	624.2±4.3
2	0.084±0.002	24.31±0.28	24.78±0.05	396.5±0.7
3	0.043±0.002	24.27±0.51	25.44±0.07	339.2±11.9
4	0.029±0.001	33.5±0.38	34.16±0.05	454.2±22.3
5	0.019±0.001	32.94±0.72	32.96±0.04	456.5±10.7
6	0.230±0.002	32.52±0.32	33.77±0.02	540.4±0.3
7	0.019±0.002	5.31±0.29	5.61±0.04	89.8±0.5
8	0.011±0.001	6.07±0.06	6.42±0.01	132.3±7.4
9	0.006±0.001	6.83±0.41	7.22±0.05	194.4±19.8
10	0.126±0.001	17.6±0.07	18.59±0.01	594.7±0.3
11	0.079±0.001	23.09±0.61	23.38±0.02	748.1±0.6
12	0.042±0.001	24.37±0.31	24.46±0.05	782.7±1.6
13	0.009±0	10.02±0	10.59±0	338.7±0
14	0.007±0.001	11.50±0.18	12.15±0.02	388.8±0.6
15	0.180±0.014	27.00±2.1	26.42±0.2	845.4±6.6
16	0.098±0.003	29.42±0.61	28.79±0.06	921.3±1.9
17	0.018±0.001	10.90±0.46	10.67±0.05	341.3±1.5
18	0.014±0.001	17.03±0.44	16.60±0.04	531.2±1.2
19	0.011±0.001	19.42±0.83	19.01±0.09	608.2±2.6
20	0.081±0	12.17±0	11.91±0	190.5±0
21	0.023±0.001	6.93±0.07	6.78±0.01	108.4±0.1
22	0.023±0.003	14.11±1.51	13.81±0.15	221.0±2.4
23	0.006±0.001	7.44±0.22	7.28±0.03	116.4±0.4
24	0.107±0.002	28.29±0.39	15.80±0.03	252.8±0.5
25	0.045±0.001	23.45±0.5	13.23±0.03	211.7±0.5
26	0.010±0.001	10.85±0.57	6.04±0.04	96.7±0.6

27	0.005±0.001	11.11±0.68	6.26±0.04	100.1±0.6
28	0.004±0.001	13.75±0.59	7.58±0.04	121.3±0.6
29	0.093±0.002	24.26±0.5	13.69±0.03	219.0±0.5
30	0.054±0.001	28.34±0.51	15.86±0.03	253.8±0.5
31	0.007±0.001	7.20±0.53	4.06±0.03	65.0±0.5
32	0.007±0.001	15.6±0.55	8.26±0.03	132.2±0.4
33	0.005±0.001	17.69±3.95	9.53±0.17	152.4±2.7
34	0.102±0.001	26.57±0.13	14.96±0.01	239.3±0.2
35	0.058±0.003	30.45±1.2	17.10±0.07	273.6±1.1
36	0.026±0.001	27.18±1	15.34±0.06	245.4±0.9
37	0.013±0.002	27.89±3.22	15.24±0.22	243.8±3.5
38	0.009±0.001	27.82±1.85	15.70±0.1	251.2±1.7
39	0.098±0.001	25.53±0.17	14.41±0.01	461.0±0.4
40	0.050±0.001	27.18±0.39	14.71±0.03	470.8±0.7
41	0.027±0.001	30.80±2.39	15.93±0.04	509.7±1
42	0.005±0.001	11.49±0.23	6.42±0.02	205.3±0.4
43	0.004±0.001	13.81±1.34	7.70±0.08	246.4±2.4
44	0.079±0.001	20.68±0.1	11.67±0.46	373.4±0.2
45	0.044±0.001	23.50±0.1	12.99±0.42	415.7±0.3
46	0.028±0.001	29.11±0.49	16.21±1.68	518.7±0.8
47	0.006±0.001	13.37±0.78	7.40±5.85	236.7±1.3
48	0.004±0.001	11.93±0.49	6.62±4.07	211.7±0.6
49	0.090±0.005	24.07±1.26	13.31±0.07	425.8±2.3
50	0.041±0.001	22.17±0.31	11.97±0.03	383.0±0.7
51	0.023±0.002	24.72±1.42	13.73±0.08	219.7±1.3
52	0.003±0	7.56±0.35	3.85±0	123.2±0
53	0.002±0.001	7.64±0.42	4.09±0.02	65.4±0.3

($F_{H_2O_2}$: hydrogen peroxide productivity in molar flowrate, TOF: turn over frequency)

4.3.1. Overall analysis of maxima and minima

One of the tools to identify the global behavior is the analysis of the maxima and minima in the overall reactor productivity (measured as mmol/min of H_2O_2 produced), as overviewed in Figure 4. At high pressures (25 – 28 barg), the maximum productivity was obtained (experiments #1, 4, 6, 5 and 16, in this order). In this case, the most experiments were carried out at low liquid flowrates. On the contrary, the lowest productivity was observed for experiments #7, 8, 9, 21 and 23, respectively. Hereupon the common denominators were higher flowrates and shorter silica bed. At low – intermediate pressures (15 barg), the productivity in general was lower. The best results were obtained for the experiments #41, 35, 46, 30 and 24, respectively, and the lowest productivity was obtained in experiments #31, 52, 53, 26 and 27, respectively. Hereupon, nevertheless, the observed tendencies were not that clear.

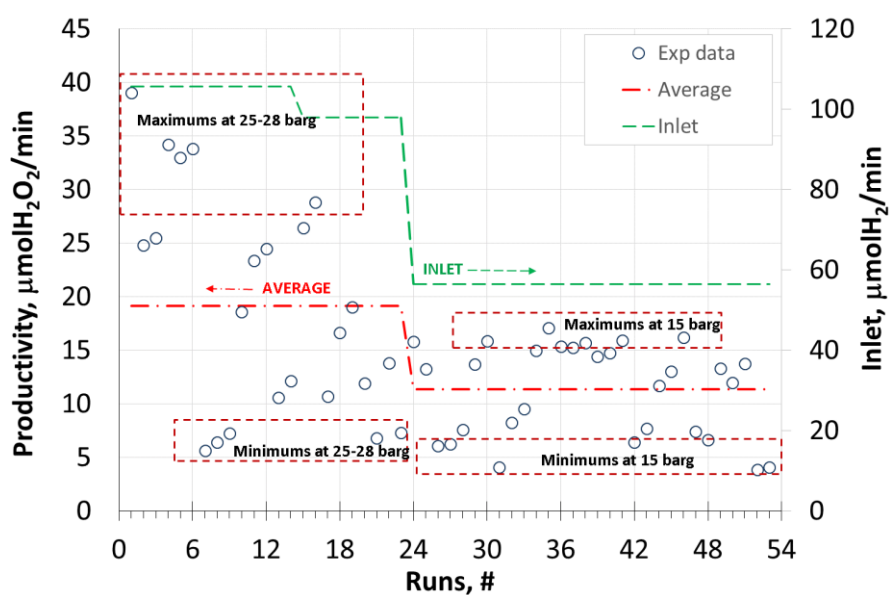


Figure 4. Overview of the experiments

Our hypotheses point out that the relationship between the concentration of H_2 and Pd is an important factor, whereupon the higher the ratio H_2/Pd the better results are obtained in terms of direct synthesis; i.e. higher productivity. Hereafter, we consider the H_2/Pd ratio directly in the catalytic microscopic terms – on the level of the active site. Thus, the H_2 has been dissolved and consequently adsorbed on the catalyst surface. Therefore, this H_2 is available for the reaction in the vicinity of the active sites. To support this hypothesis we have plotted TOF (which already considers the quantity of catalyst applied as well as the selectivity) versus the initial ratio of H_2 – to – active metal (Pd) (Figure 5). We have included a draft trend lines indicating the limits of the values obtained.

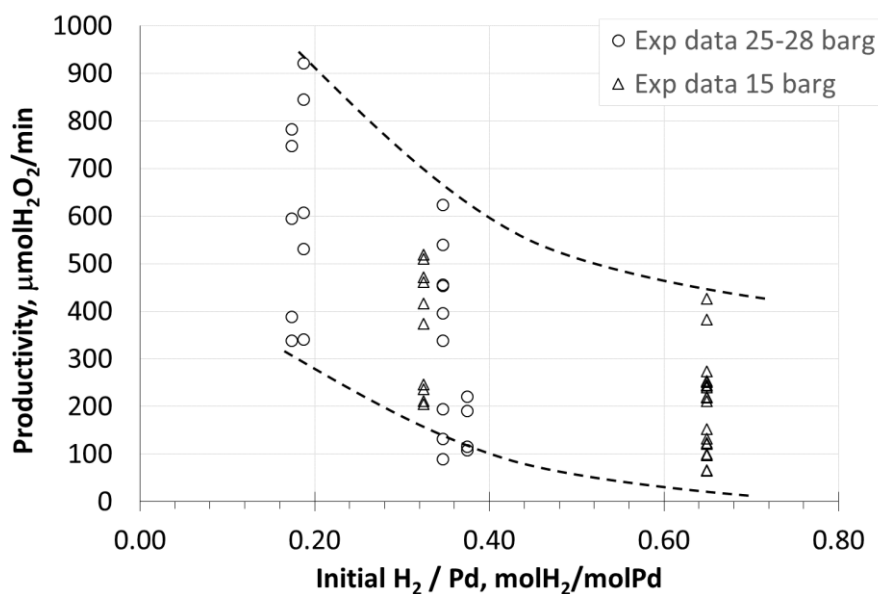


Figure 5. Turnover frequency (TOF) vs initial hydrogen/palladium ratio

Considering the system the hypothesis are:

- H-1. Lower H₂ concentration or partial pressure in the gas phase results in lower H₂/Pd.
- H-2. At lower liquid flow rates, similar amount of H₂ is dissolved, higher local H₂ concentration is achieved and the actual H₂/Pd ratio at the active site is higher.
- H-3. Increased catalyst concentration in the catalyst bed at initial reaction stages is beneficial.
- H-4. When maintaining fixed amount of catalyst, a longer catalyst bed (more SiO₂) helps to achieve improved H₂ dissolution and, thus, the H₂/Pd ratio is higher.

4.3.2. Influence of operational pressure

Hereupon we tackle a three phase system in which the reactants are gases, the product and the reaction medium are liquids (water and solubilized product) and the catalyst is a solid. In the actual three phase system gases must be dissolved in the liquid phase and, consequently, diffuses into the catalyst pores to reach the active sites. If the reaction takes place with an enough of catalyst, the gas – liquid mass transfer becomes the limiting step caused by the low H₂ and O₂ solubilities in the aqueous phase. Consequently, it is possible to enhance the gas – liquid mass transfer by increasing the reaction pressure since the solubility of these gases are higher at higher pressures and also at higher H₂ concentrations in the gas phase.

The authors studied the behavior of a similar reactor previously using 4% of H₂ at the inlet. The productivity, in most of the cases, was doubled in comparison to this work [17]. Indeed, the

maximum yield (or selectivity) reached 65%, while the best results obtained in this work rendered a value of 30.8%. Notwithstanding, the H₂O₂ concentration obtained was here higher than in previous studies [12], confirming the beneficial effect of the catalyst dilution along the reactor bed.

Considering the H₂ partial pressure, the experimental results confirmed a significant pressure effect, since the hydrogen peroxide concentrations, yields and TOFs obtained at 28 barg were higher than at 15 barg (Figure 6 – Figure 7).

At first glance, the concentration of H₂O₂ at 25 – 28 barg was between 2 – 3 fold the value at 15 barg (Figure 6). As explained before, the higher relative feed of H₂, in a system that is not kinetically limited, produced more H₂O₂. The maximum concentration was obtained, as expected, as the reaction occurred at the lowest liquid flow rate and for experiments with the higher amount of catalyst, i.e. 0.265 %wt/v (at 0.5 mL/min, 75 mg of cat. and 28 barg) in contrast to 0.093 %wt/v (at 0.5 mL/min, 75 mg of cat. and 15 barg). The observed decrease in concentration is almost proportional to the increase in the liquid flow rate.

Upon comparison of the yields, it became evident that, at low pressures (15 barg), the system was limited by mass transfer and the use of either 37.5 or 75 mg of catalyst did not affect the production. On the other hand, at 28 barg, whereupon more H₂ was available, the *doubled* amount of catalyst (75 mg) almost *tripled* the productivity. This indicated that, at 15 barg, the system is both kinetically limited by the catalyst amount and, gas – liquid mass transfer and by increasing both we can push the system to a higher production level. In view of this, we can conclude that hypothesis H-1 is valid.

4.3.3. Influence of liquid flowrate

The maximum yield was always obtained at low flowrates which were directly related to high residence times of the liquid and, probably, to higher H₂ concentrations due to a higher residence time and dissolution. There is an inflexion point around 1.0 – 2.0 mL·min⁻¹. A shorter residence time, assuming that H₂ was converted completely in all cases as the gas concentration was zero at the outlet, boosted the H₂O₂ production by minimizing the contact time with the catalyst and thus the decomposition. At higher residence times, the instabilities of the trickle flow might have compromised the results in some cases. The phenomenon was found at both 25 – 28 barg and 15 barg as depicted in Figure 6. The trends observed were very consistent and allowed to verify the

hypothesis H-2. At low pressures, as the system was limited by mass transfer, the lower the catalyst amount, the higher the TOF measured (Figure 8).

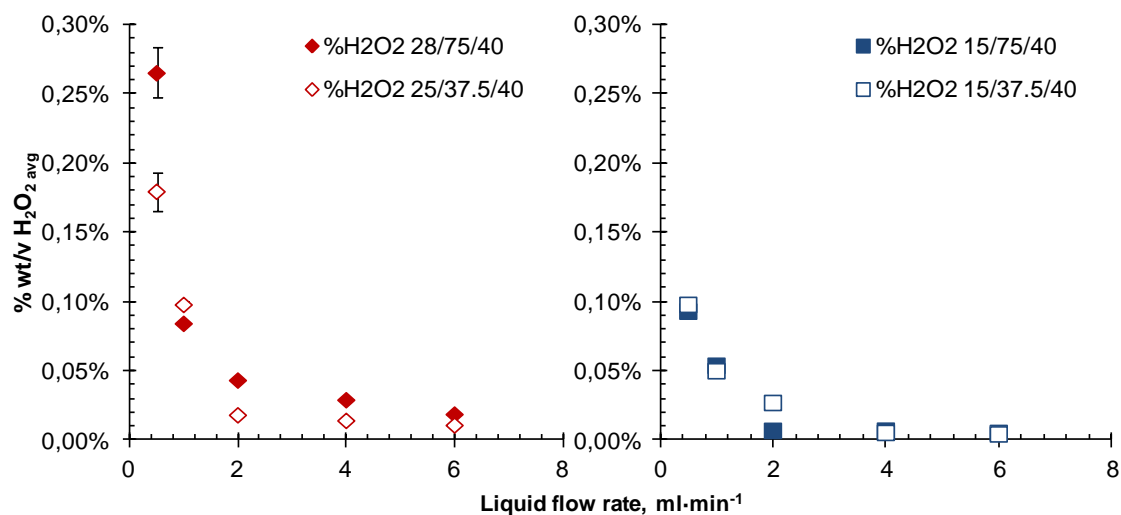


Figure 6. Influence of reactor pressure, liquid flow rate and catalyst on the final average hydrogen peroxide concentration (#1 – 5, 15 – 19, 29 – 33, 39 – 43). Uniform catalyst distribution. (Pressure (barg) /amount of catalyst (mg)/ bed volume (cm^3))

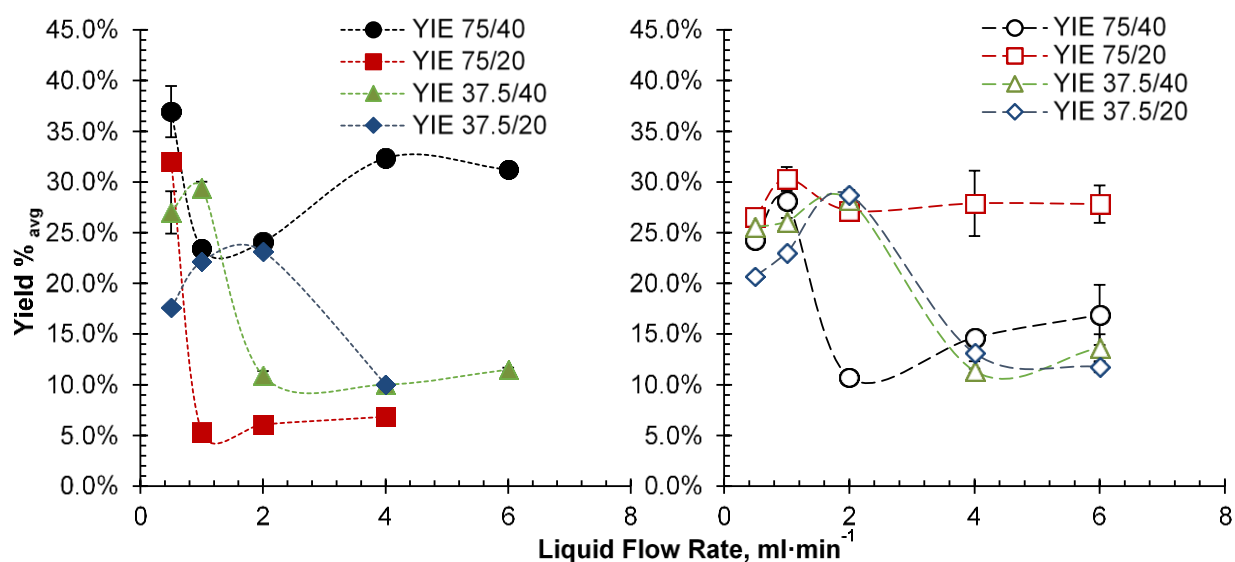


Figure 7. Influence of the catalyst on the final average yield values (#1--19, 29 – 48). Solid symbols – 28 barg; empty symbols – 15 barg. (amount of catalyst (mg)/ bed volume (cm^3))

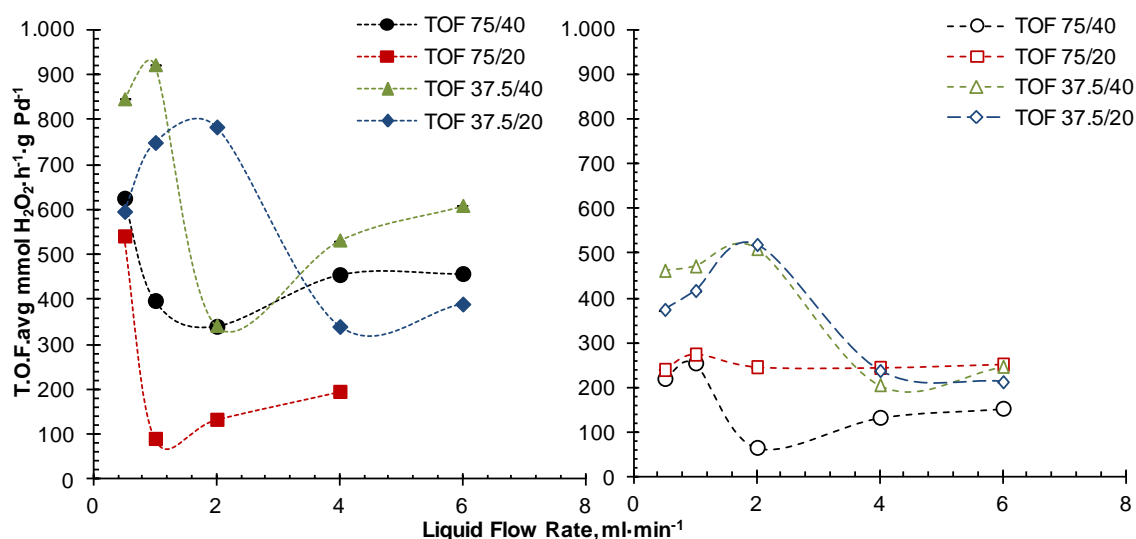


Figure 8. Influence of the catalyst on final average TOF values (#1 – 19, 29 – 48). Solid symbols – 28 barg; empty symbols – 15 barg.

4.3.4. Influence of the ratio between the catalyst, bed volume and catalyst distribution

In an industrial TBR, it is common that the bed filling is an industrial catalyst, which comprises the support and the active metal. The support contributes to the interfacial transfer. In our system, the catalyst and the inert filling were different. Therefore, we were able to modify the SiO₂ (for mass transfer) and the Pd/C (for the reaction) ratio or distribution. At first glance, the influence of the excess H₂ in the gas phase is clear, as clarified in Figure 9. The lowest productivity obtained at 25 – 28 barg was comparable with the average productivity at 15 barg. In fact, at 15 barg, the productivity was almost constant at every flow rate and, in essence, independent of the catalyst quantity or distribution. Thus, the system at 15 barg was mass transfer limited and the catalyst amount made no difference; one can also analyze this in terms of considering that only 56.42 μmol · min⁻¹ of H₂ were introduced and both 37.5 and 75 mg of catalyst could convert the reactants. At a higher pressure, with a double H₂ inflow, the catalytic effect was more clearly observed.

Second, at 25 – 28 barg, 75 and 37.5 mg of catalyst amount in 20 and 40 mL of SiO₂ were studied. It turned out that 75 mg compared to 37.5 mg was superior, thus indicating that more catalyst can convert more H₂.

Furthermore, in both cases, the uniform distribution of the catalyst in a long bed (meaning more mass transfer area and more H₂ dissolution) increased the H₂O₂ productivity. We tested three different distributions of the catalyst in the bed: uniform distributed (HD); high concentration at

the top (inlet) and low at the bottom (HTLB); and low concentration at the top (inlet) and high at the bottom (LTHB) (see also Table 1). The worst results were observed for 75 mg Pd/C with 40 mL of SiO₂ but with a lower concentration of catalyst at the beginning of the bed (LTHB). This clearly indicates that H₂/Pd ratio should be high at any reactor length. This is very important result since probably the adsorption/desorption rates on the catalyst of the reagents and of the products are strongly affected by the H₂ present in the environment. The best results were obtained at 0.5 mL/min with 75/40/HTLB (high concentration in the inlet) thus indicating the validity of H-3.

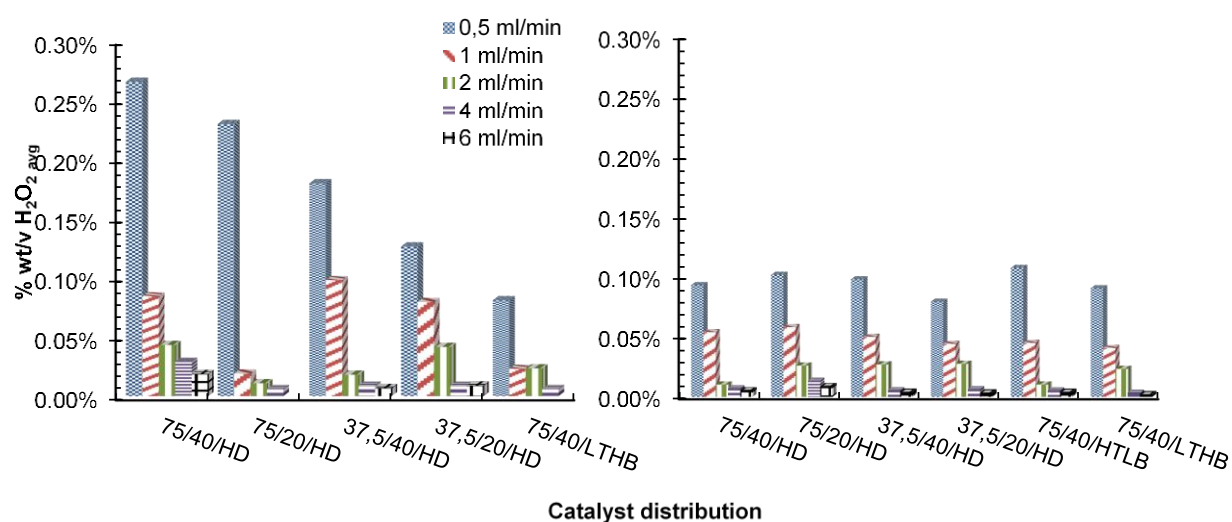


Figure 9. Influence of catalyst distribution and liquid flow rate on final average hydrogen peroxide concentration (# 1 – 23; 24 – 53). (Amount of catalyst (mg)/ bed volume (cm³)/distribution). 28 – 25 barg left figure, 15 barg right figure.

When comparing the yields obtained, it can be seen that at 15 barg the highest yield was obtained when the catalyst was more concentrated (75 mg catalyst in 20 mL), indicating that 20 mL is large enough volume to transfer 56.42 $\mu\text{mol}\cdot\text{min}^{-1}$ of H₂ but the faster the reaction the higher the production (see Figure 10). Preserving that proportion at 25 – 28 barg, 40 mL SiO₂ gave the best results. Considering the TOF, low liquid flowrates was always better compared to high liquid flowrates as plotted in Figure 11.

The palladium – to – bed volume ratio (Pd/V_b) can give a similar trends: 0.047 mgPd·cm⁻³ < Pd/V_b < 0.188 mgPd·cm⁻³ were tested. At Pd/V_b = 0.094 mgPd·cm⁻³ higher yield was attained at 0.5 mL·min⁻¹ using 75 mg of catalyst, as depicted in Figure 12. On the other hand, 0.047 mgPd·cm⁻³ exhibited the highest TOF values for 37.5 mg of catalyst, at low liquid flowrates too. In any case (exceptions apart), the best yields and TOF were obtained at low Pd/V_b ratios (Figure 12)

Figure 13). This implies that a large ‘solubilization’ area around the catalyst seems beneficial, thus confirming the hypothesis H-4. The isolated, irregular points deviating from the trend could be explained by the differences in the wetting of the reactor bed.

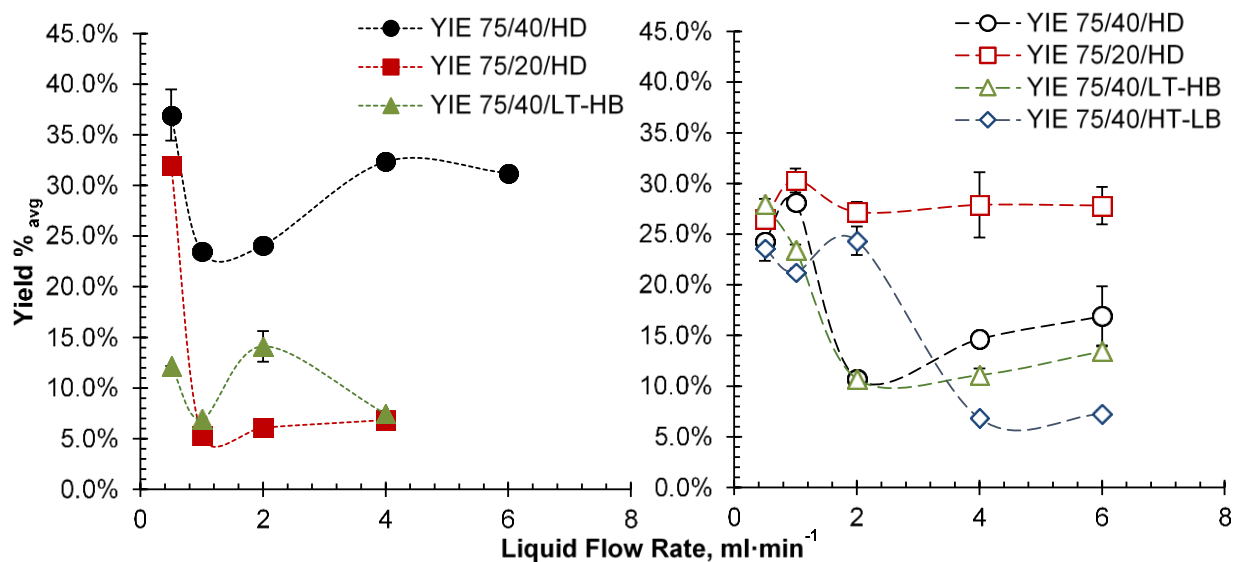


Figure 10. Influence of catalyst distribution on final average yield values. (#1 – 9, 20 – 38, 49 – 53). (Amount of catalyst (mg)/ bed volume (cm³)/distribution). Solid symbols: 28 – 25 barg, empty symbols: 15 barg.

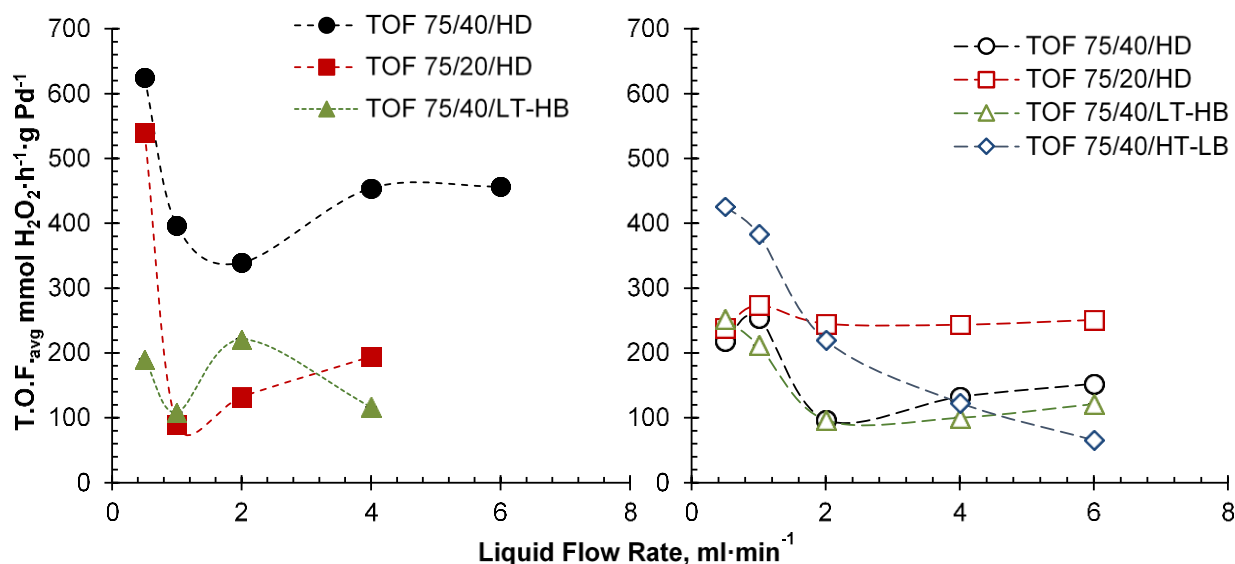


Figure 11. Influence of catalyst distribution on final average TOF values. (#1 – 9, 20 – 38, 49 – 53). (Amount of catalyst (mg)/ bed volume (cm³)/distribution). Solid symbols: 28 – 25 barg, empty symbols: 15 barg.

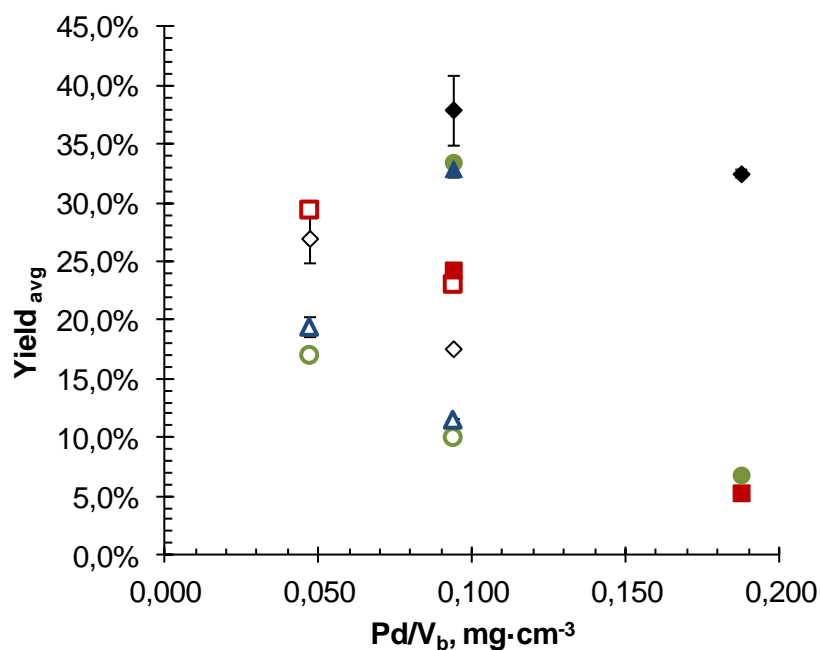


Figure 12. Influence of ratio Pd/V_b on final average yield values (#1 – 19). 75 mg of catalyst: ◆ 0.5 ml·min⁻¹; ■ 1 ml·min⁻¹; ● 4 ml·min⁻¹; ▲ 6 ml·min⁻¹ and 37.5 mg of catalyst: ◇ 0.5 ml·min⁻¹; □ 1 ml·min⁻¹; ○ 4 ml·min⁻¹; △ 6 ml·min⁻¹.

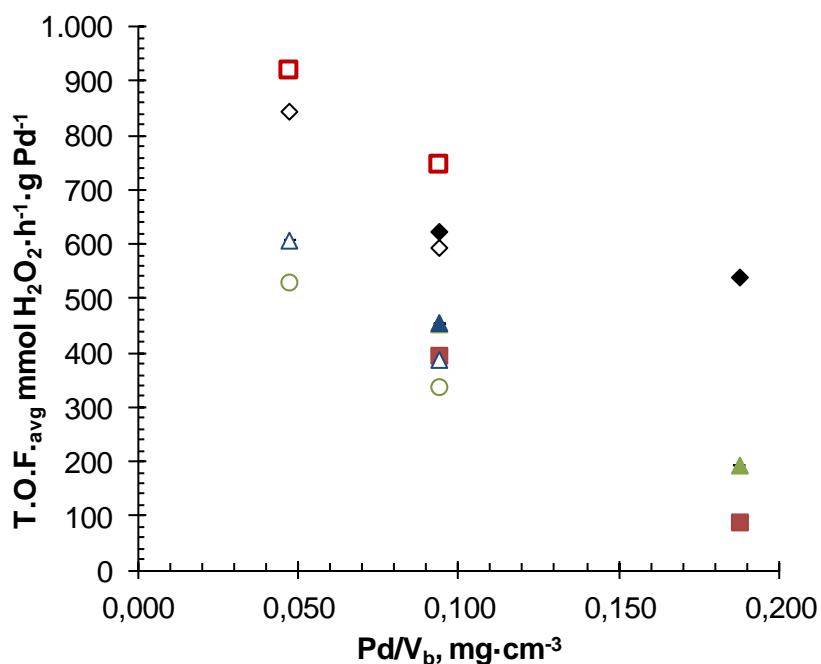


Figure 13. Influence of ratio Pd/V_b on final average TOF values (#1 – 19). 75 mg of catalyst: ◆ 0.5 ml·min⁻¹; ■ 1 ml·min⁻¹; ● 4 ml·min⁻¹; ▲ 6 ml·min⁻¹. 37.5 mg of catalyst: ◇ 0.5 ml·min⁻¹; □ 1 ml·min⁻¹; ○ 4 ml·min⁻¹; △ 6 ml·min⁻¹.

4.4. Conclusions

One of the goals in research concerning direct synthesis of H₂O₂ is to determine the truly best conditions to render the process viable. This encompasses various aspects in terms of the catalytic material, reactor design and operations as well as reactions conditions. The last two decades have been very prolific in the topic, with more than 250 – 300 journal articles related to the topic, directly or indirectly. Most of the research has been very successful in increasing the selectivity or productivity of the process, especially because of improved catalyst design. However, it is important to complement the discoveries in terms of catalyst design by an approach where the direct synthesis reaction is analyzed in detail in terms of the reaction conditions and reactor design, as demonstrated in the present work.

The first conclusion is that the use of low H₂ concentration, i.e. 2.23% molH₂ in the gas phase lead to very low productivities and reaction yields, compared to the options at 4.0% molH₂ (near the explosive limit).

The low H₂ gas concentration regime was studied in order to demonstrate that the ratio between H₂ and palladium is important in order to maximize the productivity and yield.

We found that:

- 1) Lower H₂ concentration or partial pressure (by modifying the total pressure) in the gas phase suppressed the productivity.
- 2) Lower liquid flowrate produced a higher local H₂ concentration and higher H₂O₂ concentrations, but also higher productivities.
- 3) A higher catalyst concentration in bed at initial stages (top of the downflow reactor) was better than homogeneous distribution.
- 4) At the same amount of catalyst a longer bed (more SiO₂) improved the H₂ dissolution and the production was clearly higher. Thus, a ratio of Pd/Vb < 0.094 mg/cm³ is recommended, in most cases.

In summary, in terms of productivity it is beneficial to maintain a high H₂ concentration in the liquid phase and also a high catalyst concentration in the bed in the very beginning of the reactor.

Acknowledgements

This work is part of the activities Process Chemistry Centre (PCC) at the Åbo Akademi University (ÅA). Dr. Juan Garcia Serna acknowledges the Spanish Economy and Competitiveness Ministry, Project Reference: ENE2012-33613 for funding and "Programa Salvador Madariaga 2012" for

mobility scholarship. MEng. Irene Huerta is grateful to the Johan Gadolin scholarship 2012-13 (ÅA). Financial support from Academy of Finland to Academy Professor Tapio Salmi is gratefully acknowledged. Dr². P. Biasi gratefully acknowledges to the Kempe Foundations for financial support. In Sweden, also the Bio4Energy programme is acknowledged.

This work is part of the activities Process Chemistry Centre (PCC) at the Åbo Akademi University.
Dr. Juan

References

- [1] B.H. Alsolami, R.J. Berger, M. Makkee, J.A. Moulijn, Catalyst performance testing in multiphase systems: Implications of using small catalyst particles in hydrodesulfurization, *Industrial and Engineering Chemistry Research* 52 (2013) 9069-9085.
- [2] BASF, <http://www.chemicals-technology.com/projects/basf-hppo/>, (2013).
- [3] P. Biasi, J. García-Serna, A. Bittante, T. Salmi, Direct synthesis of hydrogen peroxide in water in a continuous trickle bed reactor optimized to maximize productivity, *Green Chemistry Accepted* (2014).
- [4] P. Biasi, N. Gemo, J.R. Hernandez Carucci, K. Eranen, P. Canu, T.O. Salmi, Kinetics and Mechanism of H₂O₂ Direct Synthesis over a Pd/C Catalyst in a Batch Reactor, *Industrial & Engineering Chemistry Research* 51 (2012) 8903-8912.
- [5] P. Biasi, S. Zancanella, F. Pinna, P. Canu, T.O. Salmi, Hydrogen peroxide direct synthesis: From catalyst preparation to continuous reactors, *Chemical Engineering Transactions* 24 (2011) 49-54.
- [6] G. Blanco-Brieva, M.P. de Frutos Escrig, J.M. Campos-Martin, J.L.G. Fierro, Direct synthesis of hydrogen peroxide on palladium catalyst supported on sulfonic acid-functionalized silica, *Green Chemistry* 12 (2010) 1163-1166.
- [7] C. Burato, S. Campestrini, Y.-F. Han, P. Canton, P. Centomo, P. Canu, B. Corain, Chemoselective and re-usable heterogeneous catalysts for the direct synthesis of hydrogen peroxide in the liquid phase under non-explosive conditions and in the absence of chemoselectivity enhancers, *Applied Catalysis A* 358 (2009) 224-231.
- [8] J.M. Campos-Martin, G. Blanco-Brieva, J.L. Fierro, Hydrogen peroxide synthesis: an outlook beyond the anthraquinone process, *Angew Chem Int Ed Engl* 45 (2006) 6962-6984.
- [9] I.R. Cohen, T.C. Purcell, A.P. Altshuller, Analysis of the oxidant in photooxidation reactions, *Environmental Science and Technology* 1 (1967) 247-252.

- [10] B. Corain, K. Jerabek, P. Centomo, P. Canton, Generation of Size-Controlled Pd⁰ Nanoclusters inside Nanoporous Domains of Gel-Type Resins: Diverse and Convergent Evidence That Supports a Strategy of Template-Controlled Synthesis, *Angewandte Chemie International Edition* 43 (2004) 959–962.
- [11] ChemSystems, Hydrogen Peroxide - PERP07/08-3, 2009.
- [12] V. Choudhary, C. Samanta, Role of chloride or bromide anions and protons for promoting the selective oxidation of H₂ by O₂ to H₂O₂ over supported Pd catalysts in an aqueous medium, *Journal of Catalysis* 238 (2006) 28-38.
- [13] T. Deguchi, H. Yamano, M. Iwamoto, Dynamics of direct H₂O₂ synthesis from H₂ and O₂ on a Pd nano-particle catalyst protected with polyvinylpyrrolidone, *Journal of Catalysis* 287 (2012) 55-61.
- [14] J.K. Edwards, G.J. Hutchings, Palladium and gold-palladium catalysts for the direct synthesis of hydrogen peroxide, *Angew. Chem., Int. Ed.* 47 (2008) 9192-9198.
- [15] J.K. Edwards, B. Solsona, E.N. Ntainjua, A.F. Carley, A.A. Herzing, C.J. Kiely, G.J. Hutchings, Switching Off Hydrogen Peroxide Hydrogenation in the Direct Synthesis Process, *Science* 323 (2009) 1037-1041.
- [16] J.K. Edwards, B.E. Solsona, P. Landon, A.F. Carley, A. Herzing, C.J. Kiely, G.J. Hutchings, Direct synthesis of hydrogen peroxide from H₂ and O₂ using TiO₂-supported Au-Pd catalysts, *Journal of Catalysis* 236 (2005) 69-79.
- [17] EVONIK, <http://h2o2.evonik.com/product/h2o2/en/Pages/default.aspx>, (2013).
- [18] J. García-Serna, T. Moreno-Rueda, P. Biasi, M.J. Cocero, J.-P. Mikkola, T.O. Salmi, Engineering in direct synthesis of hydrogen peroxide: targets, reactors and guidelines for operational conditions, *Green Chemistry Advance article*, DOI: 10.1039/C3GC41600C (2014).
- [19] N. Gemo, P. Biasi, P. Canu, T.O. Salmi, Mass transfer and kinetics of H₂O₂ direct synthesis in a batch slurry reactor, *Chemical Engineering Journal* 207 (2012) 539-551.
- [20] L.W. Gosser, Catalytic process for making H₂O₂ from hydrogen and oxygen, 1987.
- [21] T. Inoue, M.A. Schmidt, K.F. Jensen, Microfabricated Multiphase Reactors for the Direct Synthesis of Hydrogen Peroxide from Hydrogen and Oxygen, *Industrial and Engineering Chemistry Research* 46 (2007) 1153-1160.
- [22] P. Landon, P.J. Collier, A.F. Carley, D. Chadwick, A.J. Papworth, A. Burrows, C.J. Kiely, G.J. Hutchings, Direct synthesis of hydrogen peroxide from H₂ and O₂ using Pd and Au catalysts, *Physical Chemistry Chemical Physics* 5 (2003) 1917 - 1923.

- [23] J. Li, A. Staykov, T. Ishihara, K. Yoshizawa, Theoretical study of the decomposition and hydrogenation of H₂O₂ on Pd and Au@Pd surfaces: Understanding toward high selectivity of H₂O₂ synthesis, *Journal of Physical Chemistry C* 115 (2011) 7392-7398.
- [24] Q. Liu, J. Lunsford, The roles of chloride ions in the direct formation of H₂O₂ from H₂ and O₂ over a Pd/SiO₂ catalyst in a H₂SO₄/ethanol system, *Journal of Catalysis* 239 (2006) 237-243.
- [25] S. Maehara, M. Taneda, K. Kusakabe, Catalytic synthesis of hydrogen peroxide in microreactors, *Chemical Engineering Research and Design* 86 (2008) 410-415.
- [26] S. Melada, R. Rioda, F. Menegazzo, F. Pinna, G. Strukul, Direct synthesis of hydrogen peroxide on zirconia-supported catalysts under mild conditions, *Journal of Catalysis* 239 (2006) 422-430.
- [27] T. Moreno Rueda, J. García Serna, M.J. Cocero Alonso, Direct production of H₂O₂ from H₂ and O₂ in a biphasic H₂O/scCO₂ system over a Pd/C catalyst: Optimization of reaction conditions, *The Journal of Supercritical Fluids* 61 (2012) 119-125.
- [28] E.N. Ntainjua, M. Piccinini, J.C. Pritchard, J.K. Edwards, A.F. Carley, J.A. Moulijn, G.J. Hutchings, Effect of Halide and Acid Additives on the Direct Synthesis of Hydrogen Peroxide using Supported Gold-Palladium Catalysts, *ChemSusChem* 2 (2009) 575-580.
- [29] N.E. Ntainjua, M. Piccinini, J.C. Pritchard, J.K. Edwards, A.F. Carley, J.A. Moulijn, G.J. Hutchings, Effect of halide and acid additives on the direct synthesis of hydrogen peroxide using supported gold-palladium catalysts, *ChemSusChem* 2 (2009) 575-580.
- [30] N. Rados, A. Shaikh, M.H. Al-Dahhan, Solids flow mapping in a high pressure slurry bubble column, *Chemical Engineering Science* 60 (2005) 6067-6072.
- [31] Y. Voloshin, A. Lawal, Overall kinetics of hydrogen peroxide formation by direct combination of H₂ and O₂ in a microreactor, *Chemical Engineering Science* 65 (2010) 1028-1036.
- [32] X. Wang, Y. Nie, J.L.C. Lee, S. Jaenicke, Evaluation of multiphase microreactors for the direct formation of hydrogen peroxide, *Applied Catalysis A* 317 (2007) 258-265.

Table Captions

Table 1. Experimental table for H ₂ O ₂ direct synthesis in a trickled bed reactor.....	146
Table 2. Summary of main experimental results and standard deviation values	150

Figure Captions

- Figure 1. Reactions involved in the direct synthesis of hydrogen peroxide.....142
- Figure 2. Scheme of the apparatus used in the H₂O₂ experiments. (1) Trickled bed reactor. (2) Liquid solvent supply. (3, 4, 5) Gas bottles, O₂, N₂ and CO₂/H₂ (97.5/2.5 %). (6) Pump. (7) Mass flow controller. (8, 9) External cooling and chiller with temperature controller. (10) Liquid collection vessel. (11) Pressure controller. (12) Vent valve. (13) Micrometric valve. (14) On/off valve. (15) Check valve. (16) Three – way valve. (17) Ball valve.145
- Figure 3. Trickle bed region and operational window (adapted from Ranade *et al.* [24]).....149
- Figure 4. Overview of the experiments152
- Figure 5. Turnover frequency (TOF) vs initial hydrogen/palladium ratio.....153
- Figure 6. Influence of reactor pressure, liquid flow rate and catalyst on the final average hydrogen peroxide concentration (#1 – 5, 15 – 19, 29 – 33, 39 – 43). Uniform catalyst distribution. (Pressure (barg) /amount of catalyst (mg)/ bed volume (cm³)).....155
- Figure 7. Influence of the catalyst on the final average yield values (#1–19, 29 – 48). Solid symbols – 28 barg; empty symbols – 15 barg. (amount of catalyst (mg)/ bed volume (cm³))155
- Figure 8. Influence of the catalyst on final average TOF values (#1 – 19, 29 – 48). Solid symbols – 28 barg; empty symbols – 15 barg.156
- Figure 9. Influence of catalyst distribution and liquid flow rate on final average hydrogen peroxide concentration (# 1 – 23; 24 – 53). (Amount of catalyst (mg)/ bed volume (cm³)/distribution). 28 – 25 barg left figure, 15 barg right figure.157
- Figure 10. Influence of catalyst distribution on final average yield values. (#1 – 9, 20 – 38, 49 – 53). (Amount of catalyst (mg)/ bed volume (cm³)/distribution). Solid symbols: 28 – 25 barg, empty symbols: 15 barg.158
- Figure 11. Influence of catalyst distribution on final average TOF values. (#1 – 9, 20 – 38, 49 – 53). (Amount of catalyst (mg)/ bed volume (cm³)/distribution). Solid symbols: 28 – 25 barg, empty symbols: 15 barg.158
- Figure 12. Influence of ratio Pd/V_b on final average yield values (#1 – 19). 75 mg of catalyst: ◆ 0.5 ml·min⁻¹; ■ 1 ml·min⁻¹; ● 4 ml·min⁻¹; ▲ 6 ml·min⁻¹ and 37.5 mg of catalyst: ◇ 0.5 ml·min⁻¹; □ 1 ml·min⁻¹; ○ 4 ml·min⁻¹; △ 6 ml·min⁻¹.....159
- Figure 13. Influence of ratio Pd/V_b t in final average TOF values (#1 – 19). 75 mg of catalyst: ◆ 0.5 ml·min⁻¹; ■ 1 ml·min⁻¹; ● 4 ml·min⁻¹; ▲ 6 ml·min⁻¹. 37.5 mg of catalyst: ◇ 0.5 ml·min⁻¹; □ 1 ml·min⁻¹; ○ 4 ml·min⁻¹; △ 6 ml·min⁻¹.....159

CHAPTER V

The development of the H₂O₂ direct synthesis process in water with a commercial catalyst in a continuous reactor: bridging the gap between chemistry and chemical engineering

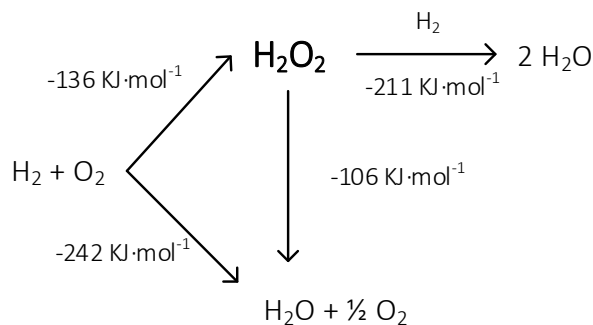
A trickle bed reactor (TBR) was used to study different parameters upon hydrogen peroxide direct synthesis. The catalysts used were commercial palladium on active carbon, with silica used to dilute the catalyst along the reactor bed. The influence of pressure (1.75 to 25 barg), temperature (5 to 60 °C), liquid flow rate (2 to 13.8 mL·min⁻¹), gas flow rate (3.39 to 58.46 mL·min⁻¹), catalyst amount (90 to 540 mg), Pd percentage on the support (5, 10 and 30% wt. Pd/C) as well as promoter concentrations (0.0005 to 0.001M) were all varied as reaction parameters to better understand the behaviour of the system. On the other hand, the gas phase molar composition of the feed (4:20:76 = H₂:O₂:CO₂) was kept constant. The strong influence between liquid flow rate, gas flow rate and catalyst amount were identified as the key parameters to tune the reaction, and related to the activity of the catalyst. In essence, these parameters must be carefully tuned to control the hydrogen consumption. The maximum productivity (288.6 μmol H₂O₂·min⁻¹) and yield (83.8%) were obtained when a diluted bed of 30%Pd/C was applied. In essence, the H₂O₂ hydrogenation was studied in order to understand its role in the H₂O₂ direct synthesis reaction network. Consequently, understanding the whole reaction mechanism and coupling it with the reaction conditions studied led to a deeper understanding of all the phenomena involved in the H₂O₂ direct synthesis. As direct consequence, it was demonstrated that a systematic analysis of the reaction parameters is needed to acquire information for an optimal catalyst design.

5.1. Introduction

The chemical industry and society have been looking for new and more sustainability products and processes for decades. One of the most used chemical products is hydrogen peroxide, with a wide range of applications primarily as an oxidant, from paper to electronic industries. Its demand still increases year after year and annual market [1-4] is close to 3000 kt/y. In fact, the traditional synthesis route, auto-oxidation process, is used to produce more than 95 % of the total production. However it is not capable to conform to the new “green” market demands, strongly related to formation of by-products and application of energy-demanding purifying stages. A viable alternative to this large scale process can be the direct synthesis (DS), due to its green philosophy and the clean byproducts produced (Scheme 1). Direct synthesis of H_2O_2 is a three phase reaction process encompassing by a one desired reaction, hydrogen peroxide synthesis, and three undesired reactions, water synthesis, H_2O_2 decomposition and H_2O_2 hydrogenation (Scheme 1). The main problem of the direct synthesis, apart from the safety concerns on the H_2/O_2 mixtures, is the selectivity. The challenge is that usually the catalysts active for the DS are also active for the H_2O formation and for the H_2O_2 hydrogenation.

Undesired reactions can be minimized at different levels. The main issue is still the design of appropriated catalysts [2] (active metal or support [3, 5, 6]), followed by the focus on the addition of promoters (acids and halides) [3, 5-8], selection of liquid solvent (water, methanol, ethanol or a mixture of them) and optimization of reaction conditions since appropriate selection of operational parameters are crucial in aiming at high selectivities in the H_2O_2 direct synthesis [9-20]. Gas phase concentration is limited by flammability limits of hydrogen – oxygen mixtures. An inert gas, typically CO_2 or N_2 , is needed to maintain the H_2 concentration below the lower inflammability limits (LFL: 3.6 – 4.0 %).

Hydrogen peroxide direct synthesis could compete with traditional auto-oxidation process only if the process will be able to produce a clean solution of H_2O_2 close to a concentration of 12-15% wt.



Scheme 1. H₂O₂ direct synthesis' reaction scheme

The direct synthesis of H₂O₂ in water over a solid catalyst is a three phase reaction and thus it is necessary to develop it in a continuous reactor that allows firstly a continuous H₂O₂ production. Also appropriate contacting between three phases (solid–liquid–gas) is important to minimize the mass transfer limitations. One of the most promising reactors for the H₂O₂ direct synthesis is a trickle bed reactor. Trickle bed reactors (TBR) are three phase fixed bed reactors widely used in petrochemical industry and bulk chemistry industry. In a TBR, liquid flows down wetting the solid particles as drops or rivulets while the gas down-flows or up-flows through the column. Henkel *et al.* patented one of the first TBRs for hydrogen peroxide direct synthesis [21]. In this patent a TBR of I.D. = 16 mm, length = 40 cm charged with 148 g of catalyst with a concentration of active metal from 0.25 to 2.5 % wt of Pd (95%) and Au (5%) was proposed. Water and ethanol mixtures were applied as solvent at 50 bar and 25 °C. Gas phase was a mixture of H₂:O₂:N₂ (3:20:77 % mol). To avoid secondary reactions, a concentration of bromide between 0.0002 and 0.001 mol·dm⁻¹ and concentration of H₂SO₄ of 0.01 mol·dm⁻³ were used. Under these conditions, conversions between 47% and 68%, selectivities ranging from 29% to 72%, and palladium productivities (or Turnover frequency, TOF) between 1.6 and 16.5 g H₂O₂·g Pd⁻¹·h⁻¹ were obtained. Later on, it was studied the direct synthesis of hydrogen peroxide in a TBR [9-12]. The effect of the catalyst supports (a commercial cross-linked polymeric matrix and sulphated zirconia (ZS)) in terms of the selectivity of palladium catalyst were evaluated. Best results were obtained with Pd – SZ catalyst reaching a selectivity of 70% [11]. Commercial polymeric matrix gave inferior results because of its morphology [10]. Using methanol as solvent and without promoters, it was found that operating at -10 °C and 10 – 20 bar, the maximum value of TOF reached was 6.1 mmol H₂O₂·g Pd⁻¹·h⁻¹ and a productivity of 0.0035 mmol H₂O₂·min⁻¹ was obtained. Further, the influence of gas phase molar ratio was also studied: when bimetallic catalyst (Pd – Au) was used the selectivity was higher at low flow rates while a hydrogen molar ratio concentration close to 4% (4:22:76 of H₂:O₂:CO₂) seemed suitable. However when only 2 mol. % of hydrogen molar ratio was present in the feed (2:22:78 – H₂:O₂:CO₂), the selectivity was

higher upon use of high liquid flow rates [12]. Direct synthesis reaction have been also studied using water as liquid phase with a 5 %Pd/C and a mixture of sodium bromide/phosphoric acid as promoters. Under these conditions a maximum productivity up to 0.15 mmol H₂O₂·min⁻¹ and 63 % of yield were obtained [9]. Later on an exhaustive study concerning the influence of the reaction conditions with the objective to maximize hydrogen peroxide productivity on a TBR was conducted. The most important parameters studied were pressure (5 to 28 barg), liquid flow rate (0.25 to 2 ml·min⁻¹), amount of catalyst (30 to 300 mg) and the total distribution of solid along the reactor. A maximum productivity of 149.4 μmol H₂O₂·min⁻¹, corresponding to and 74.1% yield was obtained [9]. It was concluded that the system performance can be optimized by an appropriate selection of catalyst distribution, trying to maintain high H₂/Pd ratio beneficial upon H₂O₂ direct synthesis.

Heterogeneous catalyzed reactions are complex and their understanding and optimization requires exhaustive investigations of the operational parameters. Indeed, thus the behavior of the system can be used to design more efficient catalysts. Moreover, if only one parameter is studied, the results are applicable only for the conditions proposed. Other studies involving the direct synthesis in a continuous reactor are shown in Table 2.

Table 1. Performance comparison of different reactor systems

Reference	Reactor Type	Catalyst	Temperature	Pressure	Solvent	H ₂ O ₂ Productivity*
Present Work	TBR	5%Pd/C	288	28	H ₂ O+acid+bromide	2000
Paunovic[22]	Microreactor	5%AuPd/SiO ₂	303	20	H ₂ O+acid+bromide	3500
Freakley[13]	Millireactor	1%PdAu/TiO ₂	275	10	66% MeOH + 34% H ₂ O	400
Inoue [23]	Microreactor	5%PdAu/TiO ₂	293	10	H ₂ O+acid+bromide	3000
Biasi[9]	TBR	5%Pd/C	288	28	H ₂ O+acid+bromide	1120
Kim[16]	Upflow	0.24%Pd/resin	295	50	MeOH+acid+bromide	5300

*mol H₂O₂·kgPd⁻¹·h⁻¹

The aim of this work is to give useful guidelines in terms of on the reaction conditions and product distribution to materials scientists aiming at designing a new generation of catalysts. It is well known that the performance of different catalysts upon H₂O₂ direct synthesis are different and depend on nanoparticle size, catalyst support, 2nd metal used, etc. Moreover, all the catalysts features have to be related to the reaction parameters to understand how to improve the catalysts for the H₂O₂ direct synthesis could be improved. The use of a continuous reactor reduces the time and the materials required. The analysis of the whole reaction parameters can give to the chemists new insight how to synthesize tailor-made catalysts for H₂O₂ direct synthesis.

The choice of the commercial catalyst and the single metal catalyst was motivated by the need of finding a catalyst available in significant amounts and to have consistent results with different batches of catalysts. All the parameters studied, from the H₂ concentration to the gas and liquid flow rate, as well as from temperature to pressure are of fundamental importance and if well integrated with catalyst characterization can give the path to follow when synthesizing new promising catalysts. Hereby we report, in an objective way, what is important to understand and analyze to control the H₂O₂ direct synthesis from the operational point of view.

5.2. Materials and methods

5.2.1 *Materials*

The TBR bed was composed of a mixture of Pd/C catalyst and SiO₂. SiO₂ microparticles (200 to 500 μm Sigma-Aldrich) were used as inert material to dilute the catalyst. The active catalyst was carbon with 5%, 10% and 30% of Pd (Sigma-Aldrich) used without any modification. Glass wool (from Carl Roth) was used as plugs inside the reactor to immobilize the SiO₂-Pd/C mixture. Hydrogen peroxide concentration in reaction was measured by iodometric titration. For the iodometric titration, potassium iodide (99.5% Sigma-Aldrich), sulphuric acid (98% J.T. Baker), starch (Merck), sodium thiosulfate pentahydrate (99.5% Sigma-Aldrich) and ammonium molybdate tetrahydrate (99.0% Fluka) were used as reagents. All the experiments were carried out using deionized water as the reaction medium. To minimize hydrogenation and decomposition, promoters were used. Phosphoric acid (99.0% Sigma-Aldrich) and sodium bromide (99.5% Sigma-Aldrich). Premium grade (99.999 %) Oxygen (O₂), Nitrogen (N₂) and hydrogen/carbon dioxide (H₂/CO₂) were supplied by AGA Oy (Linde Group, Finland).

5.2.2 *Experimental set-up*

The experimental set-up used for the experiments was quite similar to the system used in a previous work[9]. Briefly, the reactor was made of AISI 316 stainless steel, 60 cm long and with an internal diameter of 1.5 cm. The reactor was passivated with 30 wt./wt.% HNO₃ overnight to minimise hydrogen peroxide decomposition. Figure 1 shows the complete apparatus.

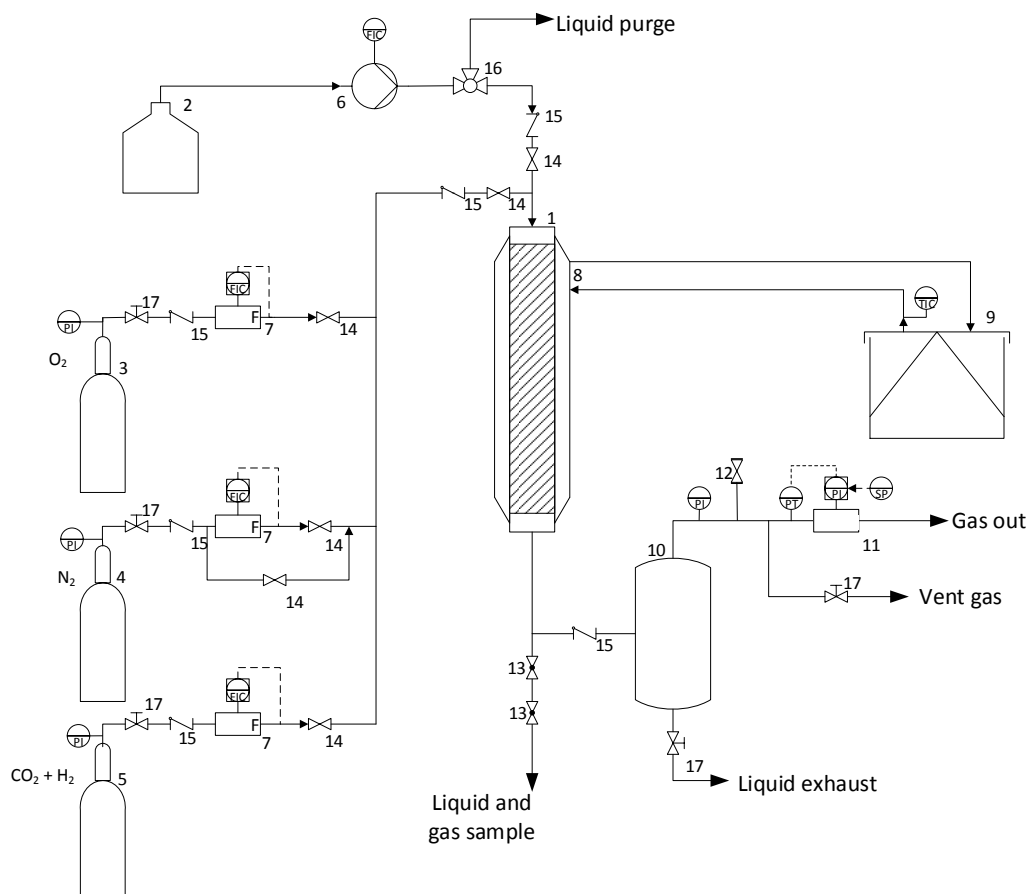


Figure 1. Scheme of the apparatus used in the H_2O_2 experiments. (1) Trickle bed reactor. (2) Liquid solvent supply. (3, 4, 5) Gas bottles, O_2 , N_2 and CO_2/H_2 (95/5 %). (6) Pump. (7) Mass flow controller. (8, 9) External cooling and chiller with temperature controller. (10) Liquid collection vessel. (11) Pressure controller. (12) Vent valve. (13) Micrometric valve. (14) On/off valve. (15) Check valve. (16) Three-way valve. (17) Ball valve.

5.2.3 Methods

Reaction progress was measured and controlled by measuring hydrogen peroxide concentration in the liquid phase, while oxygen and hydrogen were monitored in the gas phase. H_2O_2 concentration was determined by iodometric titration. The influence of pressure, temperature, liquid flow rate, gas flow rate, amount of catalyst and palladium catalyst percentage in a TBR with a high L/D ratio were monitored. The experimental conditions are summarised in Table 2. Gas composition was constant 76/20/4 %mol ($\text{CO}_2/\text{O}_2/\text{H}_2$). Volumetric gas flow rate may varied according to temperature and pressure values in order to ensure constant molar gas flow rate. Monitoring the molar gas flow rate constant, simplified the study and the comparison of the final results. Oxygen to hydrogen molar ratio (O_2/H_2) was fixed at around 5, according to the earlier

conclusions that suggest that an excess of O₂ can minimized the sites devoted to the production of water⁵.

Hydrogen peroxide production rate ($F_{H_2O_2}$) and turnover frequency (T.O.F.) values were calculated from H₂O₂ % wt/v concentration in liquid phase. Yield was defined as the moles of hydrogen peroxide produced divided by the moles of hydrogen fed into the reactor. Hydrogen concentration on gas phase at the outlet of the reactor was negligible.

5.2.4 Experimental procedure

Reactor was filled with a mixture of catalyst and quartz sand corresponding to each experiment. Care has to be taken upon reactor loading avoiding any empty spaces and assuring a homogeneous catalyst concentration along the bed. To start the reaction, the desired pressure was attained by N₂, followed by pumping of liquid for 30-60 minutes to ensure completely wetness of the catalytic bed. Correspondingly, the liquid and gas flow rate values were then adjusted as desired. During the actual experiment, gas and liquid samples were withdrawn every 15 minutes after the reactor started to operate in steady state regime.

5.3. Results and discussion

The main results are reported in Table 2 and Table 3. Table 2 summarized the conditions used upon experiments while Table 3 reports the H₂O₂ concentration, $F_{H_2O_2}$ and TOF obtained.

Table 2. Experimental table for H₂O₂ direct synthesis in a trickle bed reactor.

Run #	Press. barg	Temp. °C	Pd loading %	Catalyst mg	LFR mL·min ⁻¹	GFR mL·min ⁻¹	FH ₂ μmol·min ⁻¹	O ₂ /H ₂ mol/mol	[Br] mmol·dm ⁻³
1	25	15	5	380	4.0	3.39	143.9	4.94	5.0·10 ⁻⁴
2	25	15	5	380	4.0	5.22	221.6	4.94	5.0·10 ⁻⁴
3	25	15	5	380	4.0	8.64	366.6	4.94	5.0·10 ⁻⁴
4	25	15	5	380	4.0	11.69	496.0	4.94	5.0·10 ⁻⁴
5	25	15	5	380	6.0	3.39	143.9	4.94	5.0·10 ⁻⁴
6	25	15	5	380	6.0	5.22	221.6	4.94	5.0·10 ⁻⁴
7	25	15	5	380	6.0	8.64	366.6	4.94	5.0·10 ⁻⁴
8	25	15	5	380	6.0	11.69	496.0	4.94	5.0·10 ⁻⁴
9	25	15	5	540	4.0	3.39	143.9	4.94	5.0·10 ⁻⁴
10	25	15	5	540	4.0	5.22	221.6	4.94	5.0·10 ⁻⁴
11	25	15	5	540	4.0	8.64	366.6	4.94	5.0·10 ⁻⁴
12	25	15	5	540	4.0	11.69	496.0	4.94	5.0·10 ⁻⁴
13	25	15	5	540	6.0	3.39	143.9	4.94	5.0·10 ⁻⁴

14	25	15	5	540	6.0	5.22	221.6	4.94	$5.0 \cdot 10^{-4}$
15	25	15	5	540	6.0	8.64	366.6	4.94	$5.0 \cdot 10^{-4}$
16	25	15	5	540	6.0	11.69	496.0	4.94	$5.0 \cdot 10^{-4}$
17	25	15	5	540	5.5	11.69	496.0	4.94	$5.0 \cdot 10^{-4}$
18	25	15	5	540	8.0	11.69	496.0	4.94	$5.0 \cdot 10^{-4}$
19	25	15	5	540	7.6	3.39	143.9	4.94	$5.0 \cdot 10^{-4}$
20	25	15	5	540	12.0	3.39	143.9	4.94	$5.0 \cdot 10^{-4}$
21	25	15	5	150	3.9	3.39	143.9	4.94	$5.0 \cdot 10^{-4}$
22	25	15	5	150	3.9	5.22	221.6	4.94	$5.0 \cdot 10^{-4}$
23	25	15	5	150	3.9	8.64	366.6	4.94	$5.0 \cdot 10^{-4}$
24	25	15	5	150	3.9	11.69	496.0	4.94	$5.0 \cdot 10^{-4}$
25	25	15	5	150	5.8	3.39	143.9	4.94	$5.0 \cdot 10^{-4}$
26	25	15	5	150	5.8	5.22	221.6	4.94	$5.0 \cdot 10^{-4}$
27	25	15	5	150	5.8	8.64	366.6	4.94	$5.0 \cdot 10^{-4}$
28	23	15	5	150	5.8	11.69	496.0	4.94	$5.0 \cdot 10^{-4}$
29	23	15	5	150	13.8	11.69	496.0	4.94	$5.0 \cdot 10^{-4}$
30	23	15	5	150	11.5	8.64	366.6	4.94	$5.0 \cdot 10^{-4}$
31	23	15	5	150	12.9	5.22	221.6	4.94	$5.0 \cdot 10^{-4}$
32	23	15	5	150	12.9	3.39	143.9	4.94	$5.0 \cdot 10^{-4}$
33	20	15	5	540	6.0	14.62	496.0	4.94	$5.0 \cdot 10^{-4}$
34	15	15	5	540	6.0	19.49	496.0	4.94	$5.0 \cdot 10^{-4}$
35	10	15	5	540	6.0	29.23	496.0	4.94	$5.0 \cdot 10^{-4}$
36	4.5	15	5	540	6.0	58.46	496.0	4.94	$5.0 \cdot 10^{-4}$
37	1.75	15	5	540	6.0	58.46	496.0	4.94	$5.0 \cdot 10^{-4}$
38	20	5	5	540	6.0	14.11	496.0	4.94	$5.0 \cdot 10^{-4}$
39	20	40	5	540	6.0	15.88	496.0	4.94	$5.0 \cdot 10^{-4}$
40	20	60	5	540	6.0	16.90	496.0	4.94	$5.0 \cdot 10^{-4}$
41	20	40	5	540	6.0	15.88	496.0	4.94	$5.0 \cdot 10^{-4}$
42	20	25	5	540	6.0	15.12	496.0	4.94	$5.0 \cdot 10^{-4}$
43	15	15	10	270	6.0	3.39	143.9	4.94	$5.0 \cdot 10^{-4}$
44	15	15	10	270	6.0	5.22	221.6	4.94	$5.0 \cdot 10^{-4}$
45	15	15	10	270	6.0	8.64	366.6	4.94	$5.0 \cdot 10^{-4}$
46	15	15	10	270	6.0	11.69	496.0	4.94	$5.0 \cdot 10^{-4}$
47	15	15	10	270	6.0	11.69	496.0	4.94	$5.0 \cdot 10^{-4}$
48	15	15	10	270	4.0	11.69	496.0	4.94	$5.0 \cdot 10^{-4}$
49	15	15	30	90	6.0	11.69	496.0	4.94	$5.0 \cdot 10^{-4}$
50	15	15	30	90	6.0	8.64	366.6	4.94	$5.0 \cdot 10^{-4}$
51	15	15	30	90	6.0	5.22	221.6	4.94	$5.0 \cdot 10^{-4}$
52	15	15	30	90	6.0	3.39	143.9	4.94	$5.0 \cdot 10^{-4}$
53	15	15	30	90	4.0	11.69	496.0	4.94	$5.0 \cdot 10^{-4}$
54	10	15	5	540	2.0	5.54	141.0	4.94	$5.0 \cdot 10^{-4}$
55	10	15	5	540	2.0	5.54	141.0	4.94	$2.5 \cdot 10^{-4}$
56	10	15	5	540	2.0	5.54	141.0	4.94	$1.0 \cdot 10^{-3}$

Table 3. Summary of main experimental results and standard deviation values

Run #	[H ₂ O ₂] %wt/v	Yield %	F _{H₂O₂} μmol·min ⁻¹	T.O.F. mmol H ₂ O ₂ ·h ⁻¹ ·g Pd ⁻¹
1	0.059 ± 0.002	48.6 ± 1.2	70.0 ± 1.8	215.3 ± 5.5
2	0.1 ± 0.002	52.8 ± 0.8	117.1 ± 1.8	360.3 ± 5.6
3	0.181 ± 0	58.2 ± 0.19	213.3 ± 0.5	656.2 ± 1.4
4	0.225 ± 0	53.3 ± 0.1	264.2 ± 0.5	813 ± 1.4
5	0.056 ± 0.001	68.4 ± 0.8	98.4 ± 1.2	302.7 ± 3.8
6	0.087 ± 0.002	69.5 ± 1.4	153.9 ± 3.2	473.6 ± 9.8
7	0.109 ± 0.003	52.5 ± 1.4	192.4 ± 5.1	591.9 ± 15.7
8	0.12 ± 0.001	42.8 ± 0.4	212.3 ± 2.0	653.3 ± 6.2
9	0.056 ± 0.001	45.5 ± 1.0	65.5 ± 1.5	145.5 ± 3.3
10	0.103 ± 0.003	54.9 ± 1.4	121.6 ± 3.1	270.3 ± 6.9
11	0.175 ± 0.002	56.3 ± 0.5	206.3 ± 1.8	458.5 ± 4.0
12	0.227 ± 0.002	53.8 ± 0.4	266.8 ± 2.0	592.9 ± 4.4
13	0.053 ± 0	64.4 ± 0.5	92.0 ± 0.7	206 ± 1.6
14	0.084 ± 0.001	66.6 ± 0.8	147.6 ± 1.7	327.9 ± 3.7
15	0.133 ± 0.002	63.8 ± 0.8	233.9 ± 3.0	519.8 ± 6.6
16	0.175 ± 0.004	62.2 ± 1.4	307.3 ± 6.9	686.1 ± 15.3
17	0.19 ± 0.008	61.9 ± 2.7	307.3 ± 13.0	682.9 ± 29.6
18	0.127 ± 0.005	60.4 ± 2.6	299.4 ± 12.7	665.3 ± 28.2
19	0.042 ± 0	65.6 ± 0.4	94.4 ± 0.5	209.8 ± 1.1
20	0.029 ± 0.001	69.3 ± 2.0	99.7 ± 2.9	221.6 ± 6.4
21	0.071 ± 0.001	56.3 ± 0.8	81.1 ± 1.1	648.5 ± 9.2
22	0.113 ± 0	58.3 ± 0.2	129.2 ± 0.5	1034 ± 4.2
23	0.176 ± 0	54.9 ± 0.1	201.3 ± 0.3	1610.3 ± 2.1
24	0.217 ± 0.001	50.1 ± 0.2	248.7 ± 0.9	1989.6 ± 7.3
25	0.05 ± 0.001	59.8 ± 1.1	86.0 ± 1.5	688.3 ± 12.1
26	0.08 ± 0.002	61.3 ± 1.6	135.8 ± 3.5	1086.5 ± 27.7
27	0.094 ± 0.001	43.9 ± 0.4	161.1 ± 1.5	1288.9 ± 12.0
28	0.107 ± 0.001	36.8 ± 0.4	182.7 ± 2.0	1461.8 ± 16.1
29	0.054 ± 0	44.1 ± 0.0	219.0 ± 0	1751.7 ± 0
30	0.046 ± 0.001	42.3 ± 0.6	155.1 ± 2.1	1240.8 ± 16.6
31	0.032 ± 0	55.1 ± 0.0	122.0 ± 0	976.1 ± 0
32	0.02 ± 0	71.0 ± 1.1	102.2 ± 1.5	817.5 ± 12.2
33	0.155 ± 0.003	48.5 ± 1.0	240.8 ± 4.8	535.1 ± 10.0
34	0.135 ± 0.001	43.5 ± 0.3	215.8 ± 1.6	479.6 ± 3.6
35	0.109 ± 0.002	35.6 ± 0.5	180.2 ± 8.4	392.5 ± 5.5
36	0.088 ± 0.001	29.5 ± 0.3	146.5 ± 1.5	325.6 ± 3.4
37	0.053 ± 0	18.9 ± 0.1	93.9 ± 0.7	208.7 ± 1.6
38	0.155 ± 0.004	53.2 ± 1.5	264.1 ± 7.4	586.9 ± 16.4
39	0.165 ± 0.006	58.2 ± 1.1	288.8 ± 5.4	641.7 ± 11.9
40	0.125 ± 0.001	43.9 ± 0.3	217.5 ± 1.4	483.4 ± 3.1
41	0.179 ± 0.005	62.3 ± 1.7	309.1 ± 8.4	686.9 ± 18.6
42	0.185 ± 0.002	64.6 ± 0.6	320.2 ± 2.8	711.6 ± 6.1
43	0.046 ± 0.001	58.9 ± 1.9	84.7 ± 2.7	188.3 ± 6.0

44	0.066 ± 0.001	54.0 ± 0.6	119.6 ± 1.3	265.7 ± 2.8
45	0.09 ± 0.001	44.4 ± 0.3	162.7 ± 1.1	361.5 ± 2.4
46	0.116 ± 0.01	41.7 ± 3.7	206.7 ± 18.3	459.4 ± 40.8
47	0.137 ± 0.002	50.5 ± 0.6	250.5 ± 3.0	556.6 ± 6.7
48	0.196 ± 0.006	45.8 ± 1.5	227.1 ± 7.3	504.7 ± 16.2
49	0.168 ± 0.002	58.2 ± 0.7	288.6 ± 3.3	641.2 ± 7.4
50	0.144 ± 0.002	71.8 ± 1.1	263.3 ± 4.0	585.1 ± 8.8
51	0.097 ± 0.001	79.7 ± 1.0	176.6 ± 2.2	392.5 ± 4.9
52	0.066 ± 0.001	83.8 ± 1.5	120.4 ± 2.1	267.6 ± 4.8
53	0.203 ± 0.002	47.8 ± 0.6	236.5 ± 2.8	525.5 ± 6.3
54	0.143 ± 0.001	59.5 ± 0.5	83.9 ± 0.7	186.3 ± 1.6
55	0.102 ± 0.001	41.2 ± 0.4	58.1 ± 0.5	129.1 ± 1.2
56	0.159 ± 0.004	64.1 ± 1.5	90.4 ± 2.1	200.9 ± 4.7

In TBRs there is the possibility to work under six different flow regimes [24]. A low liquid flow rate and a low gas flow rate are generally desired for trickle bed operations. This ensures low gas – liquid interactions and liquid flows around solid particles as a film or rivulets. However, the industrial scale and laboratory scale do not necessary behave in the same way or follow the same physical rules. At industrial scale, gravity acts as the main force while capillary forces are the main ones at laboratory scale. Eötvös number ($E\ddot{o}$ = gravitational force / capillary force) calculated for this experimental system had small values (0.006 – 0.012) which confirms that capillary forces have a great influence over hydrodynamic system's behaviour [25]. The influence of the capillary force could be moderated by the high length – diameter reactor ratio ($L/D = 40$) although that effect cannot be directly measured since it is not included in the Eötvös number. In fact, not many references are available about flow regime on laboratory scale trickle bed columns, so we will accept that industrial regime flows can be extrapolated to laboratory scale with some restrictions. The study of the real hydrodynamic behavior was out of the scope of this work, but must be taken into account to ensure the correct running of the system.

To ensure that the system flow operated under trickle bed region, liquid and gas phases must flow with a Reynolds number lower than 10^3 [24]. Experiments set were designed to work in the upper part of tricked flow zone (white little dots), although some points with highest liquid and gas flow rates were in the pulsed flow region (black squares). Even if some experiments were in the border line of the pulsed flow regime, the results were consistent. Because of that, all the experiments were performed in the same series independently of the flow regime.

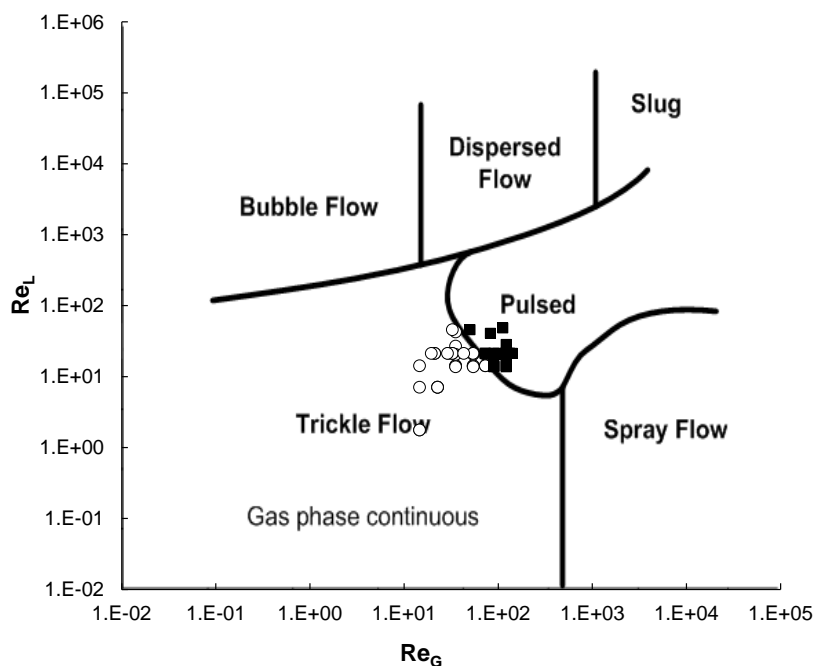


Figure 2. Trickle bed region and operational window (adapted from Ranade *et al.* [24])

Trickle bed reactor is a flexible solution to support hydrogen peroxide direct synthesis because it guarantees a high mass transfer coefficient between gas, liquid and solid phase. In general, it is quite difficult to understand the relation between the reactor system and the mechanism of the reaction studied, especially for the H₂O₂ direct synthesis. For that reason, it is important to study all the reactor parameters and to relate them to the catalyst activity and to the possible reaction mechanism. Only with this systematic work new information can be acquired and used for catalyst design [20]. Thus it is necessary to monitor the reaction variables in terms of the productivity and stability of the reaction system.

The reaction conditions must be selected carefully, avoiding that one reaction step (mass transfer or kinetic control) may limit the process. Success in hydrogen peroxide direct synthesis depends on the liquid flow rate relative to gas flow rate and the amount of catalyst: with a correct selection of them, it is possible to reduce the production of water, as already demonstrated [4, 9, 13, 20]. Liquid flow rate, gas flow rate and the catalyst amount are all coupled. Indeed, it is important to analyze them together to understand how H₂ should be fed and consumed in the reactor to minimize all the reactions that are forming water. Secondary reactions are related to the amount of hydrogen available in the liquid phase and its consumption rate [9, 26]. H₂O₂ productivity could increase with the gas flow rate (higher amount of H₂) only if the gas can be dissolved into the liquid phase (mass transfer) and further consumed (kinetics).

5.3.1. Hydrogenation experiments

Hydrogen peroxide direct synthesis reaction scheme is composed of four reaction occurring parallel and series. Although hydrogen peroxide synthesis is the main (desired) reaction, hydrogenation ($\text{H}_2\text{O}_2 + \text{H}_2 \rightarrow 2 \text{H}_2\text{O}$), decomposition ($\text{H}_2\text{O}_2 \rightarrow \text{H}_2\text{O} + \frac{1}{2} \text{O}_2$) and water formation ($\text{H}_2 + \frac{1}{2} \text{O}_2 \rightarrow \text{H}_2\text{O}$) are also present in the system. The undesired side reactions constitute one of the main disadvantages of hydrogen peroxide direct synthesis and this problem it is well known [2-4, 27]. The focus on retarding the secondary reactions, at all levels (catalyst, reactor design and reaction conditions selection), is one of the first priorities to be studied. Water formation is difficult to monitor if the secondary reactions are still present in the reaction network. In our case the decomposition reaction was negligible if NaBr and H_3PO_4 were used.

In order to introduce an analysis of the hydrogenation reaction rate for further work, hydrogenation experiments were carried out in conjunction to the experiments of the direct synthesis reaction. Hydrogenation experiments are needed to understand in which conditions hydrogenation plays an important role on the overall reaction network. Moreover hydrogenation reaction is a simple reaction that can be used to calculate the mass transfer coefficient [28] and to understand the general activity of the catalyst under the experimental conditions [2-4, 26]. Obviously no oxygen was fed into the reactor during hydrogenation experiments. Hydrogenation percentage represents the decreasing H_2O_2 productivity due to hydrogenation, based on the initial concentration in the liquid phase. Also, the influence of liquid and gas flow rates were measured. The initial concentration of the H_2O_2 used was 0.1 wt. % and the H_2O_2 was generated by the reaction.

As could be expected, hydrogenation was promoted by lower liquid flow rates and when the molar flow rate of hydrogen was higher (Figure 3 and Table 4). The decrease in hydrogen peroxide concentration was influenced mostly by an increase in the hydrogen molar flow rate ($16 \mu\text{mol H}_2\text{O}_2 \cdot \text{min}^{-1}$ to $99 \mu\text{mol H}_2\text{O}_2 \cdot \text{min}^{-1}$) compared to the liquid flow rate decrease ($16 \mu\text{mol H}_2\text{O}_2 \cdot \text{min}^{-1}$ to $4 \mu\text{mol H}_2\text{O}_2 \cdot \text{min}^{-1}$). For an easier discussion of the results, the progress of hydrogenation reaction would be measured in relation to the μmol of hydrogen peroxide hydrogenated. The influence of the liquid flow rate, on hydrogen consumption rate, indirectly represented by the hydrodynamic residence time, followed a linear tendency and confirmed that there was no relation between the amount of hydrogen peroxide inside the reactor and the hydrogenation rate. However there was a clear effect of the liquid

residence time on the hydrogenation rate. Based on these results, the first interpretation of the data could make us to conclude that hydrogenation rate could be reduced simply by decreasing the residence time of liquid inside the reactor or by reducing the amount of catalyst's active centers in the solid bed. However, a further investigation concerning the support effect over hydrogen peroxide would be needed before this statement is confirmed. The influence of the volumetric gas flow rate, represented by the molar flow rate of hydrogen (gas molar composition was kept constant for all the experiments, 5 % mol H₂) is summarized in Figure 3 (right). The rate of consumption of hydrogen increased exponentially with increasing the hydrogen molar flow rate as expected since, a value of the order of reaction higher than one is indicated by calculation of the reaction order.

Notwithstanding, it is important to note that if high concentration of H₂ is prevailing together with high concentration of H₂O₂, the preferential routes are H₂O₂ formation and direct formation of H₂O [26]. Finally, hydrogenation is to be ascribed to the conditions of high hydrogen peroxide concentration with low H₂/Pd ratio (i.e. low amount of hydrogen along the bed with HO simultaneously).

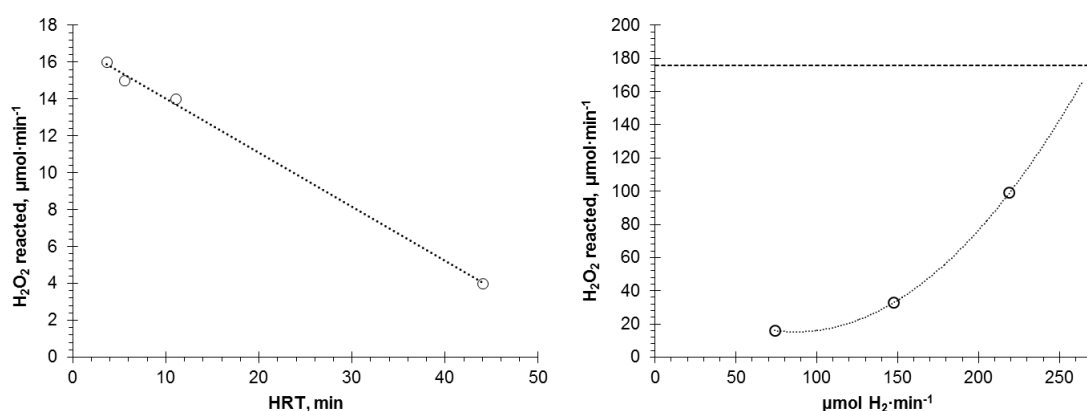


Figure 3. Influence of hydraulic residence time (left) and gas flow rate (right) on hydrogen consumption rate. (# 59 – 62 and # 57 – 59). 15 barg, 15 °C, 540 mg of catalyst 5 % Pd/C, 74.20 μmol H₂·min⁻¹ (left figure), 6 mL·min⁻¹ (right figure), [Br⁻] = 5·10⁻⁴ M

Table 4. Summary of main experimental conditions and results for hydrogenation experiments

Exp. #	LFR mL·min ⁻¹	F _{H₂} μmol·min ⁻¹	F _{H₂O₂_Initial} μmol·min ⁻¹	F _{H₂O₂_Final} μmol·min ⁻¹	% hydrogenation*	HRT min	H ₂ O ₂ reacted rate μmol·min ⁻¹
57	6	219.03	176	77	56.3 ± 7.69	3.7	99
58	6	147.73	167	134	19.8 ± 2.25	3.7	33
59	6	74.2	173	157	9.2 ± 1.64	3.7	16
60	4	74.2	121	106	12.4 ± 1.24	5.5	15
61	2	74.2	63	49	22.2 ± 1.28	11.0	14
62	0,5	74.2	14	10	28.6 ± 1.92	44.0	4

*calculated on base of the hydrogen peroxide concentration

5.3.2. Influence of liquid flow rate/gas flow rate and catalyst amount

LFR must be high enough to ensure complete and homogenous wetting of the reactor bed. In an early study, selected LFR values between 0.25 and 2 ml·min⁻¹ was chosen and was concluded that the system productivity could be thus increased because of an enhancement in mass transfer and a reduction in hydrogenation reaction rate⁹. Upper LFR value is limited by flow regime region because experimental conditions must be designed in order to ensure trickle flow regime. With these limitations, 4 ml·min⁻¹ and 6 ml·min⁻¹ were selected as the operational liquid flow rates.

For 4 ml·min⁻¹ flow rate (Figure 4) the increase in the H₂O₂ production was linear for each amount of catalyst, thus indicating that hydrogen in the liquid phase (catalyst from 150 to 580 mg) was not limiting the reaction. However, at these catalyst loadings, the production rates were very similar indicating that the mass transfer regulated the reaction. Thus, mass transfer was influencing the direct synthesis process too. The hypothesis is as follows: the direct synthesis of H₂O₂ and direct formation of H₂O are the reactions that compete at the beginning, while hydrogenation and decomposition are the reactions that are only commenced after a significant amount of H₂O₂ is produced [9, 26]. Most probably, since the liquid flow rate was not very high, the catalyst consumes all the hydrogen in the first part of the reactor, thus minimizing H₂O₂ hydrogenation. Hydrogenation for 4 ml·min⁻¹ was quite low, around 10% along the bed. That means that hydrogenation was not affecting so much the reaction, but most probably the formation of water was due to the direct synthesis of water at the beginning of the catalyst bed. For 6 ml·min⁻¹ flow rate (Figure 4) the results were different. The experiments with 540 mg of catalyst displayed a linear increase of the H₂O₂ with the H₂ content in the feed. The experiments with 380 and 150 mg of catalyst behaved differently, a linear increase of H₂O₂ was observed from

120 up to 220 $\mu\text{mol}\cdot\text{min}^{-1}$ of H₂ in the feed, while after 220 $\mu\text{mol}\cdot\text{min}^{-1}$ of H₂ a non-linear increase in H₂O₂ concentration was observed. The explanation can be quite simple: with 540 mg catalyst the reactions that consume H₂ to form H₂O₂ and H₂O take place in the first part of the reactor and all H₂ is consumed to form H₂O₂ and H₂O. Hydrogenation was not occurring in this case or was negligible.

The H₂O₂ formed could only decompose since H₂ was not anymore present in the liquid phase (and decomposition was negligible). So, the most probable reactions to occur were only the direct formation of H₂O₂ and H₂O. With 380 and 150 mg of catalyst, H₂ reacts also in the second part of the reactor (with low H₂ concentration and low H₂/Pd ratio[9]). In this case, a competition between H₂O₂ and H₂O production and H₂O₂ hydrogenation prevailed. There is a competition between the phenomena of adsorption on the catalyst surface, and these phenomena are related to the catalyst amount, H₂ concentration in the liquid phase and to the gas and liquid flow rates. Probably, at the flow rate of 4 $\text{ml}\cdot\text{min}^{-1}$, the contact time of the reagents with the catalyst was enough to minimize hydrogenation. The yield followed the same trend described previously. Yield (Figure 5) was quite stable for the experiments with 540 mg of catalyst but decreased quite rapidly for other amounts of catalysts at 6 $\text{ml}\cdot\text{min}^{-1}$. These observations are in accordance with the early findings of *Biasi et al.* and the concept of the “gradient reactors”[9]. It seems that everything depends on the palladium centers and their distribution along the reactor and as well as the equilibrium of the adsorption between H₂, O₂ and H₂O₂. This equilibrium can be shifted to minimize the hydrogenation. It seems that direct water formation only occurs on specific palladium centers of the catalyst. The last series of experiments performed with 150 mg of catalysts and 15 $\text{ml}\cdot\text{min}^{-1}$ of liquid flow rate exhibited an interesting trend: when the hydrogen flow rate was low, the production high in comparison. Upon feed rate of 120 $\mu\text{mol}\cdot\text{min}^{-1}$ of H₂ the yield was high as well, but when the H₂ feed was increased the production rate only little and the yield drastically decreased. These results are in accordance with the previous observations related to the gas-liquid mass transfer and to the possibility of the hydrogen to form directly H₂O₂ and H₂O or to hydrogenate the H₂O₂ formed (also here everything is related to contact time).

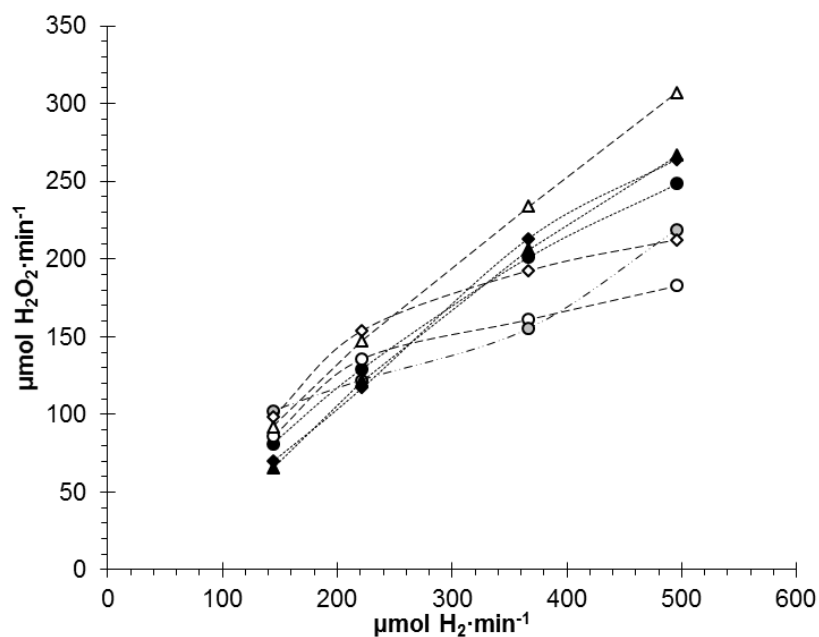


Figure 4. Influence of liquid flow rate, gas flow rate and amount of palladium on hydrogen peroxide production rate. (# 1 – 16; 21 – 32). 15 barg, 15 °C, 5% Pd/C, $[Br^-] = 5 \cdot 10^{-4}$. ● 150 mg of catalyst, 4 mL·min⁻¹; ◆ 380 mg of catalyst, 4 mL·min⁻¹; ▲ 540 mg of catalyst, 4 mL·min⁻¹; ○ 150 mg of catalyst, 6 mL·min⁻¹; ◇ 380 mg of catalyst, 6 mL·min⁻¹; △ 540 mg of catalyst, 6 mL·min⁻¹; ● 150 mg of catalyst, 15 mL·min⁻¹.

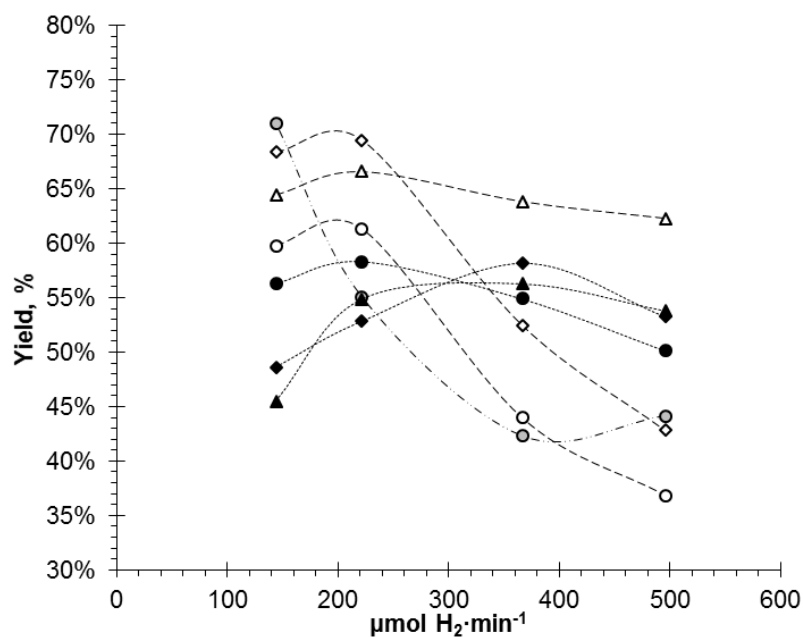


Figure 5. Influence of liquid flow rate, gas flow rate and amount of palladium on average final yield value. (# 1 – 16; 21 – 32). 15 barg, 15 °C, 5% Pd/C, $[Br^-] = 5 \cdot 10^{-4}$. ● 150 mg of catalyst, 4 mL·min⁻¹; ◆ 380 mg of catalyst, 4 mL·min⁻¹; ▲ 540 mg of catalyst, 4 mL·min⁻¹; ○ 150 mg of catalyst, 6 mL·min⁻¹; ◇ 380 mg of catalyst, 6 mL·min⁻¹; △ 540 mg of catalyst, 6 mL·min⁻¹; ● 150 mg of catalyst, 15 mL·min⁻¹.

5.3.3. Influence of total pressure

Mass transfer limitations between gaseous reactants (hydrogen and oxygen) and the active centres of the catalyst restrict system effectiveness and reduce productivity. Mass transfer can be enhanced in different ways. Thus, a higher operational pressure can improve hydrogen peroxide direct synthesis by increasing gas solubility in the liquid phase as showed in Figure 6 ($9.82 \cdot 10^{-6} \text{ molH}_2 \cdot \text{molH}_2\text{O}^{-1}$ at 28 barg and 15 °C; $1.29 \cdot 10^{-6} \text{ molH}_2 \cdot \text{molH}_2\text{O}^{-1}$ at 5 barg and 15 °C). Greater amounts of gas dissolved in the liquid phase means higher hydrogen peroxide productivity.

A comparison between experiments 16 and 35 (Table 5) showed how the volumetric flow rate plays a very important role. Hydrogen reacted to first produce H₂O₂ and H₂O. If a lot of H₂ was present in the bottom part of the reactor, competition between hydrogenation and the H₂O₂ formation present, thus favouring hydrogenation reaction (i.e. same amount of H₂, but different consumption of the H₂ along the bed and different gas solubility and H₂ in liquid phase). The pressure in the experiments 13 and 16 (Table 5) was equal and the yield was comparable even if the hydrogen molar flow rate at the experiment 13 was almost 3.5 times lower. The difference in these experiments is the H₂ concentration at the inlet. Probably the consumption rate of H₂ was similar and the main reactions involved were only the direct synthesis of H₂O₂ and H₂O. Analyzing the experiments 35 and 55, one can state that the lower liquid flow rate resulted in a high yield while higher liquid flow rate resulted in pronounced hydrogenation, as observed before. Experiments 20 demonstrated again how mass transfer and concentration of reagents and catalyst play an important role on the reaction mechanism and how the reaction network of the H₂O₂ direct synthesis should be managed. A comparison from these experiments can demonstrate that a high pressure does not guarantee a higher productivity or yield but it has to be fine tuned experimentally to achieve excellent results.

The experimental results validated previous hypothesis and were consistent with theoretical assumptions as it can be seen (Figure 6). Pressure had the same effect in terms of hydrogen peroxide direct synthesis yield. Maximum hydrogen peroxide productivity was 307.34 $\mu\text{mol H}_2\text{O}_2 \cdot \text{min}^{-1}$ obtained for 26 barg. This was also the maximum productivity obtained. As expected, the lowest productivity rate (93.93 $\mu\text{mol H}_2\text{O}_2 \cdot \text{min}^{-1}$) was obtained at the lowest pressure (2.75 barg).

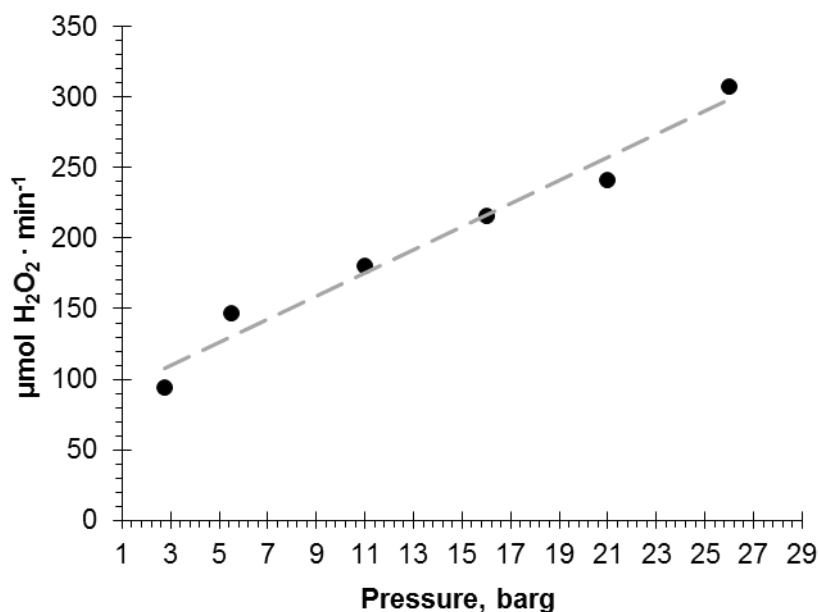


Figure 6. Influence of reactor pressure on final average hydrogen peroxide molar flow rate. (# 33 - 37). 15 °C, 540 mg of catalyst 5% Pd/C, 6 mL·min⁻¹, 469.03 μmol H₂·min⁻¹, [Br⁻] = 5·10⁻⁴

Table 5. The influence of the total pressure and H₂ molar flow rate influence

Exp. #	Pressure barg	LFR mL·min ⁻¹	GFR mLN·min ⁻¹	FH ₂ μmol·min ⁻¹	FH ₂ O ₂ μmol·min ⁻¹	Yield %
16	25	6	11.69	496,03	307,34	62%
35	10	6	26.23	496,03	180,24	36%
13	25	6	3.39	143,91	92,01	64%
20	25	12	3.39	143,91	99,71	69%
55	10	2	5.54	141,04	83,86	59%

Although it seems that productivity can increase with pressure, a maximum is reached when kinetics control the reaction and all the hydrogen dissolved in the liquid phase does not fully react (Fig. 6). Operational conditions must be selected carefully to avoid this kind of conditions. An excess of hydrogen in the liquid phase can favour hydrogenation reaction by retarding hydrogen peroxide, production (and selectivity towards it) especially when high hydrogen peroxide concentrations are obtained.

5.3.4. Influence of temperature

Experiments in series (# 38 – 42) were carried out with a high amount of catalyst (540 mg of 5% Pd/C), high liquid flow rate (6 mL·min⁻¹) and high hydrogen molar flow rate (496 μmol H₂·min⁻¹) to

ensure high mass transfer rates between gas and liquid phase. Consequently, a volcano shape trend was observed. To explain this behaviour it is appropriate to consider the activity of the catalyst. Lower temperatures retard the H₂ consumption. This can be seen clearly when observing hydrogenation reaction. Nevertheless, the temperature and the rates of the reflect different effects: H₂ consumption rate, H₂O₂ hydrogenation, synthesis of H₂O. An optimum of the above mentioned effects can be found around 20-40°C (Figure 7).

Even if selecting the most appropriate operational conditions, the results do not show a linear tendency or a clear optimum value. Within the temperature interval analysed, three different sections can be seen. At low (5 °C and 15 °C) and high (60 °C) temperatures, hydrogen peroxide productivity reflected moderate values between 218 and 264 $\mu\text{mol H}_2\text{O}_2\cdot\text{min}^{-1}$, probably due to low reaction rates and slow kinetics as well as higher hydrogenation rates when high temperatures were applied. Highest productivity values (310 and 320 $\mu\text{mol H}_2\text{O}_2\cdot\text{min}^{-1}$) were obtained at intermediate temperatures (25 °C and 40 °C). Similar tendencies were obtained in terms of yield and turnover frequency values.

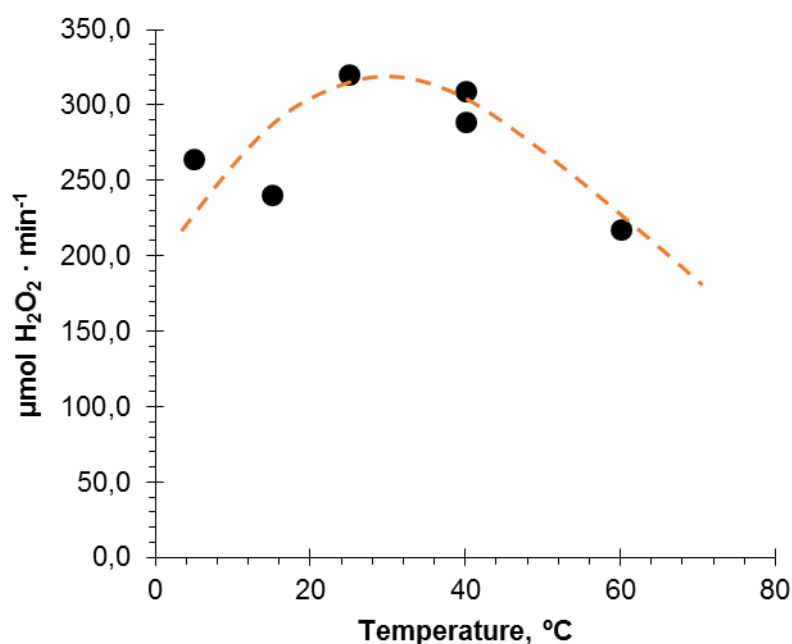


Figure 7. Reaction temperature vs. hydrogen peroxide production rate. (# 33, 38 – 42). 20 barg, 540 mg of catalyst 5% Pd/C, 6 mL·min⁻¹, 469.03 $\mu\text{mol H}_2\text{O}_2\cdot\text{min}^{-1}$, [Br] = 5·10⁻⁴

Highest catalyst activity has been found in the gap of temperature between 25 °C and 45 °C which resulted favorable for a possible application of the catalyst for industrial scale or pilot scale. Since the hydrogen peroxide synthesis is an exothermic reaction the control of the reaction temperature by cooling is need. Cooling water is typically

5.3.5. Influence of bromide concentration

Liu and Lunsford [29, 30] proposed that H^+ reacts with an active form of oxygen to produce H_2O_2 and acts over the electronic state of active metal to facilitate H_2O_2 formation. Protons could also act as boosters enhancing the adsorption of halide ions by lowering the pH below isoelectric point [17, 18]. Dissociative adsorption of O_2 and H_2O_2 as well as cleavage of the bond $O - O$ may take place over the more energetic active centers (edge, corner or defect) of the catalyst. Halide anions could block the most active sites and thus counter-effect decomposition or act as an electron scavenger and inhibit radical – type decomposition reactions.

Deguchi and Iwamoto [31, 32] proposed a reaction mechanism based on kinetic analysis. Based on this analysis it was concluded that H^+ accelerated Br^- adsorption and it was responsible for adsorption and desorption of some reaction intermediates. Irrespectively to bromide effect, Deguchi reached similar conclusions proposing that bromide is adsorbed on the most energetic active sites and thus reduces the decomposition and hydrogenation probability. It is still unclear what truly are the dynamic effects in terms of bromide on the H_2O_2 direct synthesis. Figure 8 might give some insight of this mystery.

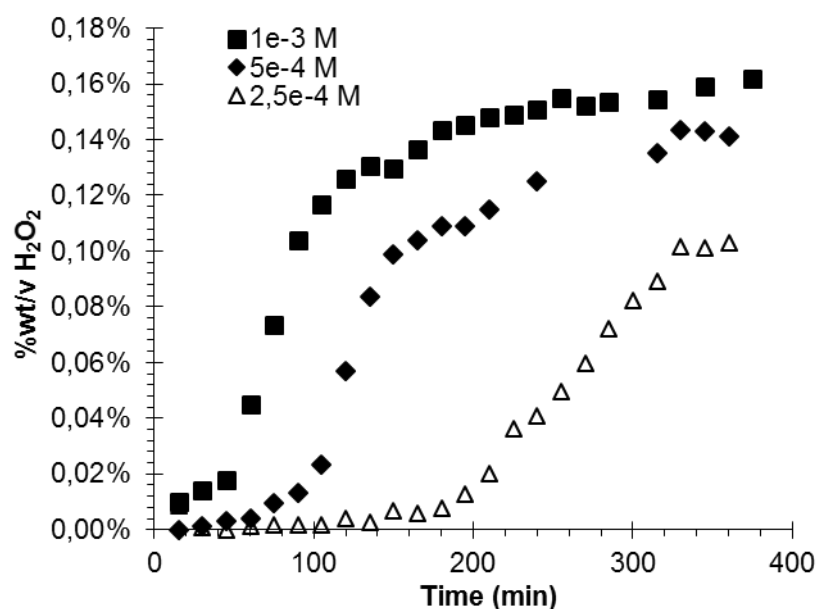


Figure 8. Evolution of hydrogen peroxide during the course of reaction and the influence of bromide concentration. (# 54 - 56). 10 barg, 15 °C, 540 mg of catalyst 5% Pd/C, 2 mL·min⁻¹, ■ [Br⁻] = 1·10⁻³ M, 214.5 μmol H₂·min⁻¹, ◆ [Br⁻] = 5·10⁻⁴ M, 147.73 μmol H₂·min⁻¹, △ [Br⁻] = 2.5·10⁻⁴ M, 74.20 μmol H₂·min⁻¹

Sodium bromide as halide and phosphoric acid were chosen as promoters. For this propose, three experiments carried out at three sodium bromide concentrations were selected ($1 \cdot 10^{-3}$ M; $5 \cdot 10^{-4}$ M; $2.5 \cdot 10^{-4}$ M). Acid concentration was kept constant (pH equal to 2). Unlike during the remaining experiments, hydrogen concentration was measured every 15 minutes from the very beginning (without waiting that the steady state condition prevails). This was the first time the H₂O₂ production was measured during the start up till the steady state with different amounts of bromide (Figure 8). The experiments performed without NaBr and H₃PO₄ resulted in assumed complete conversion of H₂ but no observed H₂O₂. It is interesting to see the non-steady state: during the first part H₂O₂ increases slowly and then (t_{st}), depending on the NaBr concentration, H₂O₂ production sharply increases to reach a steady-state (t_{ct}) (Figure 8). Previously, it was seen that as a result of NaBr addition, the shape and the dispersion of the nanoparticles of the catalyst were [9]. Most probably there is a phenomenon of adsorption/desorption of the Br⁻ to block the sites responsible for H₂O formation and activation for the reaction. Also, reconstruction of the nanocluster probably needed before active sites for H₂O₂ formation emerge [9].

These phenomena are correlated with the NaBr quantity. The more NaBr there is in the solution, the faster is the activation step of the catalyst to reach steady-state conditions (i.e. stable concentration of the H₂O₂). Moreover, more NaBr boosts higher maximum H₂O₂ concentrations reached. The liquid flow rate and the gas flow rates were fixed, and the only variable was the NaBr concentration. An analysis of the data suggests the following conclusions: Br⁻ blocks the sites for both H₂O₂ and H₂O formation, but the effect of the bromide is higher on the sites for direct formation of water. 1) The quantity of the Br⁻ not only affects the quantity of the sites but also the quality of the sites that are blocked. Indeed, doubling the concentration of Br⁻ does not mean doubled final concentration of H₂O₂. Consequently, the amount of Br⁻ influences the sites responsible for H₂O formation but also the ones for the H₂O₂ direct synthesis and for H₂O₂ hydrogenation. It seems that higher bromide concentrations influence strongly H₂O₂ hydrogenation reaction (Figure 8 and Figure 9). 2) The time to reach the steady-state for H₂O₂ production varied when different concentrations of NaBr were used. Thus, reconstruction of the metal nanoclusters and adjustments in adsorption/desorption equilibrium phenomena of the Br⁻ on the Pd surface are likely affected (Pd surface types are also related to the sites that are available for the different reactions) (Figure 8 and Figure 9).

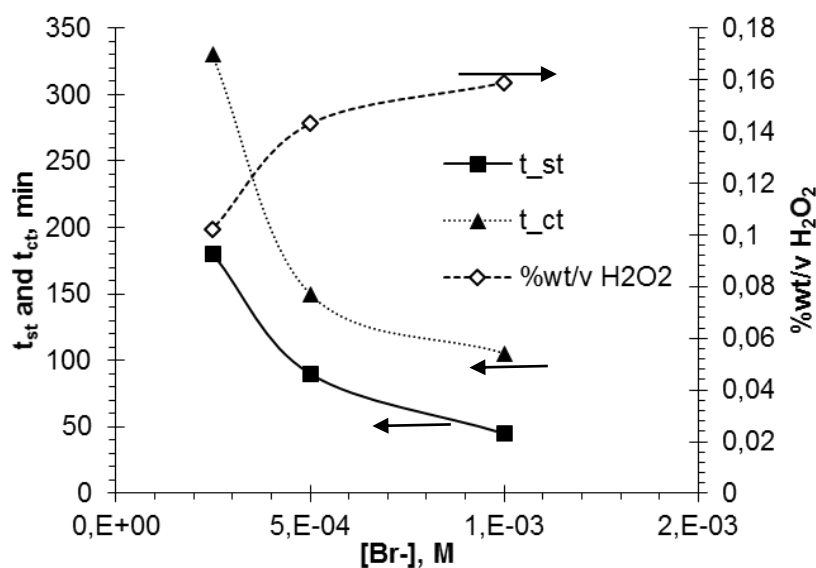


Figure 9. The bromide concentration effect. (# 54 - 56). 10 barg, 15 °C, 540 mg of catalyst 5% Pd/C, 2 mL·min⁻¹

Thus it can be stated that with a higher bromide concentration a better H₂O₂ productivity can be obtained. However, the poisoning and deactivation effects induced by bromide are well known. Samanta *et al.* [7, 33, 34] determined that 0.94 mmol·dm⁻³ (equivalent to 9.4 ·10⁻⁴ M) is the optimum bromide concentration and that higher bromide concentration can decrease the system productivity due to catalyst poisoning. For that reason, to avoid poisoning, 5·10⁻⁴ M bromide concentration was set for all remaining experiments.

5.3.6. Influence of palladium concentration in the catalyst

Three different loadings of palladium on activated carbon (i.e. 5, 10, 30 %wt.) were tried in order to see the effect of the palladium amount on the catalyst studied the influence of catalyst distribution on the reaction bed and concluded that productivity and yield are higher when catalyst's concentration is lower at the bottom of the reactor. By maintaining a low catalyst concentration at the bottom of the column, the contact between active centers and high H₂O₂ concentration could be avoided and hydrogenation is retarded. Consequently, the total amount of palladium was kept constant at 2.7 mg.

The catalyst with 30%Pd/C gave, in general, the best results. A plausible reason is the fast consumption of H₂ at the beginning of the reactor, as explained before [9]. The quantity of Pd on the support had a big influence on the reaction rate and probably the hydrogenation does not play an important role in this case because there is not enough catalyst along the bed and the

probability to hydrogenate the H₂O₂ formed was very low. Another important issue is the sintering: when the metal nanoparticles active for the direct synthesis are found in high concentration, the nanoparticles can more easily aggregated compared to lower Pd/C concentration allowing the formation of big nanoparticles that favour the H₂O₂ direct synthesis [9, 35]. The yield in this case was extremely high, around 85%. Increasing the amount of H₂ fed in the reactor increased linearly the H₂O₂ production but had an adverse effect on the yield. This can be connected to enhanced mass transfer between gas and liquid. The experiments performed over 10% Pd/C showed similar trend as 30% Pd/C albeit with lower values of productivity. On the contrary, 5% Pd/C gave rise to different trend compared to the other cases. The production of H₂O₂ increased more sharply when H₂ feed was increased. A combinatorial effect accounting for direct synthesis of H₂O₂, formation of H₂O and hydrogenation of H₂O₂ connected to the high amount of catalyst dispersed along the catalytic bed can be speculated for. The higher the catalyst amounts, the higher the probability for the reagents to react on the Pd centres. The yield observed was relatively constant for different amount of H₂ feed rates, indicating that mass transfer phenomena played a marginal role compared to the kinetics.

The maximum productivity of 250.5 $\mu\text{molH}_2\text{O}_2 \cdot \text{min}^{-1}$ (for 496.0 $\mu\text{molH}_2 \cdot \text{min}^{-1}$) and 288.6 $\mu\text{molH}_2\text{O}_2 \cdot \text{min}^{-1}$ (for 496.0 $\mu\text{molH}_2 \cdot \text{min}^{-1}$) were obtained for 10 % Pd/C and 30 % Pd/C, respectively. Yields between 84 % and 60 % for 30 % Pd/C and between 60 % and 50 % for 10 % Pd/C were measured. In general, experiments over 30%Pd/C gave the best values in terms of yield and productivity.

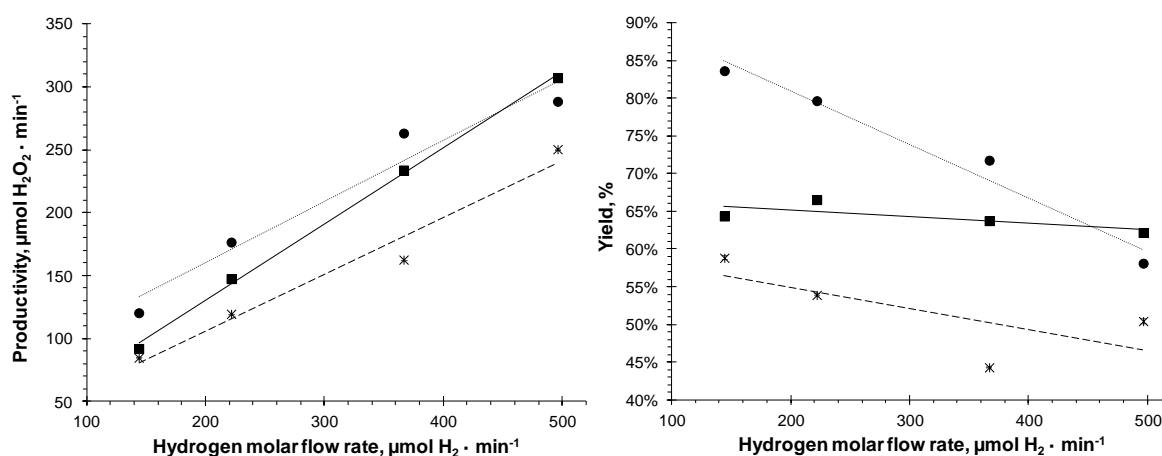


Figure 10. Influence of Pd loading on the catalyst vs. the hydrogen peroxide production rate (left) and final average yield values (right). (# 34, 43 – 53). 15 barg, 15 °C, 6 mL·min⁻¹, [Br⁻] = 5·10⁻⁴, ■ 540 mg of catalyst – 5 % Pd/C; * 270 mg of catalyst – 10 % Pd/C; ● 90 mg of catalyst – 30 % Pd/C.

5.4. Conclusions

As a summary we can conclude that H_2O_2 direct synthesis is a challenging reaction and to understand the real mechanism, different parameters have to be studied. Despite the work efforts towards tuning the reaction for maximum H_2O_2 concentration, it was more important to try to understand the mechanisms and gather important information for new catalyst design. Concerning the hydrogenation reaction, it could be concluded that a high hydrogen molar flow rate and a low liquid flow rate could increase the hydrogenation rate because of the residence time of the liquid phase is higher and the contact between hydrogen and hydrogen peroxide is enhanced. Liquid flow rate must be selected keeping in mind the objective to ensure the perfect wetting of the solid. Fast hydrogen consumption to produce the H_2O_2 was clearly seen as beneficial when high mass transfer limitations prevailed ($6 \text{ ml}\cdot\text{min}^{-1}$) or with high amount of catalyst was present (540 mg of 5 % Pd/C catalyst). On the other hand, when experimental conditions and catalyst distribution along the column did not allow for fast consumption of hydrogen, a decrease in the yield could be expected because of H_2O_2 hydrogenation. The same is true when high-loaded Pd catalyst as applied. Pressure had a promoting effect on mass transfer processes, as observed by other authors. Consequently to obtain a high productivity and yield, not only an optimum selection of the reaction conditions is needed but also high pressures. A volcano shaped temperature effect was revealed since both H_2O_2 formation and its hydrogenation rates were increased with temperature

The sintering effect due to the NaBr can help in dismissing the sites of the metal cluster that produce H_2O . The effect of the Br^- on the metal cluster is challenging to quantify but some indications can be drawn. The Br^- affects indistinctly the sites for H_2O_2 direct synthesis and water formation. Moreover, it seems that not only the phenomenon of adsorption/desorption of Br^- on the Pd surface but something more complicated occurs[9]. To summarize, the catalyst design for H_2O_2 in a continuous reactor involves: 1) low consumption of H_2 2) High concentration of H_2 at all stages 3) controlled mass transfer of the reagents through liquid-solid inter-phase 4) catalyst tailor made for the reactor.

Acknowledgements

This work is part of the activities Process Chemistry Centre (PCC) financed by the Åbo Akademi University (ÅA). Dr. Juan Garcia Serna acknowledges the Spanish Economy and Competitiveness

Ministry, Project Reference: ENE2012-33613 for funding and "Programa Salvador Madariaga 2012" for mobility scholarship. MEng. Irene Huerta is grateful to the Johan Gadolin scholarship 2012-13 (ÅA). Financial support from Academy of Finland is gratefully acknowledged. Dr. Pierdomenico Biasi gratefully acknowledges the Kempe Foundations (Kempe Stiftelserna) for financial support.

References

1. Campos-Martin, J.M., G. Blanco-Brieva, and J.L.G. Fierro, *Hydrogen Peroxide Synthesis: An Outlook beyond the Anthraquinone Process*. Angewandte Chemie International Edition, 2006. **45**(42): p. 6962-6984.
2. Edwards, J.K., et al., *The Direct Synthesis of Hydrogen Peroxide Using Platinum-Promoted Gold-Palladium Catalysts*. Angewandte Chemie International Edition, 2014. **53**(9): p. 2381-2384.
3. Edwards, J.K., et al., *The effect of heat treatment on the performance and structure of carbon-supported Au-Pd catalysts for the direct synthesis of hydrogen peroxide*. Journal of Catalysis, 2012. **292**(0): p. 227-238.
4. Edwards, J.K., et al., *Switching Off Hydrogen Peroxide Hydrogenation in the Direct Synthesis Process*. Science, 2009. **323**(5917): p. 1037-1041.
5. Ghedini, E., et al., *Mesoporous silica as supports for Pd-catalyzed H₂O₂ direct synthesis: Effect of the textural properties of the support on the activity and selectivity*. Journal of Catalysis, 2010. **273**(2): p. 266-273.
6. Melada, S., et al., *Direct synthesis of hydrogen peroxide on zirconia-supported catalysts under mild conditions*. Journal of Catalysis, 2006. **239**(2): p. 422-430.
7. Samanta, C., *Direct synthesis of hydrogen peroxide from hydrogen and oxygen: An overview of recent developments in the process*. Applied Catalysis A, 2008. **350**(2): p. 133-149.
8. Samanta, C. and V.R. Choudhary, *Direct oxidation of H₂ to H₂O₂ over Pd/Ga₂O₃ catalyst under ambient conditions: Influence of halide ions added to the catalyst or reaction medium*. Applied Catalysis A, 2007. **326**(1): p. 28-36.
9. Biasi, P., et al., *Direct synthesis of hydrogen peroxide in water in a continuous trickle bed reactor optimized to maximize productivity*. Green Chemistry, 2013. **15**(9): p. 2502-2513.

10. Biasi, P., et al., *Role of a Functionalized Polymer (K2621) and an Inorganic Material (Sulphated Zirconia) as Supports in Hydrogen Peroxide Direct Synthesis in a Continuous Reactor*. *Industrial & Engineering Chemistry Research*, 2013. **52**(44): p. 15472-15480.
11. Biasi, P., et al., *Hydrogen Peroxide Direct Synthesis: Selectivity Enhancement in a Trickle Bed Reactor*. *Industrial & Engineering Chemistry Research*, 2010. **49**(21): p. 10627-10632.
12. Biasi, P., et al., *Continuous H₂O₂ direct synthesis over PdAu catalysts*. *Chemical Engineering Journal*, 2011. **176–177**(0): p. 172-177.
13. Freakley, S.J., et al., *Effect of Reaction Conditions on the Direct Synthesis of Hydrogen Peroxide with a AuPd/TiO₂ Catalyst in a Flow Reactor*. *ACS Catalysis*, 2013. **3**(4): p. 487-501.
14. Huerta, I., et al., *Effect of the low hydrogen to palladium ratio in the direct synthesis of H₂O₂ in water in a trickle bed reactor*. *Catalysis Today* 2014. **Submitted**.
15. Huerta, I., J. García-Serna, and M.J. Cocero, *Hydrogenation and decomposition kinetic study of H₂O₂ over Pd/C catalyst in an aqueous medium at high CO₂ pressure*. *The Journal of Supercritical Fluids*, 2013. **74**(0): p. 80-88.
16. Kim, J., et al., *Palladium Nanocatalysts Immobilized on Functionalized Resin for the Direct Synthesis of Hydrogen Peroxide from Hydrogen and Oxygen*. *Acs Catalysis*, 2012. **2**(6): p. 1042-1048.
17. Moreno Rueda, T., J. García Serna, and M.J. Cocero Alonso, *Direct production of H₂O₂ from H₂ and O₂ in a biphasic H₂O/scCO₂ system over a Pd/C catalyst: Optimization of reaction conditions*. *The Journal of Supercritical Fluids*, 2012. **61**(0): p. 119-125.
18. Moreno, T., J. García-Serna, and M.J. Cocero, *Direct synthesis of hydrogen peroxide in methanol and water using scCO₂ and N₂ as diluents*. *Green Chemistry*, 2010. **12**: p. 282-289.
19. Moreno, T., et al., *Direct synthesis of H₂O₂ in methanol at low pressures over Pd/C catalyst: Semi-continuous process*. *Applied Catalysis A: General*, 2010. **386**(1-2): p. 28-33.
20. García-Serna, J., et al., *Engineering in direct synthesis of hydrogen peroxide: targets, reactors and guidelines for operational conditions*. *Green Chemistry*, 2014. **Submitted**.
21. Henkel, H. and W. Weber, *US Patent 1,108,752*, US Patent 1,752, Editor. 1914.
22. Paunovic, V., et al., *Direct synthesis of hydrogen peroxide over Au–Pd catalyst in a wall-coated microchannel*. *Journal of Catalysis*, 2014. **309**(0): p. 325-332.
23. Inoue, T., et al., *Direct synthesis of hydrogen peroxide based on microreactor technology*. *Fuel Processing Technology*, 2013. **108**(0): p. 8-11.

24. Ranade, V.V., R. Chaudhar, and P.R. Gunjal, *Trickle Bed Reactors: Reactor Engineering & Applications*. 2011, Oxford: Elsevier.
25. De Santos, J.M., T.R. Melli, and L.E. Scriven, *Mechanics of gas-liquid flow in packed-bed contactors*. Annual Review of Fluid Mechanics, 1991. **23**(1): p. 233-260.
26. Biasi, P., et al., *Kinetics and Mechanism of H₂O₂ Direct Synthesis over a Pd/C Catalyst in a Batch Reactor*. Industrial & Engineering Chemistry Research, 2012. **51**(26): p. 8903-8912.
27. Edwards, J.K., et al., *Strategies for Designing Supported Gold–Palladium Bimetallic Catalysts for the Direct Synthesis of Hydrogen Peroxide*. Accounts of Chemical Research, 2013.
28. Voloshin, Y. and A. Lawal, *Overall kinetics of hydrogen peroxide formation by direct combination of H₂ and O₂ in a microreactor*. Chemical Engineering Science, 2010. **65**(2): p. 1028-1036.
29. Liu, Q. and J.H. Lunsford, *The roles of chloride ions in the direct formation of H₂O₂ from H₂ and O₂ over a Pd/SiO₂ catalyst in a H₂SO₄/ethanol system*. Journal of Catalysis, 2006. **239**(1): p. 237-243.
30. Liu, Q. and J.H. Lunsford, *Controlling factors in the direct formation of H₂O₂ from H₂ and O₂ over a Pd/SiO₂ catalyst in ethanol*. Applied Catalysis A, 2006. **314**(1): p. 94-100.
31. Deguchi, T. and M. Iwamoto, *Reaction mechanism of direct H₂O₂ synthesis from H₂ and O₂ over Pd/C catalyst in water with H⁺ and Br⁻ ions*. Journal of Catalysis, 2011. **280**(2): p. 239-246.
32. Deguchi, T. and M. Iwamoto, *Kinetics and Simulation Including Mass-Transfer Processes of Direct H₂O₂ Synthesis from H₂ and O₂ over Pd/C Catalyst in Water Containing H⁺ and Br⁻ Ions*. Industrial & Engineering Chemistry Research, 2011. **50**(8): p. 4351-4358.
33. Samanta, C. and V.R. Choudhary, *Direct synthesis of H₂O₂ from H₂ and O₂ over Pd/H-beta catalyst in an aqueous acidic medium: Influence of halide ions present in the catalyst or reaction medium on H₂O₂ formation*. Catalysis Communications, 2007. **8**(1): p. 73-79.
34. Samanta, C. and V.R. Choudhary, *Direct formation of H₂O₂ from H₂ and O₂ and decomposition/hydrogenation of H₂O₂ in aqueous acidic reaction medium over halide-containing Pd/SiO₂ catalytic system*. Catalysis Communications, 2007. **8**(12): p. 2222-2228.
35. Menegazzo, F., et al., *When high metal dispersion has a detrimental effect: Hydrogen peroxide direct synthesis under very mild and nonexplosive conditions catalyzed by Pd supported on silica*. Journal of Catalysis, 2012. **290**: p. 143-150.

Table Captions

Table 1. Performance comparison of different reactor systems.....	169
Table 2. Experimental table for H ₂ O ₂ direct synthesis in a trickle bed reactor.....	172
Table 3. Summary of main experimental results and standard deviation values	174
Table 4. Summary of main experimental conditions and results for hydrogenation experiments	179
Table 5. The influence of the total pressure and H ₂ molar flow rate influence.....	183

Figure Captions

Figure 1. Scheme of the apparatus used in the H ₂ O ₂ experiments. (1) Trickle bed reactor. (2) Liquid solvent supply. (3, 4, 5) Gas bottles, O ₂ , N ₂ and CO ₂ /H ₂ (95/5 %). (6) Pump. (7) Mass flow controller. (8, 9) External cooling and chiller with temperature controller. (10) Liquid collection vessel. (11) Pressure controller. (12) Vent valve. (13) Micrometric valve. (14) On/off valve. (15) Check valve. (16) Three-way valve. (17) Ball valve.	171
Figure 2. Trickle bed region and operational window (adapted from Ranade <i>et al.</i> [24]).....	176
Figure 3. Influence of hydraulic residence time (left) and gas flow rate (right) on hydrogen consumption rate. (# 59 – 62 and # 57 – 59). 15 barg, 15 °C, 540 mg of catalyst 5 % Pd/C, 74.20 μmol H ₂ ·min ⁻¹ (left figure), 6 mL·min ⁻¹ (right figure), [Br ⁻] = 5·10 ⁻⁴ M.....	178
Figure 4. Influence of liquid flow rate, gas flow rate and amount of palladium on hydrogen peroxide production rate. (# 1 – 16; 21 – 32). 15 barg, 15 °C, 5% Pd/C, [Br ⁻] = 5·10 ⁻⁴ . ● 150 mg of catalyst, 4 mL·min ⁻¹ ; ◆ 380 mg of catalyst, 4 mL·min ⁻¹ ; ▲ 540 mg of catalyst, 4 mL·min ⁻¹ ; ○ 150 mg of catalyst, 6 mL·min ⁻¹ ; ◇ 380 mg of catalyst, 6 mL·min ⁻¹ ; △ 540 mg of catalyst, 6 mL·min ⁻¹ ; ● 150 mg of catalyst, 15mL·min ⁻¹	181
Figure 5. Influence of liquid flow rate, gas flow rate and amount of palladium on average final yield value. (# 1 – 16; 21 – 32). 15 barg, 15 °C, 5% Pd/C, [Br ⁻] = 5·10 ⁻⁴ . ● 150 mg of catalyst, 4 mL·min ⁻¹ ; ◆ 380 mg of catalyst, 4 mL·min ⁻¹ ; ▲ 540 mg of catalyst, 4 mL·min ⁻¹ ; ○ 150 mg of catalyst, 6 mL·min ⁻¹ ; ◇ 380 mg of catalyst, 6 mL·min ⁻¹ ; △ 540 mg of catalyst, 6 mL·min ⁻¹ ; ● 150 mg of catalyst, 15mL·min ⁻¹	181
Figure 6. Influence of reactor pressure on final average hydrogen peroxide molar flow rate. (# 33 - 37). 15 °C, 540 mg of catalyst 5% Pd/C, 6 mL·min ⁻¹ , 469.03 μmol H ₂ ·min ⁻¹ , [Br ⁻] = 5·10 ⁻⁴	183
Figure 7. Reaction temperature vs. hydrogen peroxide production rate. (# 33, 38 – 42). 20 barg, 540 mg of catalyst 5% Pd/C, 6 mL·min ⁻¹ , 469.03 μmol H ₂ O ₂ ·min ⁻¹ , [Br ⁻] = 5·10 ⁻⁴	184
Figure 8. Evolution of hydrogen peroxide during the course of reaction and the influence of bromide concentration. (# 54 - 56). 10 barg, 15 °C, 540 mg of catalyst 5% Pd/C, 2 mL·min ⁻¹ , ■ [Br ⁻] = 1·10 ⁻³ M, 214.5 μmol H ₂ ·min ⁻¹ , ◆ [Br ⁻] = 5·10 ⁻⁴ M, 147.73 μmol H ₂ ·min ⁻¹ , △ [Br ⁻] = 2.5·10 ⁻⁴ M, 74.20 μmol H ₂ ·min ⁻¹	185
Figure 9. The bromide concentration effect. (# 54 - 56). 10 barg, 15 °C, 540 mg of catalyst 5% Pd/C, 2 mL·min ⁻¹	187
Figure 10. Influence of Pd loading on the catalyst vs. the hydrogen peroxide production rate (left) and final average yield values (right). (# 34, 43 – 53). 15 barg, 15 °C, 6 mL·min ⁻¹ , [Br ⁻] = 5·10 ⁻⁴ , ■	

540 mg of catalyst – 5 % Pd/C; ✱ 270 mg of catalyst – 10 % Pd/C; ● 90 mg of catalyst – 30 % Pd/C.....188

CHAPTER VI

Determination and modeling of liquid – gas mass transfer coefficient and interfacial area in a low pressure bubble column.

The bubble column reactors are widely used in chemical and biochemical applications. Although the operation of this kind of reactors is relatively easy, the design must be complicated since the hydrodynamic and the mass transfer inside the reactor are dominated by so many parameters and phenomena. A huge amount of references and correlations for prediction of the gas hold up, bubble diameter, interfacial area and volumetric mass transfer coefficient are available in the open literature sources, although these expression not always provides good enough results. Influence of the gas flow rate (200 – 1500 ml·min⁻¹), initial liquid level on the column (40 – 75 cm) and geometry of the diffuser (1/8" O.D. tube or porous diffuser) on the hold - up (from 0.94% to 7.78%; from 0.80% to 13.13%), bubble diameter (from 0.72 cm to 1.23 cm; from 0.26 cm to 0.47 cm), interfacial area (from 0.08 cm⁻¹ to 0.43 cm⁻¹; from 0.24 cm⁻¹ to 1.89 cm⁻¹) and volumetric mass transfer coefficient (from 6.5·10⁻³ s⁻¹ to 2.8·10⁻² s⁻¹; from 1.8·10⁻² s⁻¹ to 1.1·10⁻¹ s⁻¹) have been measured and analysed in at atmospheric pressure bubble column. New expression for hold up and bubble diameter prediction are proposed. Computational fluid dynamic (CFD) analysis have been used to predict hold up, bubble diameter and mass transfer coefficient.

6.1. Introduction

There are three main kinds of multiphase reactors; the trickle bed reactor (fixed bed or packed bed), the fluidized bed reactor and the bubble column reactor. Bubble column reactors are composed by for a cylindrical vessel with a gas distributor in the bottom. The gas flow is introduced through a sparger that acts as distributor, creating a number of gas bubbles. In the case that there was a solid phase the reactor is referred as slurry bubble column reactor.

Industrial applications of the bubble column reactors and the slurry bubble column reactors are numerous, they are widely used in chemical, petrochemical, biochemical and metallurgical industries [1]. The most known application for bubble columns is the Fischer – Tropsch process, which consist in the productions of fuels, methanol synthesis, and manufacture of other synthetic fuels by the indirect coal liquefaction process. Other applications of bubble column reactors are related with chemical process such as oxidation, chlorination, alkylation, polymerization and hydrogenation, and in the biochemical industry the fermentation and the wastewater [2, 3].

The reason of the huge range of applications of the bubble column reactors is based on the number of advantages they provide in comparison to other multiphase reactors. They have an excellence heat and mass transfer coefficient, which made them a good selection for exothermic and mass transfer limited reactions. The high thermal inertia due to the big liquid volumes reduce the risk of runaway reactions. The absence of mobile parts and the simplicity of the apparatus reduce the maintenance and operational costs. Durability of the catalyst or the other packing material could be high in comparison with other reaction layouts. The addition and withdrawal of the catalyst, the operation plug – free are other of the benefits of the operation with bubble column reactors. Nevertheless, the main drawback is the need of handling the slurry and recovering the catalyst.

According to the industrial importance of bubble column reactors and its applications, the number of studies related to design and scale up and investigation of the important hydrodynamic and operational parameters have gained a great attention in the last 20 years. Researches in bubble columns are lately focused on the same topics: gas hold – up studies, bubble characteristics, flow regimen investigations, computational fluids dynamic studies and local and average mass transfer and heat transfer measurements. The influence of the column dimensions (length, diameter and gas distributor) and the operational conditions (pressure, temperature, density and viscosity of the liquid and the gas, solid concentration, superficial velocity) are commonly included into the studies of the hydrodynamics of bubble columns. In

regret of the amount of studies about bubble column and slurry bubble columns available in the literature, the phenomena on these reactors are not completely understood because the most of these studies are focus on just one of the phases.

The main interest of the study of the hydrodynamic behaviour of the bubble column reactors and the relations between its operational variables and the system behaviour it is the scale up and the design. Although the construction of bubble column reactors is simple, a successful design depends on the measurement of three aspects: heat and mass transfer phenomena, mixing characteristics and chemical kinetics of the reaction. More specifically, in order to design a bubble column reactor the next hydraulic parameters are needed, specific gas – liquid interfacial area, Sauter mean diameter of bubbles, axial dispersion coefficients of the gas and the liquid, mass transfer coefficient for all the phases involves in the system and gas hold – ups.

Although a huge amount of correlations and equations for predictions are available on the open literature sources [4-14] the range of applications of those expressions is limited by the conditions at which the expressions were obtained. CFD is routinely used today in a wide variety of disciplines and industries, including aerospace, automotive, power generation, chemical manufacturing, polymer processing, petroleum exploration, medical research, meteorology, and astrophysics. The use of CFD in the process industries has led to reductions in the cost of product and process development and optimization activities (by reducing down time), reduced the need for physical experimentation, shortened time to market, improved design reliability, increased conversions and yields, and facilitated the resolution of environmental, health, and right – to – operate issues. It follows that the economic benefit of using CFD has been substantial, although detailed economic analyses are rarely reported.

CFD has an enormous potential impact on industry because the solution of the equations of motion provides everything that is meaningful to know about the domain. For example, chemical engineers commonly make assumptions about the fluid mechanics in process units and piping that lead to great simplifications in the equations of motion. An agitated chemical reactor may be designed on the assumption that the material in the vessel is perfectly mixed, when, in reality, it is probably not perfectly mixed. Consequently, the fluid mechanics may limit the reaction rather than the reaction kinetics, and the design may be inadequate. CFD allows one to simulate the reactor without making any assumptions about the macroscopic flow pattern and thus to design the vessel properly the first time.

As a previous work before the design of a high pressure bubble column reactor a complete study of the influence of gas flow rate will be carried out. The aim of this work is to provide enough

information about the hydrodynamic of low pressure bubble column reactor (mass transfer coefficient, bubble diameter and distribution and hold – up values) that could be used to predict the behaviour of a similar reaction system at high pressures. For the prediction a review of the expressions available on literature will be carried out in order to look for one of them that could predict and adjust the experimental values with enough accuracy, if none of the models proposed would be good enough a new equation will be proposed and fitted.

6.2. Material and methods

6.2.1. *Materials*

All the experiments were carried out using deionized water as liquid phase. Premier grade oxygen (99.99 %), from Carbueros Metálicos (Valladolid, Spain) was used as gas phase. To ensure that oxygen concentration into the liquid phase is close to zero and obtained complete saturation curves anhydride sodium sulphite (Na_2SO_3) PA – ACS grade from Panreac (Barcelona, Spain) was added to the liquid phase. Sodium sulphite and solved oxygen reaction was catalysed by anhydride cobalt (II) chloride, 99 % PS grade from Panreac (Barcelona, Spain).

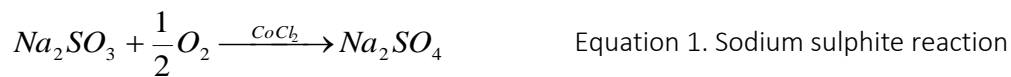
6.2.2. *Experimental setup*

Experimental setup was composed by a methacrylate column with an I.D. = 4.7 cm and 90 cm of length. Column was open at the upper side and connected to the diffuser and the volumetric flow controller in the lower side. To test the influence of the diffuser geometry, two different diffusers were used, an AISI 316 stainless steel tube with an O.D. = 1/8" and a commercial diffuser (JASCO JR – 3675 – 2) with an average porous diameter of 1 μm . Volumetric mass flow was measured and fixed by a controller BRONKHORST model EL – FLOW with an operation range from 80 $\text{mLN}\cdot\text{min}^{-1}$ to 2000 $\text{mLN}\cdot\text{min}^{-1}$. Pressure was fixed using a Bourdon type manometer and a back – pressure valve.

Saturation of liquid phase and oxygen concentration was measuring by a portable dissolved oxygen meter (WTW – OXI 330 Set) and a sensor (WTW – Cellox 325). Sensor was cleaned and the system was calibrated periodically according to the specifications to ensure measuring was correct. A video camera was used to count and measure the bubbles and their dimensions.

6.2.3. Experimental procedure

To reduce the oxygen concentration of the deionised water at the beginning of each experiment and simplified the measuring of the saturation curves sodium sulphite and cobalt (II) chloride were add to the column. Sodium sulphite and cobalt (II) chloride (as a catalyst) react with the oxygen solved in the liquid and allow us to start each curve form a value of the oxygen concentration closed to zero.



Oxygen concentration in liquid phase was measured until it reached a value closed to zero. The measurement of the dissolved oxygen meter was not reliable if it was a continuous flow of gas, as the bubbles created instability in the oxygen probe sensor. So, oxygen bubbling into the column was not constant. The experiments were divided into small time intervals with alternative periods of gas bubbling and concentration measuring. As one of the goals of this to paper it is to study the influence of the column liquid level the sensor was fixed always at 5 cm under the liquid surface.

Once the oxygen concentration in the liquid phase was closed to zero, gas valve was opened to allow the flow of the gas through the column. When oxygen concentration in liquid phase was kept constant, about two or three minutes were necessary, sensor was move away from the column and experimental set was restart.

Hold – up values were obtained directly by measuring the height of the liquid column after stabilization. Bubble diameter is calculated by two different methods according to what kind of diffusor is used. When 1/8" tube was used as diffusor, number of bubbles was low, size distribution was irregular and bubbles had a non – spherical shape. System was closed to a churn – turbulent bubbling regime [13], because of this average bubble volume was calculated from the total number of bubbles and the gas volume in the column. In order to compare experimental results, average bubbles diameter have been calculated assuming spherical shape.

On opposite case, when the porous diffuser was used, the flow regime was closed to homogeneous regime, because of this the number of bubbles was higher, the size distribution was regular and the bubbles had a more defined spherical shape. Since the amount of bubbles

was too high to count them, it is not possible to calculate bubble volume or diameter in the same way that when 1/8" O.D. tube is used. Because of this, for experiments with the porous diffuser the bubble diameter was measured directly from the photographs taken during the experiments assuming that bubbles in the picture were representative. The amount of bubbles was calculated from the gas total volume and bubble's volume calculated as spheres. Experimental interfacial area was obtained from the amount of bubbles, the average bubble volume and the gas total volume. The mass transfer coefficient was calculated from the experimental values of liquid phase saturation curves, as it was explained in section 6.3.1..

6.3. System modelling and correlations

6.3.1. Model as perfect mixed stirred tank (PMST)

From the experimental results, hold – up (ϵ) and interfacial area (a) can be calculated directly by measuring of liquid height and the size and number of bubbles. Mass transfer coefficient could be calculated from saturation liquid phase curves measured for each experiment.

Assuming that the system can be approximated to a perfect mixed stirred reactor and thus, oxygen concentration is the same at every point inside the column, mass balance equation can be written as follows (eq. 1).

$$\frac{dC_{O_2}}{dt} = k_L \cdot a \cdot (C^* - C) \quad \text{Equation 2. Mass balance equation for PMST model}$$

where C^* is the solubility of oxygen at a certain temperature, k_L is the mass transfer coefficient, a is the interfacial area and C_{O_2} is the concentration of O_2 solved in the liquid at a determinate moment.

For each experiment the value of the group $k_L \cdot a$ has been fit to minimize the objective function. The objective function (O.F.) was defined as absolute difference between experimental results, C_{O_2} , and the oxygen concentration values calculated by the model equation.

The mass balance is an ODE (Ordinary Differential Equation) that was solved using "ode45" tool from MATLAB® 7.0 R14 (Dormand – Prince algorithm from the Runge – Kutta family). The O.F. was minimized using "fminsearch" tool, varying the value of the $k_L \cdot a$ group.

6.3.2. Empirical correlations from bibliography

Hold-up and bubble diameter are key parameters in order to understand and predict the behaviour and results in bubble columns. There is a plenty of researching groups and authors that have try to obtain a mathematical expression to calculate the value of the hold – up and the bubble diameter. Most of these equations are based on results and conclusions acquired experimentally and because of this their application is only possible under the same experimental conditions.

In this section some correlations are introduce in order to compare the hold-up and bubble diameter obtained experimentally and check if some of the selected expressions could be used to predict the results. From the numerous amount of correlations for calculation of hold-up and bubble diameters available in bibliography references those that which experimental conditions are closer to the experimental conditions fixed in this work have been selected. Almost all the expressions available for hold-up predictions are based on the gas and the liquid physical proprieties although combination of these variables and the factors and coefficients on the equations varied from an author to other. Some correlations were selected from the reviews published by Kantarci *et al.* [4] and Behkish *et al.* [15] to being used as comparison in this paper, for calculation of the hold – up and the bubble diameter.

Table 1. Gas hold – up and bubble diameter correlations

Research Group	Correlation / Model equation	Gas/liquid/solid system	Exp. conditions
Kumar <i>et al.</i> (K) – [4, 6]	$\varepsilon = 0.728U - 0.485U^2 + 0.0975U^3$ $U = u_g \left(\frac{\rho_l^2}{\sigma(\rho_l - \rho_g)g} \right)^{1/4}$	Air / H ₂ O / Kerosene	P: atm, T: amb u _g : 0.0014 – 0.14 m·s ⁻¹
Hughmark (HU) – [4, 7]	$\varepsilon = \frac{1}{2 + \left(\frac{0.35}{u_g} \right) \left(\frac{\rho_l \cdot \sigma}{72} \right)^{1/3}}$	Air, H ₂ O, kerosene, oil, Na ₂ SO ₃ , and ZnCl ₂ aqueous solution, glycerol, light oil	P: atm, T: amb u _g : 0.004 – 0.45 m·s ⁻¹ D _c : 0.0245 m
Hikita <i>et al.</i> (HI) – [4, 8]	$\varepsilon = 0.672 \left(\frac{\mu_l \cdot u_g}{\sigma} \right)^{0.578} \left(\frac{\mu_l^4 \cdot g}{\rho_l \cdot \sigma^3} \right)^{-0.131} \left(\frac{\rho_g}{\rho_l} \right)^{0.062} \left(\frac{\mu_g}{\mu_l} \right)^{0.107}$	Air, H ₂ , CO ₂ , CH ₄ , C ₃ H ₈ /H ₂ O, 30 – 50 % wt sucrose, methanol, n – butanol, anilina	P: atm, T: amb u _g : 0.042 – 0.38 m·s ⁻¹ D _c : 0.1 m; H _c : 1.5 m

Hikita and Kikukawa (HK) – [4, 9]	$\varepsilon = 0.505 \cdot u_g^{0.47} \cdot \left(\frac{0.072}{\sigma} \right)^{2/3} \cdot \left(\frac{0.001}{\mu_l} \right)^{0.05}$	Air, H ₂ O, methanol aqueous sol (8–53 % wt), cane sugar aqueous sol (35–50 % wt)	u_g : 0.043–0.34 m·s ⁻¹ D_c : 0.01–0.019 m; H_c : 1.5–2.4 m
Gaddis and Vogelpohl (GV) – [10]	$V_B = c_0 + \frac{c_1}{V_B^{1/3}} + \frac{c_2}{V_B^{2/3}}$ $c_0 = \frac{\pi \cdot d_0 \cdot \sigma}{\rho_l \cdot g}; \quad c_1 = 10.9 \frac{Q_0 \cdot \nu}{g}; \quad c_2 = 1.16 \frac{Q_0^2}{g}$	N/A	$0 < We < 4$ $10^{-3} < \mu < 1 \text{ Pa} \cdot \text{s}$ $0.2 < d_0 < 6 \text{ mm}$
Moo – Young and Blanch (MYB) – [4, 11]	$d_b = 0.19 \cdot d_0^{0.48} \cdot \text{Re}_0^{2/3}; \quad \text{Re}_0 = \frac{4 \cdot Q_0 \cdot \rho_l}{\pi \cdot d_0 \cdot \mu_l}$	N/A	N/A
Leibson (L) – [4, 12]	$d_b = 0.18 \cdot d_0^{1/2} \cdot \text{Re}_0^{1/3}$	Air, water, 1.6% butanol aqueous sol.	P : 20 lb·sp ⁻¹ abs H_c : 50 in D_c : 8 in Air: 0.40–11.0 std. cu. ft. ·min ⁻¹
Bhavaraju <i>et al.</i> (B) – [4, 13, 14]	$\frac{d_b}{d_0} = 3.23 \cdot \left(\frac{4 \cdot \rho_l \cdot Q_0}{\pi \cdot \mu_l \cdot d_0} \right)^{-0.1} \cdot \left(\frac{Q_0^2}{d_0^5 \cdot g} \right)^{0.21}$	Air, water, CMC aqueous sol. (0.5–3.0%); HEC aqueous sol. (1.14 %), carbopol aqueous sol. (0.15 %)	$\text{Re}_0 < 2000$

In the case that none of the correlation summarized on Table 1 could predict with a good enough accuracy the experimental values a different expression will be proposed on base on the experimental results and the bibliography studied.

6.3.3. CFD model of the bubble column

There are two main methods to determine the interfacial area in a bubble column. The first method consists in the development of the empirical correlations as a function of experimental parameters such as the gas velocity, and some physical properties of the liquid and gas phase, as density, viscosity and surface tension. However, none of these correlations take in account the influence of the bubble size distribution in the system. It is assumed that the physical properties of the fluids and the column dimensions fix the bubble size distribution and the concentration. That assumption is only true within the dynamic equilibrium region, in which the number of bubbles for each size approximately constant. The second method uses direct phenomenological modelling and it takes into account the coalescence and break out of the bubbles inside the column. Prince and Blanch [16] were the first to propose and validate a working model, and some years after Pohorecki *et al.* [17] used it to predict the dynamic equilibrium's bubble size distribution in a specific region for various gas – liquid systems. More recently, approximations

were based on the computational fluid dynamics techniques. In this paper, it have been used the simplified model proposed by Chen *et al.* [18] complemented with the coalescence and aggregation nuclei proposed by Luo [19] to study the development of bubble size distribution in a column. In that way it is possible to predict the final size of the bubbles from the resolution of the liquid and gas phase equations and from the application of a suitable turbulence model. An extensive discussion about this and others methods to model multiphase systems can be found in Fox and Marchisio [20]. Bubble size distribution in the column was obtained by the system modelling solved using the flow analysis modelling software FLUENT developed by ANSYS.

From the size distribution is possible to calculate distribution moments (M_k), the Sauter mean bubble diameter (d_{sauter}) and the turbulent dissipation coefficient at the liquid phase (ϵ_L).

$$M_k = \int_{-\infty}^{\infty} L^k \cdot n(L) \cdot dL \quad \text{Equation 3. Moment's distribution}$$

$$d_{sauter} = d_{32} = \frac{M_3}{M_2} \quad \text{Equation 4. Sauter's mean bubble diameter}$$

Some authors have proposed different expressions to obtain the value of the mass transfer coefficient from model's results. Penetration theory developed by Higbie [21] and the model of surface renewal proposed by Danckwerts [22] are two methods widely used to calculate mass transfer coefficient when the bubble size is known. Danckwerts modified Higbie's model suggesting an improvement by assuming that k_L value is related with the average rate of renovation of the interphase surface between the bubbles and the turbulent eddies in a variable contact time, where parameter "s" is the fractional rate of surface – element replacement.

$$k_L = \sqrt{D_l \cdot s} \quad \text{Equation 5. Danckwerts' correlation}$$

Lamont and Scott assumed that turbulence movement at small scale affects the mass transfer rate, in consequence 's' can be calculated using the theory of isotropic turbulence developed by Kolmogorov. As it was suggested by Lamont and Scott [23] the mass transfer coefficient is calculated according to the next equation.

$$k_L = C_L \cdot D^{0.5} \left(\frac{\xi}{\nu_l} \right)^{0.25} \quad \text{Equation 6. Lamont and Scott equation}$$

where, ξ is the turbulence dissipation rate in the liquid phase, ν_l is the liquid kinematic viscosity, D is the molecular diffusivity of the chemical species, and C_L is the fitting constant (0.4) proposed by Lamont and Scott.

6.4. Results and discussion

Aimed at determining the influence of operational variables in the hold – up, bubble diameter and mass transfer we have studied the influence of the initial liquid column length (ILL), from 40 cm to 75 cm, the gas flow rate, from 200 mLN·min⁻¹ to 1500 mLN·min⁻¹ and the influence of the diffuser geometry has been studied. All the experiments were carried out at atmospheric pressure and ambient temperature. In order to reduce the errors of the values due to experimental deviations each experiment was repeated three times.

Table 2. Summarized experimental conditions and main results

#	ILL (h_0), cm	GFR, ml·min ⁻¹	Diffuser	Bubble diam (D_b), cm	Hold – up (ϵ), %	Interfacial área (a) cm ⁻¹	Volumetric mass transfer coefficient ($k_L \cdot a$), s ⁻¹
1	40	200.0	1/8" tube	0.72 ± 1.9·10 ⁻²	1.00 ± 0	0.08 ± 0.00	6.5·10 ⁻³ ± 9.3·10 ⁻⁴
2	40	500.0	1/8" tube	0.88 ± 8.3·10 ⁻²	2.08 ± 5.2·10 ⁻³	0.14 ± 0.02	1.0·10 ⁻² ± 1.4·10 ⁻³
3	40	823.7	1/8" tube	1.04 ± 8.1·10 ⁻²	2.75 ± 5.0·10 ⁻³	0.15 ± 0.02	1.3·10 ⁻² ± 1.7·10 ⁻³
4	40	1221.1	1/8" tube	0.90 ± 2.0·10 ⁻²	4.50 ± 2.5·10 ⁻³	0.29 ± 0.02	1.3·10 ⁻² ± 1.3·10 ⁻³
5	40	1459.4	1/8" tube	0.93 ± 3.0·10 ⁻²	7.17 ± 3.8·10 ⁻³	0.43 ± 0.01	2.4·10 ⁻² ± 9.6·10 ⁻⁴
6	50	200.0	1/8" tube	0.85 ± 1.8·10 ⁻²	1.73 ± 1.1·10 ⁻³	0.12 ± 0.00	1.1·10 ⁻² ± 1.8·10 ⁻³
7	50	500.0	1/8" tube	0.92 ± 7.3·10 ⁻²	2.87 ± 9.5·10 ⁻³	0.17 ± 0.06	1.1·10 ⁻² ± 1.1·10 ⁻³
8	50	856.3	1/8" tube	1.23 ± 7.5·10 ⁻²	4.07 ± 6.1·10 ⁻³	0.19 ± 0.02	1.2·10 ⁻² ± 1.6·10 ⁻³
9	50	1175.7	1/8" tube	0.95 ± 4.4·10 ⁻²	5.07 ± 2.3·10 ⁻³	0.30 ± 0.02	1.5·10 ⁻² ± 2.8·10 ⁻³
10	50	1485.9	1/8" tube	0.90 ± 8.7·10 ⁻²	5.20 ± 1.2·10 ⁻²	0.37 ± 0.04	1.9·10 ⁻² ± 4.2·10 ⁻⁴

Determination and modeling of liquid – gas k_L and interfacial area in a low pressure bubble column

11	60	200.0	1/8" tube	$0.71 \pm 2.9 \cdot 10^{-2}$	$0.94 \pm 9.6 \cdot 10^{-4}$	0.08 ± 0.00	$6.7 \cdot 10^{-3} \pm 1.1 \cdot 10^{-3}$
12	60	500.0	1/8" tube	$0.82 \pm 1.9 \cdot 10^{-1}$	$1.56 \pm 1.2 \cdot 10^{-2}$	0.14 ± 0.05	$1.5 \cdot 10^{-2} \pm 2.7 \cdot 10^{-3}$
13	60	848.5	1/8" tube	$0.87 \pm 2.0 \cdot 10^{-1}$	$2.61 \pm 1.5 \cdot 10^{-2}$	0.16 ± 0.07	$1.2 \cdot 10^{-2} \pm 2.3 \cdot 10^{-3}$
14	60	1228.9	1/8" tube	$1.09 \pm 9.6 \cdot 10^{-2}$	$6.56 \pm 1.3 \cdot 10^{-2}$	0.33 ± 0.04	$1.7 \cdot 10^{-2} \pm 1.3 \cdot 10^{-3}$
15	60	1502.2	1/8" tube	$1.03 \pm 6.0 \cdot 10^{-2}$	$7.78 \pm 7.9 \cdot 10^{-3}$	0.42 ± 0.02	$2.0 \cdot 10^{-2} \pm 2.4 \cdot 10^{-3}$
16	70	200.0	1/8" tube	$0.85 \pm 2.6 \cdot 10^{-2}$	$1.62 \pm 8.2 \cdot 10^{-4}$	0.11 ± 0.00	$8.3 \cdot 10^{-3} \pm 2.2 \cdot 10^{-3}$
17	70	500.0	1/8" tube	$0.96 \pm 4.1 \cdot 10^{-2}$	$2.00 \pm 1.4 \cdot 10^{-3}$	0.12 ± 0.00	$1.3 \cdot 10^{-2} \pm 2.1 \cdot 10^{-3}$
18	70	836.3	1/8" tube	$1.12 \pm 4.1 \cdot 10^{-2}$	$4.24 \pm 5.8 \cdot 10^{-3}$	0.22 ± 0.02	$1.4 \cdot 10^{-2} \pm 1.8 \cdot 10^{-3}$
19	70	1300.8	1/8" tube	$0.95 \pm 3.6 \cdot 10^{-2}$	$4.86 \pm 1.4 \cdot 10^{-3}$	0.29 ± 0.02	$1.9 \cdot 10^{-2} \pm 3.6 \cdot 10^{-3}$
20	70	1489.0	1/8" tube	$0.99 \pm 3.4 \cdot 10^{-2}$	$7.14 \pm 3.8 \cdot 10^{-3}$	0.40 ± 0.01	$2.8 \cdot 10^{-2} \pm 6.2 \cdot 10^{-3}$
21	75	200.0	1/8" tube	$0.92 \pm 3.3 \cdot 10^{-2}$	-	0.12 ± 0.01	$8.6 \cdot 10^{-3} \pm 4.3 \cdot 10^{-4}$
22	75	500.0	1/8" tube	$0.95 \pm 6.0 \cdot 10^{-2}$	$2.13 \pm 3.5 \cdot 10^{-3}$	0.13 ± 0.14	$1.1 \cdot 10^{-2} \pm 1.2 \cdot 10^{-3}$
23	75	823.3	1/8" tube	$0.95 \pm 3.6 \cdot 10^{-2}$	$3.11 \pm 3.4 \cdot 10^{-3}$	0.19 ± 0.01	$1.7 \cdot 10^{-2} \pm 7.5 \cdot 10^{-3}$
24	75	1228.1	1/8" tube	$0.86 \pm 5.3 \cdot 10^{-2}$	$3.78 \pm 2.2 \cdot 10^{-2}$	0.32 ± 0.11	$2.4 \cdot 10^{-2} \pm 9.4 \cdot 10^{-4}$
25	75	1517.7	1/8" tube	$0.93 \pm 1.6 \cdot 10^{-2}$	$6.44 \pm 5.0 \cdot 10^{-3}$	0.39 ± 0.02	$2.4 \cdot 10^{-2} \pm 3.2 \cdot 10^{-3}$
26	40	247.5	Porous	$0.27 \pm 4.4 \cdot 10^{-2}$	$1.33 \pm 1.4 \cdot 10^{-3}$	0.29 ± 0.02	$1.9 \cdot 10^{-2} \pm 1.4 \cdot 10^{-3}$
27	40	541.0	Porous	$0.35 \pm 3.9 \cdot 10^{-2}$	$3.08 \pm 9.5 \cdot 10^{-3}$	0.52 ± 0.20	$3.6 \cdot 10^{-2} \pm 5.4 \cdot 10^{-3}$
28	40	774.0	Porous	$0.37 \pm 4.2 \cdot 10^{-2}$	$5.58 \pm 1.2 \cdot 10^{-2}$	0.86 ± 0.12	$5.8 \cdot 10^{-2} \pm 1.6 \cdot 10^{-2}$
29	40	1356.4	Porous	$0.43 \pm 3.3 \cdot 10^{-2}$	$9.58 \pm 5.2 \cdot 10^{-3}$	1.23 ± 0.04	$8.3 \cdot 10^{-2} \pm 2.5 \cdot 10^{-2}$
30	40	1695.2	Porous	$0.37 \pm 2.7 \cdot 10^{-2}$	$11.8 \pm 5.2 \cdot 10^{-3}$	1.74 ± 0.14	$8.0 \cdot 10^{-2} \pm 1.7 \cdot 10^{-2}$
31	50	240.9	Porous	$0.28 \pm 2.9 \cdot 10^{-2}$	$1.13 \pm 3.1 \cdot 10^{-3}$	0.24 ± 0.07	$1.8 \cdot 10^{-2} \pm 1.1 \cdot 10^{-3}$
32	50	552.1	Porous	$0.36 \pm 4.5 \cdot 10^{-2}$	$2.87 \pm 3.1 \cdot 10^{-3}$	0.47 ± 0.11	$4.1 \cdot 10^{-2} \pm 1.4 \cdot 10^{-2}$
33	50	828.6	Porous	$0.39 \pm 5.5 \cdot 10^{-2}$	$6.60 \pm 5.3 \cdot 10^{-3}$	0.96 ± 0.10	$6.7 \cdot 10^{-2} \pm 2.0 \cdot 10^{-3}$
34	50	1313.4	Porous	$0.46 \pm 7.5 \cdot 10^{-2}$	$9.00 \pm 1.4 \cdot 10^{-2}$	1.10 ± 0.26	$8.6 \cdot 10^{-2} \pm 1.1 \cdot 10^{-2}$
35	50	1566.6	Porous	$0.38 \pm 6.8 \cdot 10^{-2}$	$13.13 \pm 4.2 \cdot 10^{-3}$	1.89 ± 0.35	$9.4 \cdot 10^{-2} \pm 7.3 \cdot 10^{-3}$
36	60	257.1	Porous	$0.26 \pm 3.6 \cdot 10^{-2}$	$1.28 \pm 1.3 \cdot 10^{-2}$	0.27 ± 0.25	$1.8 \cdot 10^{-2} \pm 3.9 \cdot 10^{-3}$
37	60	514.3	Porous	$0.30 \pm 3.5 \cdot 10^{-2}$	$3.89 \pm 9.6 \cdot 10^{-4}$	0.76 ± 0.09	$3.5 \cdot 10^{-2} \pm 9.6 \cdot 10^{-3}$
38	60	908.1	Porous	$0.40 \pm 1.2 \cdot 10^{-1}$	$6.33 \pm 1.7 \cdot 10^{-3}$	0.93 ± 0.23	$5.8 \cdot 10^{-2} \pm 6.2 \cdot 10^{-3}$
39	60	1337.6	Porous	$0.30 \pm 5.5 \cdot 10^{-2}$	$9.44 \pm 3.8 \cdot 10^{-3}$	1.79 ± 0.27	$1.1 \cdot 10^{-1} \pm 3.6 \cdot 10^{-2}$
40	60	1653.1	Porous	$0.43 \pm 7.6 \cdot 10^{-2}$	$12.56 \pm 1.9 \cdot 10^{-3}$	1.60 ± 0.34	$7.9 \cdot 10^{-2} \pm 5.1 \cdot 10^{-3}$
41	70	240.7	Porous	$0.31 \pm 1.6 \cdot 10^{-2}$	$1.81 \pm 3.6 \cdot 10^{-3}$	0.34 ± 0.07	$2.2 \cdot 10^{-2} \pm 3.4 \cdot 10^{-3}$
42	70	538.5	Porous	0.36 ± 0	3.86 ± 0	0.61 ± 0.00	$4.0 \cdot 10^{-2} \pm 7.0 \cdot 10^{-3}$
43	70	924.9	Porous	$0.34 \pm 2.9 \cdot 10^{-2}$	$5.86 \pm 2.5 \cdot 10^{-3}$	0.98 ± 0.12	$6.3 \cdot 10^{-2} \pm 5.6 \cdot 10^{-3}$
44	70	1336.4	Porous	$0.39 \pm 2.3 \cdot 10^{-2}$	$10.00 \pm 2.9 \cdot 10^{-3}$	1.40 ± 0.11	$5.6 \cdot 10^{-2} \pm 4.1 \cdot 10^{-3}$
45	70	1734.7	Porous	$0.42 \pm 6.6 \cdot 10^{-2}$	$13.14 \pm 2.9 \cdot 10^{-3}$	1.69 ± 0.25	$5.7 \cdot 10^{-2} \pm 1.7 \cdot 10^{-2}$
46	75	254.3	Porous	0.30 ± 0	$0.80 \pm 2.7 \cdot 10^{-3}$	0.16 ± 0.05	$1.9 \cdot 10^{-2} \pm 1.2 \cdot 10^{-3}$
47	75	550.5	Porous	0.41 ± 0	$4.09 \pm 4.1 \cdot 10^{-3}$	0.58 ± 0.06	$3.9 \cdot 10^{-2} \pm 9.3 \cdot 10^{-3}$
48	75	838.8	Porous	$0.38 \pm 7.1 \cdot 10^{-2}$	$8.62 \pm 2.8 \cdot 10^{-3}$	1.30 ± 0.27	$3.2 \cdot 10^{-2} \pm 2.5 \cdot 10^{-2}$
49	75	1343.2	Porous	$0.40 \pm 4.1 \cdot 10^{-2}$	$10.36 \pm 7.7 \cdot 10^{-4}$	1.42 ± 0.13	$6.0 \cdot 10^{-2} \pm 9.4 \cdot 10^{-3}$
50	75	1616.1	Porous	$0.47 \pm 5.8 \cdot 10^{-2}$	$12.58 \pm 4.7 \cdot 10^{-3}$	1.45 ± 0.20	$7.8 \cdot 10^{-2} \pm 1.5 \cdot 10^{-2}$

As at any heterogeneous system some different flow regimens could be expected. According to literature and experimental results obtained, as a function of the gas superficial velocity four typical flow regimens are commonly observed in bubble columns: homogeneous regime (bubbly flow), heterogeneous regime (churn – turbulent), slug flow regime and the “foaming – regime” which it is not as common as the previous ones [24]. Homogeneous flow is obtained in semicontinuous columns with a low gas superficial velocity and it is characterized by uniform small size distribution bubbles. At homogeneous regime there is no practically coalescence or break up thus bubble diameter depends only on the diffuser’s geometry and system properties [25]. Heterogeneous flow regime appears at high gas superficial velocities and it enhances gas turbulence and liquid recirculation. As result of these flow irregularities the size and the number of the bubbles varies along the column because coalescence and rupture phenomena. In spite of the gas turbulence and liquid recirculation enhancement, the mass transfer coefficient use to be higher when system works under homogeneous flow regime, although bubble columns operated at industrial scale are kept at heterogeneous regime [4].

6.4.1. Hold – up

Hold – up (ϵ) is an adimensional parameter key for mass transfer design of bubble columns. It is basically defined as the volume fraction occupied by gas phase, although it is possible to calculate hold – up values for liquid and solid phase too. Basic factors that influence hold – up are: gas and liquid properties, gas superficial velocity, column geometry and dimensions and operation conditions. Some authors [2, 4] have suggested that the main influence factor is the superficial gas velocity, and that hold – up increased with gas superficial velocity [24, 26, 27]. Bubble size distributions had also influence over hold – up values. For bubbly regime hold-up’s increase because of superficial gas velocity was more pronounced than the increase when flow regime was close to churn – turbulent region [28]. Hyndman *et al.* [24] studied the effect of small and large bubbles in hold – up values and concluded that in churn – turbulent regime the hold – up increased with superficial gas velocity because of large bubbles’ hold – up increased also, while small bubbles’ hold – up remained constant. In bubbly regime, there was a narrower bubble size distribution and on consequence hold – up increase was due to overall bubble’s hold-up.

In terms of absolute values, hold – up is higher when porous diffuser was used at high flow rates, even if the gas flow rate was the same (maximum $\epsilon = 13.14\%$ for diffuser experiments, maximum

$\epsilon = 7.17\%$ for 1/8" O.D. tube experiments). These results could be explained according to the rise velocity of the bubbles. Small bubbles, produced when porous diffuser was used, had a lower rise velocity, on consequence the amount of gas in the column and the values of hold – up were higher. Some authors [29, 30] also noted the effect of small orifice diameters and the diffuser type in the hold – up values and concluded that when porous diffusers were used the hold – up value obtained was greater specially for gas velocities below $6\text{ cm}\cdot\text{s}^{-1}$.

As it could be expected, hold – up values increased lineally with the gas flow rate (GFR) since the amount of gas that flowed through the liquid phase increased. At low GFR hold – up was quite similar for both experiment conditions, independently of the what type of diffuser was used (from 0.94 % to 1.82 % for 1/8" O.D. tube and from 0.80 % to 1.81 % for porous diffuser at $200\text{ mL}\cdot\text{min}^{-1}$ and different ILL values). The difference between both experimental series increased with the gas flow rate, and at high gas flow rate hold – up for experiments with porous diffuser it was almost the double at same conditions (from 5.20 % to 7.78 % for 1/8" O.D. tube and from 11.83 % to 13.14 % for porous diffuser at $1500\text{ mL}\cdot\text{min}^{-1}$ and different ILL values). There was not a clear influence of the initial liquid level for the experiments realised either with the 1/8" O.D. tube or the diffuser. From Figure 1 and Figure 2, it could be also deduced that system was too much stable when a porous diffuser was used, because of the deviations of experimental results were smaller. That effect could be explained because of the coalescence and rupture of the big bubbles produced on the column was greater when the 1/8" O.D. tube is used.

For experiments from #1 to #25, experiments with 1/8" O.D. tube, all correlations gave results closed to experimental values (*average* standard deviation values: 18.7 % for Kumar *et al.* correlation, 39.3 % for Hughmark correlation, 62.6 % for Hikita and Kikukawa correlation and 25.6 % for Hikita *et al.* correlation) and predicted correctly the experimental tendency. However, because of the great experimental deviations it was difficult to find or develop an expression that could be adjusted to the hold – up values in all the experimental interval, although Kumar *et al.* expression could be used to obtain a relative good approximation. When a porous diffuser was used (experiments from #26 to #50) the hold – up values obtained with bibliography correlations were too much lower than experimental ones specially at medium and high gas flow rate (*average* standard deviation values: 39.2 % for Kumar *et al.* correlation, 59.8 % for Hughmark correlation, 53.2 % for Hikita and Kikukawa correlation and 44.3 % for Hikita *et al.* correlation). As none of the correlations from bibliography could predicted the experimental values with enough accuracy, a new correlation was proposed.

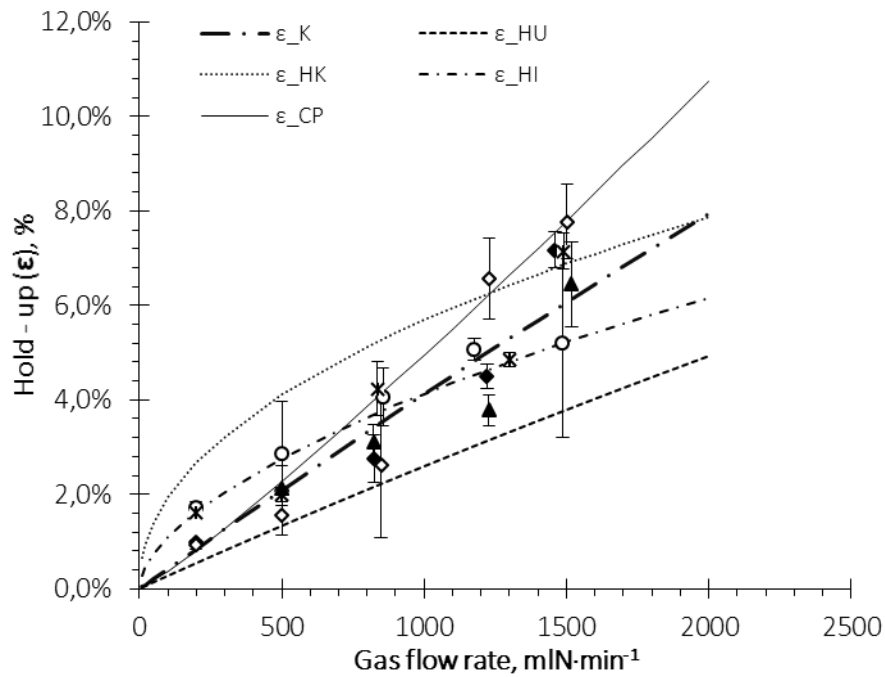


Figure 1. Influence of gas flow rate and initial liquid level on hold-up. 1/8" O.D. tube, \blacklozenge $h_0 = 40$ cm; \circ $h_0 = 50$ cm; \diamond $h_0 = 60$ cm; $*$ $h_0 = 70$ cm; \blacktriangle $h_0 = 75$ cm.

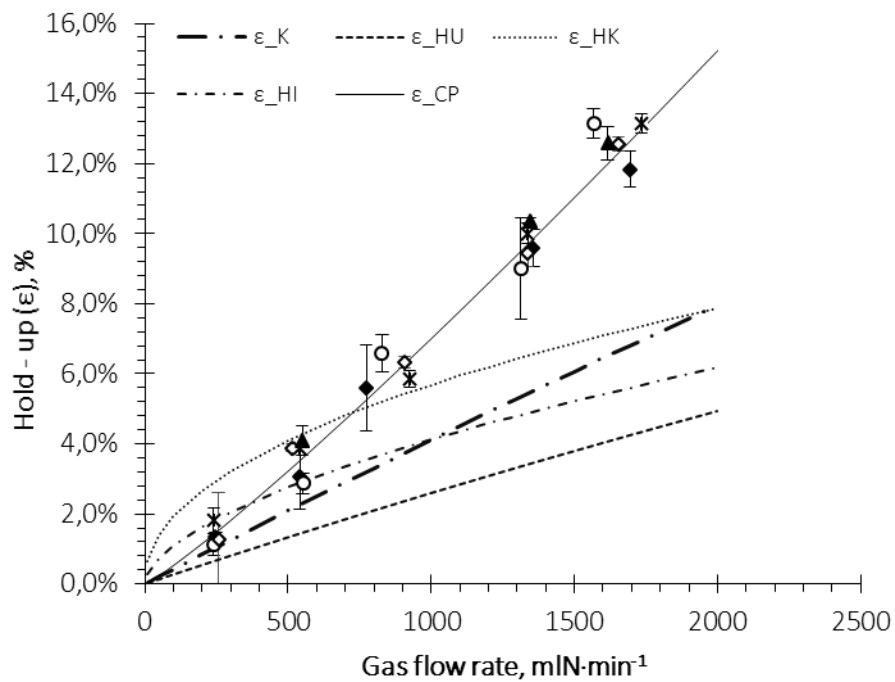


Figure 2. Influence of gas flow rate and initial liquid level on hold-up. Porous diffuser, \blacklozenge $h_0 = 40$ cm; \circ $h_0 = 50$ cm; \diamond $h_0 = 60$ cm; $*$ $h_0 = 70$ cm; \blacktriangle $h_0 = 75$ cm.

From the observation of the experimental results and the review of some authors' models, the main parameters which hold – up depends on could be estimated. Reynolds number (Re), which groups the gas properties, column dimensions and operation conditions, and bubble diameter which depends on the diffusor geometry and the orifice diameter were selected as correlation variables. However, bubble diameter is not a value that could be obtained directly on system design step or predict easily, and its participation in hold-up's calculation could complicate the application of the correlation. Replacing the bubble diameter by an expression for bubble diameter calculation (section 6.4.2) a new equation for hold – up prediction based exclusively on fluids physical properties, column dimensions and operation conditions was obtained.

$$\varepsilon = f_{\varepsilon} \cdot d_0 \cdot \text{Re}^{0.7} \cdot \left(\frac{u_g}{d_0^5 \cdot g} \right)^{0.21} \quad \text{Equation 7. Proposed correlation for hold – up calculation } (\varepsilon_{\text{PC}})$$

The independent factor (f_{ε}) was calculated by minimization of difference between experimental values and model prediction's values. It was not possible to find a value of f_{ε} capable to adjust both experiments' group with a small deviation values. Although the values of f_{ε} that minimize experimental values (Table 3) are quite similar, the difference suggests that there was some other effect that it had not been taking account in the correlation, probably system's hydrodynamic or bubbles distribution along the column (when 1/8" O.D. tube was used as diffusor bubbles did not take up totally the column section). Average standard deviation was smaller for experiments #26 to #50 than for experiments #1 to #25, because equations used for bubble diameter calculation predicts those values with a better accuracy. Correlation proposed on this paper can predict hold – up values for all gas flow rate range with a relatively low standard deviation at the specific experimental conditions summarized in Table 2, however some additional information and more experiments at different flow regimens would be need to determinate the optimum value of f_{ε} .

Table 3. Summarized results for hold – up adjustment with Equation 7

#	f_{ε}	Average standard deviation
1 - 50	$4.03 \cdot 10^{-2}$	25.6 % and 16.0 %
1 – 25	$3.41 \cdot 10^{-2}$	21.20%
26 – 50	$4.82 \cdot 10^{-2}$	9.9%

6.4.2. Bubble diameter

Bubble diameter is a basic parameter on bubble columns because mass transfer mechanism and system hydrodynamics depend on the bubble size. As bubble rise velocity and its contribution to hold – up are related to bubble diameter, a good prediction of bubble diameters is mandatory for bubble column design. Average bubble size in a bubble column is influenced by the superficial gas velocity, liquid properties, gas properties, gas distribution, column dimensions and operating pressure. Because the objective of this work, only the influence of superficial gas velocity and gas distribution were studied.

In relation to the superficial gas velocity influence over bubble diameter several authors had obtained different and opposite conclusions and statements. Akita and Yoshida [31] decreed that bubble size diameter decreased with increasing gas flow rate, while in opposite Fukuma *et al.* [32] and Saxena *et al.* [33] concluded that bubble size increased with gas flow rate until it reached a constant maximum value at a certain gas superficial velocity. Prakash *et al.* [3] studied not only the influence of operation conditions but also the distribution of the bubble size along the column section. It was concluded that larger bubbles were dominant in the centre of the column and smaller bubbles could be found densely closed to the wall. Some differences between small and big bubbles were related; small bubbles contribution to general hold – up values is higher than big bubbles, the rise velocity of small bubbles decreased with increasing gas flow rate whereas rise velocity of big bubbles increased. Schumpe and Grund [34] studied also the variations of the rise velocity of small and big bubbles with the gas flow rate. According to the paper of Schumpe and Grund rise velocity of small bubbles decreased gradually while the superficial velocity increased and it attained almost constant value afterwards, but large bubbles' rise velocity increased continuously with gas superficial velocity.

As it could be expected bubble average diameter obtained for experiments #1 to #50 (using 1/8" O.D. tube as diffuser) were greater (0.71 cm to 1.23 cm) than values obtained for experiments with the porous diffuser (0.27 cm to 0.46 cm). Difference between average bubble diameter on both experiments groups could be explained not only on base on the orifice diameter but also because the hydrodynamic regimen. When a 1/8" O.D. tube was used as diffuser, the system flow regimen was closed to turbulent region which imply that coalescence and rupture phenomena could affected to the initial bubble size and it would increase while the bubble rose up through the column. This phenomenon can be confirmed by the experimental results for the first group of experiments (#1 to #25) as it could be seen in Figure 3. Bubble size variation with liquid initial column level did not follow a clear tendency that could be justified with any of the

experimental parameters, that chaotic behavior could be related whit coalescence or breaking phenomena that acted in a random way. The same behavior could be found in bubble size values on Figure 4 when gas flow rate is upper to $1300 \text{ mLN}\cdot\text{min}^{-1}$, which suggest that at high gas flow rate the system had a heterogeneous flow regimen even when a porous diffuser was used.

Regarding to the influence of the gas flow rate on bubble average diameter it could be statement, in general terms, that our system behaved as Fukuma *et al.* and Saxena *et al.* reported and that bubble size increased with gas superficial velocity until it reached at maximum value (0.98 cm for experiments #1 to #25 and 0.40 cm for experiments #26 to #50) at approximately $1300 \text{ mLN}\cdot\text{min}^{-1}$.

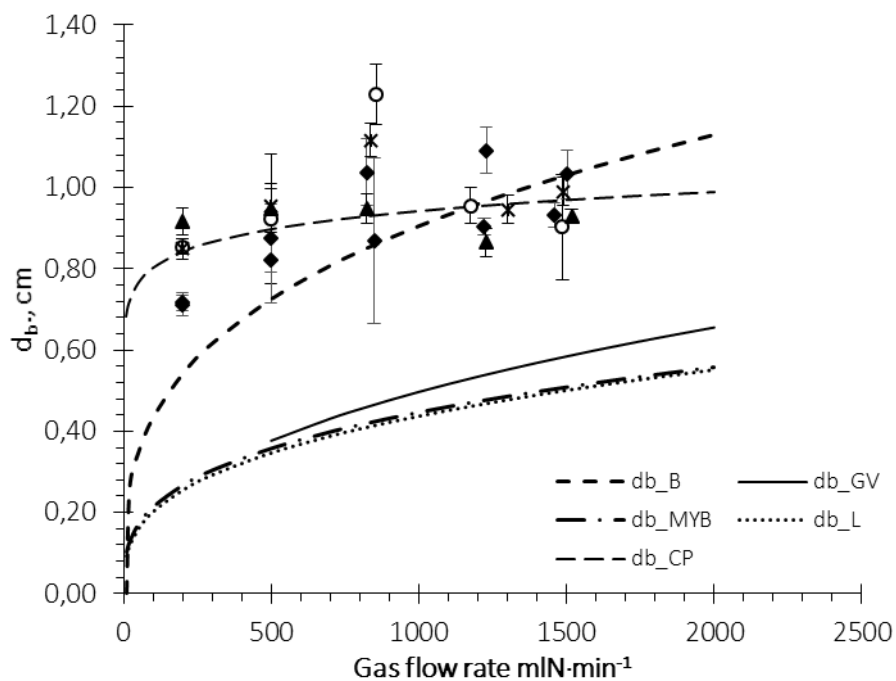


Figure 3. Influence of gas flow rate and initial liquid level on bubble diameter. 1/8" O.D. tube, ◆ $h_0 = 40 \text{ cm}$; ○ $h_0 = 50 \text{ cm}$; ◇ $h_0 = 60 \text{ cm}$; * $h_0 = 70 \text{ cm}$; ▲ $h_0 = 75 \text{ cm}$.

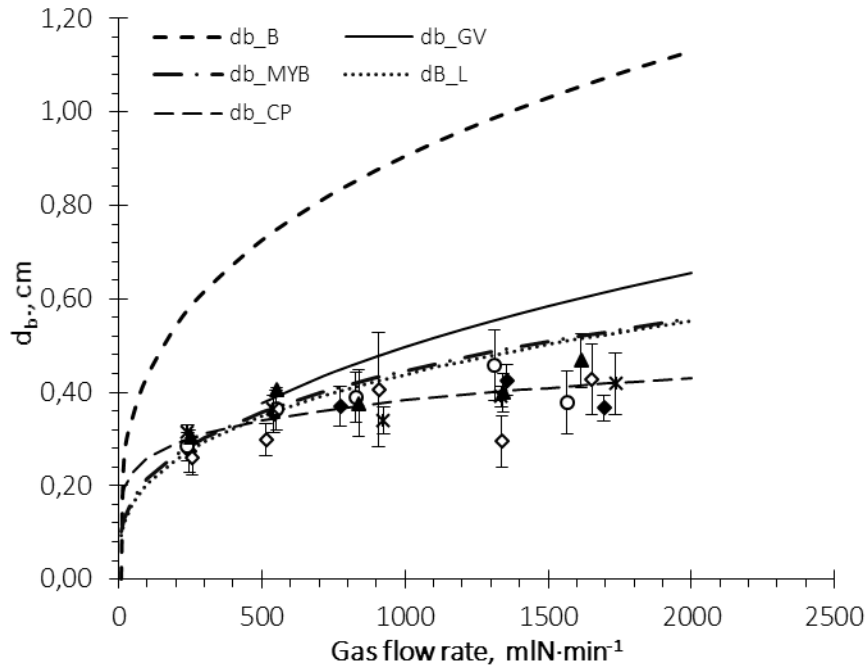


Figure 4. Influence of gas flow rate and initial liquid level on bubble diameter. Porous diffuser, \blacklozenge $h_0 = 40$ cm; \circ $h_0 = 50$ cm; \diamond $h_0 = 60$ cm; $*$ $h_0 = 70$ cm; \blacktriangle $h_0 = 75$ cm.

A bibliographic review have been carried out in order to found one expression that allows to calculated bubble diameters only using design parameters and operation conditions. The equations and models compared are summarized on Table 1, Figure 3 and Figure 4. They have been selected according to the conditions they have been obtained and the variables and parameters needed for their application. None of the correlations selected could predict the flattening of the results at high gas flow rate even for the first group of experiments (#1 to #25) or the second one (#26 to #50,) although predictions at high gas flow rate were better when the porous diffuser was used because the change of tendency is softer. Even if none of the proposed correlations predicted the rupture of the experiments' tendency, in absolute terms, they could give a relatively good approximation for the value of the bubble's diameter. For experiments with 1/8" O.D. tube, correlation of Bhavaraju *et al.* was the only one that provided values of the bubble diameter closed to the experimental results (standard deviation from 0 % to 37 %) meanwhile the others models proposed on Table 1 gave lower values of the bubble's diameters (average standard deviation values: 52 % for Gaddis and Vogelpohl correlation, 56 % for Moo – Young and Blanch correlation and 57 % for Leibson correlation). Opposite results were obtained for the experiments from #26 to #50 (using porous diffuser). As the average bubble diameter is smaller, Gaddis and Vogelpohl correlation, Moo – Young and Blanch correlation and Leibson correlation predicted the bubble diameter with relatively low standard deviation values (28 %,

17% and 15% respectively) while Bhavaraju correlation predict bubble diameter with an average standard deviation of 132%.

Due to that results of the adjustments using papers and references from bibliography were not good enough, a new correlation was proposed. The correlation proposed (CP) in this work had the same mathematical structure that the equations looked up on bibliography review. The bubbles diameter were calculated as a function of the orifice Reynolds number (that groups fluids properties, column dimensions and operation conditions) and some independent factors that take different values depending on the system that had been studied, and that only could be calculated by iteration and adjustment of the experimental values. The values of the average standard deviations obtained were small, as it could be expected since independent factors were calculated in order to ensure a good fitting between the proposed correlation and the experimental values.

$$d_b = f_{db_1} \cdot \text{Re}_0^{f_{db_2}}$$

Equation 8. Proposed correlation for the bubbles' diameter calculation (d_{b_CP})

Table 4. Summarized results for bubble's diameter adjustment with Equation 8

#	f_{db_1}	f_{db_2}	Average standard deviation
1 – 25	0.482	0.0704	8%
26 – 50	0.076	0.1683	7%

6.4.3. Mass transfer coefficient and interfacial area

The mass transfer rate per unit of volume is governed by the liquid phase, its properties and the phenomena that took place in that phase if it is assumed that gas phase resistance is negligible. A good calculation of the mass transfer coefficient and an extensive knowledge about how experimental conditions could influence it are need for an optimum design of a bubble column reactor. Although the most of researching are focus on the calculation of the volumetric mass transfer coefficient, this is a global parameter that does not provide all the information about the mass transfer phenomenon needed to obtain a complete understanding of the process.

Calculation of interfacial area (a) and mass transfer coefficient (k_L) individually could give extra information about the mass transfer mechanism and also allow to identify which parameter controls the mass transfer. Volumetric mass transfer coefficient has been calculated from the experimental curves of liquid saturation as it has been explained on section 6.3.1. The interfacial area (a) could be calculated from the fraction of the volume of the column occupied by the gas and the bubble diameter (Equation 9).

$$a = \frac{6 \cdot V_g}{d_b} \quad \text{Equation 9. Interfacial area}$$

As it could be expected, mass transfer coefficient depends on the superficial gas velocity, fluids properties and column dimensions and geometry. So many authors [35-38] have studied the influence of the gas superficial velocity on the volumetric mass transfer coefficient by different methods (CFD modelling, dynamic pressure step method, electrochemical technique) and for all the cases it was concluded that $k_L \cdot a$ increased with increasing gas velocity. Influence of the liquid properties on mass transfer coefficient is mainly related to the liquid viscosity, higher viscosities led to increase the volume fraction of bigger bubbles which supposed a decreased in the interfacial area and on consequence a reduction on the value of the mass transfer coefficient [32, 36]. Muller and Davidson studied the addition of surfactants and the concluded that they could increase volumetric mass transfer coefficient because of the amount of small bubbles was enhanced and the coalescence of bubbles was reduced [39]. Vandu and Krishna [40] reported that $k_L \cdot a$ values followed the same tendency of the values of hold – up and that the ratio $k_L \cdot a - \epsilon_g$ depended on the liquid – phase Schmidt number ($Sc = \nu/D$). In relation to the effect of the properties of the bubbles on the mass transfer coefficient, a proportionality relation between the mass transfer coefficient and the volume – surface mean bubble diameter was suggested by Fukuma *et al.* [32]. Some authors studied the influence of the flow regime [36, 38] and they reported that although the mass transfer was enhanced by the coalescence and break up phenomena that occurred typically in the heterogeneous regime, for industrial bubble column's applications the presence of small bubbles (produced typically in homogeneous flow regimen) should be preferred. Respect to the effect of the experimental conditions and column dimensions, Verma and Rai [37] suggested that initial bed height has not influence over the mass transfer coefficient and that the reason because the higher values were obtained when spargers and porous diffusers were used is due to the gas hold – up values were also higher.

Experimental results obtained in this work are consistent with some of the conclusions and the statements found on the bibliography review. Volumetric mass transfer coefficient increased with gas flow rate, an overview of interfacial area and mass transfer coefficient values showed up that increment on $k_L \cdot a$ values was due to the increased of the interfacial area (interfacial area increased because the amount of gas inside the column is higher) and that gas flow rate had a small influence on mass transfer coefficient.

A strong influence of the geometry of the diffusor on the interfacial area and the volumetric mass transfer coefficient had been reported, according the results showed in Figure 5 and Figure 6. When porous diffusor was used interfacial area values varied between 0.16 cm^{-1} and 1.89 cm^{-1} while an interfacial area with values between 0.08 cm^{-1} and 0.43 cm^{-1} were obtained when a 1/8" O.D. tube was used as diffusor. This huge difference between interfacial area values was not due only to the fact that hold – up values were higher for the experiments with the porous diffusor, but also because of the porous diffusor produced smaller bubbles. Diffuser geometry's influence could be appreciate in the values of the volumetric mass transfer coefficient (from $6.48 \cdot 10^{-3} \text{ s}^{-1}$ to $2.81 \cdot 10^{-2} \text{ s}^{-1}$ for experiments # 1 to #25 and from $1.81 \cdot 10^{-2} \text{ s}^{-1}$ to $1.06 \cdot 10^{-1} \text{ s}^{-1}$ for experiments # 26 to #50) but not in the values of mass transfer coefficient (from $4.63 \cdot 10^{-2}$ to $1.22 \cdot 10^{-1} \text{ cm} \cdot \text{s}^{-1}$ for experiments # 1 to #25 and from $2.52 \cdot 10^{-2}$ to $1.34 \cdot 10^{-1} \text{ cm} \cdot \text{s}^{-1}$ for experiments # 26 to #50) what suggested that this parameter does not depend on the geometry and the dimensions of the diffusor. Variations of the mass transfer coefficient with the initial height column were not related with any experimental variables and disagree with the results and conclusions of some papers consulted during the bibliographical review, because of that, it could be assumed that variations of the mass transfer coefficient were due to experimental irregularities.

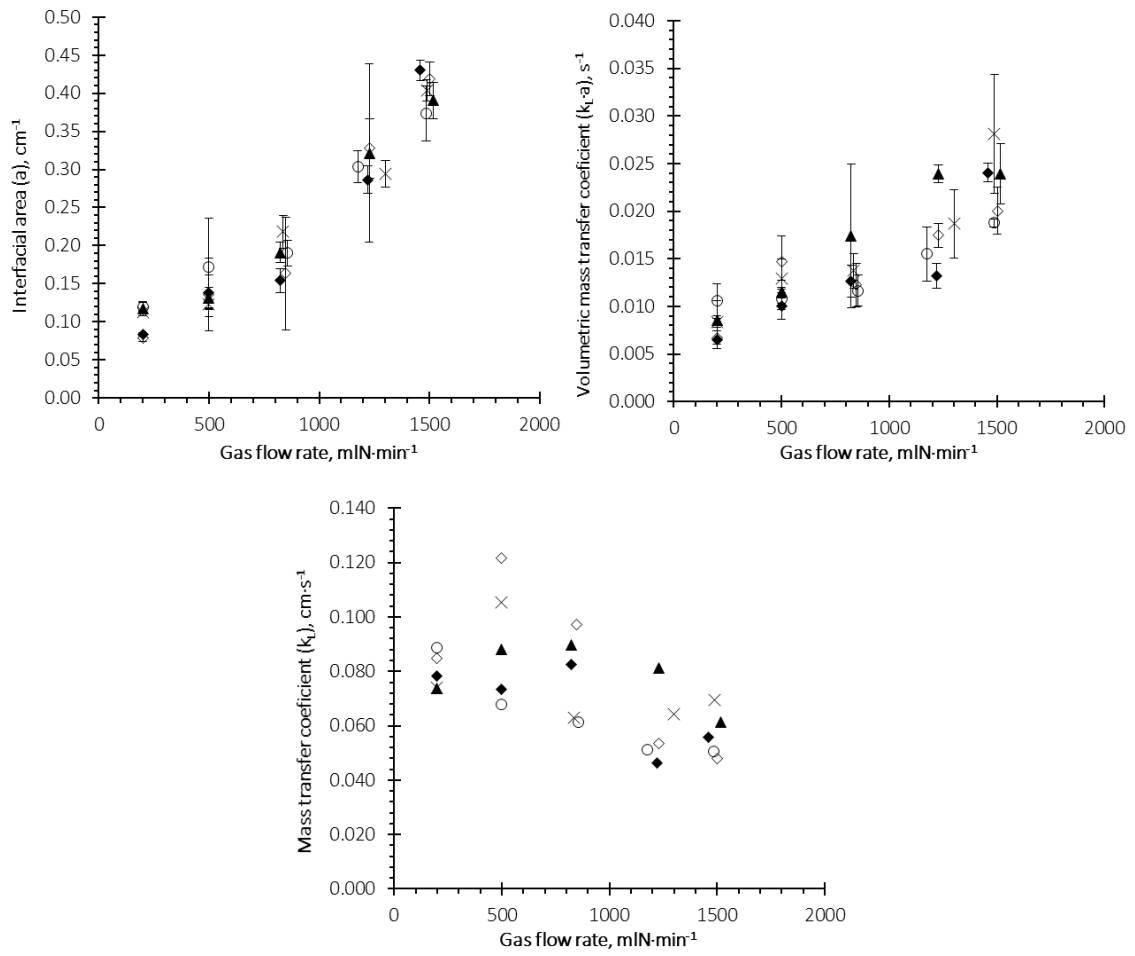


Figure 5. Influence of gas flow rate and initial liquid level on interfacial area (left), volumetric mass transfer coefficient (right) and mass transfer coefficient (center). 1/8" O.D. tube. ◆ $h_0 = 40$ cm; ○ $h_0 = 50$ cm; ◇ $h_0 = 60$ cm; * $h_0 = 70$ cm; ▲ $h_0 = 75$ cm.

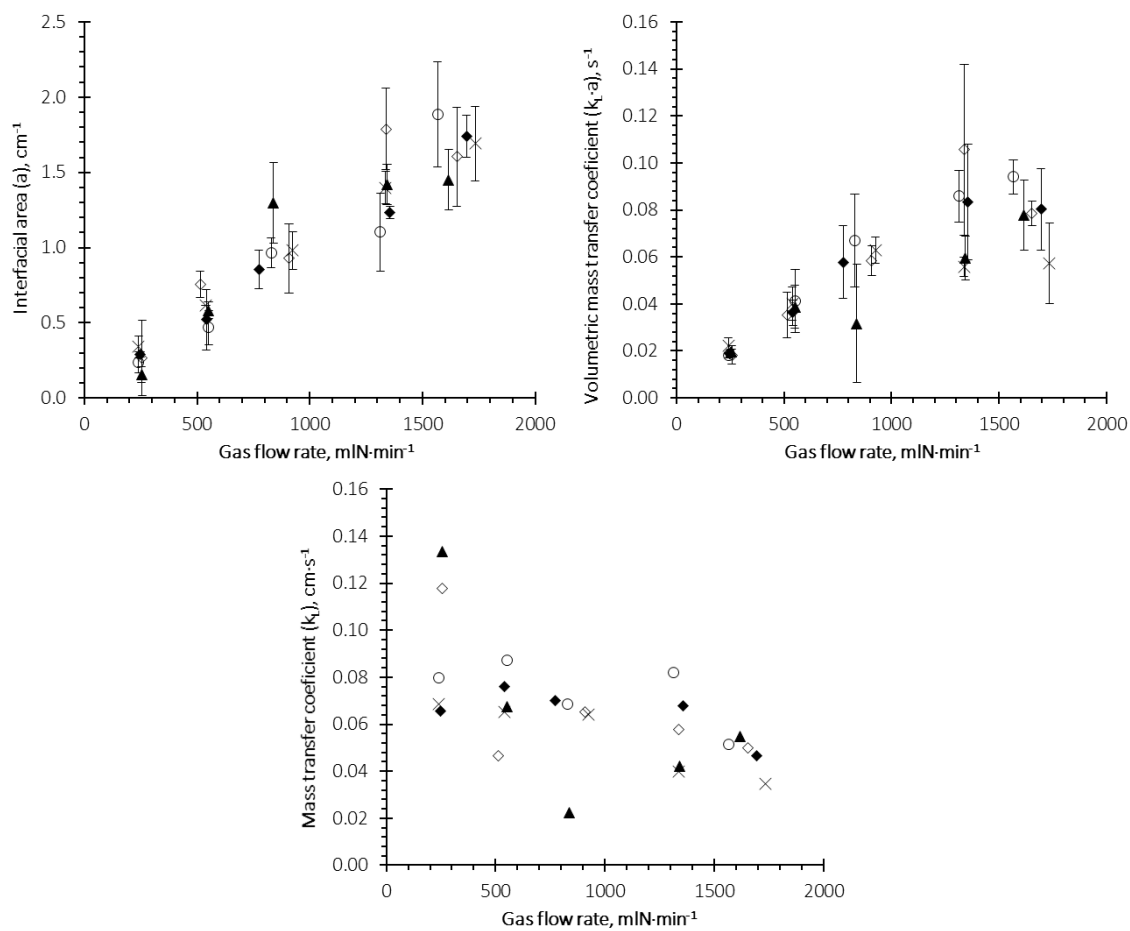


Figure 6. Influence of gas flow rate and initial liquid level on interfacial area (left), volumetric mass transfer coefficient (right) and mass transfer coefficient (center). Porous diffuser. ◆ $h_0 = 40$ cm; ○ $h_0 = 50$ cm; ◇ $h_0 = 60$ cm; * $h_0 = 70$ cm; ▲ $h_0 = 75$ cm.

6.4.4. CFD modelling; results and conclusions

As it could be seen according to the discussion on the previous section, the correlations obtained from bibliography reviews could not always predict the values of hold – up and the diameter of bubbles with the enough accuracy. A detailed knowledge of these parameters is need if a good design of a bubble column reactor is desired. One of the main issues for the prediction of hold – up and bubble diameter is the optimum selection of the suitable equation from all the correlations available on bibliography; each correlation have been obtained for a very specific conditions and it can be used exclusively in a similar experimental context.

The use of computational fluid dynamic's model to predict a system behavior remove this drawback because CFD's solving methods are based on general models applicable to all the

systems without almost any limitations. CFD modelling requires a huge amount of resources to solve each calculation step and because of this only three case studies will be calculated.

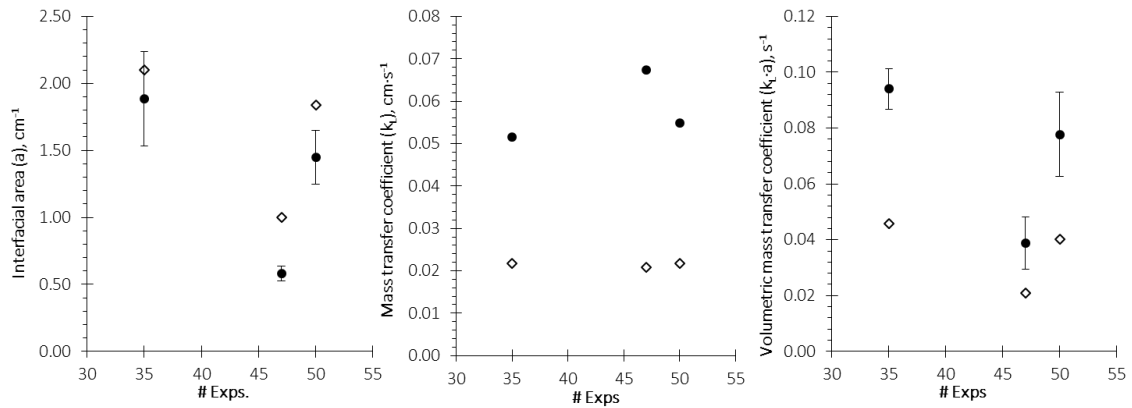


Figure 7. Comparison of experimental results and values obtained by CFD modeling. (# Exp. 35, 47 and 50).

● Experimental values; ◇ CFD model.

Table 5. Summarize results of CFD modeling for hold – up and volumetric and mass transfer coefficient prediction

	47	35	50
h_0 (cm)	75	50	75
GFR ($ml \cdot min^{-1}$)	550.5	1566.6	1616.1
Diffuser	Porous	Porous	Porous
ξ ($m^2 \cdot s^{-3}$)	$1.81 \cdot 10^{-4}$	$2.16 \cdot 10^{-4}$	$2.16 \cdot 10^{-4}$
k_L ($cm \cdot s^{-1}$)	$2.09 \cdot 10^{-2}$	$2.18 \cdot 10^{-2}$	$2.18 \cdot 10^{-2}$
h_f (cm)	76.5	52.3	78
ε_g (%)	2.0	4.4	3.8
D_b (cm)	0.12	0.12	0.12
a (cm^{-1})	1.00	2.10	1.84
$k_L \cdot a$ (s^{-1})	$2.08 \cdot 10^{-2}$	$4.58 \cdot 10^{-2}$	$4.01 \cdot 10^{-2}$

CFD modeling generated results exclusively based on the theoretical hypothesis and statements, and because of that not influence of the initial column level could be seen in the results of the Figure 7 and Table 5. For experiments number 35 and 50, although the initial level of liquid is different (50 and 75 cm respectively) the values of turbulence dissipation rate in the liquid phase, diameter of the bubble, and the mass transfer coefficient are the same due to the gas flow rate is $1500 \text{ ml} \cdot \text{min}^{-1}$ for both experiments. Also not influence of the experimental conditions over the bubble diameter have been found even if the gas flow rate or the initial liquid level changed, that

suggested that, in opposition of the results of the section 6.4.2, for the CFD model only the orifice diameter had influence over the final bubble size.

Bubble diameter value obtained by CFD is much lower than the experimental ones measured directly on the column, since the real coalescence phenomena and the growing of the bubbles along the column were not perfectly predicted. On consequence the interfacial area for the CFD results was slightly higher. By the modelling of the system by CFD it also possible to generate the size distribution of the bubbles. As it can be seen on Figure 8, the distribution of the size of the bubbles is relatively narrow since almost the 65% of the bubbles in the column have a diameter of 0.1 cm approximately.

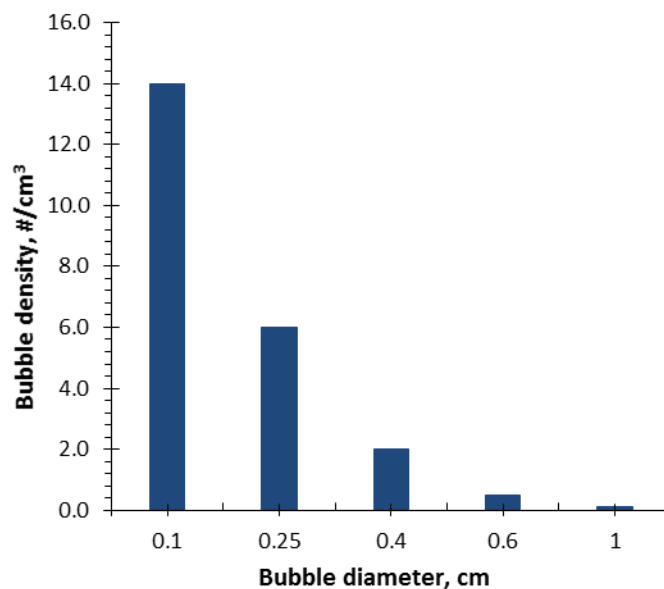


Figure 8. Bubble size distribution obtained by CFD (results for experiment # 35)

Also the mass transfer coefficient (k_L) was lower than the values obtained experimentally. The equation developed by Lamont and Scott [23, 41] proposed a different value of the parameter C_L in function of which kind of system it has been study. For instance, $C_L = 1.13$ resulted in good prediction of the mass transfer in stirred tanks, meanwhile, due to the low turbulence levels a $C_L = 0.4$ was recommended for bubble columns. Extremely low values of k_L were obtained when a $C_L = 0.4$ was used, which suggested that the turbulence of the fluids phases inside the column is too much higher than the value of turbulence of the regular bubble columns, maybe due to the geometry or the experimental conditions of the system. If a value of $C_L = 2.5$ was used (Lamont and Scott sentenced that the order of magnitude of C_L must be the unit, but did not limit the value) values of k_L closed to the experimental ones were obtained.

6.5. Conclusions

Complexity of the bubble columns and of the hydrodynamic process that take place inside are one of the main drawbacks on the design and scale up of bubble column reactors or slurry bubble column reactors. By the analysis of the main operation parameters and its influence over system hydrodynamic and the mass transfer mechanisms it could be concluded that:

- The initial liquid level of the column had not influence over the hold – up, the diameter of the bubbles or the mass transfer coefficient in the operational interval analysed.
- The gas hold – up increases with the gas flow rate, since higher the GFR higher the amount of gas in the column and on consequence higher the fraction of the volume filled by the gas. By the same reason the interfacial area increased also with the gas flow rate.
- The bubble size increased with gas flow rate until it reached a constant maximum value at a certain gas superficial velocity.
- Increasing of the volumetric mass transfer coefficient ($k_L \cdot a$) is mainly due to increasing of the interfacial area; the mass transfer coefficient (k_L) has not a clear dependence of any operational conditions.
- Also influence of the diffuser geometry have been found, and in general terms it could be said that when a porous diffuser was used the mass transfer inside the column was enhanced.

A review of expression for hold – up and bubble diameter prediction has been done, although none of the correlations selected have provide a good approximation to the experimental results. Because of that, new expressions, based on easy measuring parameters (column geometry, superficial gas velocity and fluids properties), have been proposed and fitted to our experimental values. Also utility of the computational fluid dynamic analysis for the prediction of hold – up, bubble diameter and volumetric mass transfer coefficient have been studied. Results obtained by CFD are quite better than the values obtained using the references from the open literature, and they could be used for first approximation.

Acknowledgements

The authors thank the Spanish Economy and Competitiveness Ministry (former Science and Innovation Ministry) Project Reference: CTQ2011-23293 and Junta de Castilla y León Project

Reference: VA254B11-2 for funding. The authors also wish to thank Centro de Tecnología de REPSOL (Móstoles, Spain) for scientific advice and project funding.

Symbols and nomenclature

a	interfacial area, cm^{-1}
C	dissolved oxygen concentration, $\text{mg}\cdot\text{dm}^{-3}$
C*	saturation dissolved oxygen concentration, $\text{mg}\cdot\text{dm}^{-3}$
D	Mass diffusivity
d_0	orifice diameter
d_b	bubble diameter
Fr	Froude number
f_s	Independent coefficient for Equation 7
g	gravitational acceleration
h_0	initial column liquid level (ILL), cm
$k_L\cdot a$	gas – liquid volumetric mass transfer coefficient, s^{-1}
$k_L\cdot a$	gas – liquid mass transfer coefficient, $\text{cm}\cdot\text{s}^{-1}$
Q_0	gas flow rate
Re	Reynolds number
t	time, min
u_g	mean superficial velocity
V_B	volume of bubble
V_g	fraction of the column volume occupied by the gas
We	Weber number
ξ	turbulence dissipation rate in the liquid phase
ε	gas hold – up, %
μ_g	viscosity of the gas phase
μ_l	viscosity of the liquid phase
ρ_g	density of the gas phase
ρ_l	density of the liquid phase
σ	surface tension
ν	kinematic viscosity of the liquid phase
K	Kumar <i>et al.</i> correlation
HU	Hughmark correlation

HK	Hikita and Kikukawa correlation
HI	Hikita correlation
GV	Gaddis and Vogelpohl model
MYB	Moo – Young and Blanch correlation
L	Leibson <i>et al.</i> correlation
B	Bhavaraju <i>et al.</i> correlation

References

1. Degaleesan, S., M. Dudukovic, and Y. Pan, *Experimental study of gas-induced liquid-flow structures in bubble columns*. AIChE Journal, 2001. **47**(9): p. 1913-1931.
2. Shah, Y.T., et al., *Design parameters estimations for bubble column reactors*. AIChE Journal, 1982. **28**(3): p. 353-379.
3. Prakash, A., et al., *Hydrodynamics and local heat transfer measurements in a bubble column with suspension of yeast*. Biochemical Engineering Journal, 2001. **9**(2): p. 155-163.
4. Kantarci, N., F. Borak, and K.O. Ulgen, *Bubble column reactors*. Process Biochemistry, 2005. **40**(7): p. 2263-2283.
5. Behkish, A., et al., *Gas holdup and bubble size behavior in a large-scale slurry bubble column reactor operating with an organic liquid under elevated pressures and temperatures*. Chemical Engineering Journal, 2007. **128**(2-3): p. 69-84.
6. Kumar, A., et al., *Bubble swarm characteristics in bubble - columns*. Canadian Journal of Chemical Engineering, 1976. **54**(6): p. 503-508.
7. Hughmark, G.A., *Hold up and mass transfer in bubble columns*. Industrial & Engineering Chemistry Process Design and Development, 1967. **6**(2): p. 218-&.
8. Hikita, H., et al., *Gas hold up in bubble columns*. Chemical Engineering Journal and the Biochemical Engineering Journal, 1980. **20**(1): p. 59-67.
9. Hikita, H. and H. Kikukawa, *Liquid-phase mixing in bubble columns: Effect of liquid properties*. The Chemical Engineering Journal, 1974. **8**(3): p. 191-197.
10. Gaddis, E.S. and A. Vogelpohl, *Bubble formation in quiescent liquids under constant flow conditions*. Chemical Engineering Science, 1986. **41**(1): p. 97-105.
11. Moo-Young, M. and H.W. Blanch, *Design of biochemical reactors. Mass transfer criteria for simple and complex systems*. Advances in Biochemical Engineering, 1981. **19**: p. 1-69.

12. Leibson, I., et al., *Rate of flow and mechanics of bubble formation from single submerged orifices*. Aiche Journal, 1956. **2**(3): p. 296-306.
13. Bhavaraju, S.M., R.A. Mashelkar, and H.W. Blanch, *Bubble motion and mass transfer in non - newtonian fluids. 1. Single bubble in power law and Bingham fluids*. Aiche Journal, 1978. **24**(6): p. 1063-1070.
14. Bhavaraju, S.M., R.A. Mashelkar, and H.W. Blanch, *Bubble motion and mass transfer in non - newtonian fluids. 2. Swarm of bubbles in a power law fluid*. Aiche Journal, 1978. **24**(6): p. 1070-1076.
15. Behkish, A., et al., *Novel correlations for gas holdup in large-scale slurry bubble column reactors operating under elevated pressures and temperatures*. Chemical Engineering Journal, 2006. **115**(3): p. 157-171.
16. Prince, M.J. and H.W. Blanch, *Bubble coalescence and break - up in air - sparged bubble columns*. Aiche Journal, 1990. **36**(10): p. 1485-1499.
17. Pohorecki, R., et al., *Modelling of the coalescence/redispersion processes in bubble columns*. Chemical Engineering Science, 2001. **56**(21-22): p. 6157-6164.
18. Chen, P., J. Sanyal, and M.P. Dudukovic, *Numerical simulation of bubble columns flows: effect of different breakup and coalescence closures*. Chemical Engineering Science, 2005. **60**(4): p. 1085-1101.
19. Luo, H. and H.F. Svendsen, *Theoretical model for drop and bubble breakup in turbulent dispersions*. Aiche Journal, 1996. **42**(5): p. 1225-1233.
20. Marchisio, D.L., Fox, Rodney O., *Multiphase reacting flows: modelling and simulation*. Vol. VII. 2007, London: Springer.
21. Higbie, R., *The rate of absorption of a pure gas into a still liquid during short periods of exposure*. Transactions of the American Institute of Chemical Engineers, 1935. **31**: p. 365-389.
22. Danckwerts, P.V., *Significance of liquid - film coefficients in gas absorption*. Industrial and Engineering Chemistry, 1951. **43**(6): p. 1460-1467.
23. Lamont, J.C. and D.S. Scott, *An eddy cell model of mass transfer into the surface of a turbulent liquid*. AIChE Journal, 1970. **16**(4): p. 513-519.
24. Hyndman, C.L., F. Larachi, and C. Guy, *Understanding gas-phase hydrodynamics in bubble columns: a convective model based on kinetic theory*. Chemical Engineering Science, 1997. **52**(1): p. 63-77.
25. Thorat, B.N. and J.B. Joshi, *Regime transition in bubble columns: experimental and predictions*. Experimental Thermal and Fluid Science, 2004. **28**(5): p. 423-430.

26. Daly, J.G., S.A. Patel, and D.B. Bukur, *Measurement of gas holdups and sauter mean bubble diameters in bubble column reactors by dynamics gas disengagement method*. Chemical Engineering Science, 1992. **47**(13–14): p. 3647-3654.
27. Krishna, R., et al., *Gas Holdup in Slurry Bubble Columns: Effect of Column Diameter and Slurry Concentrations*. AIChE Journal, 1997. **43**(2): p. 311-316.
28. Kara, S., et al., *Hydrodynamics and axial mixing in a three-phase bubble column*. Industrial & Engineering Chemistry Process Design and Development, 1982. **21**(4): p. 584-594.
29. Bouaifi, M., et al., *A comparative study of gas hold-up, bubble size, interfacial area and mass transfer coefficients in stirred gas–liquid reactors and bubble columns*. Chemical Engineering and Processing: Process Intensification, 2001. **40**(2): p. 97-111.
30. Luo, X., et al., *Maximum stable bubble size and gas holdup in high-pressure slurry bubble columns*. AIChE Journal, 1999. **45**(4): p. 665-680.
31. Akita, K. and F. Yoshida, *Gas Holdup and Volumetric Mass Transfer Coefficient in Bubble Columns*. Effect of Liquid Properties, Ind. Eng. Chem. Process. Des. Dev., 1974. **12**: p. 76.
32. Fukuma, M., K. Muroyama, and A. Yasunishi, *Properties of bubble swarm in a slurry bubble column*. Journal of Chemical Engineering of Japan, 1987. **20**(1): p. 28-33.
33. Saxena, S.C., N.S. Rao, and A.C. Saxena, *Heat-transfer and gas-holdup studies in a bubble column: Air-water-glass bead system*. Chem. Eng. Commun., 1990. **96**: p. 31-55.
34. Schumpe, A. and G. Grund, *Gas disengagement technique for studying gas hold up structure in bubble columns*. Canadian Journal of Chemical Engineering, 1986. **64**(6): p. 891-896.
35. Letzel, H.M., et al., *Gas holdup and mass transfer in bubble column reactors operated at elevated pressure*. Chemical Engineering Science, 1999. **54**(13-14): p. 2237-2246.
36. Behkish, A., et al., *Mass transfer characteristics in a large-scale slurry bubble column reactor with organic liquid mixtures*. Chemical Engineering Science, 2002. **57**(16): p. 3307-3324.
37. Verma, A.K. and S. Rai, *Studies on surface to bulk ionic mass transfer in bubble column*. Chemical Engineering Journal, 2003. **94**(1): p. 67-72.
38. Krishna, R. and J.M. van Baten, *Mass transfer in bubble columns*. Catalysis Today, 2003. **79–80**(0): p. 67-75.
39. Muller, F.L. and J.F. Davidson, *On the effects of surfactants on mass transfer to viscous liquids in bubble columns*. Chemical Engineering Research and Design, 1995. **73**(A3): p. 291-296.

40. Vandu, C.O. and R. Krishna, *Volumetric mass transfer coefficients in slurry bubble columns operating in the churn-turbulent flow regime*. Chemical Engineering and Processing, 2004. **43**(8): p. 987-995.
41. Buffo, A., et al., *Simulation of polydisperse multiphase systems using population balances and example application to bubbly flows*. Chemical Engineering Research and Design, 2013. **91**(10): p. 1859-1875.

Table Captions

Table 1. Gas hold – up and bubble diameter correlations.....	202
Table 2. Summarized experimental conditions and main results	205
Table 3. Summarized results for hold – up adjustment with Equation 7.....	210
Table 4. Summarized results for bubble’s diameter adjustment with Equation 8.....	214
Table 5. Summarize results of CFD modeling for hold – up and volumetric and mass transfer coefficient prediction	219

Figure Captions

Figure 1. Influence of gas flow rate and initial liquid level on hold-up. 1/8” O.D. tube, ◆ $h_0 = 40$ cm; ○ $h_0 = 50$ cm; ◇ $h_0 = 60$ cm; ✱ $h_0 = 70$ cm; ▲ $h_0 = 75$ cm.....	209
Figure 2. Influence of gas flow rate and initial liquid level on hold-up. Porous diffuser, ◆ $h_0 = 40$ cm; ○ $h_0 = 50$ cm; ◇ $h_0 = 60$ cm; ✱ $h_0 = 70$ cm; ▲ $h_0 = 75$ cm.....	209
Figure 3. Influence of gas flow rate and initial liquid level on bubble diameter. 1/8” O.D. tube, ◆ $h_0 = 40$ cm; ○ $h_0 = 50$ cm; ◇ $h_0 = 60$ cm; ✱ $h_0 = 70$ cm; ▲ $h_0 = 75$ cm.	212
Figure 4. Influence of gas flow rate and initial liquid level on bubble diameter. Porous diffuser, ◆ $h_0 = 40$ cm; ○ $h_0 = 50$ cm; ◇ $h_0 = 60$ cm; ✱ $h_0 = 70$ cm; ▲ $h_0 = 75$ cm.	213
Figure 5. Influence of gas flow rate an initial liquid level on interfacial area (left), volumetric mass transfer coefficient (right) and mass transfer coefficient (center). 1/8” O.D. tube. ◆ $h_0 = 40$ cm; ○ $h_0 = 50$ cm; ◇ $h_0 = 60$ cm; ✱ $h_0 = 70$ cm; ▲ $h_0 = 75$ cm.	217
Figure 6. Influence of gas flow rate an initial liquid level on interfacial area (left), volumetric mas transfer coefficient (right) and mass transfer coefficient (center). Porous diffuser. ◆ $h_0 = 40$ cm; ○ $h_0 = 50$ cm; ◇ $h_0 = 60$ cm; ✱ $h_0 = 70$ cm; ▲ $h_0 = 75$ cm.	218
Figure 7. Comparison of experimental results and values obtained by CDF modeling. (# Exp. 35, 47 and 50). ● Experimental values; ◇ CFD model.	219
Figure 8. Bubble size distribution obtained by CFD (results for experiment # 35)	220

CONCLUSIONS

This work has contributed to the analysis of the secondary reactions that take place during the direct synthesis of hydrogen peroxide, the utilization of nitrogen as inert compound of the gas phase and the development of continuous triphase reactors for direct synthesis of hydrogen peroxide. The best results of hydrogen peroxide productivity, the yield of the reaction and the turnover frequency of each chapter (III, IV and V) are summarized on the next figures. Also the main conditions of each experiments are indicated.

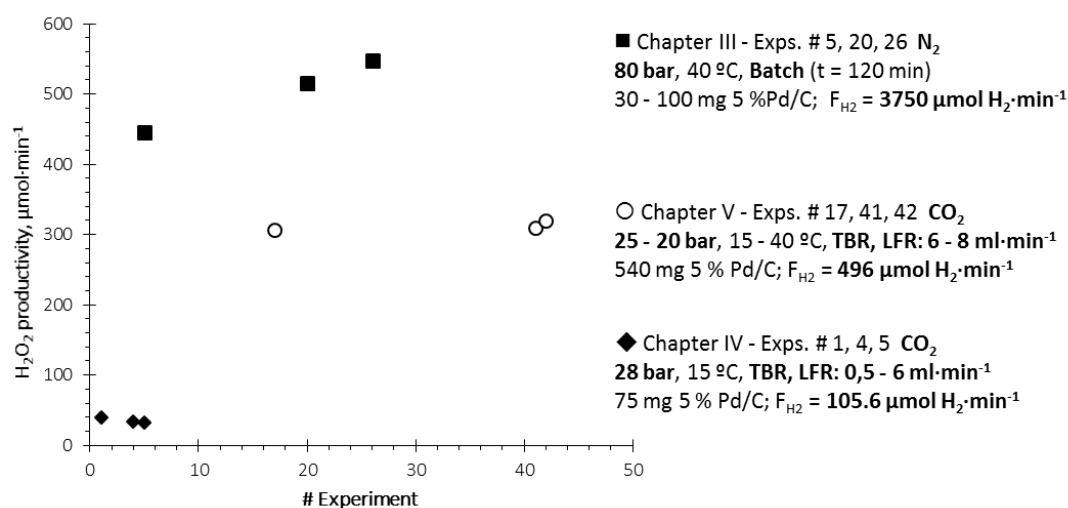


Figure 1. Maxima values of productivity obtained for the chapters III, IV and V

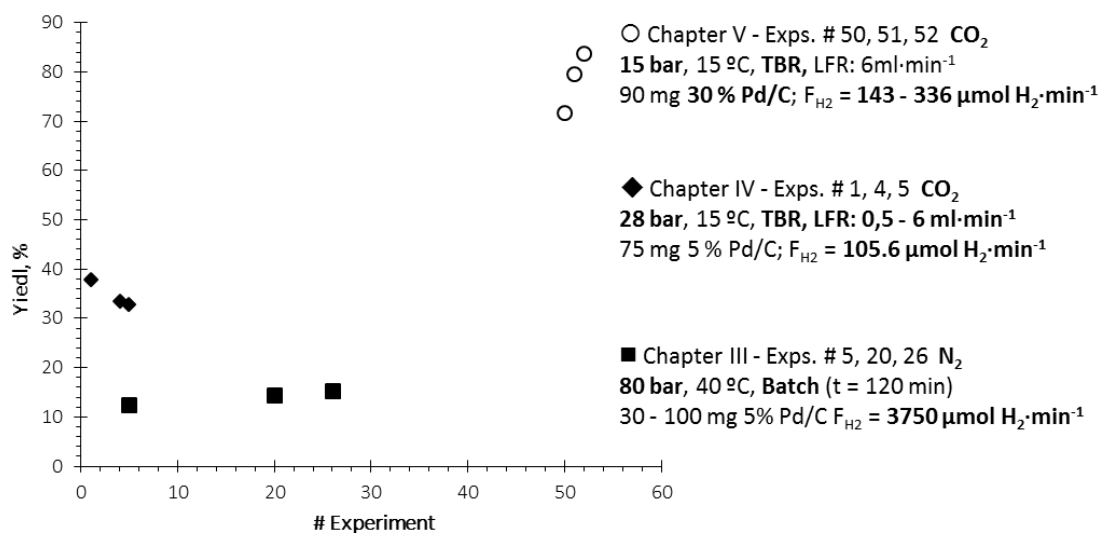


Figure 2. Maxima values of yield obtained for the chapters III, IV and V

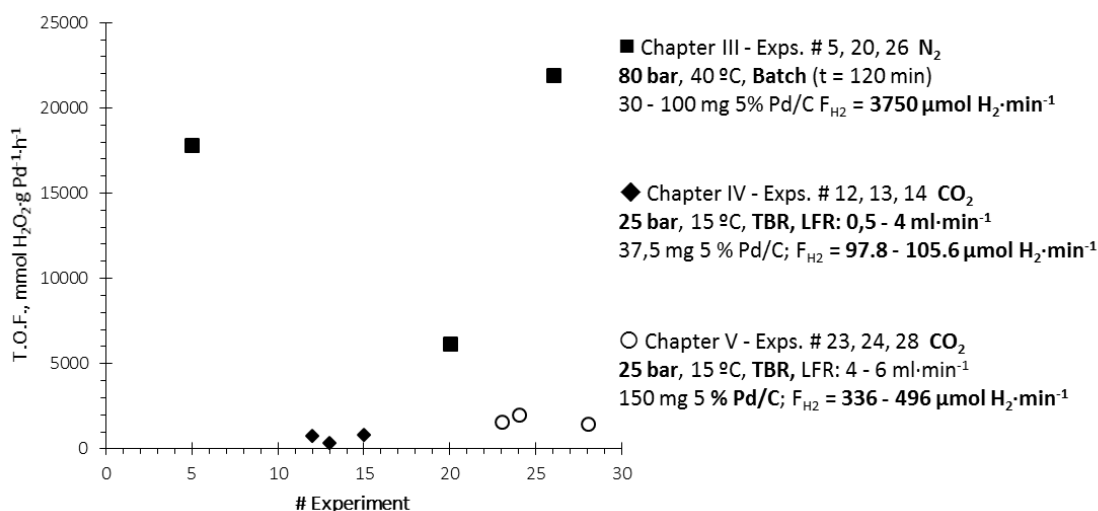


Figure 3. Maxima values of T.O.F obtained for the chapters III, IV and V

For chapter IV, as low pressure and low hydrogen molar flow rate was used, the productivity and T.O.F obtained was lower in comparison with the results of the chapter III and V. These results are not unexpected, since during the design of the experiments productivity was gave up in favor of an easier analysis of the influence of the reaction conditions.

Maximum productivity (Figure 1) was obtained at chapter III since the hydrogen flow rate was the higher ($446, 516$ and $548 \mu mol H_2O_2 \cdot min^{-1}$). Although at chapter V a similar value of productivity was reached ($307, 309$ and $320 \mu mol H_2O_2 \cdot min^{-1}$), that suggest that with a correct selection of the operation conditions a trickle bed reactor could be as efficient as a semicontinuous reactor even if the pressure at the TBR was too much lower (80 bar vs. 28 bar) and if the hydrogen molar flow rate it is almost 10 times lower. Higher selectivity was obtained when a catalyst with a high palladium percentage (30 %) was used. The beneficial effect of a high concentration of the actives sites is clear in that case, although a further investigation of the catalyst structure is need to understand the reason of this result. Values of T.O.F produced at chapter III are too much higher than the values of the chapters IV and V since for the chapter III the calculation of T.O.F. was made on base on the accumulated hydrogen peroxide concentration and for the chapters IV and V it was made on base on the instantaneous value.

On base on the analysis and discussion of the experimental results the main conclusions of this thesis could be summarized as follows:

Chapter II: Hydrogenation and decomposition kinetic study of H₂O₂ over Pd/C catalyst in an aqueous medium at high CO₂ pressure

- Hydrogenation and decomposition must be deeply studied since they could reveal key information of the direct synthesis process and enhanced the optimization of the process variables.
- Hydrogenation was higher at low H₂O₂ concentrations and decomposition increased with the H₂O₂ concentration. Reaction order of hydrogenation and decomposition, obtained for experimental data, were -0.16 and 1.03 respectively.
- Selection of the optimum value of the concentration of acid and the ratio Br/Pd could reduce the effect of the secondary reactions. A pH = 2 or closed to that value was enough to protect the hydrogen peroxide already formed. A ratio halide – palladium between 3.0 and 5.0 decreased the hydrogenation and a value of 8.0 it was optimum to reduce the decomposition.
- Number of actives sites had a strong influence over the catalyst behaviour, but also the support, the catalyst preparation, history etc. must be taken into account. The kinetics of reaction of three different catalyst have been compared and the order of reaction in function of the number or active metal sites have been calculated. The order of reaction as a function of the number of sites has been 0.812 – 0.981 for decomposition at low Pd amounts and up to 1.444 at high Pd amounts. For hydrogenation the order was 0.710 – 1.078. This indicates that not all of the Pd sites are available or active.
- The activation energies values have been calculated for both reactions, $E_{a_d} = 18803.6$ J/mol (decomposition) and $E_{a_h} = 7746.2$ J/mol (hydrogenation) as average values for all the catalysts used, obtaining average errors of %AAD_d = 0.6% and %AAD_h = 2.20% respectively.

Chapter III: Direct synthesis of H₂O₂ in water using nitrogen as inert over Pd/C catalysts in semicontinuous mode

- The utilization of nitrogen as inert compound of the gas phase was a viable alternative to produce hydrogen peroxide in a semicontinuous stirring reactor. Hydrogen peroxide concentration values of 1.13 % wt/v and values of selectivity and conversion of 70% and 35% respectively were obtained.
- Productivity (CO₂: 1.58 % wt/v vs. N₂: 0.647 % wt/v) and selectivity (CO₂: 88% vs. N₂: 48%) were higher when carbon dioxide was used as inert since the CO₂ acted as co – solvent increasing the mass transfer between the gas and the liquid and stabilized the H₂O₂ already produced.
- Mass transfer phenomena act as the controlling step of the reaction for amount of catalyst lower than 30 mg of 5 %Pd/C. This value has been found as the optimum, since if the number of active sites in the reactor was lower the hydrogen was not consumed quickly enough and the hydrogenation of the H₂O₂ was produced. As the mass transfer is the limiting stage of the process, selectivity or productivity could not be increased by the increasing of the amount catalyst. Even a high number of active sites in the reaction medium could be harmful since could cause the decomposition of the hydrogen peroxide.
- Global pressure had a positive influence over conversion (13.2 % – 30.2 %), selectivity (15.8 % – 47.8 %) and T.O.F (0.897 mol·h⁻¹·g Pd⁻¹ – 6.193 mol·h⁻¹·g Pd⁻¹), since all of them increased with the pressure (if the molar fraction of hydrogen was kept constant).
- The influence of the hydrogen partial pressure was also analyzed. Conversion and productivity increased with the hydrogen partial pressure independently if the variation was due to variation of the global pressure or the composition of the gas phase. Selectivity followed a different tendency. Selectivity was constant (30 % – 35 %) when hydrogen molar flow rate varied and global pressure was kept constant (80 bar). On the opposite case, the selectivity increased with the hydrogen partial pressure if the ratio O₂/H₂ was kept constant but the global pressure increased. Influence of the O₂/H₂ on the

amount of oxygen available for reaction, adsorption mechanism and oxidation state of the active metal might be the reason of the different behavior.

- From the observed reaction rate the values of the pre – exponential factor ($272.15 \text{ mmol}\cdot\text{min}^{-1}$, $520.54 \text{ mmol}\cdot\text{min}^{-1}$ and $766.51 \text{ mmol}\cdot\text{min}^{-1}$ for 1 % Pd/C, 3 % Pd/C and 5 % Pd/C catalyst respectively) and the ratio and the ratio E_a/R (2306.7 K, 2348.4 K and 2588.2 K for 1 % Pd/C, 3 % Pd/C and 5 % Pd/C catalyst respectively) have been calculated. A dependence of the pre – exponential factor on the palladium percentage has been found, and as higher the palladium percentage higher the pre – exponential factor. Any influence of the number of active sites have been found on the kinetic parameters, that suggested that the method of preparation of the catalyst might or the aggregation of the particles could be the reason of these results.
- As the reaction conditions were kept constant, not influence of the gas flow rate over the selectivity was seen. The conversion decreased when high flow rates were set since the residence time of the gas inside the reactor was lower.
- Nitrogen has not the good properties that the carbon dioxide has, and on consequence the productivity and selectivity obtained when nitrogen was used as inert were lower in comparison with the values obtained with carbon dioxide. However, with a further investigation, the correct selection of the reaction conditions, the development of more efficient catalyst and the construction of a new reactor the direct synthesis of hydrogen peroxide using nitrogen could be a process to be taking into consideration.

Chapter IV: Effect of the low hydrogen to palladium ratio in the direct synthesis of H_2O_2 in water in a trickle bed reactor

- It is possible to produce hydrogen peroxide by direct synthesis in a continuous trickle bed reactor at high pressure. The best conditions to ensure the viability of the process must be optimized.
- The used of a low concentration of hydrogen (2.3 % mol) in the phase gas lead to very low productivities and yield values (maxima values: $39.02 \mu\text{mol H}_2\text{O}_2\cdot\text{min}^{-1}$; 37.9 % yield).

- Value of the ratio H_2/Pd is a key parameter in the optimization of the productivity and the yield.
- Higher the total pressure on the reaction, higher the concentration of the hydrogen solved into the liquid phase and on consequence higher the amount of hydrogen available for reaction. At low pressure, 15 barg, system was limited by the mass transfer phenomena and no enhancement of the productivity was obtained when the amount of catalyst in the reactor was increased (15.86 $\mu\text{mol } H_2O_2 \cdot \text{min}^{-1}$ with 1 $\text{ml} \cdot \text{min}^{-1}$ and 75 mg of 5 % Pd/C in 40 ml of volume bed vs. 14.71 $\mu\text{mol } H_2O_2 \cdot \text{min}^{-1}$ with 1 $\text{ml} \cdot \text{min}^{-1}$ and 37.5 mg of 5 % Pd/C in 40 ml of volume bed).
- Lower liquid flow rate (0.05 – 0.1 $\text{ml} \cdot \text{min}^{-1}$) produced a higher local H_2 concentration and higher H_2O_2 concentrations but also higher productivities. Very high residence time may cause an incomplete wetting of the reaction bed and reduce the efficiency of the process.
- A non – uniform catalyst distribution reduced losses of productivity due to the secondary reactions (decomposition and hydrogenation). A higher catalyst concentration in the bed at the initial part of the reactor reduced the possibilities of contact between high concentrations of hydrogen peroxide, the actives sites and an excess of the hydrogen.
- At the same amount of catalyst a longer bed (more SiO_2) helped in a higher H_2 dissolution and the production was clearly higher. Thus, a ratio of $\text{Pd}/V_b < 0.094 \text{ mg}/\text{cm}^3$ was recommended, in most cases.

Chapter V: The development of the H_2O_2 direct synthesis process in water with a commercial catalyst in a continuous reactor: bridging the gap between chemistry and chemical engineering

- Hydrogen peroxide direct synthesis is a challenging reaction and so many efforts have been done in order to try to understand the reaction mechanism and gather important information for the design and preparation of specifically design catalyst.
- The hydrogenation reaction is responsible of the low yield and productivity obtained. A strong influence of the gas flow rate have been found, as higher the amount of hydrogen

available for reaction higher the percentage of hydrogen peroxide hydrogenated (9.2 % of hydrogenation with $74.2 \mu\text{mol}\cdot\text{min}^{-1}$ and 56.3% of hydrogenation with $219.03 \mu\text{mol}\cdot\text{min}^{-1}$ at $6 \text{ ml}\cdot\text{min}^{-1}$ of liquid flow rate). Also a linear relation between the hydrodynamic residence time of the liquid phase and the hydrogenation rate has been observed. Logically as higher the residence time higher the hydrogenation rate since the contact between the hydrogen and the hydrogen peroxide was increased (12.4 % of hydrogenation when $\text{HRT} = 5.5 \text{ min}$ to 28.6% of hydrogenation when $\text{HRT} = 44 \text{ min}$ and $74.2 \mu\text{mol}\cdot\text{min}^{-1}$).

- Selection of the liquid flow rate must be done to ensure that the reaction bed is completely wetted but also that a flow regime is trickle type.
- A fast consumption of the hydrogen is necessary to avoid secondary reactions and obtained a high yield and productivity; it could be obtained when the high mass transfer limitations prevailed ($6 \text{ ml}\cdot\text{min}^{-1}$) or when high amount of catalyst was used (540 mg of 5 % Pd/C). Decreasing of productivity and yield were obtained if the reaction conditions did not allow the fast consumption of the hydrogen. Also with a catalyst rich in palladium percentage (30 % Pd/C) a faster consumption of the hydrogen is possible.
- Pressure had a beneficial effect over productivity and yield. High pressure did not guarantee a high productivity if the rest of the operational parameters (liquid flow rate, amount of the catalyst, gas flow rate) were not correctly selected.
- Not a clear effect of the temperature has been found. High temperatures values increased hydrogenation and decomposition rates. Low temperature values gave a low value of reaction rate and decreased the production of hydrogen peroxide. An intermediate temperature value was the optimum.
- Concentration of bromide on the liquid phase affected on the final hydrogen peroxide concentration but also on the time need to reach the steady – state. Higher the concentration of bromide lower the time need to the hydrogen peroxide concentration started to increased ($45 \text{ min} - 1\cdot 10^{-3} \text{ M}$; $90 \text{ min} - 5\cdot 10^{-4} \text{ M}$; $180 \text{ min} - 2.5\cdot 10^{-4} \text{ M}$) and higher the time to the system to stabilized ($105 \text{ min} - 1\cdot 10^{-3} \text{ M}$; $150 \text{ min} - 5\cdot 10^{-4} \text{ M}$; 330

min - $2.5 \cdot 10^{-4}$ M). Results suggested that the Br^- blocked the sites both for H_2O_2 and water formation but also that the concentration of Br^- affected to the quantity of the sites and the quality. Reconstruction of the metal nanoclusters, adsorption and desorption phenomena are affected by the concentration of Br^- on the liquid phase.

- Concentration of the active metal on the catalyst has also showed up have influence on the hydrogen peroxide productivity. The maximum productivity of $250.5 \mu\text{molH}_2\text{O}_2 \cdot \text{min}^{-1}$ (for $496.0 \mu\text{molH}_2 \cdot \text{min}^{-1}$) and $288.6 \mu\text{molH}_2\text{O}_2 \cdot \text{min}^{-1}$ (for $496.0 \mu\text{molH}_2 \cdot \text{min}^{-1}$) were obtained for 10 % Pd/C and 30 % Pd/C, respectively. Yields between 84 % and 60 % for 30 % Pd/C and between 60 % and 50 % for 10 % Pd/C were measured Higher the palladium percentage on the catalyst higher the productivity and the selectivity of the solid since the amount of catalyst along the bed was not higher enough to hydrogenate the H_2O_2 already produced. High palladium percentage allows also the formation of big nanoparticles that enhanced the direct synthesis of hydrogen peroxide.

Chapter VI: Determination and modelling of liquid – gas mass transfer coefficient and interfacial area in a low pressure bubble column.

- None of the correlations from bibliography were capable to predict the values of the hold-up or the bubble diameter with the enough accuracy. No influence of the initial column liquid level has been found.
- The gas hold-up increased with the gas flow rate. Higher the gas flow rate higher the volume of the column occupied by the gas phase. When a porous diffuser was used the maximum value of hold-up obtained was around the 14% while only an 8 % was reached when a 1/8" O.D. tube was used.
- The interfacial area also increased with the gas flow rate. Smaller bubbles generated with the porous diffuser rose up the column slower (1/8" tube O.D.: 0.71 cm to 1.23 cm and porous diffuser: 0.27 cm to 0.46 cm), on consequence the residence time of the bubbles in the column is higher and the amount of gas inside the system per unit of time is higher too.

-
- None a clear dependence of the mass transfer coefficient (k_L) (1/8" O.D.: from $4.63 \cdot 10^{-2}$ to $1.22 \cdot 10^{-1} \text{ cm}\cdot\text{s}^{-1}$ and porous diffuser: from $2.52 \cdot 10^{-2}$ to $1.34 \cdot 10^{-1} \text{ cm}\cdot\text{s}^{-1}$) on the gas flow rate has been found but there was a strong influence of the gas flow rate on the volumetric mass transfer ($k_L\cdot a$) (1/8" tube O.D.: from $6.48\cdot 10^{-3} \text{ s}^{-1}$ to $2.81\cdot 10^{-2} \text{ s}^{-1}$ and porous diffuser: from $1.81\cdot 10^{-2} \text{ s}^{-1}$ to $1.06\cdot 10^{-1} \text{ s}^{-1}$) and the interfacial area (a) (1/8" tube O.D.: 0.08 cm^{-1} and 0.43 cm^{-1} and porous diffuser: 0.16 cm^{-1} and 1.89 cm^{-1}).
 - As none of the expressions and correlations from the bibliography was capable to predict the bubble diameter and the hold-up with a small enough error new correlations based on the Reynolds number and the fluids properties have been proposed.
 - The CFD model generated similar results and predicted the influence of the main variables of the system. A more detailed modeling was needed to predict the results with a lower deviation.

FUTURE WORK

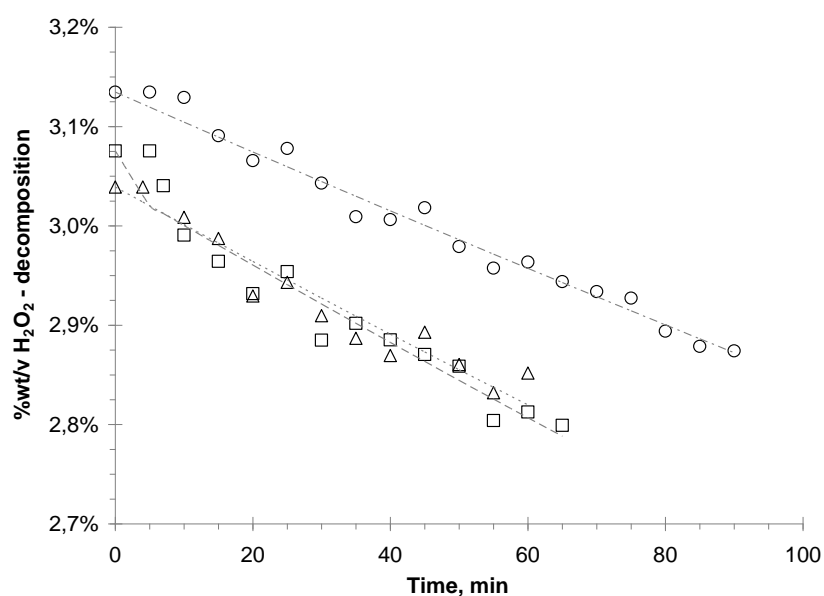
On the last chapters it have been show up that the direct synthesis of hydrogen peroxide in a continuous reactor is a feasible process. However further investigation focus on some aspects of the process are needed in order to complete the researching about the direct synthesis.

- Analysis of the commercial catalyst after and before the reaction. Measure of the diameter of the particles, porous size and area and determination of the oxidation state of the active metal.
- Development of the kinetic model integrating the kinetic data for the four reactions that take place during the direct synthesis of the hydrogen peroxide.
- Design and preparation of a specific catalyst. The used of different metal combination (Pd – Au) and the functionalization of the support have reported an increasing on the productivity and selectivity on the direct synthesis of the hydrogen peroxide. The combination of specifically design catalyst and the optimized reaction conditions obtained in this work might be necessary in order to determinate the maximum productivity and selectivity that the system could reach.
- Substitution of carbon dioxide and oxygen by air. The use of air as inert (N_2) and reagent (O_2) could reduce the global cost of production of hydrogen peroxide, and help to the development of the direct synthesis as an industrial process for hydrogen peroxide synthesis. As it is logical the optimization of the reaction variables will be need.
- Start up, optimization and analysis of the influence of the reaction conditions for direct synthesis of hydrogen peroxide in a continuous slurry bubble column reactor. Along with the trickle bed reactor the slurry bubble columns are the main alternative for continuous direct synthesis of hydrogen peroxide. Influence of the main reaction parameters on the system hydrodynamic and reaction productivity should be analyzed in detail.

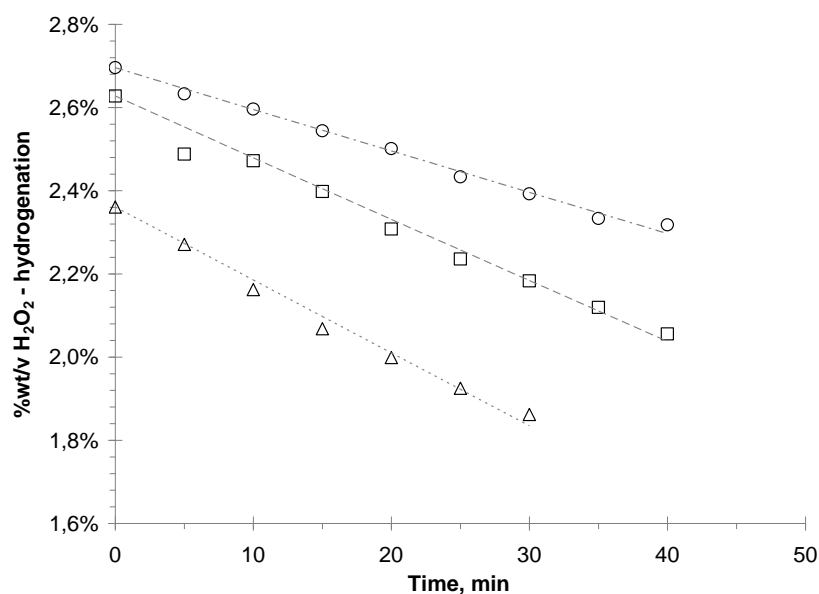
APPENDIX I

Supplementary figures for chapter II

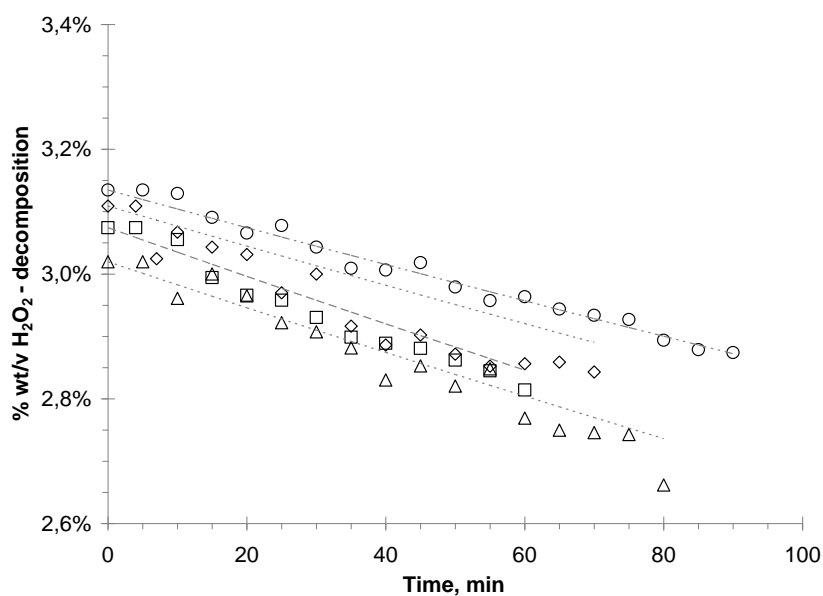
Hydrogen peroxide decomposition and hydrogenation reaction are quite complex, because of this it is required a large number of experiments' data in order developed a model that allows to obtain the best adjustment possible. Figures summarized in this appendix have been built from the hydrogen peroxide concentration values obtained during experimentation and give complementary information to the discussion of the chapter II.



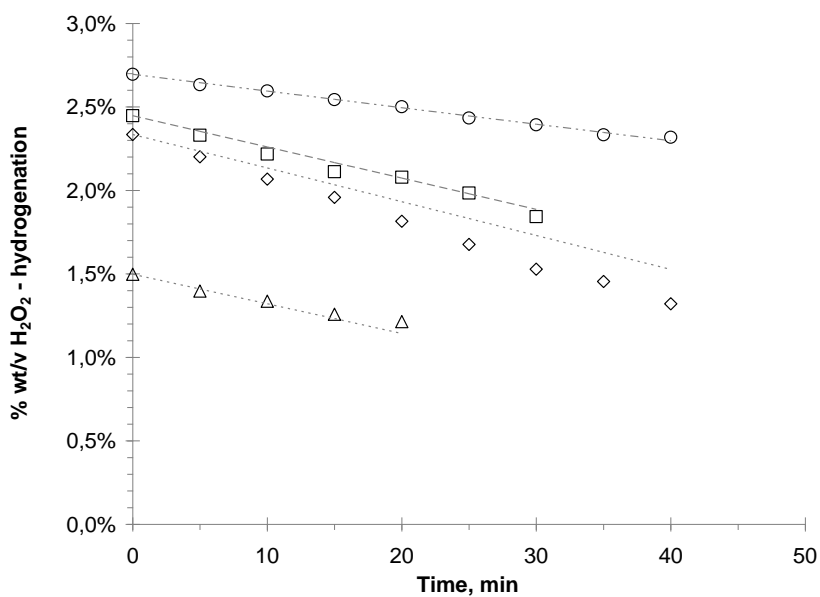
Supplementary figure 1. Effect of rate Br^-/Pd on H_2O_2 decomposition (runs # 1, 8, 9), $T^a = 40\text{ }^\circ\text{C}$, 100 mg 5% Pd/C, 100 mL, 3 %wt/v H_2O_2 initial, pH= 2, 80 bar CO_2 . \circ $\text{Br}^-/\text{Pd} = 8.5$; \triangle $\text{Br}^-/\text{Pd} = 5$; \square $\text{Br}^-/\text{Pd} = 3$. Dashed line represents the values of the simulation.



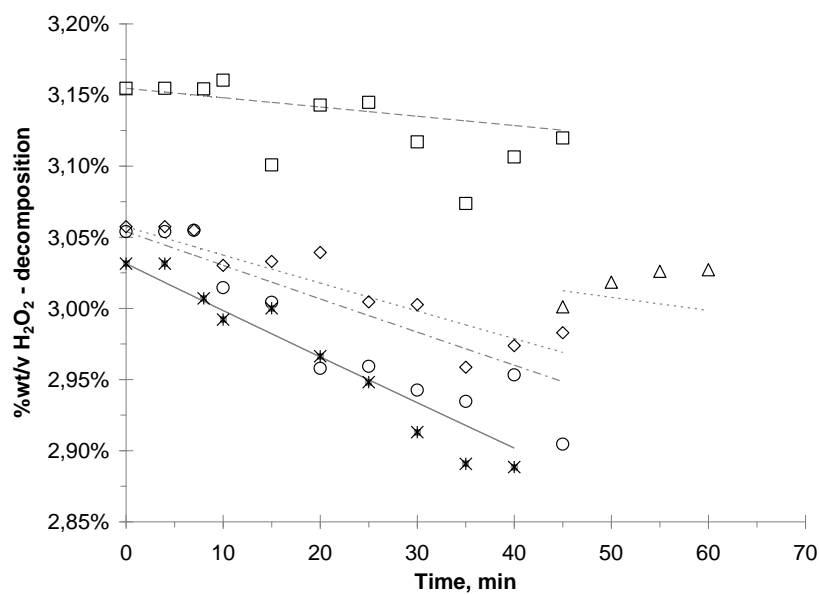
Supplementary figure 2. Effect of rate Br^-/Pd on H_2O_2 hydrogenation (runs # 1, 8, 9), $T^a = 40\text{ }^\circ\text{C}$, 100 mg 5% Pd/C, 100 mL, 3 %wt/v H_2O_2 initial, pH= 2, 80 bar CO_2 . \circ $\text{Br}^-/\text{Pd} = 8.5$; \triangle $\text{Br}^-/\text{Pd} = 5$; \square $\text{Br}^-/\text{Pd} = 3$. Dashed line represents the values of the simulation.



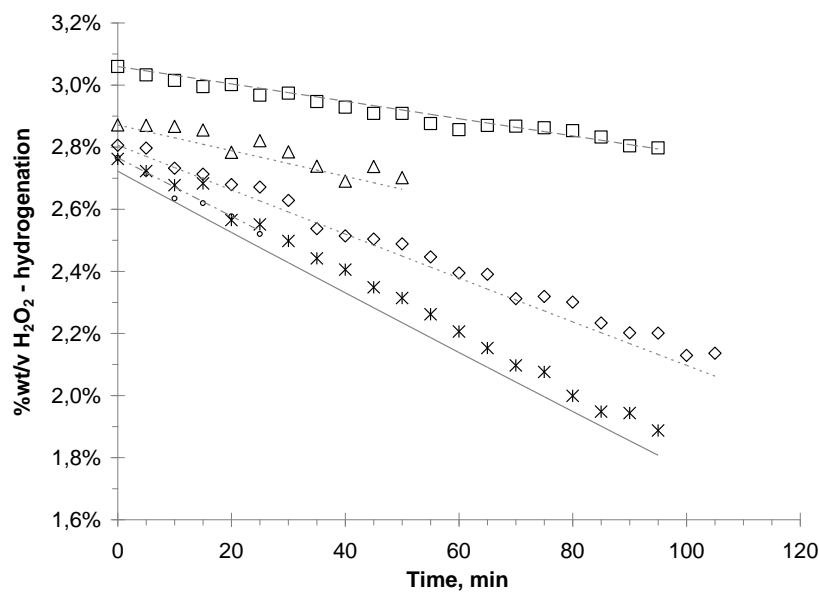
Supplementary figure 3. Effect of temperature on H_2O_2 decomposition (runs # 1, 5 - 7), 100 mg 5% Pd/C, 100 mL, 3 %wt/v H_2O_2 initial, Br/Pd = 8, pH = 2, 80 bar CO_2 . o $T^a = 40^\circ\text{C}$; ◇ $T^a = 50^\circ\text{C}$; △ $T^a = 58^\circ\text{C}$; □ $T^a = 60^\circ\text{C}$. Dashed line represents the values of the simulation.



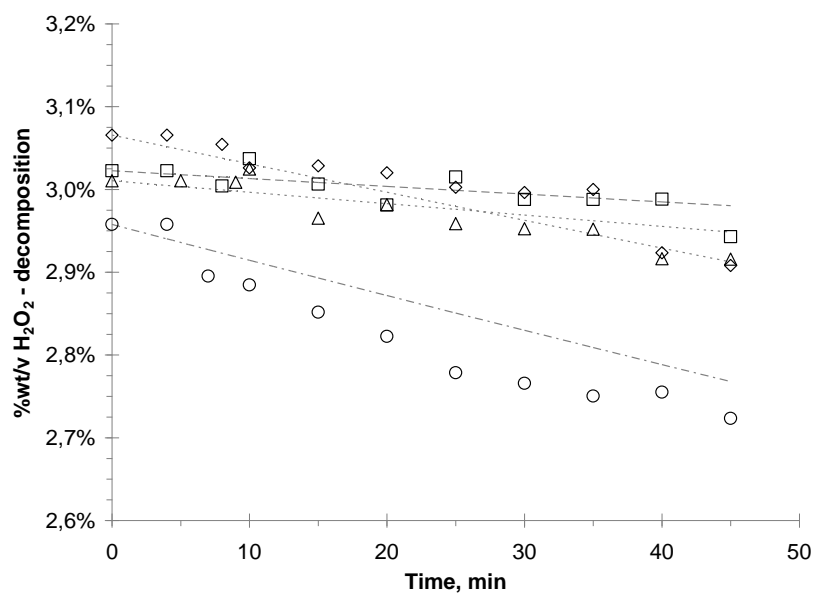
Supplementary figure 4. Effect of temperature on H_2O_2 hydrogenation (runs # 1, 5 - 7), 100 mg 5% Pd/C, 100 mL, 3 %wt/v H_2O_2 initial, Br/Pd = 8, pH = 2, 80 bar CO_2 . o $T^a = 40^\circ\text{C}$; ◇ $T^a = 50^\circ\text{C}$; △ $T^a = 58^\circ\text{C}$; □ $T^a = 60^\circ\text{C}$. Dashed line represents the values of the simulation.



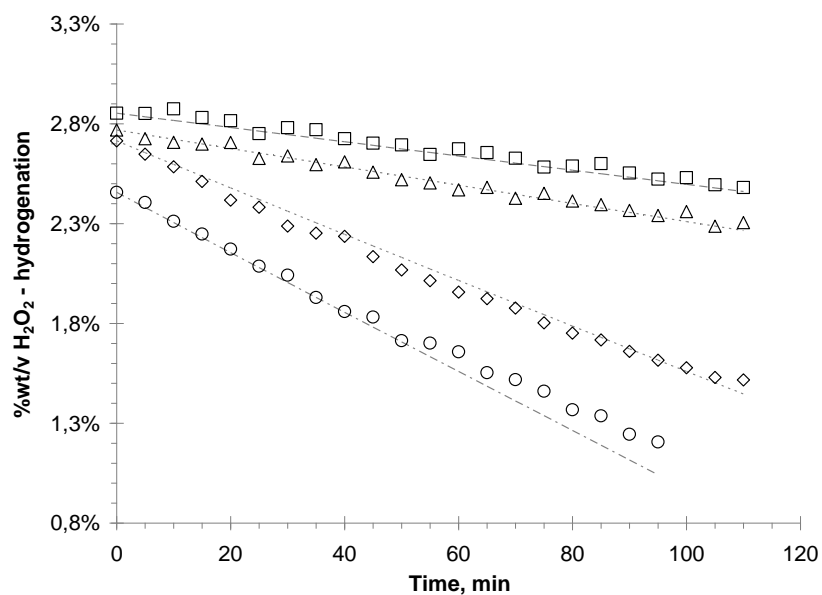
Supplementary figure 5. Effect of amount of 1% Pd/C catalyst on H_2O_2 decomposition rate (runs #13 - 17) at 40 °C, 100 mL, 3 %wt/v H_2O_2 initial, $\text{Br}^-/\text{Pd} = 8$, $\text{pH} = 2$, 80 bar CO_2 . \square 15 mg 1% Pd/C; \triangle 25 mg 1% Pd/C; \diamond 75 mg 1% Pd/C; \circ 100 mg 1% Pd/C; $*$ 200 mg 1% Pd/C. Dashed line represents the values of the simulation.



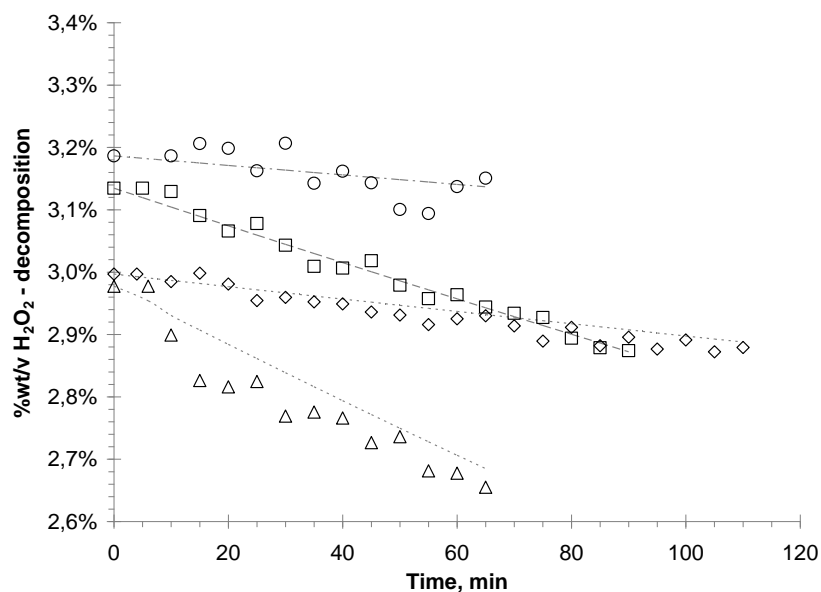
Supplementary figure 6. Effect of amount of 1% Pd/C catalyst on H_2O_2 hydrogenation rate (runs # 13 - 17) at 40 °C, 100 mL, 3 %wt/v H_2O_2 initial, $\text{Br}^-/\text{Pd} = 8$, $\text{pH} = 2$, 80 bar CO_2 . \square 15 mg 1% Pd/C; \triangle 25 mg 1% Pd/C; \diamond 75 mg 1% Pd/C; \circ 100 mg 1% Pd/C; $*$ 200 mg 1% Pd/C. Dashed line represents the values of the simulation.



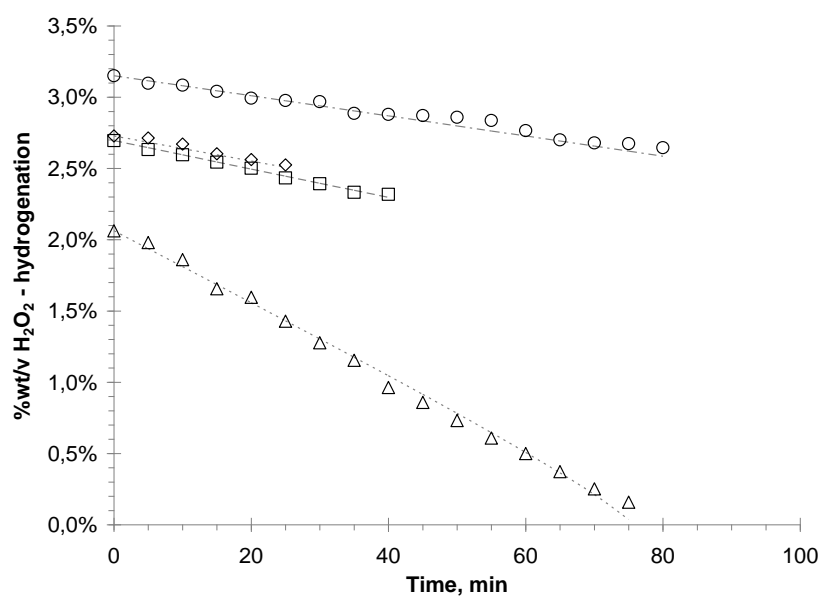
Supplementary figure 7. Effect of amount of 3% Pd/C catalyst on H_2O_2 decomposition rate (runs # 18 - 21) at 40 °C, 100 mL, 3 %wt/v H_2O_2 initial, $\text{Br}^-/\text{Pd} = 8$, $\text{pH} = 2$, 80 bar CO_2 . □ 15 mg 3% Pd/C; △ 25 mg 3% Pd/C; ◇ 100 mg 3% Pd/C; ○ 200 mg 3% Pd/C. Dashed line represents the values of the simulation.



Supplementary figure 8. Effect of amount of 3% Pd/C catalyst on H_2O_2 hydrogenation rate (runs #18 - 21) at 40 °C, 100 mL, 3 %wt/v H_2O_2 initial, $\text{Br}^-/\text{Pd} = 8$, $\text{pH} = 2$, 80 bar CO_2 . □ 15 mg 3% Pd/C; △ 25 mg 3% Pd/C; ◇ 100 mg 3% Pd/C; ○ 200 mg 3% Pd/C. Dashed line represents the values of the simulation.



Supplementary figure 9. Effect of amount of 5% Pd/C catalyst on H_2O_2 decomposition rate (runs #1 - 4) at 40 °C, 100 mL, 3 %wt/v H_2O_2 initial, $\text{Br}^-/\text{Pd} = 8$, pH = 2, 80 bar CO_2 . ○ 20 mg 5% Pd/C; ◇ 50 mg 5% Pd/C; □ 100 mg 5% Pd/C; △ 200 mg 5% Pd/C. Dashed line represents the values of the simulation.



Supplementary figure 10. Effect of amount of 5% Pd/C catalyst on H_2O_2 hydrogenation rate (runs #1 - 4) at 40 °C, 100 mL, 3 %wt/v H_2O_2 initial, $\text{Br}^-/\text{Pd} = 8$, pH = 2, 80 bar CO_2 . ○ 20 mg 5% Pd/C; ◇ 50 mg 5% Pd/C; □ 100 mg 5% Pd/C; △ 200 mg 5% Pd/C. Dashed line represents the values of the simulation.

APPENDIX II

Supplementary figures for chapter VI

Values summarized in the chapter VI have been obtained for the experimental results showed up in the next tables.

Table 1. Detailed results of the experiments # 1 to # 25, 1/8" O.D. tube used as diffuser

# exp.	ILL (h_0), cm	GFR, $\text{ml}\cdot\text{min}^{-1}$	Bubble diam. (D_b), cm	Hold – up (ϵ),%	a , cm^{-1}	k_L , $\text{cm}\cdot\text{s}^{-1}$	$k_L\cdot a$, s^{-1}
1_a	40	200.0	0.69	1.00	0.09	$6.45\cdot 10^{-2}$	$5.51\cdot 10^{-3}$
1_b	40	200.0	0.72	1.00	0.08	$8.90\cdot 10^{-2}$	$7.35\cdot 10^{-3}$
1_c	40	200.0	0.73	1.00	0.08	$8.13\cdot 10^{-2}$	$6.59\cdot 10^{-3}$
2_a	50	200.0	0.83	1.60	0.11	$1.11\cdot 10^{-1}$	$1.26\cdot 10^{-2}$
2_b	50	200.0	0.87	1.80	0.12	$8.30\cdot 10^{-2}$	$1.01\cdot 10^{-2}$
2_c	50	200.0	0.86	1.80	0.12	$7.24\cdot 10^{-2}$	$8.94\cdot 10^{-3}$
3_a	60	200.0	0.72	1.00	0.08	$7.08\cdot 10^{-2}$	$5.80\cdot 10^{-3}$
3_b	60	200.0	0.68	0.83	0.07	$8.59\cdot 10^{-2}$	$6.28\cdot 10^{-3}$
3_c	60	200.0	0.73	1.00	0.08	$9.75\cdot 10^{-2}$	$7.91\cdot 10^{-3}$
4_a	70	200.0	0.83	1.57	0.11	$9.74\cdot 10^{-2}$	$1.09\cdot 10^{-2}$
4_b	70	200.0	0.84	1.57	0.11	$6.38\cdot 10^{-2}$	$7.04\cdot 10^{-3}$
4_c	70	200.0	0.88	1.71	0.12	$6.08\cdot 10^{-2}$	$7.00\cdot 10^{-3}$
5_a	75	200.0	0.95	0.00	0.12	$6.53\cdot 10^{-2}$	$8.08\cdot 10^{-3}$
5_b	75	200.0	0.89	0.00	0.11	$8.27\cdot 10^{-2}$	$8.82\cdot 10^{-3}$
5_c	75	200.0	0.91	0.00	0.12	$7.32\cdot 10^{-2}$	$8.84\cdot 10^{-3}$
6_a	40	500.0	0.92	2.25	0.14	$6.27\cdot 10^{-2}$	$8.95\cdot 10^{-3}$
6_b	40	500.0	0.78	1.50	0.11	$8.41\cdot 10^{-2}$	$9.56\cdot 10^{-3}$
6_c	40	500.0	0.92	2.50	0.16	$7.32\cdot 10^{-2}$	$1.16\cdot 10^{-2}$
7_a	50	500.0	0.82	3.40	0.24	$4.59\cdot 10^{-2}$	$1.11\cdot 10^{-2}$
7_b	50	500.0	0.85	1.60	0.11	$1.19\cdot 10^{-1}$	$1.32\cdot 10^{-2}$
7_c	50	500.0	1.11	3.60	0.19	$6.18\cdot 10^{-2}$	$1.16\cdot 10^{-2}$
8_a	60	500.0	0.94	2.00	0.12	$1.28\cdot 10^{-1}$	$1.60\cdot 10^{-2}$
8_b	60	500.0	0.73	1.17	0.09	$1.76\cdot 10^{-1}$	$1.66\cdot 10^{-2}$
8_c	60	500.0	0.79	1.50	0.11	$1.76\cdot 10^{-1}$	$1.97\cdot 10^{-2}$
9_a	70	500.0	0.93	1.86	0.12	$1.27\cdot 10^{-1}$	$1.50\cdot 10^{-2}$
9_b	70	500.0	0.93	2.00	0.13	$8.64\cdot 10^{-2}$	$1.09\cdot 10^{-2}$
9_c	70	500.0	1.00	2.14	0.13	$1.02\cdot 10^{-1}$	$1.29\cdot 10^{-2}$
10_a	75	500.0	0.95	2.27	0.14	$9.27\cdot 10^{-2}$	$1.29\cdot 10^{-2}$
10_b	75	500.0	1.01	2.40	0.14	$7.98\cdot 10^{-2}$	$1.11\cdot 10^{-2}$
10_c	75	500.0	0.89	1.73	0.12	$9.17\cdot 10^{-2}$	$1.06\cdot 10^{-2}$
11_a	40	800.0	1.01	2.75	0.16	$9.17\cdot 10^{-2}$	$1.45\cdot 10^{-2}$
11_b	40	860.1	0.97	2.25	0.14	$8.35\cdot 10^{-2}$	$1.14\cdot 10^{-2}$
11_c	40	811.1	1.13	3.25	0.17	$7.20\cdot 10^{-2}$	$1.21\cdot 10^{-2}$
12_a	50	862.5	1.16	3.40	0.17	$6.46\cdot 10^{-2}$	$1.10\cdot 10^{-2}$
12_b	50	811.8	1.31	4.60	0.20	$5.18\cdot 10^{-2}$	$1.04\cdot 10^{-2}$
12_c	50	894.4	1.22	4.20	0.20	$6.80\cdot 10^{-2}$	$1.35\cdot 10^{-2}$

13_a	60	894.1	0.63	0.83	0.08	$1.83 \cdot 10^{-1}$	$1.43 \cdot 10^{-2}$
13_b	60	830.1	0.99	3.50	0.20	$6.19 \cdot 10^{-2}$	$1.27 \cdot 10^{-2}$
13_c	60	821.2	0.98	3.50	0.21	$4.69 \cdot 10^{-2}$	$9.72 \cdot 10^{-3}$
14_a	70	801.6	1.15	4.57	0.23	$6.62 \cdot 10^{-2}$	$1.51 \cdot 10^{-2}$
14_b	70	848.0	1.07	3.57	0.19	$6.04 \cdot 10^{-2}$	$1.17 \cdot 10^{-2}$
14_c	70	859.3	1.13	4.57	0.23	$6.21 \cdot 10^{-2}$	$1.44 \cdot 10^{-2}$
15_a	75	883.1	0.91	2.80	0.18	$8.21 \cdot 10^{-2}$	$1.48 \cdot 10^{-2}$
15_b	75	788.7	0.96	3.07	0.19	$6.18 \cdot 10^{-2}$	$1.15 \cdot 10^{-2}$
15_c	75	798.3	0.97	3.47	0.21	$1.25 \cdot 10^{-1}$	$2.59 \cdot 10^{-2}$
16_a	40	1205.1	0.89	4.75	0.31	$4.33 \cdot 10^{-2}$	$1.33 \cdot 10^{-2}$
16_b	40	1202.2	0.90	4.25	0.27	$4.35 \cdot 10^{-2}$	$1.19 \cdot 10^{-2}$
16_c	40	1256.0	0.93	4.50	0.28	$5.19 \cdot 10^{-2}$	$1.45 \cdot 10^{-2}$
17_a	50	1192.2	0.91	5.20	0.33	$5.53 \cdot 10^{-2}$	$1.81 \cdot 10^{-2}$
17_b	50	1131.3	0.99	5.20	0.30	$4.17 \cdot 10^{-2}$	$1.24 \cdot 10^{-2}$
17_c	50	1203.5	0.96	4.80	0.29	$5.62 \cdot 10^{-2}$	$1.60 \cdot 10^{-2}$
18_a	60	1223.3	1.06	6.33	0.34	$5.50 \cdot 10^{-2}$	$1.85 \cdot 10^{-2}$
18_b	60	1262.0	1.16	7.50	0.36	$4.94 \cdot 10^{-2}$	$1.79 \cdot 10^{-2}$
18_c	60	1201.4	1.05	5.83	0.31	$4.23 \cdot 10^{-2}$	$1.33 \cdot 10^{-2}$
19_a	70	1310.0	0.99	4.71	0.27	$8.26 \cdot 10^{-2}$	$2.26 \cdot 10^{-2}$
19_b	70	1370.9	0.92	4.86	0.30	$5.89 \cdot 10^{-2}$	$1.78 \cdot 10^{-2}$
19_c	70	1221.5	0.93	5.00	0.31	$5.09 \cdot 10^{-2}$	$1.56 \cdot 10^{-2}$
20_a	75	1220.3	0.86	3.47	0.23	$8.96 \cdot 10^{-2}$	$2.10 \cdot 10^{-2}$
20_b	75	1220.2	0.90	4.80	0.30	$7.50 \cdot 10^{-2}$	$2.28 \cdot 10^{-2}$
20_c	75	1243.8	0.83	3.07	0.21	$1.14 \cdot 10^{-1}$	$2.44 \cdot 10^{-2}$
21_a	40	1546.5	0.94	7.50	0.45	$5.49 \cdot 10^{-2}$	$2.45 \cdot 10^{-2}$
21_b	40	1483.8	0.96	7.25	0.42	$5.85 \cdot 10^{-2}$	$2.47 \cdot 10^{-2}$
21_c	40	1348.0	0.90	6.75	0.42	$5.44 \cdot 10^{-2}$	$2.30 \cdot 10^{-2}$
22_a	50	1552.0	0.78	3.20	0.24	$8.94 \cdot 10^{-2}$	$2.13 \cdot 10^{-2}$
22_b	50	1447.1	0.89	5.20	0.33	$5.60 \cdot 10^{-2}$	$1.86 \cdot 10^{-2}$
22_c	50	1458.6	1.03	7.20	0.39	$4.95 \cdot 10^{-2}$	$1.93 \cdot 10^{-2}$
23_a	60	1492.9	1.05	7.50	0.40	$4.63 \cdot 10^{-2}$	$1.85 \cdot 10^{-2}$
23_b	60	1509.8	0.96	7.17	0.42	$5.50 \cdot 10^{-2}$	$2.29 \cdot 10^{-2}$
23_c	60	1504.0	1.08	8.67	0.44	$4.26 \cdot 10^{-2}$	$1.88 \cdot 10^{-2}$
24_a	70	1527.0	1.03	7.43	0.40	$8.32 \cdot 10^{-2}$	$3.35 \cdot 10^{-2}$
24_b	70	1453.4	0.97	7.29	0.42	$7.04 \cdot 10^{-2}$	$2.95 \cdot 10^{-2}$
24_c	70	1486.7	0.97	6.71	0.39	$5.45 \cdot 10^{-2}$	$2.13 \cdot 10^{-2}$
25_a	75	1524.6	0.95	6.80	0.40	$6.68 \cdot 10^{-2}$	$2.70 \cdot 10^{-2}$
25_b	75	1524.4	0.91	5.87	0.36	$6.64 \cdot 10^{-2}$	$2.41 \cdot 10^{-2}$
25_c	75	1504.2	0.93	6.67	0.40	$5.10 \cdot 10^{-2}$	$2.06 \cdot 10^{-2}$

Table 2. Detailed results of the experiments # 26 to # 50, porous sparger used as diffuser

# exp.	ILL (h_0), cm	GFR, $\text{ml}\cdot\text{min}^{-1}$	Bubble diameter (D_b), cm	Hold – up (ϵ), %	a , cm^{-1}	k_L , $\text{cm}\cdot\text{s}^{-1}$	$k_L\cdot a$, s^{-1}
26_a	40	259.4	0.32	1.50	0.27	$6.41\cdot 10^{-2}$	$1.75\cdot 10^{-2}$
26_b	40	229.6	0.25	1.25	0.29	$6.71\cdot 10^{-2}$	$1.95\cdot 10^{-2}$
26_c	40	253.6	0.24	1.25	0.31	$6.57\cdot 10^{-2}$	$2.01\cdot 10^{-2}$
27_a	50	237.4	0.30	1.40	0.27	$6.70\cdot 10^{-2}$	$1.83\cdot 10^{-2}$
27_b	50	253.8	0.25	1.20	0.28	$6.72\cdot 10^{-2}$	$1.91\cdot 10^{-2}$
27_c	50	231.4	0.30	0.80	0.16	$1.05\cdot 10^{-1}$	$1.69\cdot 10^{-2}$
28_a	60	261.6	0.26	0.50	0.12	$1.90\cdot 10^{-1}$	$2.21\cdot 10^{-2}$
28_b	60	257.4	0.29	2.83	0.56	$2.58\cdot 10^{-2}$	$1.44\cdot 10^{-2}$
28_c	60	252.2	0.22	0.50	0.13	$1.38\cdot 10^{-1}$	$1.83\cdot 10^{-2}$
29_a	70	257.8	0.30	1.86	0.37	$5.04\cdot 10^{-2}$	$1.86\cdot 10^{-2}$
29_b	70	233.8	0.32	2.14	0.40	$5.65\cdot 10^{-2}$	$2.23\cdot 10^{-2}$
29_c	70	230.4	0.33	1.43	0.26	$9.83\cdot 10^{-2}$	$2.53\cdot 10^{-2}$
30_a	75	254.0	0.30	0.80	0.16	$1.33\cdot 10^{-1}$	$2.09\cdot 10^{-2}$
30_b	75	255.0	0.30	1.07	0.21	$9.15\cdot 10^{-2}$	$1.91\cdot 10^{-2}$
30_c	75	254.0	0.30	0.53	0.10	$1.76\cdot 10^{-1}$	$1.85\cdot 10^{-2}$
31_a	40	533.0	0.35	3.50	0.57	$6.04\cdot 10^{-2}$	$3.46\cdot 10^{-2}$
31_b	40	538.6	0.31	3.75	0.69	$6.12\cdot 10^{-2}$	$4.24\cdot 10^{-2}$
31_c	40	551.4	0.39	2.00	0.30	$1.06\cdot 10^{-1}$	$3.19\cdot 10^{-2}$
32_a	50	544.3	0.39	2.80	0.42	$1.01\cdot 10^{-1}$	$4.22\cdot 10^{-2}$
32_b	50	556.2	0.39	2.60	0.39	$6.99\cdot 10^{-2}$	$2.73\cdot 10^{-2}$
32_c	50	555.8	0.32	3.20	0.60	$9.09\cdot 10^{-2}$	$5.43\cdot 10^{-2}$
33_a	60	558.0	0.32	4.00	0.73	$6.05\cdot 10^{-2}$	$4.41\cdot 10^{-2}$
33_b	60	491.8	0.26	3.83	0.86	$4.29\cdot 10^{-2}$	$3.67\cdot 10^{-2}$
33_c	60	493.2	0.32	3.83	0.69	$3.65\cdot 10^{-2}$	$2.52\cdot 10^{-2}$
34_a	70	543.0	0.36	3.86	0.61	$5.33\cdot 10^{-2}$	$3.27\cdot 10^{-2}$
34_b	70	542.2	0.36	3.86	0.61	$6.69\cdot 10^{-2}$	$4.10\cdot 10^{-2}$
34_c	70	530.4	0.36	3.86	0.61	$7.59\cdot 10^{-2}$	$4.65\cdot 10^{-2}$
35_a	75	554.2	0.40	4.53	0.64	$5.01\cdot 10^{-2}$	$3.21\cdot 10^{-2}$
35_b	75	536.6	0.40	4.00	0.57	$8.68\cdot 10^{-2}$	$4.94\cdot 10^{-2}$
35_c	75	560.8	0.40	3.73	0.53	$6.55\cdot 10^{-2}$	$3.49\cdot 10^{-2}$
36_a	40	802.9	0.39	5.00	0.73	$1.03\cdot 10^{-1}$	$7.54\cdot 10^{-2}$
36_b	40	672.8	0.40	7.00	0.99	$4.65\cdot 10^{-2}$	$4.58\cdot 10^{-2}$
36_c	40	846.4	0.32	4.75	0.85	$6.14\cdot 10^{-2}$	$5.21\cdot 10^{-2}$
37_a	50	786.0	0.41	6.40	0.88	$5.52\cdot 10^{-2}$	$4.85\cdot 10^{-2}$
37_b	50	847.0	0.33	6.20	1.07	$8.19\cdot 10^{-2}$	$8.78\cdot 10^{-2}$
37_c	50	852.9	0.43	7.20	0.94	$6.88\cdot 10^{-2}$	$6.47\cdot 10^{-2}$
38_a	60	870.8	0.35	6.17	1.00	$6.54\cdot 10^{-2}$	$6.56\cdot 10^{-2}$
38_b	60	870.0	0.54	6.50	0.67	$8.13\cdot 10^{-2}$	$5.46\cdot 10^{-2}$
38_c	60	983.6	0.32	6.33	1.11	$4.93\cdot 10^{-2}$	$5.49\cdot 10^{-2}$
39_a	70	931.5	0.31	6.14	1.12	$6.04\cdot 10^{-2}$	$6.77\cdot 10^{-2}$
39_b	70	928.4	0.37	5.71	0.88	$6.42\cdot 10^{-2}$	$5.68\cdot 10^{-2}$

39_c	70	914.9	0.34	5.71	0.94	$6.80 \cdot 10^{-2}$	$6.39 \cdot 10^{-2}$
40_a	75	840.7	0.45	8.40	1.02	$9.58 \cdot 10^{-3}$	$9.80 \cdot 10^{-3}$
40_b	75	773.8	0.36	8.53	1.31	$2.00 \cdot 10^{-2}$	$2.61 \cdot 10^{-2}$
40_c	75	901.8	0.31	8.93	1.56	$3.79 \cdot 10^{-2}$	$5.92 \cdot 10^{-2}$
41_a	40	1375.2	0.42	9.75	1.25	$5.26 \cdot 10^{-2}$	$6.59 \cdot 10^{-2}$
41_b	40	1389.2	0.39	9.00	1.26	$5.73 \cdot 10^{-2}$	$7.24 \cdot 10^{-2}$
41_c	40	1304.8	0.46	10.00	1.19	$9.39 \cdot 10^{-2}$	$1.12 \cdot 10^{-1}$
42_a	50	1311.6	0.54	8.60	0.87	$1.12 \cdot 10^{-1}$	$9.79 \cdot 10^{-2}$
42_b	50	1311.6	0.41	7.80	1.05	$7.90 \cdot 10^{-2}$	$8.33 \cdot 10^{-2}$
42_c	50	1317.1	0.42	10.60	1.38	$5.53 \cdot 10^{-2}$	$7.64 \cdot 10^{-2}$
43_a	60	1333.6	0.36	9.67	1.48	$4.36 \cdot 10^{-2}$	$6.44 \cdot 10^{-2}$
43_b	60	1352.4	0.26	9.00	1.94	$6.20 \cdot 10^{-2}$	$1.20 \cdot 10^{-1}$
43_c	60	1326.9	0.27	9.67	1.95	$6.80 \cdot 10^{-2}$	$1.33 \cdot 10^{-1}$
44_a	70	1247.6	0.41	10.00	1.32	$4.15 \cdot 10^{-2}$	$5.49 \cdot 10^{-2}$
44_b	70	1383.6	0.39	9.71	1.35	$3.87 \cdot 10^{-2}$	$5.23 \cdot 10^{-2}$
44_c	70	1378.0	0.37	10.29	1.52	$3.97 \cdot 10^{-2}$	$6.04 \cdot 10^{-2}$
45_a	75	1325.6	0.45	10.40	1.27	$4.32 \cdot 10^{-2}$	$5.46 \cdot 10^{-2}$
45_b	75	1365.6	0.37	10.27	1.51	$4.67 \cdot 10^{-2}$	$7.04 \cdot 10^{-2}$
45_c	75	1338.4	0.38	10.40	1.49	$3.60 \cdot 10^{-2}$	$5.37 \cdot 10^{-2}$
46_a	40	1656.0	0.39	12.25	1.67	$5.97 \cdot 10^{-2}$	$9.96 \cdot 10^{-2}$
46_b	40	1826.0	0.37	11.25	1.65	$4.00 \cdot 10^{-2}$	$6.60 \cdot 10^{-2}$
46_c	40	1603.6	0.34	12.00	1.90	$3.97 \cdot 10^{-2}$	$7.54 \cdot 10^{-2}$
47_a	50	1555.7	0.36	12.80	1.91	$4.59 \cdot 10^{-2}$	$8.77 \cdot 10^{-2}$
47_b	50	1537.6	0.45	13.00	1.52	$6.70 \cdot 10^{-2}$	$1.02 \cdot 10^{-1}$
47_c	50	1606.6	0.32	13.60	2.22	$4.16 \cdot 10^{-2}$	$9.24 \cdot 10^{-2}$
48_a	60	1630.8	0.48	12.33	1.38	$5.48 \cdot 10^{-2}$	$7.56 \cdot 10^{-2}$
48_b	60	1639.2	0.34	12.67	1.98	$4.26 \cdot 10^{-2}$	$8.44 \cdot 10^{-2}$
48_c	60	1689.2	0.46	12.67	1.45	$5.20 \cdot 10^{-2}$	$7.55 \cdot 10^{-2}$
49_a	70	1658.0	0.49	13.14	1.43	$4.73 \cdot 10^{-2}$	$6.77 \cdot 10^{-2}$
49_b	70	1607.6	0.41	13.43	1.71	$2.20 \cdot 10^{-2}$	$3.75 \cdot 10^{-2}$
49_c	70	1938.4	0.35	12.86	1.93	$3.45 \cdot 10^{-2}$	$6.65 \cdot 10^{-2}$
50_a	75	1731.0	0.42	12.53	1.58	$3.83 \cdot 10^{-2}$	$6.05 \cdot 10^{-2}$
50_b	75	1534.0	0.53	12.13	1.22	$7.00 \cdot 10^{-2}$	$8.53 \cdot 10^{-2}$
50_c	75	1583.2	0.45	13.07	1.55	$5.64 \cdot 10^{-2}$	$8.75 \cdot 10^{-2}$

Table 3. Values of the hold – up predicted by the correlations selected

# exp.	Kumar (K), %	Hughmark (HU), %	Hikita (HI), %	Hikita and Kikukawa (HK), %	Correlation proposed (CP), %
1	0.85	0.54	1.63	2.67	0.81
2	2.10	1.33	2.77	4.11	2.04
3	3.42	2.16	3.68	5.18	3.35
4	4.99	3.13	4.61	6.22	4.97
5	5.91	3.70	5.13	6.78	5.94
6	0.85	0.54	1.63	2.67	0.81
7	2.10	1.33	2.77	4.11	2.04
8	3.55	2.24	3.76	5.27	3.49
9	4.81	3.02	4.51	6.11	4.79
10	6.01	3.76	5.19	6.85	6.05
11	0.85	0.54	1.63	2.67	0.81
12	2.10	1.33	2.77	4.11	2.04
13	3.52	2.22	3.75	5.25	3.45
14	5.02	3.15	4.64	6.25	5.00
15	6.08	3.80	5.22	6.88	6.12
16	0.85	0.54	1.63	2.67	0.81
17	2.10	1.33	2.77	4.10	2.04
18	3.47	2.19	3.72	5.22	3.40
19	5.30	3.33	4.79	6.42	5.30
20	6.03	3.77	5.19	6.85	6.06
21	0.85	0.54	1.63	2.67	0.81
22	2.10	1.33	2.77	4.10	2.04
23	3.42	2.16	3.68	5.18	3.35
24	5.02	3.15	4.64	6.25	5.00
25	6.14	3.84	5.26	6.92	6.18
26	1.05	0.67	1.84	2.95	1.22
27	2.27	1.44	2.90	4.27	3.02
28	3.22	2.03	3.55	5.03	4.75
29	5.52	3.46	4.90	6.53	10.16
30	6.81	4.25	5.60	7.28	14.08
31	1.02	0.65	1.82	2.91	1.18
32	2.31	1.47	2.93	4.30	3.10
33	3.44	2.17	3.69	5.19	5.18
34	5.35	3.36	4.81	6.44	9.70
35	6.32	3.95	5.35	7.02	12.51
36	1.09	0.69	1.89	3.00	1.27
37	2.16	1.37	2.81	4.16	2.85
38	3.76	2.37	3.89	5.42	5.85
39	5.44	3.41	4.87	6.50	9.96
40	6.65	4.15	5.52	7.20	13.54
41	1.02	0.65	1.81	2.91	1.18
42	2.26	1.43	2.89	4.25	3.01

43	3.82	2.41	3.94	5.47	5.99
44	5.44	3.41	4.87	6.50	9.95
45	6.95	4.34	5.67	7.35	14.60
46	1.08	0.69	1.87	2.99	1.25
47	2.31	1.46	2.92	4.29	3.09
48	3.48	2.20	3.72	5.23	5.27
49	5.47	3.43	4.89	6.52	10.02
50	6.51	4.07	5.45	7.12	13.11

Table 4. Values of the diameter of the bubble predicted by the correlations selected

# Exp.	Bhavaraju et al (B), cm	Gaddis and Vogelphol (GV), cm	Moo - Young and Blanch (MYB), cm	Leibson (L), cm	Proposed correlation, cm
1	0.54	0.26	0.27	0.26	0.59
2	0.72	0.38	0.36	0.35	0.79
3	0.85	0.46	0.42	0.41	0.93
4	0.97	0.54	0.48	0.47	1.06
5	1.02	0.58	0.50	0.50	1.12
6	0.54	0.26	0.27	0.26	0.59
7	0.72	0.38	0.36	0.35	0.79
8	0.86	0.47	0.43	0.42	0.95
9	0.96	0.53	0.47	0.46	1.05
10	1.03	0.58	0.51	0.50	1.12
11	0.54	0.26	0.27	0.26	0.59
12	0.72	0.38	0.36	0.35	0.79
13	0.86	0.47	0.42	0.42	0.94
14	0.97	0.54	0.48	0.47	1.06
15	1.03	0.58	0.51	0.50	1.13
16	0.54	0.26	0.27	0.26	0.59
17	0.72	0.38	0.36	0.35	0.79
18	0.86	0.46	0.42	0.41	0.94
19	0.99	0.55	0.49	0.48	1.08
20	1.03	0.58	0.51	0.50	1.13
21	0.54	0.26	0.27	0.26	0.59
22	0.72	0.38	0.36	0.35	0.79
23	0.85	0.46	0.42	0.41	0.93
24	0.97	0.54	0.48	0.47	1.06
25	1.03	0.59	0.51	0.50	1.13
26	0.58	0.28	0.29	0.28	0.24
27	0.74	0.39	0.37	0.36	0.31
28	0.83	0.45	0.41	0.40	0.35
29	1.01	0.56	0.49	0.49	0.42
30	1.07	0.61	0.53	0.52	0.45
31	0.57	0.28	0.28	0.27	0.24
32	0.75	0.39	0.37	0.36	0.31

33	0.86	0.46	0.42	0.41	0.36
34	0.99	0.55	0.49	0.48	0.42
35	1.04	0.59	0.52	0.51	0.44
36	0.58	0.29	0.29	0.28	0.25
37	0.73	0.38	0.36	0.35	0.31
38	0.88	0.48	0.43	0.43	0.37
39	1.00	0.56	0.49	0.48	0.42
40	1.06	0.61	0.52	0.52	0.45
41	0.57	0.28	0.28	0.27	0.24
42	0.74	0.39	0.37	0.36	0.31
43	0.88	0.48	0.44	0.43	0.37
44	1.00	0.56	0.49	0.48	0.42
45	1.08	0.62	0.53	0.53	0.45
46	0.58	0.29	0.29	0.28	0.25
47	0.75	0.39	0.37	0.36	0.31
48	0.86	0.46	0.42	0.41	0.36
49	1.00	0.56	0.49	0.48	0.42
50	1.05	0.71	0.52	0.51	0.44

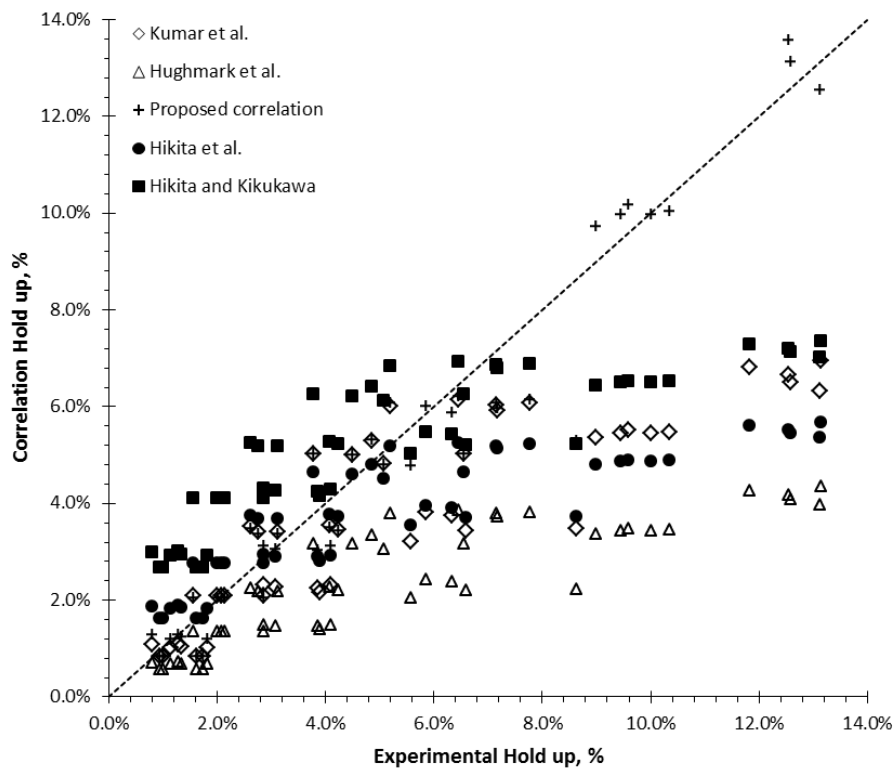


Figure 1. Comparison of the accuracy of the correlations used to the prediction of the hold – up values

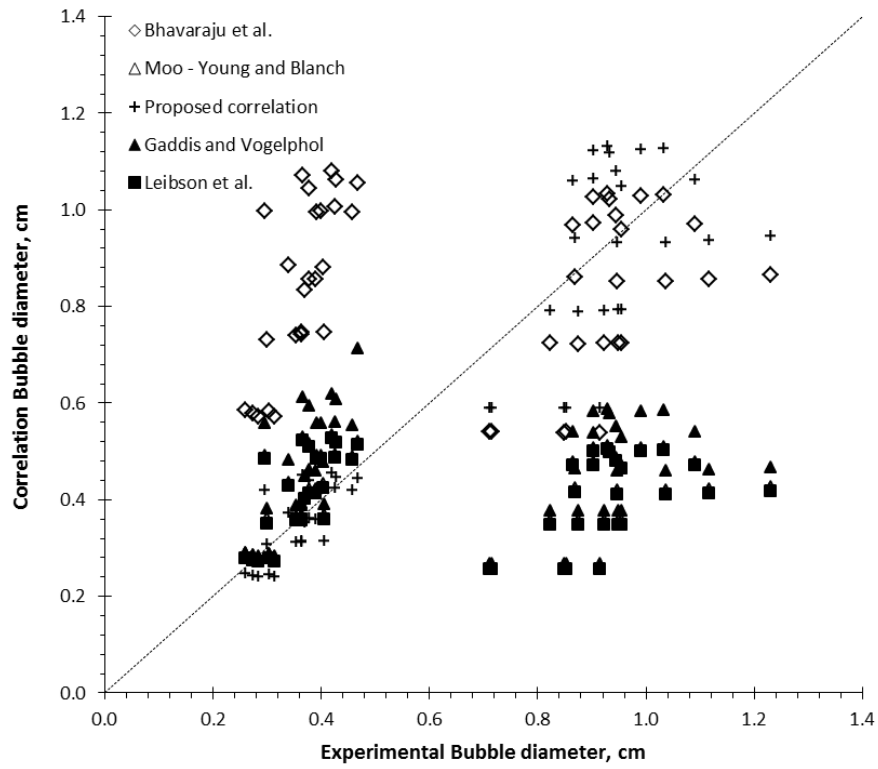


Figure 2. Comparison of the accuracy of the correlations used to the prediction of the bubble's diameter values

APPENDIX III

Direct synthesis of H_2O_2 in a slurry bubble column.

Design and preliminar analysis

A.1. Slurry bubble columns. Applications and design.

Heterogeneous reactions (between gas, liquid and solid phases) are important in so many industrial processes. The bubble column reactors (BCR) (or slurry bubble column reactor (SBCR) if there is a solid phase) offers an attractive alternative to carry out gas – liquid and gas – liquid – solid reactions. Although the BC has a simple construction and operation the bubble column reactors have an inherent limitation since the system presents some degrees of freedom that depend on the system characteristics and the operation conditions. Applications of bubble column and slurry bubble column reactor on industrial processes are large (Table 1), since these types of reactors provide a high mass and heat transfer coefficients.

Table 1. Some applications of bubble column and slurry bubble column reactors[1, 2]

Process	Reactants	Main Products
Oxidation	ethylene, cumene, butane, toluene, xylene, ethylbenzene, acetaldehyde, cyclohexane, cyclohexene, n-paraffins, glucose	vinyl acetate, phenol, acetone, methyl ethyl ketone, benzoic acid, phthalic acid, acetophenone, acetic acid, acetic anhydride cyclohexanol and cyclohexanone, adipic acid, sec-alcohols, glutonic acid
Chlorination	aliphatic hydrocarbons, aromatic hydrocarbons	chloroparaffins, chlorinated aromatics
Alkylation	ethanol, propylene, benzene, toluene	ethyl benzene, cumene, iso-butyl benzene
Hydroformylation	olefins	aldehydes, alcohols
Carbonylation	methanol, ethanol	acetic acid, acetic anhydride, propionic acid
Hydrogenation	benzene, adipic acid dinitrile, nitroaromatics, glucose, ammonium nitrate, unsaturated fatty acids, CO/H ₂	cyclohexane, hexamethylene diamine, amines, sorbitol, hydroxyl amines, methanol, Fischer – Tropsch synthesis
Gas to Liquid fuels	F–T synthesis, methanol from syngas	liquid fuels
Coal liquification	coal	liquid fuels
Desulfurization	desulfurized fractions	petroleum fractions
Aerobic Bio – chemical processes	molasses	ethanol

As for the rest of the reactor type, the engineering and design of a bubble column begins with the analysis of the process requirement and the selection of the reaction configuration. So many types of bubble columns and slurry bubble columns reactors are possible according to the system configuration and the operation mode selected (Figure 1).

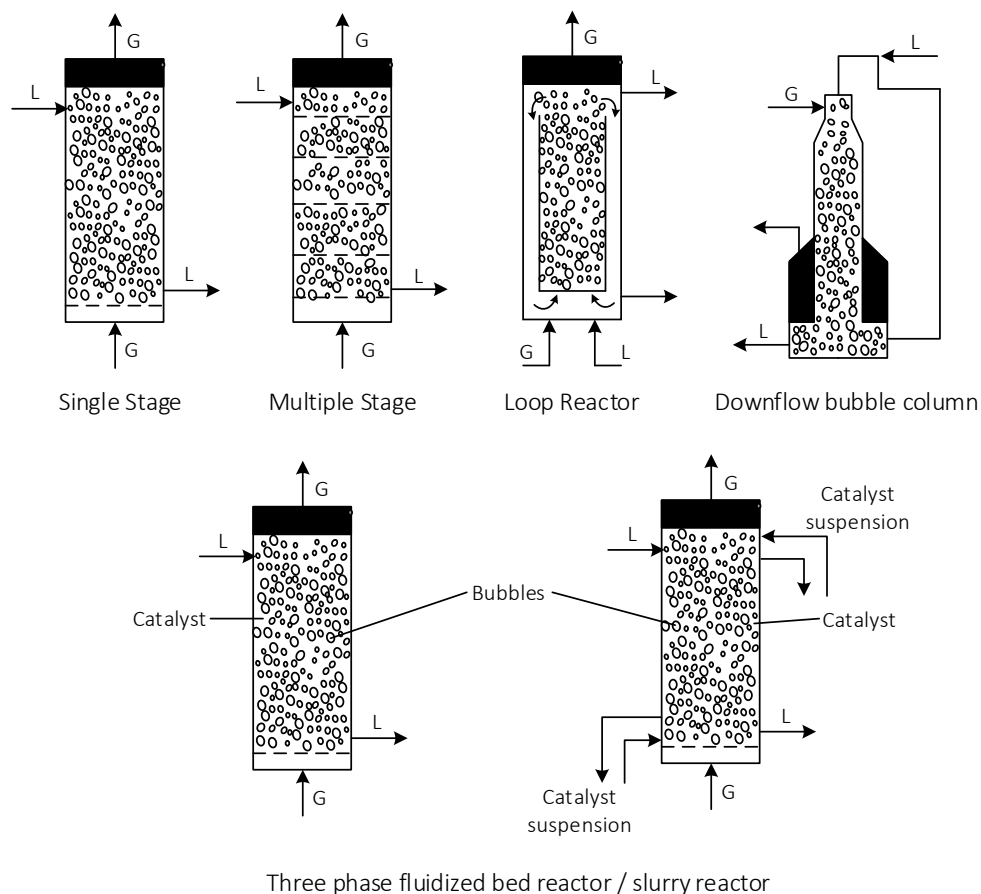


Figure 1. Types of bubble column reactors (adapted form Lee and Tsui) [3]

The use of solid catalyst on liquid – gas columns is key for heterogeneous processes that will be not possible without the addition of the solid. In the slurry bubble columns the solid is used in powdered form by what it is supposed that the solid is distributed along the column and it moves according to its interactions with the gas phase and the liquid phase. The presence of solid particles inside the reactor could further complicated the fluid dynamic of a bubble reactor since the influence of the solid particles on the interaction between the liquid phase and the bubbles depends on mean particle size, size distribution, particle density and solid volume fraction.

Slurry catalytic reactors are a viable alternative for high pressure reactions since this reactor configuration provides:

- a wide range of available reaction pressure (5 – 150 bar)

- a high heat transfer coefficient, if the absorption of the heat reaction is required with a slurry bubble column reactor an isothermal process is possible
- low pressure drop along the reactor
- an excellent wetting of the solid particles

As for the design and operation of a bubble column reactor, backmixing of the liquid phase must be taken into the account but also the needed of the separation of the liquid and the solid phase after the reaction.

A.1.1. General aspects for the design of slurry bubble column reactors

Liquid – solid phase properties. The effective properties of the liquid – solid suspension is necessary for the application of the prediction equations. The slurry could be a heterogeneous or homogeneous solid – liquid phase in function to the density, size and concentration of the particles. If the particle size is smaller than 50 μm and the concentration (in mass) is lower than the 16 % it could be assumed that the suspension is homogeneous and the equivalent suspension density could be calculated on base on the solid and liquid proportional density[4]. For the calculation of viscosity and other properties needed for the design the concentration of the suspension must be considered. Different expressions are available for dilute or concentrated suspensions.

Flow regime. As for all the systems in which some phases are involved different flow regimen could be expected. In bubble columns and slurry bubble columns the gas is sparer from the bottom of the reactor through the liquid column. The net liquid flow rate might be co – current or counter – current to the gas flow direction or the system could operate with a batch liquid phase. The bubbling of the gas phase into the liquid phase generated some different flow regimes, homogeneous, heterogeneous regime and slug flow (Figure 2). The kind of flow regime that dominates the system depends greatly on the size of the bubble inside the liquid column. When porous plates are uses as sparger uniform size bubbles are created and the gas is uniformly distributed across the bottom of the column.

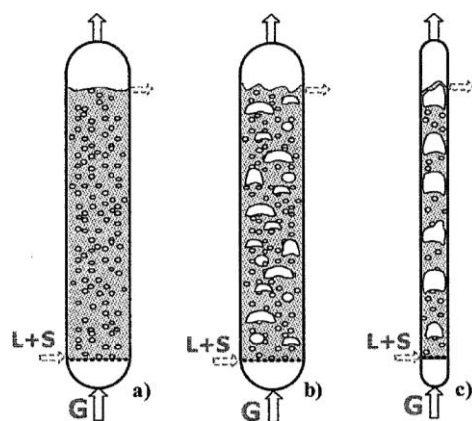


Figure 2. Schematic representation of slurry bubble columns. a) Homogeneous bubble flow, b) heterogeneous churn – turbulent flow, c) Slug flow

In general it is accepted that homogenous regime occurs when a low gas velocity are used ($< 5 \text{ cm}\cdot\text{s}^{-1}$) and a narrow bubble size distribution is observed. At higher velocities ($< 7 \text{ cm}\cdot\text{s}^{-1}$) heterogeneous and churn – turbulent flow regime could appears. The slug flow regime generally only appears in small diameter column ($< 0.15 \text{ m}$). Transitional velocities from homogeneous to heterogeneous regime are only approximately values, since it is not possible to set a single value. Thorat and Joshi [5] reported that the transitional velocity depends on the column geometry, the sparger design and the physical properties of the system. On Table 2 the value of the transitional velocities proposed by some authors are summarized.

Table 2. Experimental values of transition velocity for bubble columns (air – water)

Research Group	$V_{g,trans} \text{ (m}\cdot\text{s}^{-1}\text{)}$
Bach and Pilhofer [6]	0.046
Oels <i>et al.</i> [7]	0.039
Krishna <i>et al.</i> [8]	0.033
Yamashita and Inuoe [7]	0.040
Hyndman <i>et al.</i> [9]	0.037

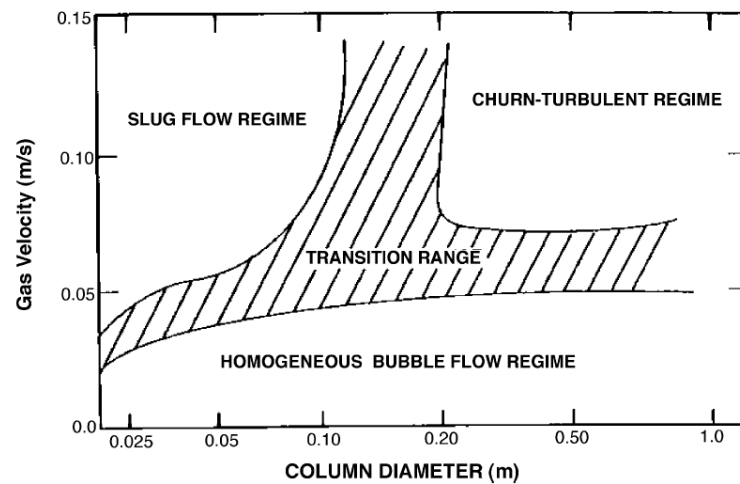


Figure 3. Flow regime map for bubble columns [7]

Homogeneous regime is unstable and a small variation on the gas flow rate or perturbations of the process can cause the transition to the heterogeneous regime. In the heterogeneous regime significant bubble – bubble interactions occur and the break up and coalescence phenomena generate that the bubble size distribution change along the column. The analysis of some authors showed up that the bubbles move to the centre of the column while they rose along the column and that on consequence the hold – up profile was not uniform, with a maximum on the column centre. The non – uniform movement of the bubbles leads to strong macroscopic internal liquid circulation in the column with upflow in the central region and downflow in the near – wall region. On consequence, the internal re – circulation generated an increasing backmixing that it is considered one of the main drawbacks of the bubble column reactors. Backmixing effect could be reduce by the design and selection of an internal devices, like draft tubes, radial baffles, *etc.* that control the flow inside the column.

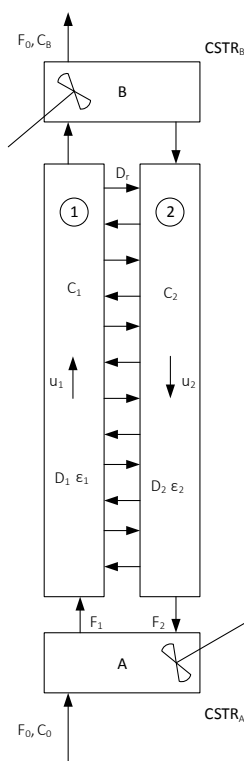
Distributor design. Orifice diameter and its distribution along the sparger surface have a vital importance on the column hydrodynamics. Wilkinson *et al.* [10] concluded that for sparger orifice larger than 1 to 2 mm the sparger design has not influence over the system behavior. Spargers with small holes generate higher hold – up values but the risk of clogging is higher and the system should be carefully controlled. For sparger design is very important to keep the same flow rate in each orifice to ensure that that the gas is homogeneously distributed. Three factors have to be calculated:

- the kinetic energy of the gas at the inlet pipe
- the pressure lost along the pipe
- the pressure lost along each orifice

Mass and heat transfer parameters. For the design of a slurry bubble column reactor so many other parameters might be to be calculated. Some of them are: the critical gas velocity for complete particle suspension [11], gas hold – up [12], gas/liquid mass transfer coefficients [2, 13], axial dispersion coefficients [14, 15] and heat transfer coefficients[4]. There is not just one equation or expression to the calculation of these parameters since they are based on experimental observation and the adjustment of experimental values. Because of that the most appropriate expression should be selected according to the experimental conditions are fixed. Even if none of the correlations found out on the bibliography references are good enough a specific expression could be obtained by the building of a similar small scale device.

Slurry bubble columns modelling: axial dispersion model. The axial dispersion model is the most popular model for describing a slurry bubble column reactor. Although this model allows introducing the backmixing phenomena, some aspects of the applicability of the axial dispersion model on the slurry bubble columns might be considered as [2]:

- the use of a unique dispersion coefficient for the macroscopic circulation and axial and radial flow in the continuous phase
- the capability to differentiate between the different classes of bubbles that may exist



One of the models proposed on literature is the two – compartment convective – diffusion model [16] (Figure 4). An extensive study using the computer – aided radioactive particle tracking method showed up that, if the superficial gas velocity is high enough and for high aspect ratio columns, the large – scale liquid circulation cells occupies most of the column height, whit the liquid phase ascending along the central core region and descending by the annular section between the core and the column’s walls. The liquid recirculation is due to the non – uniform radial hold – up profiles (since there is more gas in the center of the column).

Figure 4. Model schematic for slurry bubble column reactors (adapted from [16])

In a general view, some of the main issues that must be taken into account for the design of a bubble column reactor or a slurry bubble column reactor are summarized in the Figure 5. Most of the design applications are based on models that combine empirical correlations, pilot scale experiments and CFD prediction modelling. Typical models available on bibliography references are used to select the feasible operational window and determinate the sensitivity of the reactor to the backmixing, mass transfer coefficient, heat transfer coefficient, interfacial area and operating regime. However, even the most detailed models are not capable to predict in a detailed way the influence of the reaction conditions and the characteristics of the system.

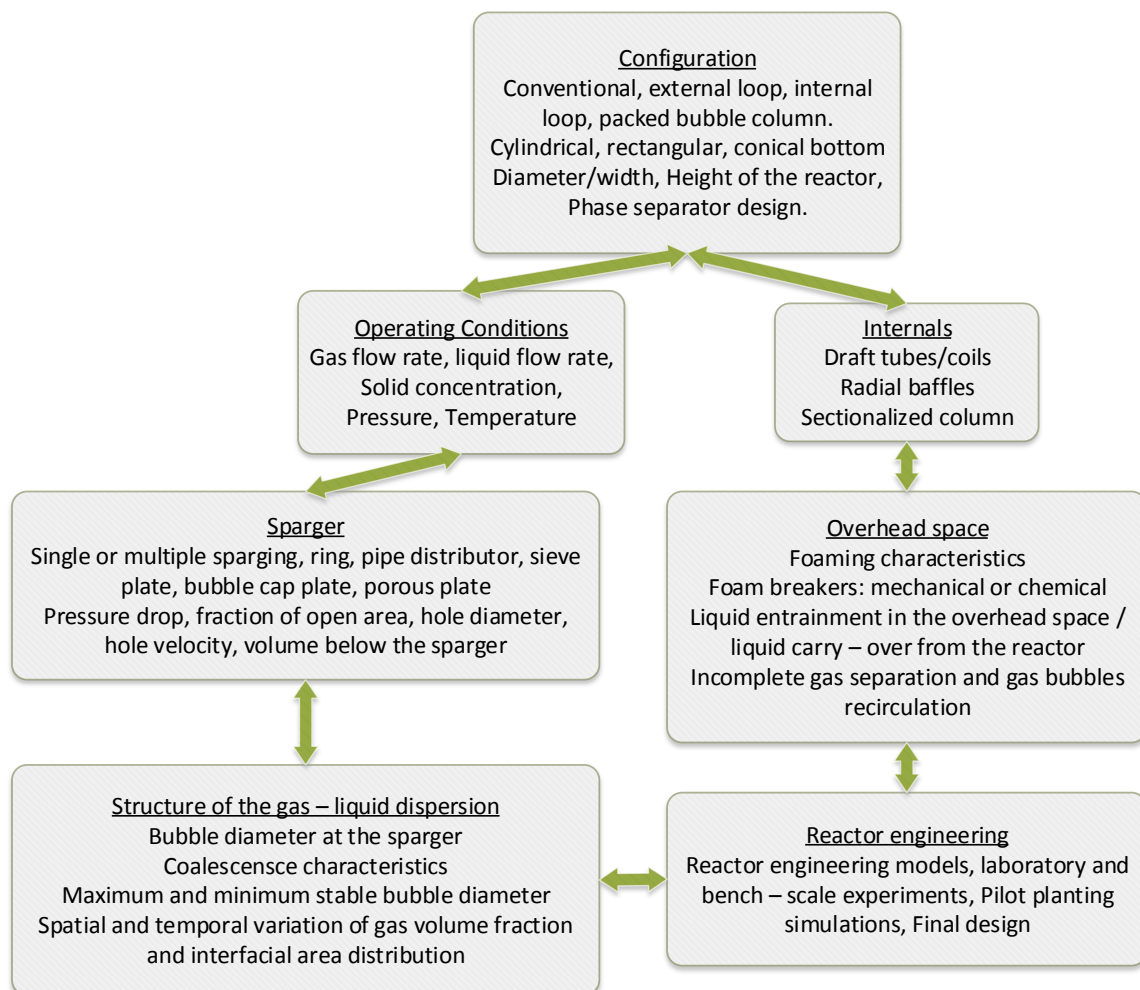


Figure 5. Relevant issues on the design of a slurry bubble column reactor

According to some of the engineering models for the design of a slurry bubble column reactor the design must ensure that:

- the system operates in a churn – turbulent regime over the specific gas flow rate range

- a minimum volumetric mass transfer coefficient and heat transfer coefficient are provided
- the gas distribution is radially and axially uniform
- the mixing is adequate and the mixing time is lower than the specific time
- the liquid droplets with the escaping gas are less than the specified mass flow rate

As it could be deduced for the discussion of the previous paragraphs, the design of a slurry bubble column reactor could be a very complicated and delicate process in which some many variables and phenomena must be taken into an account. Before the design and build of a high pressure SBCR a step by step approximation to the final design have been carried out in order to determinate if the process is possible and what could be the most optimal conditions and dimensions.

A.1.2. Pre – design of a slurry bubble column reactor: calculation of hydrodynamic parameters

In order to determinate the capability of the bibliographic references in the design of a slurry bubble column reactor a simplified calculation of the most important hydrodynamic parameters have been done. A huge amount of models and equations for the calculation of the hydrodynamic parameters are available on the bibliography libraries, however most of these researches are focus on the calculation of just one of the parameters needed. That difficult enormously the complete design of a slurry bubble column since the conditions of applicability of each correlation are different. Luft *et al.* [2] proposed a group of equations obtained by some different authors but completely compatible. Only final calculations are reported.

Definition of the design specifications

Influence of some of the operation conditions were analysed. As the system has to operate at different values of pressure, temperature, gas flow rate and liquid flow rate so different design cases (DC) have been defined. Maxima and minima values have been fixed according to the reaction conditions for the hydrogen peroxide direct synthesis (Table 3). Gas composition (H₂/O₂/N₂: 4%/20.2%/75.8% mass), column dimensions (height: 760 cm, internal diameter: 4.7 cm) and sparger geometry (microporous plate) were kept constant.

Table 3. Design specification for preliminary design calculations

# DC	Gas flow rate mlN·min ⁻¹	Pressure barg	Temperature °C	Liquid flow rate ml·min ⁻¹
01	200	20	10	0.1
02	200	20	10	10
03	200	20	60	0.1
04	200	20	60	10
05	200	90	10	0.1
06	200	90	10	10
07	200	90	60	0.1
08	200	90	60	10
09	3500	20	10	0.1
10	3500	20	10	10
11	3500	20	60	0.1
12	3500	20	60	10
13	3500	90	10	0.1
14	3500	90	10	10
15	3500	90	60	0.1
16	3500	90	60	10

Effective properties

Properties of the gas phase have been calculated from the properties of the pure gases and the molar fraction of each gas. Catalyst activity has proved to be extremely high and on consequence the amount of catalyst needed in the reaction is too much lower (10 mg – 500 mg). Since the maximum catalyst concentration in the liquid phase is about 0.05 % wt., properties of the slurry phase (liquid + solid) can be compared to the properties of the liquid phase.

Table 4. Gas, slurry and solid phase's basic properties

Pressure barg	Temperature °C	ρ_{SL} kg·m ⁻³	μ_{SL} kg·m ⁻¹ ·s ⁻¹	ρ_G kg·m ⁻³	μ_G kg·m ⁻¹ ·s ⁻¹	ρ_s kg·m ⁻³	σ N·m ⁻¹	Diffusivity m ² ·s ⁻¹
20	10	1000.6	$1.30 \cdot 10^{-3}$	24.63	$1.80 \cdot 10^{-5}$			
20	60	984.02	$4.67 \cdot 10^{-4}$	20.77	$2.03 \cdot 10^{-5}$	1491.9	$7.28 \cdot 10^{-2}$	$2.58 \cdot 10^{-9}$
90	10	1003.9	$1.30 \cdot 10^{-3}$	112.1	$1.96 \cdot 10^{-5}$			
90	60	987.05	$4.68 \cdot 10^{-4}$	92.57	$2.16 \cdot 10^{-5}$			

Flow regime

Flow regime inside the column is determinate by the column geometry and the superficial gas velocity. As the column has a small diameter (4.7 cm) the flow regime for all the design cases proposed is homogeneous, although for the highest superficial gas velocity proposed the flow regime was closed to the transitional zone from the homogeneous to the slug flow regime.

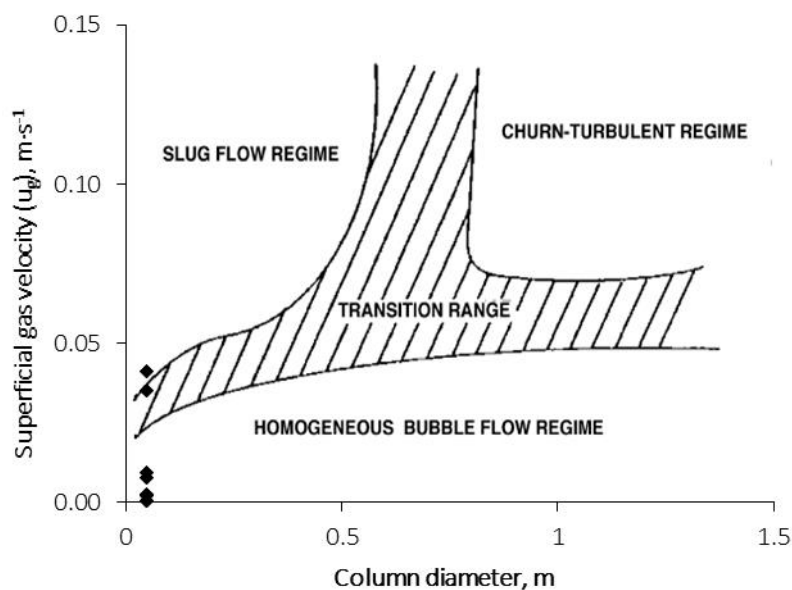


Figure 6. Flow regime diagram for design cases selected (adapted from [7])

Hydrodynamic parameters

Using the equations proposed by Luft *et al.* [2] the main hydrodynamic parameters have been calculated. All the parameters have been calculated using the basic properties summarized in the Table 4 and the operation conditions on the Table 3. Values obtained with the expressions proposed by Luft *et al.* will be compared with the values obtained experimentally when it would be possible.

Table 5. Summary of the hydrodynamic parameters obtained with the method proposed by Luft *et al.* [2]

# DC	u_{gc}/u_s	Mo_L	ε_G , %	d_b , mm	k_L , $m \cdot s^{-1}$
01	2.84	$3.39 \cdot 10^{-11}$	0.11%	5.60	$3.22 \cdot 10^{-4}$
02	0.94	$3.39 \cdot 10^{-11}$	0.11%	5.60	$3.22 \cdot 10^{-4}$
03	2.93	$5.97 \cdot 10^{-13}$	0.13%	4.70	$3.82 \cdot 10^{-4}$
04	0.97	$5.97 \cdot 10^{-13}$	0.13%	4.70	$3.82 \cdot 10^{-4}$
05	2.82	$3.27 \cdot 10^{-11}$	0.19%	3.81	$3.23 \cdot 10^{-4}$
06	0.93	$3.27 \cdot 10^{-11}$	0.19%	3.81	$3.23 \cdot 10^{-4}$
07	2.91	$5.97 \cdot 10^{-13}$	0.22%	3.24	$3.81 \cdot 10^{-4}$
08	0.96	$5.97 \cdot 10^{-13}$	0.22%	3.24	$3.81 \cdot 10^{-4}$
09	2.84	$3.39 \cdot 10^{-11}$	0.85%	2.98	$3.22 \cdot 10^{-4}$
10	0.94	$3.39 \cdot 10^{-11}$	0.85%	2.98	$3.22 \cdot 10^{-4}$
11	2.93	$5.97 \cdot 10^{-13}$	0.91%	2.50	$3.82 \cdot 10^{-4}$
12	0.97	$5.97 \cdot 10^{-13}$	0.91%	2.50	$3.82 \cdot 10^{-4}$
13	2.82	$3.27 \cdot 10^{-11}$	1.40%	2.03	$3.23 \cdot 10^{-4}$
14	0.93	$3.27 \cdot 10^{-11}$	1.40%	2.03	$3.23 \cdot 10^{-4}$
15	2.91	$5.97 \cdot 10^{-13}$	1.53%	1.73	$3.81 \cdot 10^{-4}$
16	0.96	$5.97 \cdot 10^{-13}$	1.53%	1.73	$3.81 \cdot 10^{-4}$

A.2. Direct synthesis of H₂O₂ in a low pressure slurry bubble column

As the main objective of the design of a slurry bubble column is the direct synthesis of hydrogen peroxide it could be logical to assume that the first stage on the design might be the related with the reaction. The build-up of a low pressure slurry bubble column reactor allowed us to confirm that the direct synthesis of hydrogen peroxide in a slurry bubble column reactor it is possible and gave us some information about the fluidization properties of the catalyst.

A.2.1. *Materials*

All the experiments have been carried out using deionized water as liquid phase. To avoid decomposition and hydrogenation of the hydrogen peroxide, phosphoric acid and sodium bromide (PRS-Codex, Panreac Química, Spain) have been used as promoter. KI (PRS-Codex, Panreac Química), H₂SO₄ (PA-ISO, Panreac Química) and Na₂S₂O₃·5H₂O (PA-ACS, Panreac Química) were used for conventional iodometric titration. Catalysts used for these experiments was active carbon microparticles with an palladium concentration of 5 % wt. Pd₀ (3–5 nm size) purchased from Aldrich and used fresh without pretreatment for each experiment. Compressed air and premier grade hydrogen and argon were purchased from Carburros Metálicos (Spain) and used without further modification.

A.2.2. *Experimental setup*

Experimental setup was composed by a see-through methacrylate column with an I.D. = 4.7 cm and 90 cm of length (R – 01). A porous plate with an average porous diameter of 1 μm was used as diffuser. To avoid that the liquid phase carried out the catalyst out of the column a microporous filter was set on the top of the reactor. Volumetric mass flow was measured and fixed by a controller BRONKHORST model EL – FLOW with an operation range from 80 mLN·min⁻¹ to 2000 mLN·min⁻¹ for the air stream and for 20 mLN·min⁻¹ to 400 for the hydrogen mLN·min⁻¹ (.). Pressure was fixed using a Bourdon type manometer and a back – pressure valve. A product vessel connected with the out stream act as gas – liquid separator (D – 04). Hydrogen and air were provided from the gas cylinders (D – 02 and D – 03). Liquid phase, composed by the water and the promoters provided for the liquid phase tank (D – 01) and was pumped to the reactor by a Jasco HPLC pump (0.1 – 10 ml·min⁻¹) (P – 01).

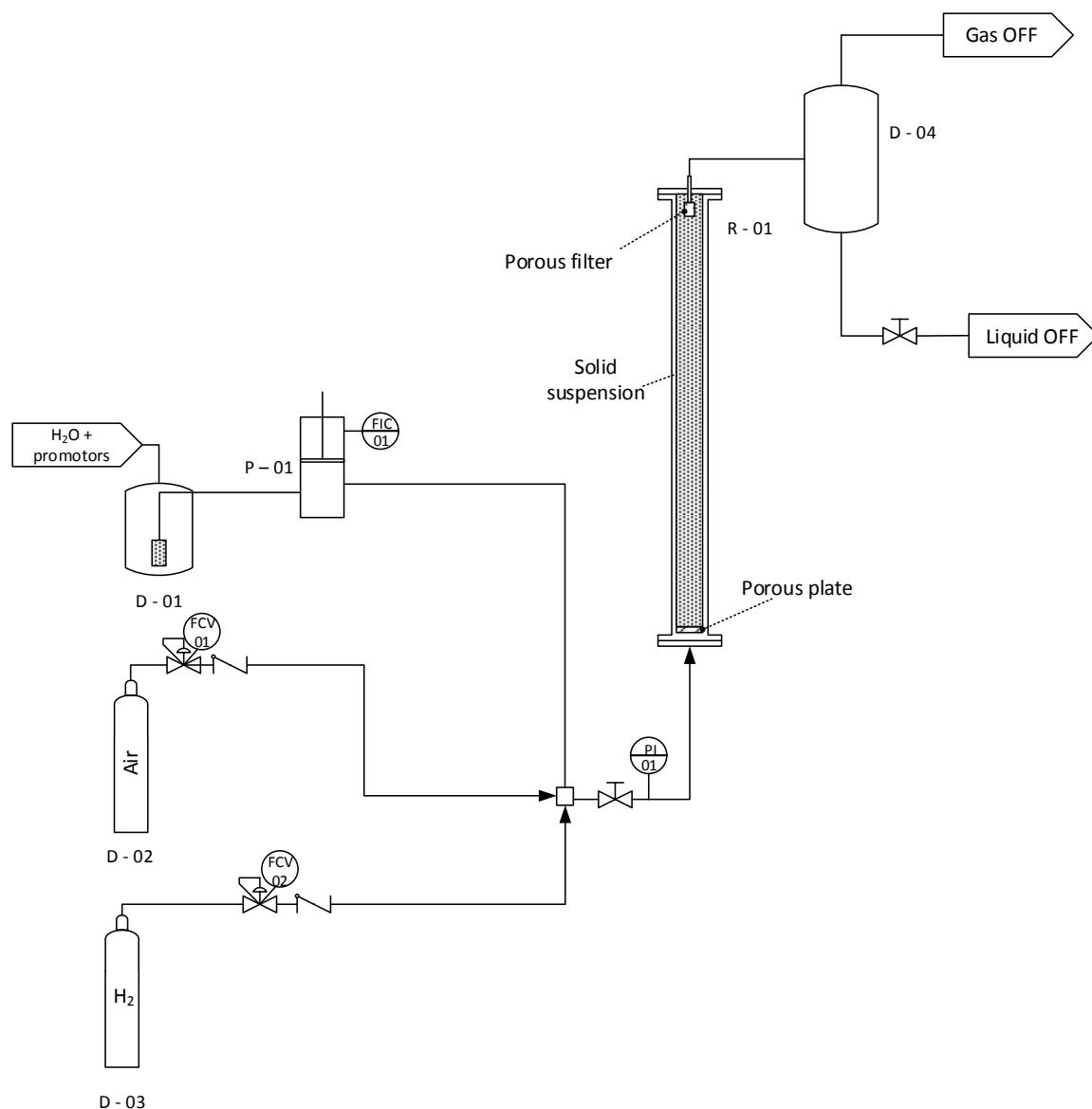


Figure 7. Scheme of the apparatus used for direct synthesis of H_2O_2 at low pressure

The reaction progress was measured by the hydrogen peroxide concentration control. The determination of the H_2O_2 concentration of the liquid phase was due by iodometric titration [17]. Turnover frequency (T.O.F.) values were calculated from H_2O_2 % wt/v concentration in liquid phase

A.2.3. Results and discussion

All the experiments were carried out at atmospheric pressure and ambient temperature. For the selection of the reaction conditions (pH, Br^-/Pd , amount of catalyst and gas flow rate) the results of previous experiments were taken into account (Chapter II and Chapter III).

Table 6. Results of low pressure H₂O₂ direct synthesis experiments

# Experiment	1	2	3
Gas flow rate (GFR), mlN·min ⁻¹	1220	1020	1020
F _{H₂} , mmol·min ⁻¹	0.93	0.91	0.91
O ₂ /H ₂	12.6	10.5	10.5
H ₂ , %	1.7	2	2
Br ⁻ /Pd	8.0	12.8	12.8
pH	2	2	2
Liquid flow rate (LFR), ml·min ⁻¹	batch	batch	2.8
Pd % wt.	5.0	5.0	5.0
Amount of catalyst, mg	100	100	100
% H ₂ O ₂ wt/v	0.008	0.009	0.0049
Accumulate H ₂ O ₂ , mmol	211.8	238.2	113.0
T.O.F, mmol H ₂ O ₂ ·h ⁻¹ ·g Pd ⁻¹	28235	35735	4519.3
Total reaction time, min	90	80	300

For the experiments #1 and #2 only the final value of the hydrogen peroxide was measured. For the experiment #3 a continuous control of the concentration was done and a sample of the liquid phase was taken every 15 minutes. As it could be expected a low hydrogen peroxide concentration was obtained, since the reaction conditions are not the optima (low pressure, not an optimum LFR – GFR ratio). Hydrogen peroxide concentration, and the accumulate H₂O₂ produced, reached when the system operated in a semicontinuous mode (continuous gas phase and batch liquid phase) was almost the double that the value obtained when a continuous system is used. Reason of the higher values of productivity obtained when a batch configuration of the liquid phase was used could be related with the reactor hydrodynamic and the catalyst distribution.

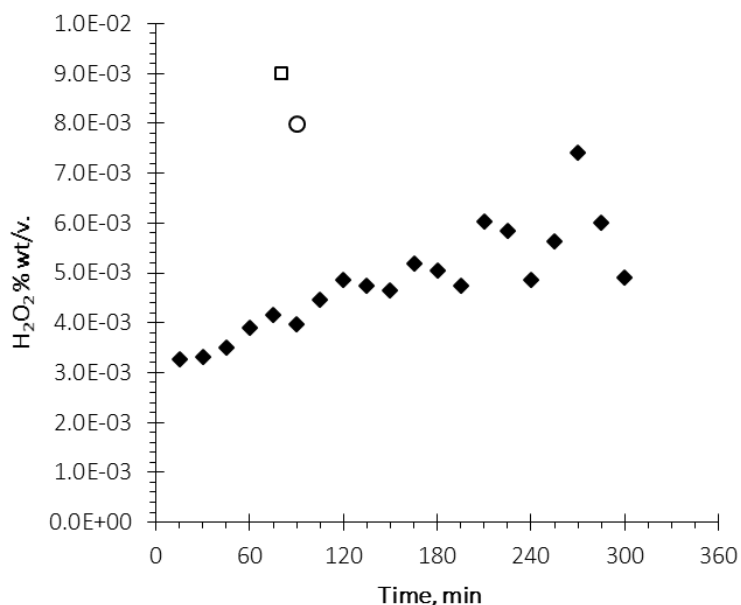


Figure 8. Hydrogen peroxide concentration for synthesis at low pressure using a SBC reactor. ○ Exp. #1; □ Exp. #2; ◆ Exp. #3

Selection of the materials and the design of this experimental apparatus was made with the objective of allow the observation of the catalyst behaviour along the reactor. One of the most important aspects for the design of a slurry bubble column is related with the catalyst, its properties and the suspension of the solid in the liquid phase. In both cases, when the liquid phase was continuous and when the liquid phase was steady, the gas flow was enough to ensure that the catalyst was homogeneously distributed along the liquid column in a short period of time, even when high amount of catalyst (more than 300 mg) were tested. However, when the reactor operated under a semicontinuous regime the liquid phase drag the catalyst along the column until a filter installed on the top of the reactor. That caused that the real amount of catalyst inside the column decreased with the reaction time and, on consequence the productivity of the system could not reach a steady value quickly.



Figure 9. Accumulation of the catalyst on the outstream filter (LFR: 2.8 ml·min⁻¹; 300 min)

A.3. Design of a high pressure slurry bubble column reactor

The mechanical design of the high pressure slurry bubble column had been done according to the specifications and limitations of the code AD-Merkblätter [18]:

- Section B0. Design of pressure vessels. Edition January 1995
- Section B1. Cylindrical and spherical shells subjected to internal pressure. Edition June 1986
- Section B5. Unstayed and stayed flat ends and plates. Edition May 1999
- Section B7. Boltings. Edition June 1986
- Section B8. Flanges. Edition February 1998
- Section B9. Openings in cylindrical, conical and spherical shells. Edition July 1995

Not only the design limitations of the design code should be taken into account since the design must be mainly limited by process itself and the laboratory facilities. On consequence for the design and built of the slurry bubble column reactor, the next points must be considered:

- The volume of the reactor should be lower than 1 dm³. According to the European standard UNE – EN 13445 and the European directive 97/23/CE [19] if the volume of the vessel is lower than 1 dm³ there would be not necessary the certification of the equipment, and the design and building would be easier and cheaper.
- Stainless steel SS316 was selected as material.
- The complete system (reactor, support, pipes and instrumentation) should not have a height greater than 1.70 m, since the system will be installed inside a bunker to ensure the security of the process.
- Reactor design should as simple and versatile as possible. The final reaction condition were not completely fixed, and the bibliography references consulted on the firsts stages of the design suggested that some modifications of the reactor configuration should be necessary in order to achieve the maximum productivity and reduce the losses of efficiency (sparger geometry, radial baffles, draft tubes, *etc.*).
- The design pressure and the design temperature were fixed at 200 bar and 200 °C respectively. Although those values are too much higher than the needed for the direct

synthesis of hydrogen peroxide, the range of operation of the reactor is extended greatly without incurring a big difference in the design or construction of the reactor.

- Although the upper and lower flask have been designed following the AD – Merkblätter code a modification of the design have been done in order to allow the joint responsible for the hermetic seal. O – ring joints have proved to be an efficient solution for the seal of a high pressure vessel since substitution of the joint is easy and quick. Dimensions of the lodging ring have been calculated following the specifications of the joint manufacturer company. The material of the joint would be selected according to the specifications of the process.
- All the dimensions and references of the tube fitting have been obtained from the Fitting Installation Manual for Hoke Gyrolock and Pipe Fitting supplied by Hoke ®.

The blueprints of the mechanical design of the slurry bubble column reactor are attached at the end of this appendix. The experimental set – up is divide in three sections: gas phase fitting – up, liquid fitting – up and reaction and phase separation and analysis.

Reactant gases, hydrogen and air, are stored in gas cylinders (D – 02 and D - 03) and connected to an appropriated system to avoid the reflux of the gases and the measuring and control of the gas pressure (PICV 11, PICV 12, PICV 13). Due to the dangerousness of the hydrogen a nitrogen cylinder (D – 01) is used to purge the hydrogen line after that any modification of the set – up would be done. The nitrogen cylinder has also all the instrumentation and control devices needed for its correct use (PICV 14). A compressor (C – 02) is used to provide that the air cylinder could be used even when the pressure on the reactor is higher than the pressure in the cylinder. High pressure air compressor is pneumatically activated by the air stream generated at the low pressure compressor (C – 01). Flow rate of the air and the hydrogen are measured and controlled by a Bronkhorst EL-FLOW mass flow meter controllers (FICV 11 and FICV 12). An automatic vale (V – 01) is installed at the hydrogen line, the valve close the hydrogen supply if a failure of the electrical supply happens. Gas phase is introduced to the reactor trough a connection at the bottom of the column.

The liquid phase (water and the promoters) is stored in an agitated and heated vessel (D - 05). The liquid phase is pump to the reactor using a HPLC pump (P – 03) which also measured and controlled the liquid flow rate (FIC 21) and have an alarm to avoid overpressure failures (PSH 21). Although the catalyst would be introduce into the reactor through the upper flange after the reaction starts, a small vessel is connected with the liquid phase line (D – 06). Filling this intermediate vessel whit a high catalyst concentrated slurry it could be possible to increase the

catalyst concentration in the reactor without stopping the process and opening the reactor. The liquid / slurry phase is introduced to the reactor through a lateral connection that it is also connected to a drain by a three ways valve. This drain could be used to empty the reactor after the experimentation.

To control the temperature inside the reactor (R – 01) a heater jacket is used. As the reaction temperatures are not extreme, water is used as cooling / heating fluid. All the reactor is also isolated. The reaction temperature is controlled at the bottom (TI 22), the middle (TI 24) and the top (TI 23) of the column. Pressure inside the reactor is measured directly in the top of the column (PI 21 and PI 22). Two safety valves are also connected to the outflow line (PSV 21 and PSV 22). Reactor pressure is controlled by a manual valve (V – 02)

The gas and liquid phases are separated in the flash (S – 01) in order to the hydrogen peroxide concentration on the liquid phase and gas composition could be measured. Temperature (TIC 31) and pressure (PICV 32) are controlled in the flash. To avoid that the catalyst particles could reach the chromatograph (A – 02) or the high pressure cell (A – 01) so many filters are installed in both gas and liquid lines. The gas micro chromatograph uses argon gas as carrier for the analysis. The argon is supplied from a cylinder (D -05) and its pressure until it reach the chromatograph is carefully controlled, also some filters are used to ensure that any particle could reach the equipment. Also gas pressure out the flash is controlled (PICV 33). Liquid phase fills the high pressure cell for Raman spectroscopy due to the pressure of the flash. As the maximum pressure that the quartz window is capable to support a safety valve is need (PSV 31). At the end of this appendix the piping and instrumentation diagrams are attached.

A.4. Measuring and analysis of the reaction conditions on the system hydrodynamic

The analysis of the column hydrodynamic is a key stage for the complete comprehension of the system and the influence of some of the reaction parameters. Before the synthesis experimentation the analysis of the gas hold - up has been done. Influence of the liquid flow rate ($2 - 16 \text{ ml}\cdot\text{min}^{-1}$), gas flow rate ($100 - 3500 \text{ mlN}\cdot\text{min}^{-1}$), pressure ($1 - 80 \text{ barg}$) and temperature ($17 - 60 \text{ }^\circ\text{C}$) have been measured and analysed. For the measured of the hold – up a simplification of the experimental set–up for the direct synthesis of hydrogen peroxide was needed. Water and air were used as liquid and gas phase respectively. No solid phase was added since the concentration of the catalyst on the reaction system will be so lower that it could be expected that it will not interfere with the hydrodynamic system.

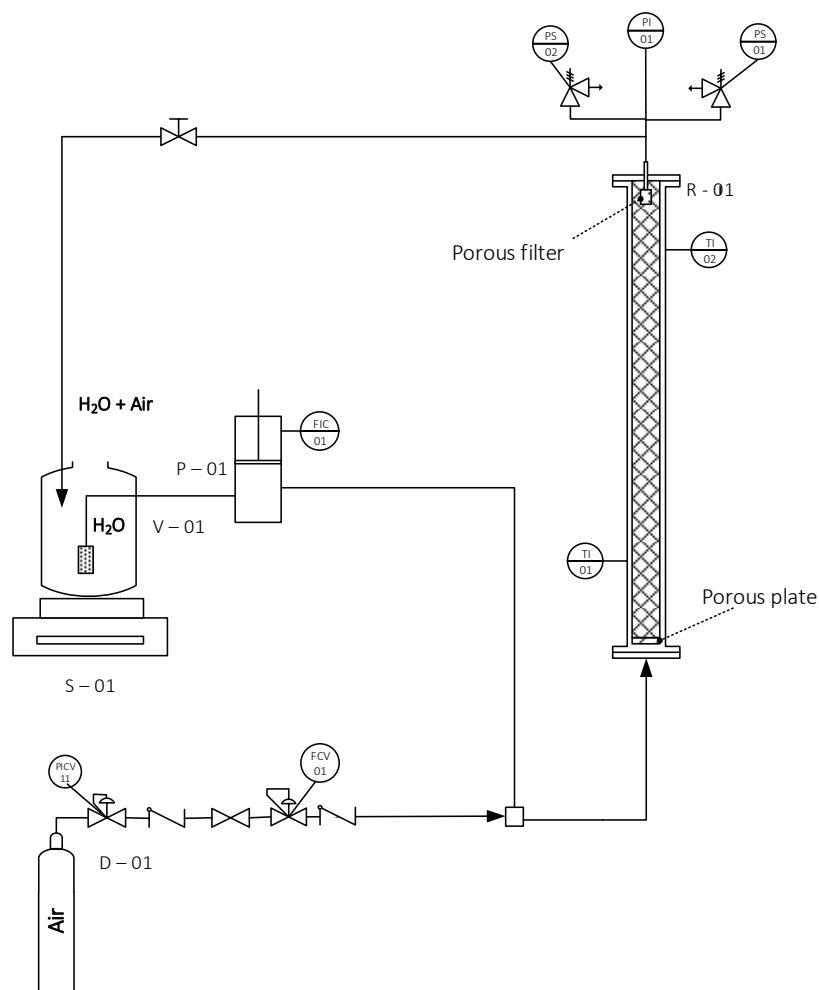


Figure 10. Experimental set – up for hold – up measuring and analysis

The gas hold – up was measuring indirectly by the measuring of the amount of water inside the reactor. Outflow and inflow liquid lines were both connected to the same vessel (V – 01) which weight was continuously controlled by a balance (S – 01). At the beginning of each test the water was pumped (P – 01) to the reactor (R – 01) until the weight of the vessel was constant, which implied that the system had reached a steady state and that the amount of water that left the reactor was the same that was pumped into it. Once the steady sate was reached the gas phase (air from the cylinder D – 01) was feeding to the column. The gas phase replace the liquid phase inside the reactor. The increase of the water amount on the vessel is directly related with the volume of the column occupied by the gas. On Table 7 the experimental average values of the gas hold – up are summarized.

Table 7. Summarized experimental conditions and selected values of the gas hold – up*.

Pressure barg	Temperature °C	Liquid flow rate ml·min ⁻¹	Gas flow rate interval mlN·min ⁻¹	Hold – up (min. – max.) %
1	17	3.9	100 – 3500	2.51 ± 0.06 – 10.58 ± 0.25
1	17	15.6	100 – 3500	0.21 ± 0.09 – 7.68 ± 0.07
1	17	2	100 – 3500	1.68 ± 0.04 – 9.04 ± 0.01
1	17	8	100 – 3500	1.66 ± 0.05 – 6.35 ± 0.03
1	17	6	100 – 3500	1.58 ± 0.02 – 7.12 ± 0.13
1	17	12	100 – 3500	2.19 ± 0.01 – 6.63 ± 0.04
1	17	16	100 – 3500	2.09 ± 0.01 – 7.11 ± 0.05
10	17	2	500 – 2000	3.38 ± 0.05 – 4.47 ± 0.02
20	17	2	500 – 2000	3.42 ± 0.04 – 4.28 ± 0.08
40	17	2	500 – 2000	3.01 ± 0.01 – 3.79 ± 0.02
80	17	2	500 – 2000	3.10 ± 0.06 – 3.40 ± 0.04
10	17	4	500 – 2000	2.13 ± 0.01 – 3.28 ± 0.02
20	17	4	500 – 2000	3.07 ± 0.04 – 4.13 ± 0.06
40	17	4	500 – 2000	2.40 ± 0.01 – 3.27 ± 0.01
80	17	4	500 – 2000	0.68 ± 0.01 – 1.21 ± 0.02
10	17	6	500 – 2000	1.50 ± 0.02 – 4.51 ± 0.02
20	17	6	500 – 2000	2.67 ± 0.02 – 3.67 ± 0.02
40	17	6	500 – 2000	2.79 ± 0.01 – 3.36 ± 0.02
80	17	6	500 – 2000	2.78 ± 0.01 – 3.36 ± 0.02
80	30	2	500 – 2000	3.54 ± 0.01 – 4.20 ± 0.03
80	30	4	500 – 2000	2.98 ± 0.03 – 2.70 ± 0.01
80	30	6	500 – 2000	0.63 ± 0.03 – 1.04 ± 0.03
80	40	2	500 – 2000	3.10 ± 0.06 – 3.64 ± 0.32
80	40	4	500 – 2000	0.72 ± 0.01 – 1.20 ± 0.03
80	40	6	500 – 2000	0.69 ± 0.06 – 1.24 ± 0.08
80	60	2	500 – 2000	3.33 ± 0.01 – 3.94 ± 0.03
80	60	4	500 – 2000	1.66 ± 0.01 – 2.35 ± 0.05
80	60	6	500 – 2000	0.64 ± 0.01 – 1.07 ± 0.01

* Only maxima and minima values have been summarized in Table 7. Complete information is showed up in the Figure 11 and Figure 12

In the same way as it was seen in the chapter VI the gas hold – up increased with the gas flow rate since the amount and the volume of gas inside the column were higher (Figure 11). On chapter VI the maxima values of the gas hold – up were closed to the 13 % and they were obtained when a porous diffuser and the maximum gas flow rate (1500 mlN·min⁻¹) were used. For the experiments carried out in this section a maximum hold – up around the 10 % was obtained even if the gas flow rate was higher (3500 mlN·min⁻¹). The reason of the differences

might be related with the reactor geometry, the characteristics of the diffuser or maybe the liquid flow rate since for all the experiments of the chapter VI the liquid phase was kept steady while for the experiments of this section the liquid phase is a continuous phase.

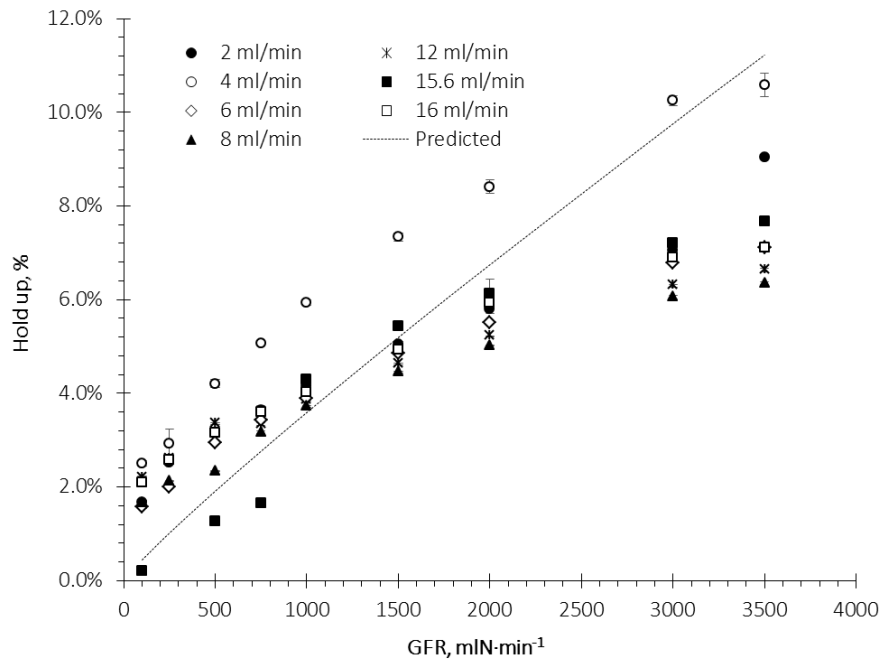


Figure 11. Influence of the liquid flow rate and the gas flow on the gas hold – up values. 1 barg, 17 °C

The equation created on the chapter VI for the prediction of the gas hold – up was not capable to calculate the hold - up values. Using the factor optimized for the low pressure bubble column ($f_c = 4.82 \cdot 10^{-2}$) the values for the hold – up were too much higher than the experimental ones. A new value for the factor have been proposed ($f_c = 7.5 \cdot 10^{-3}$) although the adjustment was not quite enough since the equation was no capable to predict the no – linear tendency when higher gas flow rates were fixed.

$$\varepsilon = f_{\varepsilon} \cdot d_0 \cdot \text{Re}^{0.7} \cdot \left(\frac{u_g}{d_0^5 \cdot g} \right)^{0.21} \quad \text{Equation 1. Proposed equation for hold – up prediction}$$

Influence of the liquid flow rate was also analysed. According to the bibliographic review did in the chapter VI the liquid flow rate should not have any direct influence on the gas hold – up (although its influence over the system hydrodynamic should be taken into account). Maxima hold – up values were obtained when 4 ml·min⁻¹ was fixed as liquid flow rate independently of the gas flow rate. When other liquid flow rate was used (2, 6, 8, 12 and 16 ml·min⁻¹) not influence of the liquid flow rate has been found, what is coherent with the observations did on the chapter

VI. Reasons of these results could be related with the specific geometry of the system, the position of the liquid phase inlet in relation with the reactor geometry and the hydrodynamic regime of the column. It should be taken into account that although according to the flow regime diagram proposed by Kantaci *et al.* [7] the regimen inside the column was homogeneous this diagram gives just an approximation to the flow regime and on consequence for our specific system the real flow rate inside the column could be different.

Hold – up decreased with the pressure since the gas volume inside the column decreased also (at $4 \text{ ml}\cdot\text{min}^{-1}$ and $2000 \text{ mlN}\cdot\text{min}^{-1}$: 1 barg – 8.4%; 10 barg – 3.3%; 40 barg – 3.3%; 80 barg – 1.2%). As the pressure increased, the influence of the liquid flow rate changed; maximum hold – up was obtained when the liquid flow rate was $2 \text{ ml}\cdot\text{min}^{-1}$ and it decreased when liquid flow rate increased. Influence of the gas flow rate was also reduced when the pressure was increased. At 80 bar the hold – up values obtained for $500 \text{ mlN}\cdot\text{min}^{-1}$ and $2000 \text{ mlN}\cdot\text{min}^{-1}$ were almost the same (at 1 bar, $2 \text{ ml}\cdot\text{min}^{-1}$: $500 \text{ mlN}\cdot\text{min}^{-1}$ – 3.2 %; $2000 \text{ mlN}\cdot\text{min}^{-1}$ – 5.8 % and at 80 bar, $2 \text{ ml}\cdot\text{min}^{-1}$: $500 \text{ mlN}\cdot\text{min}^{-1}$ – 3.1 %; $2000 \text{ mlN}\cdot\text{min}^{-1}$ – 3.4 %). Effect of the temperature is almost negligible, as it could be seen on the Figure 12, since the influence of the temperature on the properties of the fluids is really small.

Even if the results obtained in this section are not as good as they were expected and it has not been possible to generated a correlation for the prediction of the hold – up values as a function of the operational parameters, the individual values of the hold – up could be extremely useful for the modelling of the slurry bubble column reactor at next design stages.

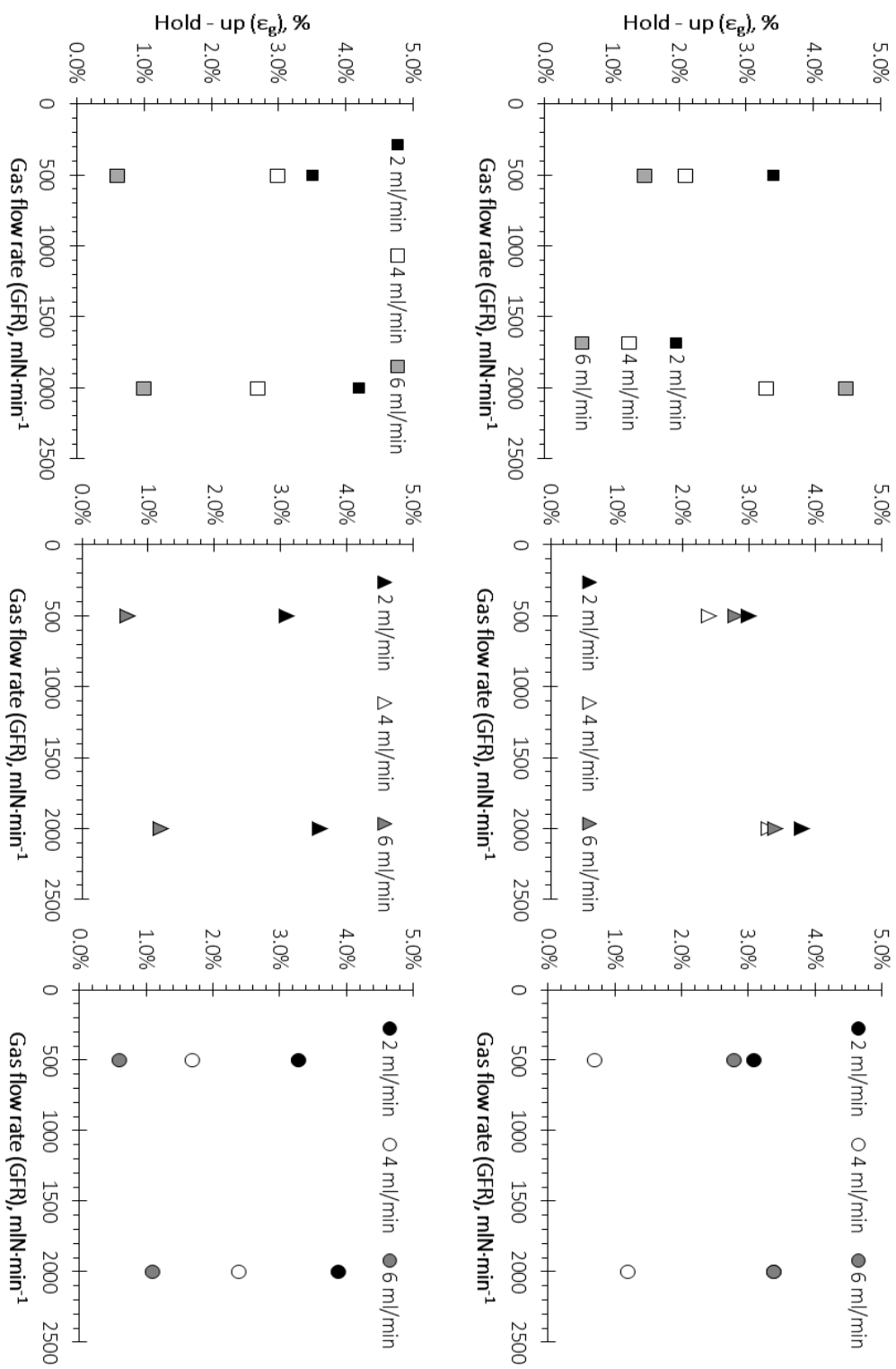


Figure 12. Influence of pressure (top) and temperature (bottom) on the gas hold – up. Pressure: 10 bar, 17 °C (left); 40 bar, 17 °C (center), 80 bar, 17 °C (right); Temperature: 80 bar, 30 °C (left); 80 bar, 40 °C (center); 80 bar, 60 °C (right)

List of symbols

D	mass diffusivity for the air – water system
d_b	bubble diameter
k_L	gas – liquid mass transfer coefficient
u_{gc}/u_s	critical gas velocity for complete solid suspension / settling velocity of a single solid particle
ε	gas hold-up, %
μ_g	viscosity of the gas phase
μ_l	viscosity of the liquid phase
ρ_G	density of the gas phase
ρ_L	density of the liquid phase
ρ_{SL}	density of the slurry phase
ρ_S	density of the solid phase
σ	surface tension

References

1. Vivek, V.R., *11 Bubble Column Reactors*, in *Process Systems Engineering*, V.R. Vivek, Editor. 2002, Academic Press. p. 327-366.
2. Luft, G., et al., *Chapter 5 Industrial reaction units*, in *Industrial Chemistry Library*, A. Bertucco and G. Vetter, Editors. 2001, Elsevier. p. 243-350.
3. Lee, S.Y. and Y.P. Tsui, *Chem, Eng. Prog.*, 1999. **July**: p. 23-49.
4. Deckwer, W.D., et al., *Hydrodynamic properties of the Fischer-Tropsch slurry process*. *Industrial & Engineering Chemistry Process Design and Development*, 1980. **19**(4): p. 699-708.
5. Thorat, B.N. and J.B. Joshi, *Regime transition in bubble columns: experimental and predictions*. *Experimental Thermal and Fluid Science*, 2004. **28**(5): p. 423-430.
6. Bach, H.F. and T. Pilhofer, *Variation of gas hold-up in bubble columns with physical properties of liquids and operating parameters of columns*. *Ger Chem Eng*, 1978. **1**(5): p. 270-275.
7. Kantarci, N., F. Borak, and K.O. Ulgen, *Bubble column reactors*. *Process Biochemistry*, 2005. **40**(7): p. 2263-2283.

8. Krishna, R., P.M. Wilkinson, and L.L. Van Dierendonck, *A model for gas holdup in bubble columns incorporating the influence of gas density on flow regime transitions*. Chemical Engineering Science, 1991. **46**(10): p. 2491-2496.
9. Hyndman, C.L., F. Larachi, and C. Guy, *Understanding gas-phase hydrodynamics in bubble columns: a convective model based on kinetic theory*. Chemical Engineering Science, 1997. **52**(1): p. 63-77.
10. Wilkinson, P.M., A.P. Spek, and L.L. Vandierendonck, *Design parameters estimation for scale up of high pressure bubble columns*. AIChE Journal, 1992. **38**(4): p. 544-554.
11. Koide, K., et al., *Critical gas velocity required for complete suspension of solid particles in solid-suspended bubble columns*. Journal of Chemical Engineering of Japan, 1983. **16**(1): p. 7-12.
12. Luo, X., et al., *Maximum stable bubble size and gas holdup in high-pressure slurry bubble columns*. AIChE Journal, 1999. **45**(4): p. 665-680.
13. Sano, Y., N. Yamaguchi, and T. Dachi, *J. Chem. Eng.*, 1974. **7**: p. 255.
14. Matsumoto, T., N. Hidaka, and S. Morooka, *Axial distribution of solid holdup in bubble column for gas-liquid-solid systems*. AIChE Journal, 1989. **35**(10): p. 1701-1709.
15. Deckwer, W.D., et al., *Fischer-Tropsch synthesis in the slurry phase on Mn/Fe catalysts*. Industrial and Engineering Chemistry Process Design and Development, 1982. **21**(2): p. 222-231.
16. Degaleesan, S., et al., *A Two-Compartment Convective-Diffusion Model for Slurry Bubble Column Reactors*. Industrial and Engineering Chemistry Research, 1997. **36**(11): p. 4670-4680.
17. Cohen, I.R., T.C. Purcell, and A.P. Altshuller, *Analysis of the oxidant in photooxidation reactions*. Environmental Science and Technology, 1967. **1**(3): p. 247-252.
18. *AD - Merkblätter. Technical Rules for Pressure Vessels 2002*, Verband der Technischen Überwachungs - Vereine e.V., Essen.
19. *Pressure Equipment Directive (97/23/EC)*. 1997.

Table Captions

Table 1. Some applications of bubble column and slurry bubble column reactors[1, 2].....	261
Table 2. Experimental values of transition velocity for bubble columns (air – water).....	264
Table 3. Design specification for preliminary design calculations	269
Table 4. Gas, slurry and solid phase's basic properties	269

Table 5. Summary of the hydrodynamic parameters obtained with the method proposed by Luft et al. [2]	270
Table 6. Results of low pressure H ₂ O ₂ direct synthesis experiments	273
Table 7. Summarized experimental conditions and selected values of the gas hold – up*.	279

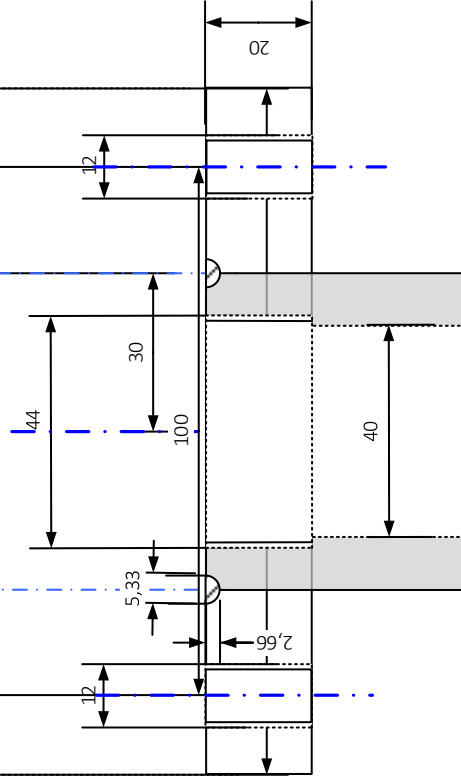
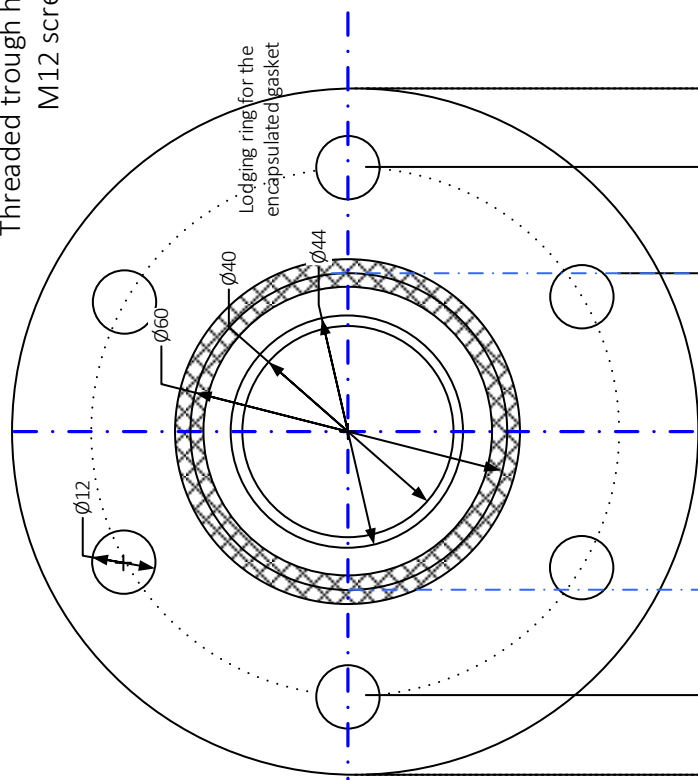
Figure Captions

Figure 1. Types of bubble column reactors (adapted form Lee and Tsui) [3].....	262
Figure 2. Schematic representation of slurry bubble columns. a) Homogeneous bubble flow, b) heterogeneous churn – turbulent flow, c) Slug flow.....	264
Figure 3. Flow regime map for bubble columns [7]	265
Figure 4. Model schematic for slurry bubble column reactors (adapted from [16])	266
Figure 5. Relevant issues on the design of a slurry bubble column reactor	267
Figure 6. Flow regime diagram for design cases selected (adapted from [7])	270
Figure 7. Scheme of the apparatus used for direct synthesis of H ₂ O ₂ at low pressure	272
Figure 8. Hydrogen peroxide concentration for synthesis at low pressure using a SBC reactor. ○ Exp. #1; □ Exp. #2; ◆ Exp. # 3	274
Figure 9. Accumulation of the catalyst on the outstream filter (LFR: 2.8 ml·min ⁻¹ ; 300 min)	274
Figure 10. Experimental set – up for hold – up measuring and analysis	278
Figure 11. Influence of the liquid flow rate and the gas flow on the gas hold – up values. 1 barg, 17 °C	280
Figure 12. Influence of pressure (top) and temperature (bottom) on the gas hold – up. Pressure: 10 bar, 17 °C (left); 40 bar, 17 °C (center), 80 bar, 17 °C (right). Temperature: 80 bar, 30 °C (left); 80 bar, 40 °C (center); 80 bar, 60 °C (right)	281

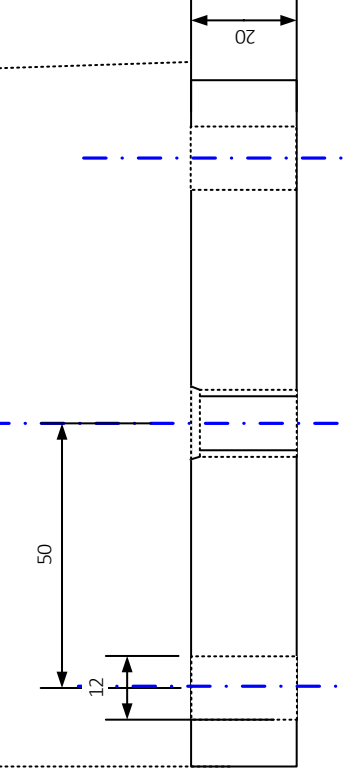
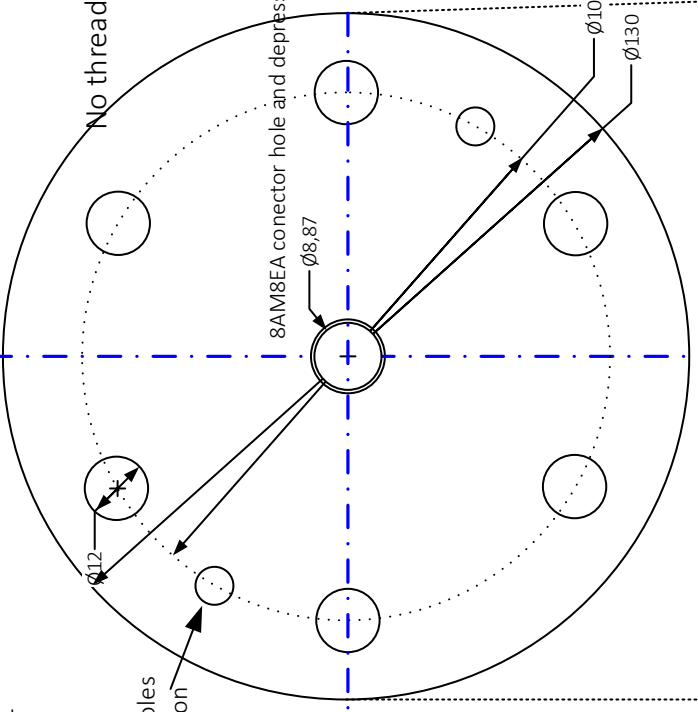
SLURRY BUBBLE COLUMN REACTOR.

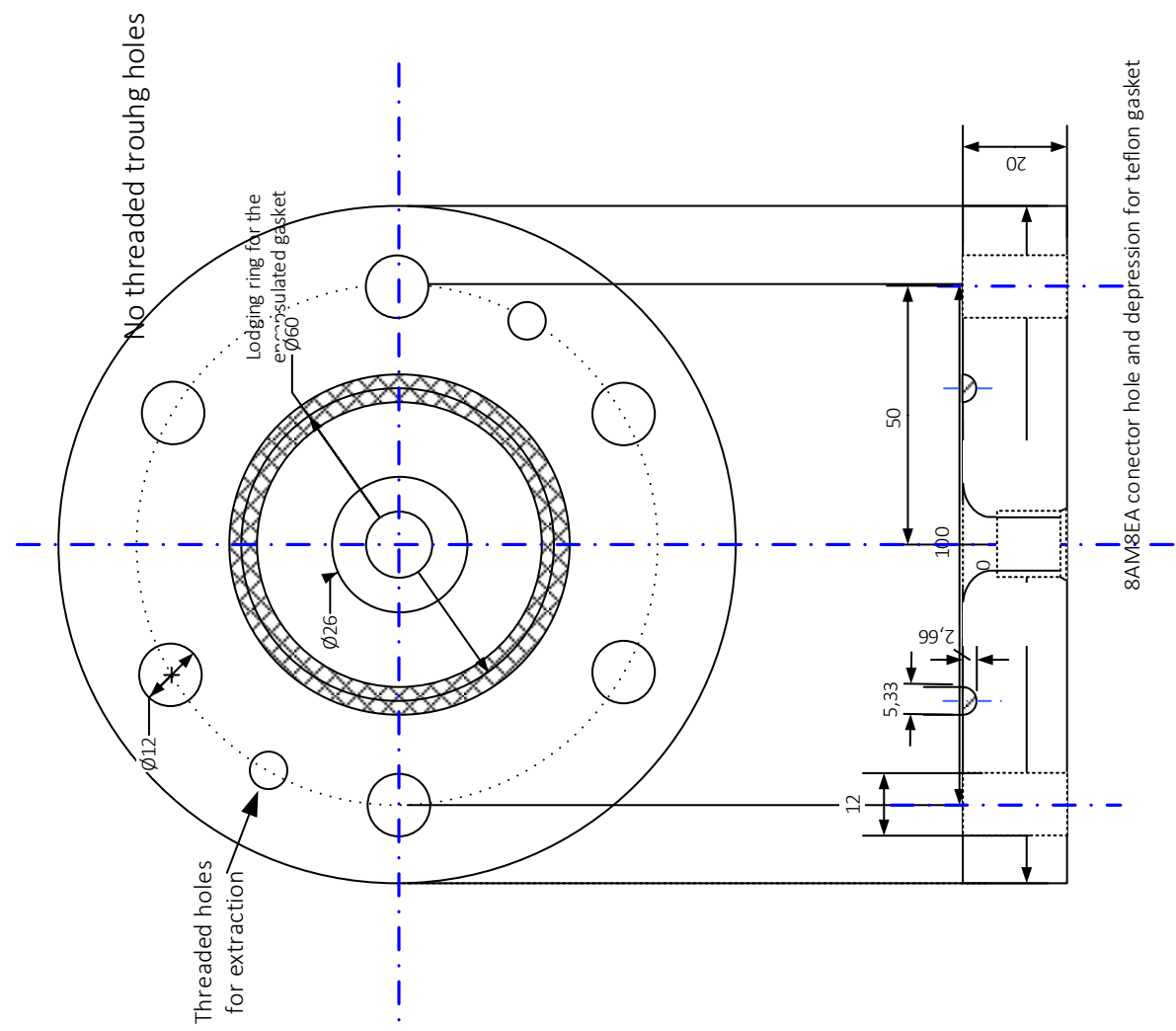
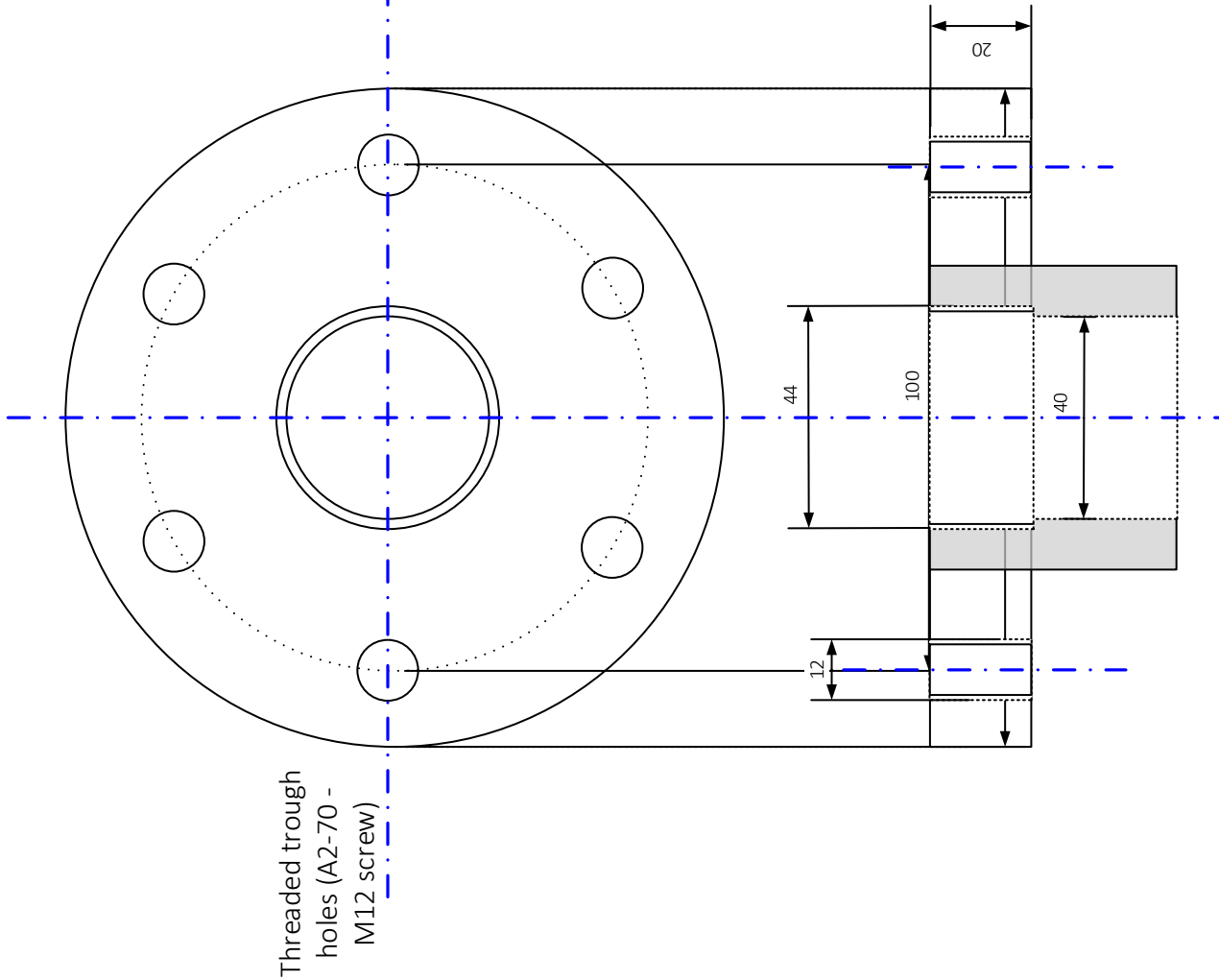
MECHANICAL DESIGN

Threaded trough holes (A2-70 - M12 screw)



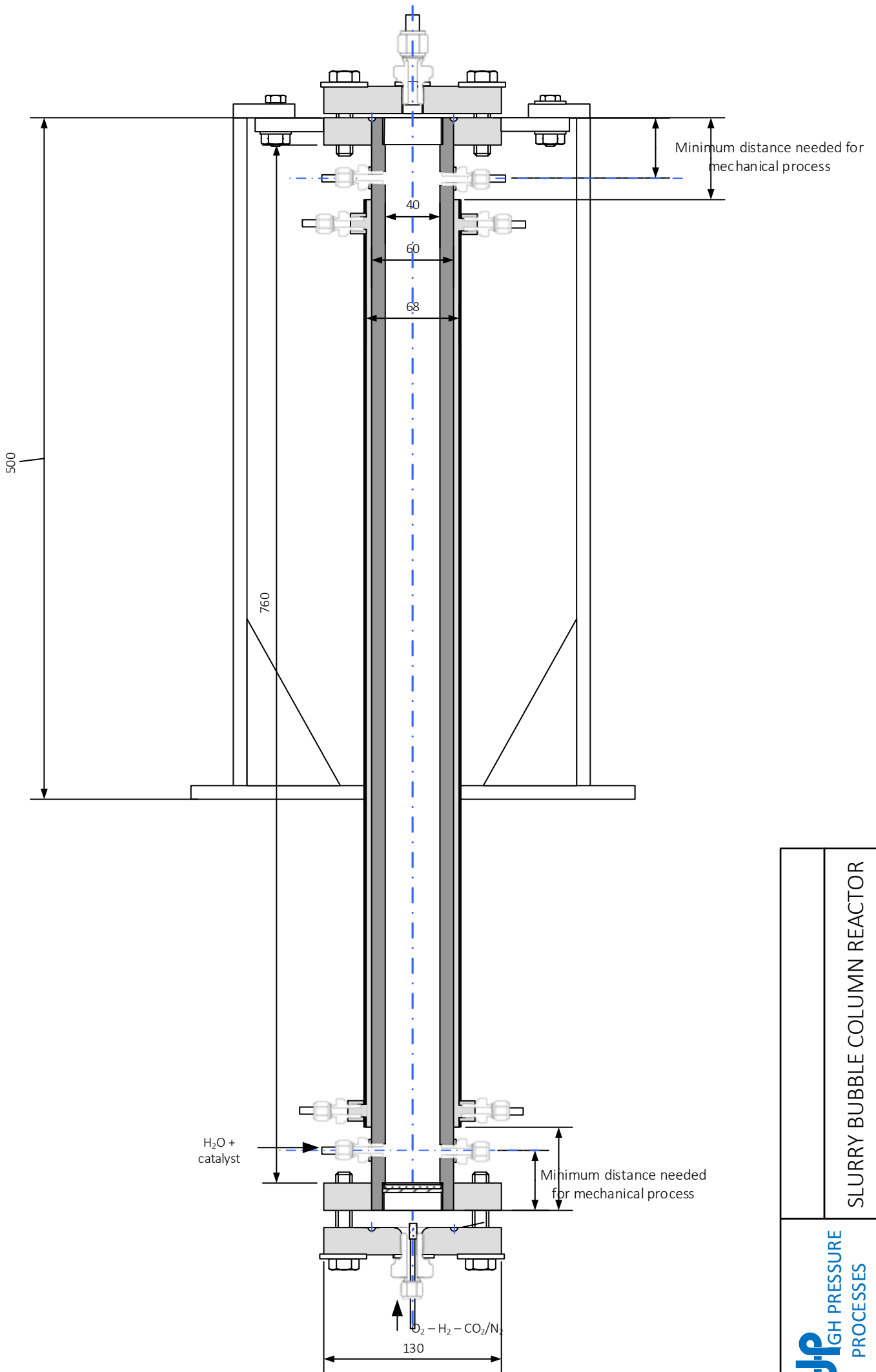
No threaded trough holes




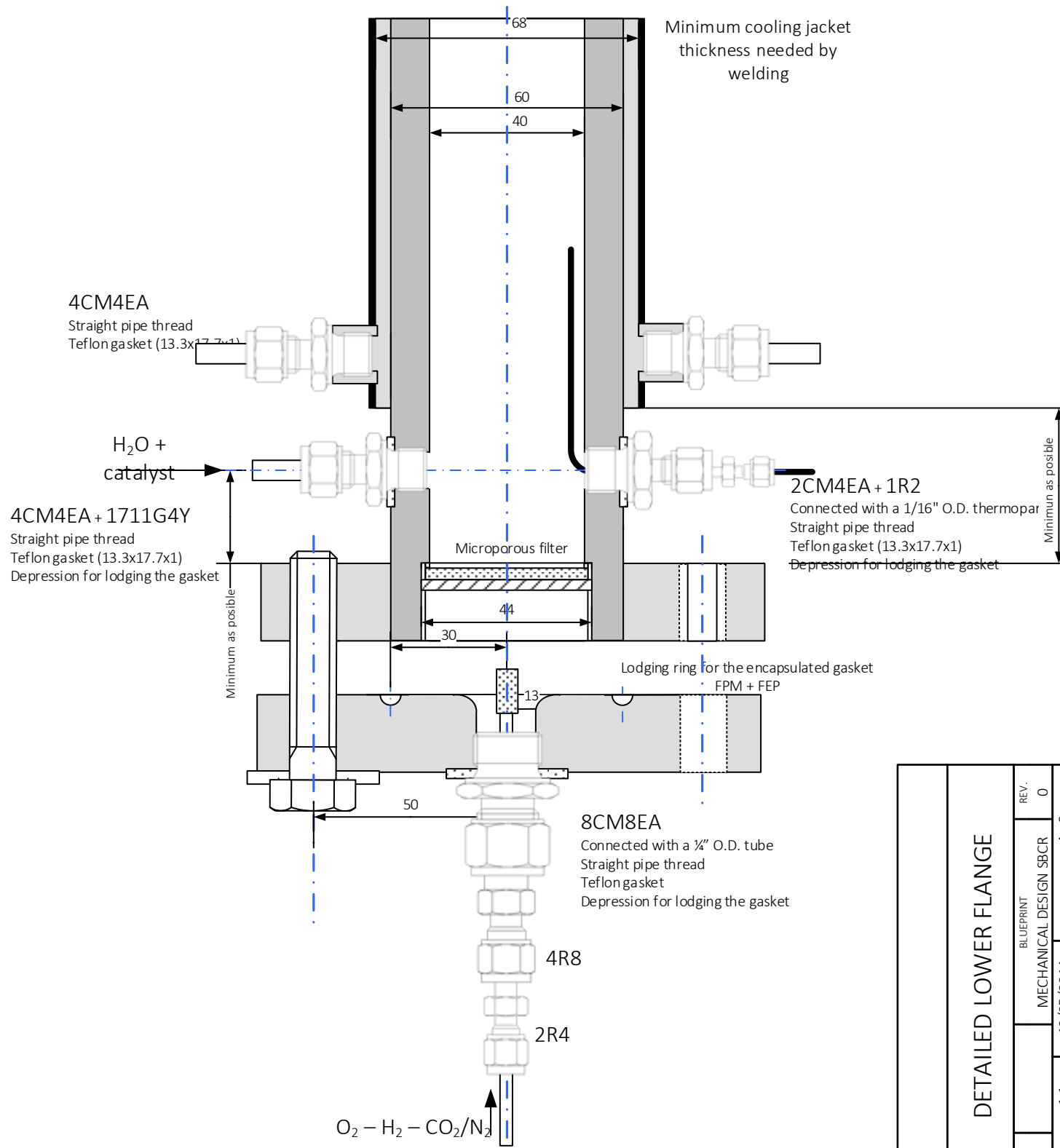


LOWER FLANGE

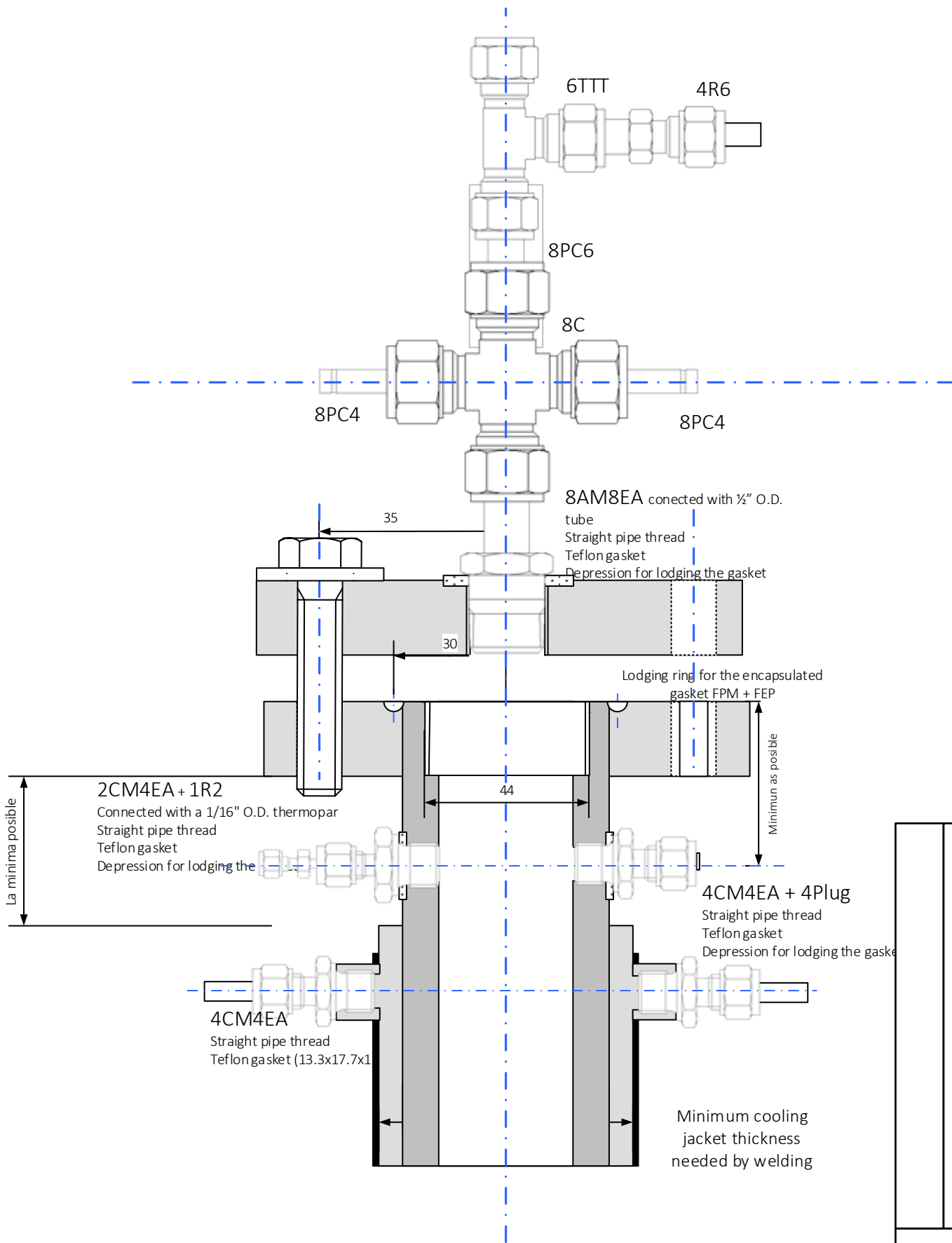
SCALE	1:1	12/05/2014	SHEET	2 DE 6
SIZE	A4	MECHANICAL DESIGN SBCR	REV.	0




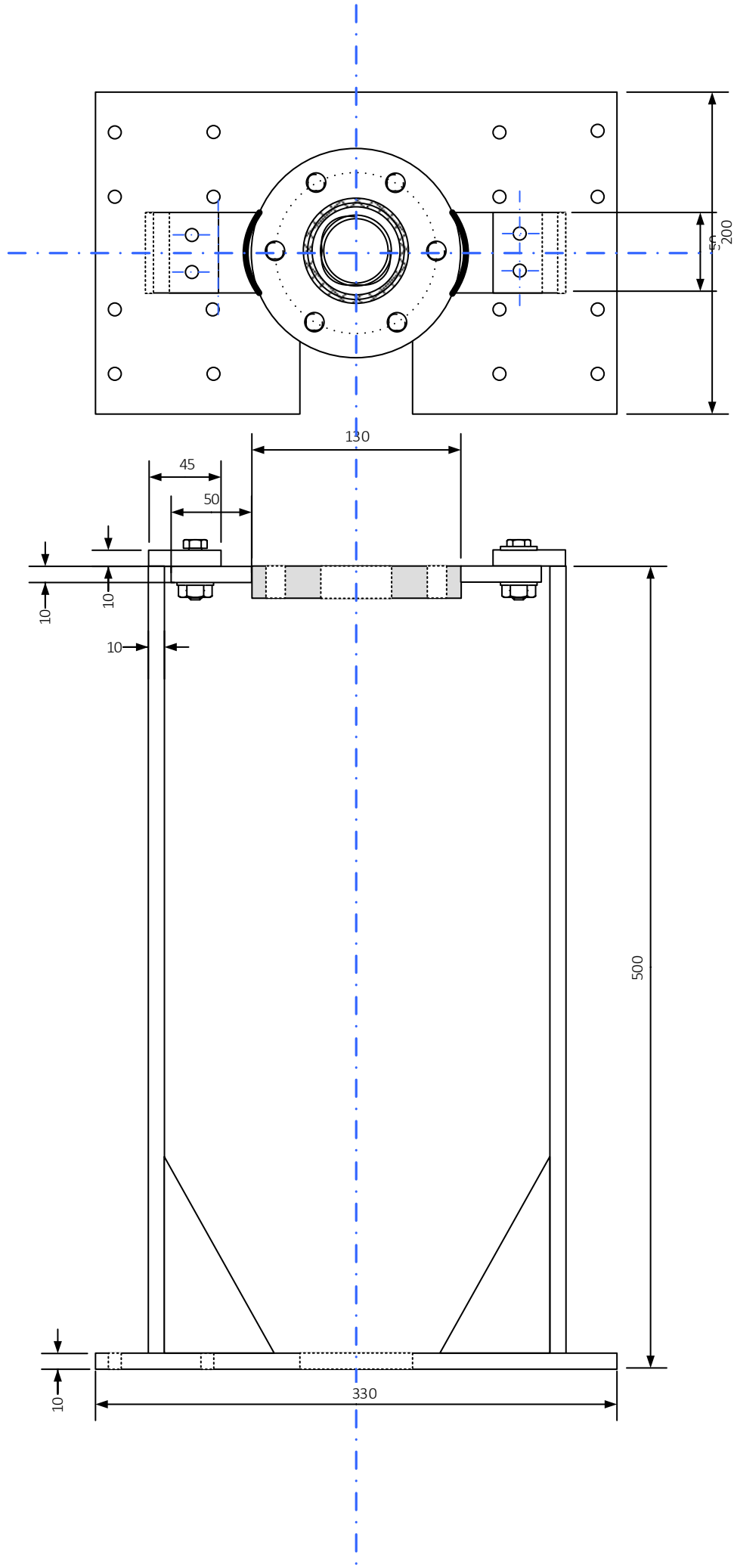
		SLURRY BUBBLE COLUMN REACTOR	
		SIZE A4	REV. 0
SCALE 1:2,5	12/05/2014	MECHANICAL DESIGN SBCR	SHEET 3 - 6




		DETAILED LOWER FLANGE	
		SIZE A4	REV. 0
SCALE 1:1	SHEET 4 - 6	MECHANICAL DESIGN SBCR	
12/05/2014		BLUEPRINT	



		DETAILED UPPER FLANGE	
		SCALE 1:1	SHEET 5 - 6
SIZE A4	BLUEPRINT	MECHANICAL DESIGN SBCR	REV. 0
SCALE 1:1	12/05/2014	SHEET	5 - 6



		REACTOR SUPPORT		
		SIZE A4	BLUEPRINT MECHANICAL DESIGN SBCR	REV. 0
SCALE 1:2.5	DATE 12/05/2014	SHEET 6 - 6		

SLURRY BUBBLE COLUMN REACTOR

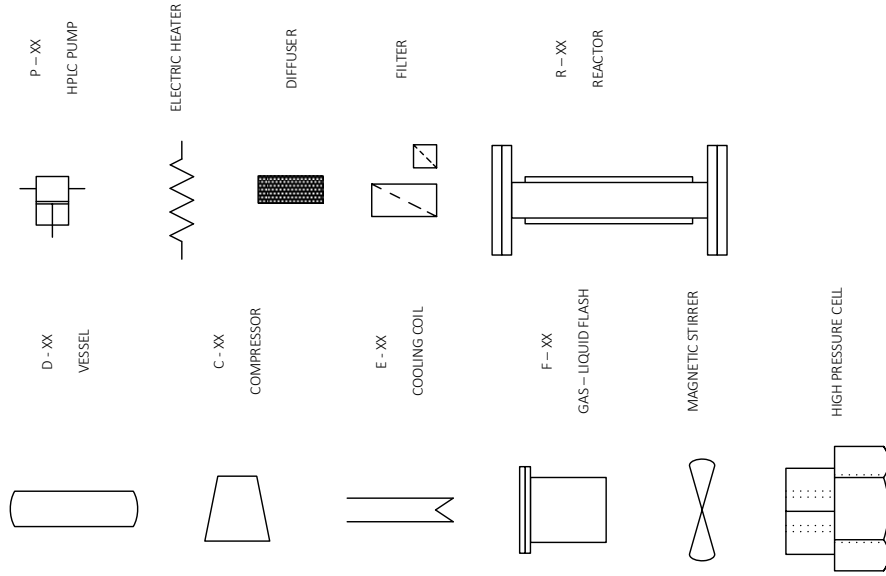
PIPING AND INSTRUMENTATION DIAGRAMS

GENERAL NOTES

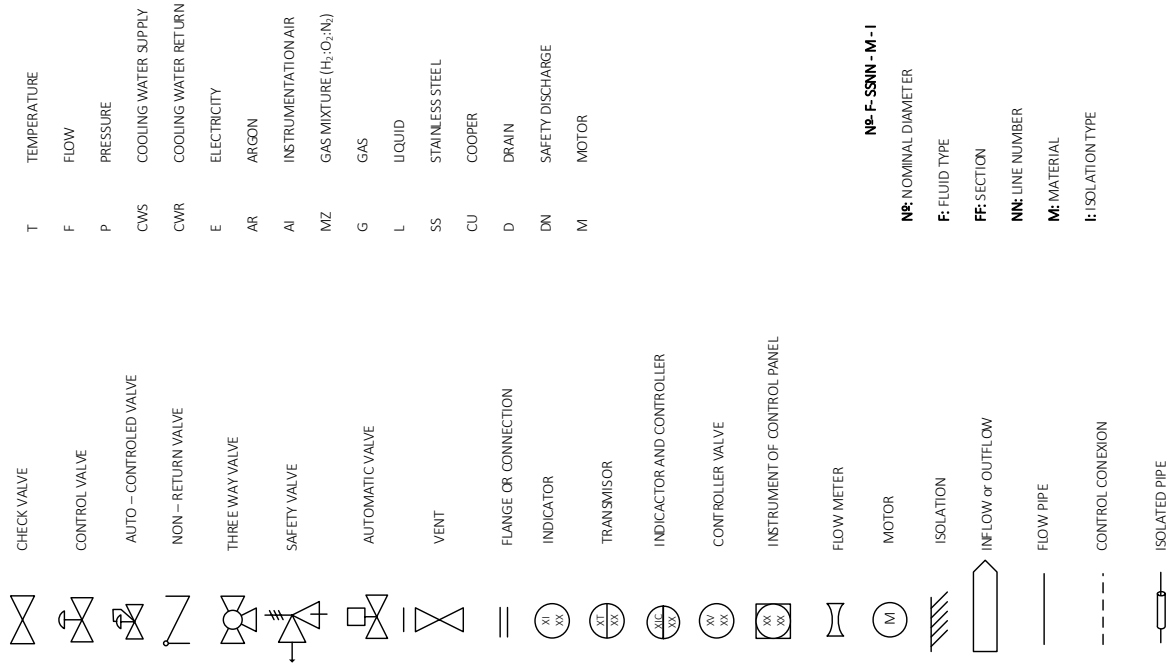
1. TO REVIEW DURING THE DETAILED DESIGN

NOTES:

EQUIPMENT SYMBOLS



CONTROLS SYMBOLS



T TEMPERATURE

F FLOW

P PRESSURE

CWS COOLING WATER SUPPLY

CWR COOLING WATER RETURN

E ELECTRICITY

AR ARGON

AI INSTRUMENTATION AIR

MZ GAS MIXTURE (H₂, O₂, N₂)

G GAS

L LIQUID

SS STAINLESS STEEL

CU COPPER

D DRAIN

DN SAFETY DISCHARGE

M MOTOR

Nº. F-SSNN - M - I

Nº: NOMINAL DIAMETER

F: FLUID TYPE

FF: SECTION

NN: LINE NUMBER

M: MATERIAL

I: ISOLATION TYPE



PROCESS: H₂O₂ Direct synthesis - SBCR

TITLE

SYMBOLS AND NOMENCLATURE

DESCRIPTION		Nº	
P&L DIAGRAM		PI-A4-00-0	
REV.	DESCRIPTION	DATE	BY
0	BASIC ENG.	12/05/2014	

GENERAL NOTES

1. TO REVIEW DURING THE DETAILED DESIGN

NOTES:

1. AUTOMATIC VALVE ELECTRICALLY ACTIVATE. THE VALVE CLOSES THE LINE IF THE ELECTRIC SUPPLIED FAILS

Equipment list:

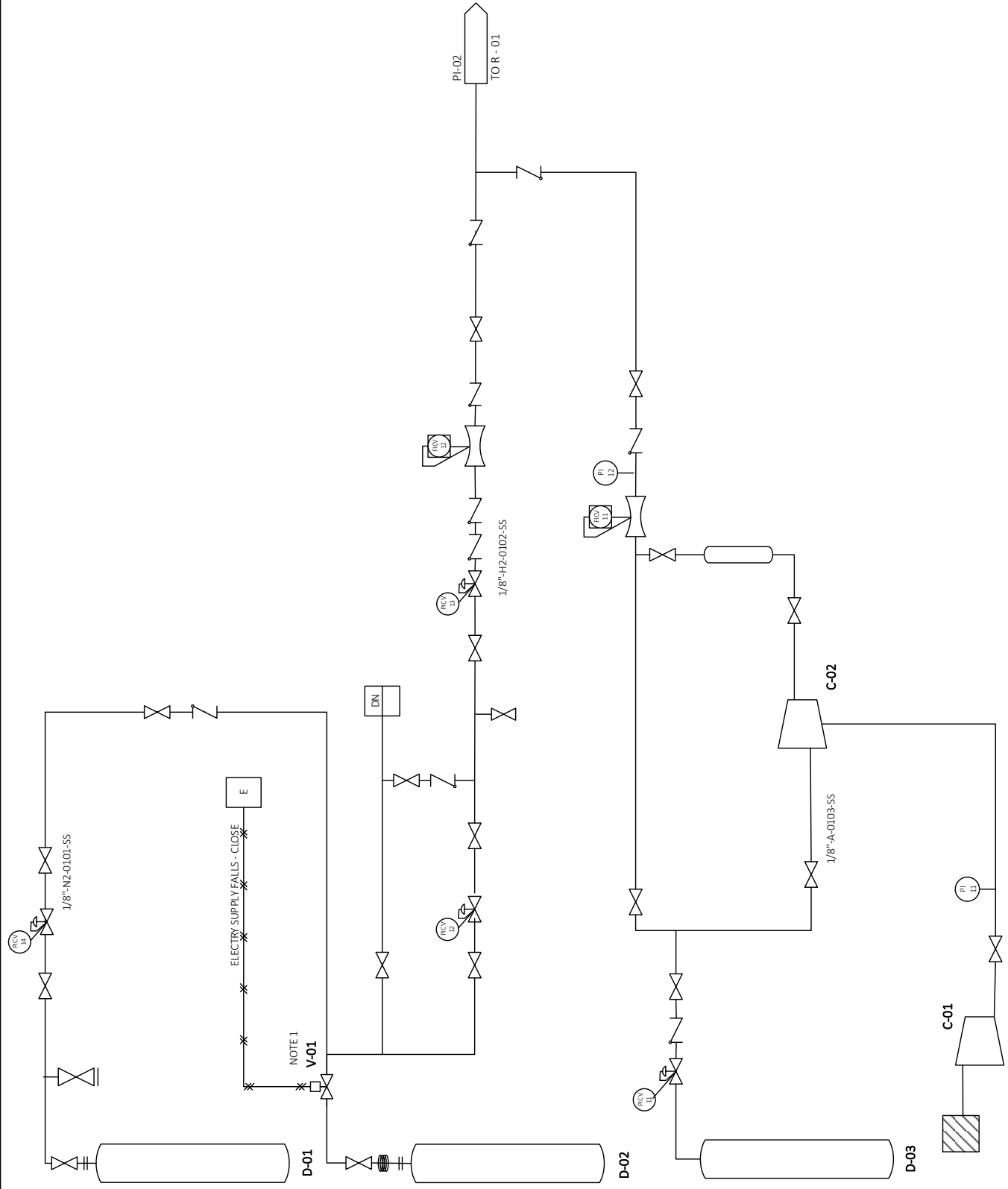
- D-01
- D-02
- D-03
- C-01
- C-02
- V-01



TAG: H₂O₂ Direct synthesis - SBOR

TITLE: GAS FITTING - OUT

REV.	DESCRIPTION	DATE	BY
0	BASIC ENG.	12/05/2014	



TAG	DESCRIPTION	UNIT	VALUE	UNIT	VALUE	UNIT	VALUE	UNIT	VALUE
D-01	DESCRIPTION: NITROGEN CYLINDER	VOLUME (m ³)	0.05						
		H (mm)	1570						
		D (mm)	230						
		P ₁ (kg/cm ² g)	220						
		T ₁ (°C)	50						
		MAT.	SS						
D-02	DESCRIPTION: HYDROGEN CYLINDER	VOLUME (m ³)	0.05						
		H (mm)	1570						
		D (mm)	230						
		P ₁ (kg/cm ² g)	220						
		T ₁ (°C)	50						
		MAT.	SS						
D-03	DESCRIPTION: AIR CYLINDER	VOLUME (m ³)	0.05						
		H (mm)	1570						
		D (mm)	230						
		P ₁ (kg/cm ² g)	12.0						
		T ₁ (°C)	50						
		MAT.	AC						
C-01	DESCRIPTION: LOW PRESSURE AIR COMPRESSOR	FLOW (mlN/min)	325						
		ΔP (kg/cm ²)	5						
		P ₁ (kg/cm ² g)	140						
		T ₁ (°C)	375						
		MAT.	SS316						
C-02	DESCRIPTION: HIGH PRESSURE AIR COMPRESSOR	FLOW (mlN/min)	2.744						
		ΔP (kg/cm ²)	90.7						
		P ₁ (kg/cm ² g)	140						
		T ₁ (°C)	375						
		MAT.	SS316						
V-01	DESCRIPTION: AUTOMATIC ELECTRIC VALVE FOR THE CONTROL OF THE FLOW OF HYDROGEN	P ₁ (kg/cm ² g)	--						
		T ₁ (°C)	--						

GENERAL NOTES

1. TO REVIEW DURING THE DETAILED DESIGN

NOTES:

1. INSTALLED INSIDE THE PUMPP - 01
2. MANUAL CONTROL TYPE VALVE. INSTALLED IN THE CONTROL PANEL.
3. SLURRY PHASE INCOMING TO THE REACTOR IS MADE THROUGH A LATERAL ACCESS SINCE AT THE BOTTOM OF THE REACTOR A POROUS PLATE IS INSTALLED TO ENSURE A GOOD DISPERSION OF THE BUBBLES
4. CATALYST COULD BE ADDED TO THE REACTION USING AN INTERMEDIATE VESSEL FULL OF A HIGH SOLID CONCENTRATED SLURRY.

Equipment list

- D-05
- P-01
- D-06
- R-01
- V-03

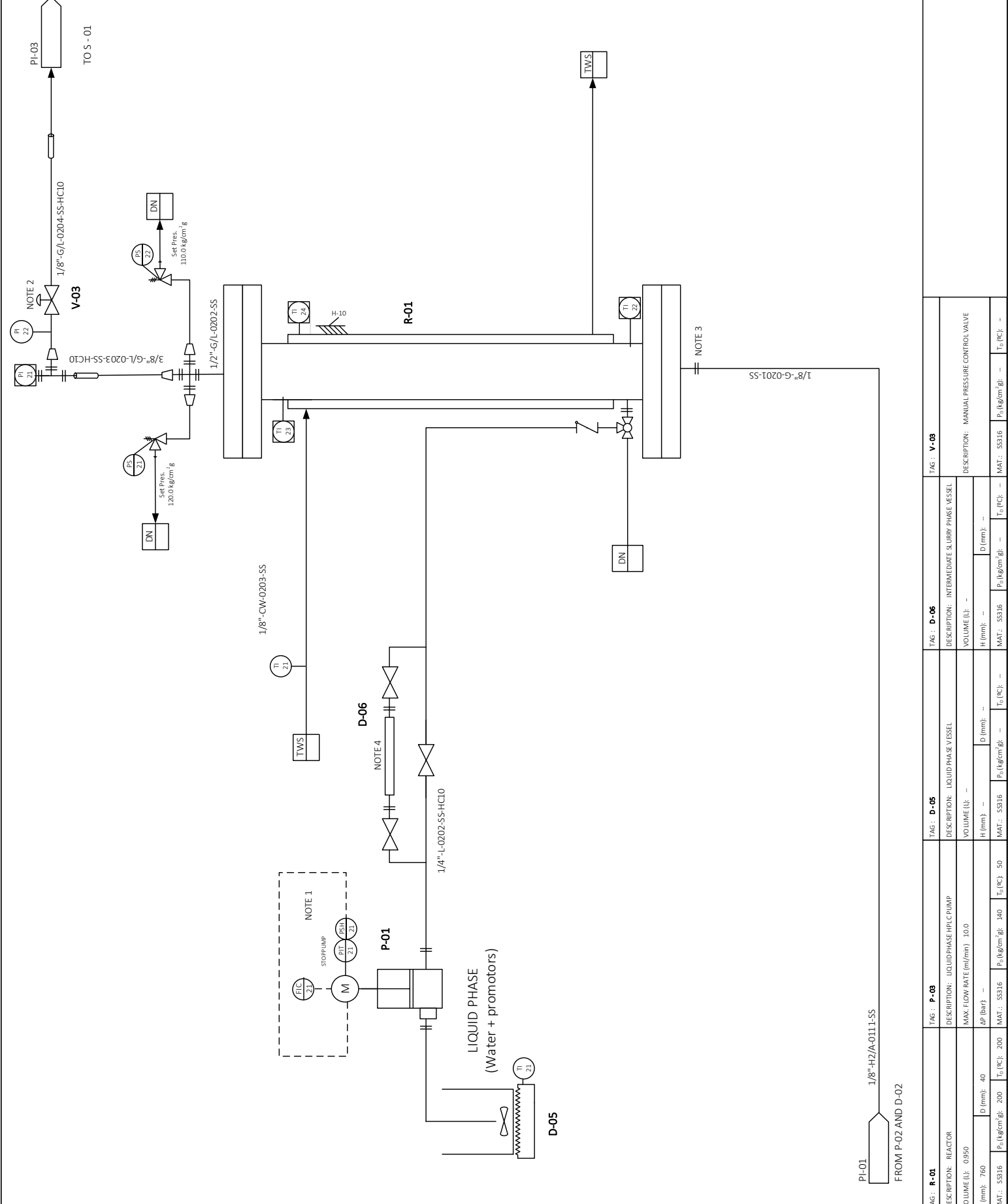


PROCESS: H₂O₂ Direct synthesis - SBCR

TITLE:

REACTION STAGE AND LIQUID PHASE FITTING - OUT

DESCRIPTION	REV.	P&ID DIAGRAM	DATE	BY
	0	BASIC ENG.	08/05/2014	



TAG	DESCRIPTION	VOLUME (L)	H (mm)	D (mm)	P ₁ (kg/cm ² g)	T ₁ (°C)	P ₂ (kg/cm ² g)	T ₂ (°C)
P-01	LIQUID PHASE HPLC PUMP	10.0	--	--	--	--	--	--
D-05	LIQUID PHASE VESSEL	--	--	--	--	--	--	--
D-06	INTERMEDIATE SLURRY PHASE VESSEL	--	--	--	--	--	--	--
V-03	MANUAL PRESSURE CONTROL VALVE	--	--	--	--	--	--	--

PI-01 1/8"-H2/A-0111-SS

FROM P-02 AND D-02

GENERAL NOTES

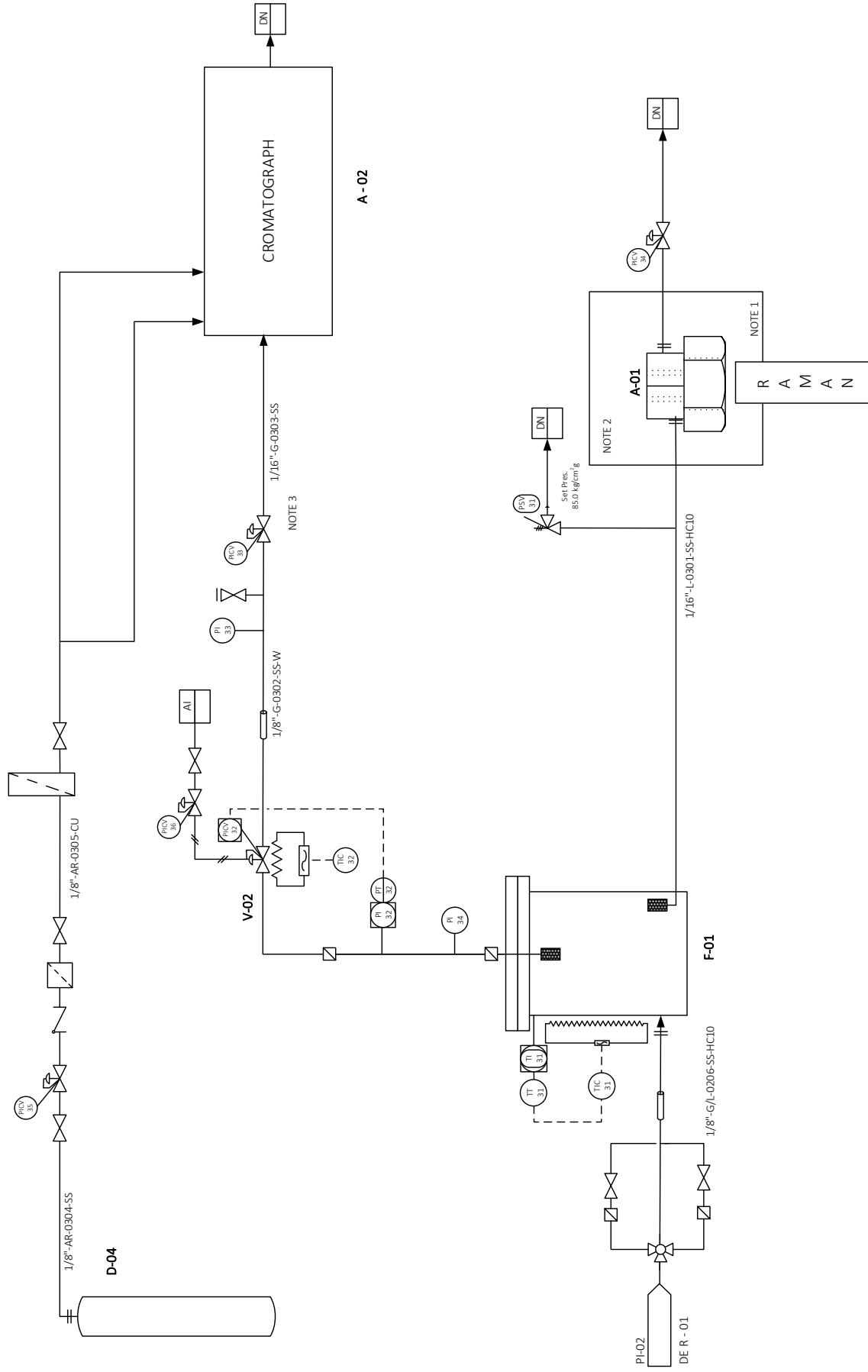
1. TO REVIEW DURING THE DETAILED DESIGN

NOTES :

1. DESCARGA DE LIQUIDO LO MAS CERCA DE LA CELDA, RELLENO PARA REDUCIR EL VOLUMEN
2. ISOLATED FORM THE NATURAL LIGHT
3. CROMATOGRAPH INLET PRESSURE MUST BE CAREFULLY KEEP CLOSE TO 1.1-2 bar

Equipment list:

- S-01
- A-01
- A-02
- D-04
- V-02



TAG		PROCESS	
H ₂ O ₂ Direct synthesis - SBRC		TITLE	
PHASE SEPARATION AND ANALYSIS			
DESCRIPTION	PI	REV.	DATE
P&L DIAGRAM	PI-A4-03-0	0	08/05/2014
REV.	DESCRIPTION	BY	
0	BASIC ENG.		

<table border="1"> <tr> <td>DESCRIPTION: GAS-LIQUID FLASH</td> <td>DESCRIPTION: ARGON CYLINDER</td> </tr> <tr> <td>VOLUME (L): 0.330</td> <td>VOLUME (m³): 0.05</td> </tr> <tr> <td>H (mm): 104.4</td> <td>D (mm): 68.3</td> </tr> <tr> <td>MAT.: S5316</td> <td>P₁ (kg/cm²g): 200</td> </tr> <tr> <td></td> <td>T₁ (°C): 200</td> </tr> </table>	DESCRIPTION: GAS-LIQUID FLASH	DESCRIPTION: ARGON CYLINDER	VOLUME (L): 0.330	VOLUME (m ³): 0.05	H (mm): 104.4	D (mm): 68.3	MAT.: S5316	P ₁ (kg/cm ² g): 200		T ₁ (°C): 200	<table border="1"> <tr> <td>DESCRIPTION: MICRO GAS CHROMATOGRAPH</td> <td>DESCRIPTION: RAMAN SPECTROMETER</td> </tr> <tr> <td>MAT.: S5316</td> <td>P₁ (kg/cm²g): 220</td> </tr> <tr> <td></td> <td>T₁ (°C): 50</td> </tr> </table>	DESCRIPTION: MICRO GAS CHROMATOGRAPH	DESCRIPTION: RAMAN SPECTROMETER	MAT.: S5316	P ₁ (kg/cm ² g): 220		T ₁ (°C): 50	<table border="1"> <tr> <td>DESCRIPTION: PRESSION CONTROL AUTOMATIC VALVE</td> <td>DESCRIPTION: PRESSION CONTROL AUTOMATIC VALVE</td> </tr> <tr> <td>MAT.: S5316</td> <td>P₁ (kg/cm²g): --</td> </tr> <tr> <td></td> <td>T₁ (°C): --</td> </tr> </table>	DESCRIPTION: PRESSION CONTROL AUTOMATIC VALVE	DESCRIPTION: PRESSION CONTROL AUTOMATIC VALVE	MAT.: S5316	P ₁ (kg/cm ² g): --		T ₁ (°C): --
DESCRIPTION: GAS-LIQUID FLASH	DESCRIPTION: ARGON CYLINDER																							
VOLUME (L): 0.330	VOLUME (m ³): 0.05																							
H (mm): 104.4	D (mm): 68.3																							
MAT.: S5316	P ₁ (kg/cm ² g): 200																							
	T ₁ (°C): 200																							
DESCRIPTION: MICRO GAS CHROMATOGRAPH	DESCRIPTION: RAMAN SPECTROMETER																							
MAT.: S5316	P ₁ (kg/cm ² g): 220																							
	T ₁ (°C): 50																							
DESCRIPTION: PRESSION CONTROL AUTOMATIC VALVE	DESCRIPTION: PRESSION CONTROL AUTOMATIC VALVE																							
MAT.: S5316	P ₁ (kg/cm ² g): --																							
	T ₁ (°C): --																							
TAG : F-01	TAG : A-01	TAG : V-02																						

ACKNOWLEDGEMENTS

En primer lugar mi más profundo agradecimiento a María José Cocero y a Juan García Serna. Sin la oportunidad que ellos me dieron nada de lo ocurrido en estos últimos años habría sido posible. Su labor como tutores, sus ideas, críticas, paciencia y apoyo incondicional ha sido imprescindible. Todo lo que ellos me han enseñado lo recordaré siempre y sé que me será de gran utilidad en cualquiera de los proyectos que emprenda.

Of course I would like to thank to Tapio Salmi and Pierdiomenico Biasi from the Department of Chemical Engineering of Åbo Akademi University of Turku (Finland) for the extraordinary experience they offered to me by allowing me to work with them and to participate into their investigations. Also I would like to thank them for all the good advices and comments because without them I could not finish this thesis.

To Alice, Lotta, Victoria and Kari because their inestimable help inside and outside the laboratory. Without you my experience in Finland would have been too much tough.

A Teresa Moreno que tuvo la inmensa paciencia de enseñarme y explicarme todo sobre el funcionamiento del laboratorio y del peróxido de hidrogeno y cuya tesis me ha sido extraordinariamente útil. A Álvaro que siempre estaba disponible cuando le necesitaba y que ha dedicado una gran cantidad de horas para el montaje. A Adrián por su aportación a esta tesis gracias a su trabajo en el laboratorio.

A todos los compañeros, los que están y los que se fueron. A Cristina, Danilo y Joao, Miriam, Luismi, Óscar, Esther, Alex, Kati, Flor, Lara, Gerardo, María y resto de compañeros del departamento. Sin duda alguna los buenos ratos superan a los malos y eso es gracias a vosotros. Gracias también a Bri y a mis chicas, aunque nos vemos poco siempre conseguimos mantenernos al día.

Por supuesto a mi maravillosa familia. Todo lo que consiga en mi vida, empezando por esta tesis, os lo deberé siempre. Nadie tiene más suerte que yo. Por último, pero no por eso menos importante a Rubén, por confiar en mí más que yo misma y por animarme siempre a seguir con tu ejemplo y tú cariño.

LIST OF PUBLICATIONS

Publications

Huerta, Irene; Biasi, Pierdomenico; García-Serna, Juan; Cocero, Maria Jose; Mikkola, Jyri-Pekka; Salmi, Tapio, Continuous H₂O₂ direct synthesis process in water: bridging the gap between chemistry and chemical engineering, *ACS Catalysis* (2014), **Submitted**

I. Huerta, P. Biasi, J. García-Serna, M.J. Cocero, Jyri-Pekka Mikkola and T. Salmi, Effect of low hydrogen to palladium molar ratios in the direct synthesis of H₂O₂ in water in a trickle bed reactor, *Catalysis Today* (2014), **Accepted**

Irene Huerta Illera, Juan Garcia-Serna, María J. Cocero, Direct synthesis of H₂O₂ in water using nitrogen as inert over Pd/C catalysts in semicontinuous mode, *The Journal of Supercritical Fluids* (2014), **Submitted**

Irene Huerta, Juan García-Serna, María José Cocero, Hydrogenation and decomposition kinetic study of H₂O₂ over Pd/C catalyst in an aqueous medium at high CO₂ pressure, *The Journal of Supercritical Fluids* (2013), 74, (80 – 88)

T. Moreno, M.A. Morán López, I. Huerta Illera, C.M. Piqueras, A. Sanz Arranz, J. García Serna, M.J. Cocero, Quantitative Raman determination of hydrogen peroxide using the solvent as internal standard: Online application in the direct synthesis of hydrogen peroxide, *Chemical Engineering Journal* (2011), 166, (1061-1065)

Oral presentation

Irene Huerta Illera, Teresa Moreno, Juan García Serna and María José Cocero. *Direct synthesis of hydrogen peroxide in a slurry bubble column reactor in water with and without a supercritical CO₂ gas phase. Process and reactor design considerations.* Catalysis in Multiphase Reactors CAMURE-8 + International Symposium on Multifunctional Reactors ISMR-7. Naantali (Finland) 22-25 May 2011

Irene Huerta Illera, Juan García Serna y María José Cocero Alonso. *Direct synthesis of hydrogen peroxide in water in slurry bubble column reactors at high pressures. Study of decomposition, hydrogenation and synthesis.* ANQUE ICCE 2012. Sevilla, 24-27 Junio de 2012

Poster

Irene Huerta, Juan García Serna, María José Cocero. Pautas de diseño de un reactor “slurry bubble column” para la síntesis directa de H_2O_2 en continuo. V Reunión de expertos en Tecnologías de Fluidos Comprimidos, FLUCOMP2011. Burgos, 15-17 de Junio de 2011

Irene Huerta, Juan García Serna, María José Cocero. *Direct synthesis of hydrogen peroxide at high pressure. Study of decomposition and hydrogenation*. ANQUE ICCE 2012. Sevilla, 24-27 Junio de 2012

